

~~CONFIDENTIAL~~

Copy

5

RM A54G13

FOR REFERENCE

~~NACA~~

NOT TO BE TAKEN FROM THIS ROOM

RESEARCH MEMORANDUM

INVESTIGATION OF THE NACA 4-(5)(05)-037 SIX- AND EIGHT-BLADE,
DUAL-ROTATION PROPELLERS AT POSITIVE AND NEGATIVE THRUST
AT MACH NUMBERS UP TO 0.90, INCLUDING SOME AERODYNAMIC
CHARACTERISTICS OF THE NACA 4-(5)(05)-041 TWO- AND
FOUR-BLADE, SINGLE-ROTATION PROPELLERS

By John H. Walker and Robert M. Reynolds

Ames Aeronautical Laboratory
Moffett Field, Calif.

CLASSIFICATION CANCELLED

Authority NACA Rev. sheet + Date Eff. 1/20
5-14-56
LN-1A-1
By N.B. - E-20-56 See

LIBRARY COPY

OCT 10 1954

LANGLEY AERONAUTICAL LABORATORY
LEAFLET NACA
LANGLEY FIELD, VIRGINIA

This material contains information affecting the National Defense of the United States within the meaning of the espionage laws, Title 18, U.S.C., Secs. 793 and 794, the transmission or revelation of which in any manner to an unauthorized person is prohibited by law.

NATIONAL ADVISORY COMMITTEE
FOR AERONAUTICS

WASHINGTON

October 8, 1954

~~CONFIDENTIAL~~



NATIONAL ADVISORY COMMITTEE FOR AERONAUTICS

RESEARCH MEMORANDUM

INVESTIGATION OF THE NACA 4-(5)(05)-037 SIX- AND EIGHT-BLADE,
DUAL-ROTATION PROPELLERS AT POSITIVE AND NEGATIVE THRUST
AT MACH NUMBERS UP TO 0.90, INCLUDING SOME AERODYNAMIC
CHARACTERISTICS OF THE NACA 4-(5)(05)-041 TWO- AND
FOUR-BLADE, SINGLE-ROTATION PROPELLERS

By John H. Walker and Robert M. Reynolds

SUMMARY

An investigation has been made to determine the aerodynamic characteristics of the NACA 4-(5)(05)-037 six- and eight-blade, dual-rotation propellers when operating at positive and negative thrust at Mach numbers up to 0.90 and when operating at near static conditions. The dual-rotation propellers were operated in combination with a long spinner and at blade angles from -20° to 70° . The aerodynamic characteristics of the six-blade propeller when operating at positive thrust with an NACA 1-series spinner were also determined through a Mach number range from 0.60 to 0.90 for a blade angle of 65° . Results of limited tests made to determine the aerodynamic characteristics of the NACA 4-(5)(05)-041 two- and four-blade, single-rotation propellers when operating at negative thrust are also included for comparison. All tests were made at an angle of attack of 0° , and the majority of tests were conducted at a Reynolds number of 1.0 million per foot.

The performance of the dual-rotation propellers was not adversely affected by compressibility up to a Mach number of about 0.65. At this Mach number, and for a blade angle of 65° , the six- and eight-blade propellers had maximum efficiencies of about 85 percent.

Increasing the total solidity by increasing the number of blades from six to eight resulted in a nearly proportional increase in power absorption with an accompanying decrease in maximum efficiency of about 2 percent.

The efficiencies of the propeller in combination with an NACA 1-series spinner were lower, by about 2 percent, than those of the propeller with a longer spinner.

There were no significant compressibility effects on the negative-thrust characteristics of the dual-rotation propellers up to a Mach number of 0.60.

The thrust per horsepower for operation of the six- and eight-blade propellers at near static conditions varied with power disc loading as predicted by actuator-disc theory for static conditions, but the values measured were lower by about 28 and 26 percent, respectively. For the design power disc loading of about 21 horsepower per square foot, the dual propellers produced about three pounds of thrust per horsepower at near static conditions.

INTRODUCTION

The high power available from modern gas-turbine engines has indicated a need for additional research on propellers. This is especially true in regard to dual-rotation propellers since the advantages of these propellers, over the single-rotation type capable of absorbing equal power, are smaller diameter, higher efficiency, absence of reaction torque, and less noise. However, the increased weight and complexity of the dual-rotation propeller are disadvantages that must be considered. Whereas much research has been conducted on single-rotation propellers during the past five years, such as reported in references 1 to 7, only limited research on dual-rotation propellers has been carried out during this period. One investigation of a dual-rotation propeller (ref. 8) has been carried to high subsonic speeds but the propeller used for those tests was designed for an advance-diameter ratio of 7.15 which is considerably higher than the advance-diameter ratios being considered for current designs.

In addition to the need for more data in the positive-thrust range, there has been an increase in the demand for data on propeller performance characteristics in the negative-thrust range, because of the desire to utilize the negative thrust for landing and maneuvering and because of the need to calculate the extremely large drag of turbine-engine-propeller combinations which results in the event of engine failure. To alleviate the large drag forces which result when the propeller is driving an engine requires automatic propeller controls to either declutch the propeller from the engine or feather the propeller. The design of these controls requires detailed information on the thrust-torque characteristics of the propeller throughout a wide range of propeller blade angles and airspeeds. There are available a number of reports relating to the performance of propellers operating at negative thrust. However, most of the data, such as those presented in reference 9 for propellers of older design and in references 4 and 5 for propellers of more current design, were obtained at low speeds. The negative-thrust characteristics of a three-blade propeller of current design operating at Mach numbers up to 0.80 are presented in reference 6.

Inasmuch as one of the greatest advantages of the turbine-propeller combination over other means of airplane propulsion is the reduction in take-off run resulting from the large thrust available at low speed, there

is a need for additional data pertaining to the thrust-torque relationship for propellers at static and near static conditions. The most recent data concerning this condition for single-rotation propellers are reported in references 4, 5, 6, and 10; and results of previous investigations of numerous single- and dual-rotation propellers are correlated in reference 11.

An investigation has been made in the Ames 12-foot pressure wind tunnel to provide additional data useful in the design and development of modern high-speed propellers. Presented herein are the force-test results for the NACA 4-(5)(05)-037 six- and eight-blade, dual-rotation propellers when producing positive and negative thrust at Mach numbers to 0.90 and when producing positive thrust at near static conditions. Comparisons have been made to show the effects of total solidity, of spinner shape, and of blade-angle differential between the front and rear units of the dual propeller. Results of limited tests of the NACA 4-(5)(05)-041 two- and four-blade, single-rotation propellers are included for purposes of comparison. All tests were made at an angle of attack of 0° and most of the data were obtained at a Reynolds number of 1.0 million per foot.

NOTATION

- a speed of sound
- B number of blades
- b blade width
- C_P power coefficient, $\frac{P}{\rho n^3 D^5}$
- C_P' power coefficient corrected for activity factor, integrated lift coefficient, and thickness ratio (ref. 11)
- C_T thrust coefficient, $\frac{T}{\rho n^2 D^4}$
- c_{ld} blade section design lift coefficient
- D propeller diameter
- HP horsepower
- h maximum thickness of blade section
- J advance-diameter ratio, $\frac{V_o}{nD}$
- M Mach number, $\frac{V}{a}$

M_t	tip Mach number, $M\sqrt{1+(\pi/J)^2}$
n	propeller rotational speed
P	power
R	propeller tip radius
Rn	Reynolds number per foot, $\frac{\rho V}{\mu}$
r	blade section radius
S	propeller disc area
T	thrust
T_c	thrust coefficient, $\frac{T}{\rho V^2 D^2}$
V	velocity
V_o	equivalent free-air velocity
β	propeller blade angle at 0.75 R
β_d	design propeller section blade angle
$\Delta\beta$	difference in blade angle between the front and rear components of the dual-rotation propeller, $\beta_F - \beta_R$
η	efficiency, $\frac{C_T}{C_P} J$
μ	air viscosity
ρ	air density

Subscripts

F	front component of dual-rotation propeller
R	rear component of dual-rotation propeller

MODEL AND APPARATUS

1000-Horsepower Propeller Dynamometer

The 1000-horsepower propeller dynamometer used for this investigation in the Ames 12-foot pressure wind tunnel is described in reference 4. The dynamometer was modified for the testing of dual-rotation propellers by the installation of a gear box within the dynamometer housing and a torquemeter on each of two concentric propeller drive shafts. The rotational speeds of the front and rear propellers were the same. The torqueometers were mounted in such a manner that mechanical losses in the gear box were not present in the measured torque. The only frictional losses included in the measured torque were from a roller bearing and a neoprene pressure seal between the propeller shafts, and from the carbon-ring pressure seal described in reference 4. These losses were small and were accounted for by calibrations. A photograph of the dynamometer with the six-blade, dual-rotation propeller is shown in figure 1.

Propellers

The NACA 4-(5)(05)-037 six- and eight-blade, dual-rotation propellers and the NACA 4-(5)(05)-041 four-blade, single-rotation propeller (described in ref. 4) were models of propellers designed for the following full-scale conditions:

Altitude, ft	35,000
Mach number	0.80
Horsepower	5,600
Advance-diameter ratio	
Six- and eight-blade dual	4.2
Four-blade single	3.7
Diameter, ft	
Six-blade dual	19
Eight-blade dual	18
Four-blade single	23
Total activity factor, $\left[\frac{100,000}{16} B \int_{0.2}^{1.0} \left(\frac{b}{D} \right) \left(\frac{r}{R} \right)^3 d\left(\frac{r}{R} \right) \right]$	
Six-blade dual	694
Eight-blade dual	925
Four-blade single	514

The NACA 16-series airfoil section was used for the blade sections. Blade width ratio, thickness ratio, section design lift coefficient, and twist distribution are shown by the blade-form curves in figure 2. It may

be noted that for this investigation, the four-blade propeller described in reference 4 was modified inboard of $r/R = 0.25$.

Except for total solidity, the NACA 4-(5)(05)-037 six-blade, dual-rotation propeller was identical to the eight-blade propeller and the NACA 4-(5)(05)-041 two-blade, single-rotation propeller was identical to the four-blade propeller.

Spinners

Most of the tests of the dual-rotation propellers were made with a spinner having a maximum diameter of 6.51 inches and a length of 22.71 inches. The forward portion (9.77 inches) was contoured to the NACA 1-series profile. This long spinner was used so the inboard blade sections would operate in a nearly uniform air stream. A photograph and details of this spinner, designated as spinner A, are shown in figures 3(a) and 4(a).

Limited tests were made of the six-blade, dual-rotation propeller with an NACA 1-46.5-085 spinner (ref. 12), having a maximum diameter of 7.23 inches and a length of 13.22 inches. This spinner is designated as spinner B and is described in figures 3(b) and 4(b).

The NACA 1-46.5-047 spinner (ref. 13), having a maximum diameter of 6.51 inches and a length of 6.58 inches, was used with the single-rotation propellers. A photograph and details of this spinner, designated as spinner C, are shown in figures 3(c) and 4(c).

The platform junctures used with each propeller-spinner combination are also shown in figures 3 and 4.

Instrumentation and Calibrations

The instrumentation of the dynamometer for the single-rotation propeller tests was identical to that described in reference 4. The dual-rotation dynamometer instrumentation differed only in that there were two torquemeters. They were similar in design and operation to the torque meter used for the single-rotation dynamometer, each having half the capacity and twice the sensitivity of the single-rotation torque meter. The torque measured by each torque meter was indicated by a manual balancing potentiometer. A description of the methods used in calibrating the thrust gages and torque meters, and a discussion of typical calibration results are presented in reference 4.

TEST CONDITIONS AND REDUCTION OF DATA

Preliminary tests were made with the six-blade dual-rotation propeller to determine the rear blade angle setting (β_R) that would cause the rear component of the propeller to absorb the same power as the front component near the advance-diameter ratio for maximum efficiency. The optimum blade-angle difference ($\Delta\beta = \text{optimum}$) determined from these tests is shown as a function of the front blade angle (β_F) in figure 5. Subsequently, the thrust, torque, and rotational speed were measured for the six- and eight-blade, dual-rotation propellers for both the optimum blade-angle settings (fig. 5) and the design blade-angle setting ($\Delta\beta = 0.8^\circ$) for the various values of front blade angle and Mach number shown in table I. Also shown in table I are the conditions for the limited tests of the two- and four-blade, single-rotation propellers.

Propeller thrust as used herein is the algebraic difference between the longitudinal force produced by the propeller-spinner combination and the longitudinal force produced by the spinner alone at the same air velocity and density. The method used in determining the propeller thrust is discussed in detail in reference 4.

The total torque required for operation of the dual-rotation propeller was ascertained by adding the torque of the front and rear components. Torque was determined for each component by the method described for the single-rotation propeller in reference 4.

The Mach number used in this report is the average Mach number over the disc area determined by the velocity surveys reported in reference 4. The air-stream velocity (and, consequently, propeller advance-diameter ratio and efficiency) was corrected for wind-tunnel-wall constraint on the propeller slipstream by the method of reference 14. Experimental data have shown good agreement with the correction presented in figure 6 (see refs. 4 and 6). The data included herein are for advance-diameter ratios at which the thrust-coefficient parameter ($T_c/1-M^2$) was greater than -0.55.

Analyses of the accuracy of the separate measurements of thrust, torque, and air-stream velocity indicate that errors in the propeller efficiencies reported herein are probably less than 2 percent.

RESULTS AND DISCUSSION

Most of the results of this investigation are presented graphically in figures 7 through 34. An index of these figures is presented in table II and gives the propeller configuration and the range of variables for each figure. Inasmuch as it did not appear advantageous to plot the

individual power coefficients for the front and rear propeller units at conditions of negative and near static thrust, these data have been tabulated in tables III to V.

Positive Thrust

Effects of Mach number.- The effects of Mach number on the aerodynamic characteristics of the propellers are shown in figures 7 through 17. The over-all propeller characteristics are presented in figures 7 through 12, and the power coefficients for the front and rear components of the dual-rotation propellers are shown in figures 13 through 17.

The effects of Mach number on maximum efficiency are shown in figure 18. As previously shown in other investigations, propeller efficiency losses due to compressibility effects were delayed to higher Mach numbers by increasing blade angle. The highest Mach number at which the dual-rotation propellers with spinner A operated without marked compressibility losses was about 0.65 for a blade angle of 65°, at which condition the propeller efficiency was about 85 percent. Maximum efficiency of the six-blade propeller varied from 87 percent at a Mach number of 0.40 to 61 percent at a Mach number of 0.84.

As shown in figure 18(f), the maximum efficiency of the two-blade propeller compares favorably with the results from reference 4 for the four-blade propeller at a blade angle of 60°.

The variation of maximum efficiency with advance-diameter ratio for the dual-rotation propellers is shown in figure 19. Figure 20 presents the variation of maximum efficiency with tip Mach number. These data, in conjunction with figure 18, indicate that at Mach numbers above 0.80, higher efficiencies could probably be obtained by operation of the propellers at lower blade angles and lower advance-diameter ratios.

Comparison of the characteristics of the six- and eight-blade, dual-rotation propellers.- As shown in figure 21, the basic characteristics of the six- and eight-blade propellers are in good agreement when compared on the basis of equal total activity factor. At all except the highest Mach numbers, the maximum efficiency of the eight-blade propeller was about 2 percent below that of the six-blade propeller, as shown in figures 18 and 19.

In the following table the full-scale characteristics of the six- and eight-blade, dual-rotation propellers at the design Mach number (0.80) and altitude (35,000 feet), calculated from the data in figures 7 and 8, are compared with the design characteristics calculated by the method of reference 15 with an assumed loss in efficiency of 8 percent due to compressibility effects.

Characteristics	Condition for B = 6				Condition for B = 8			
	Design	A	B	C	Design	A	B	C
HP	5600	5600	5600	6240	5600	5600	5600	8100
η	0.80	0.64	0.65	0.65	0.80	0.62	0.62	0.65
J	4.20	4.20	3.94	3.87	4.20	4.20	4.10	3.80
β_F	63	67	65	65	63	66	65	65
C_P	1.81	1.81	1.50	1.58	2.02	2.02	1.88	2.17
T	3160	2530	2570	2860	3160	2450	2450	3700

Condition A shows that for operation at the design power and advance-diameter ratio, blade angles higher than the design value would be required. By reducing the advance-diameter ratio and blade angles, the efficiency would be increased slightly as indicated under condition B for the design horsepower. To enable the propellers to operate with maximum efficiency at the design Mach number would require a further reduction in advance-diameter ratio and an increase in power as shown under Condition C. At the design Mach number of 0.80, there was no operating condition where the efficiency approached the calculated value of 0.80. Subsequent calculations for the eight-blade propeller using the method of reference 16 and the airfoil section data from reference 17 indicated a still higher efficiency of 86 percent. The calculated efficiencies for the design condition are unrealistically high primarily because losses due to compressibility occurred at a considerably lower Mach number than the calculations indicated. Figure 20 shows that at the design tip Mach number of 1.0 and a blade angle of 65° , the maximum efficiency had decreased more than 20 percent from its low-speed value whereas the anticipated decrease was about 8 percent.

In consideration of the effects of compressibility with regard to the spinner, it would be expected that with the shorter spinner (spinner B), the local velocities on the inner portion of the propeller blades would be considerably higher than the free-stream Mach number and, as a result, it would be anticipated that calculations based on free-stream conditions would overestimate the Mach number for the onset of compressibility effects. With the long spinner (spinner A), however, the local velocity at the blade shank is calculated to be only about 1 or 2 percent higher than the free-stream velocity, and it should be possible to neglect this velocity increment in the propeller performance analysis without introducing large losses. While the effect of the propeller inflow on the drag of the long spinner would be expected to be of appreciable magnitude, it would not be anticipated that this contribution would be particularly dependent on Mach number below a Mach number of 0.85 or 0.90.

In regard to the airstream velocity it may be stated that the velocity surveys (ref. 4) which were used to establish the free-stream Mach number

were carried out in such a manner that it is difficult to conceive them to be in error by a significant amount. However, there is no way to evaluate accurately the effect of the propeller slipstream on the flow field induced by the dynamometer structure. It is felt that this effect of slipstream was small, as indicated by the data in reference 4 which show no large effect of Mach number on the velocity induced by the dynamometer.

A point that should be made with regard to the calculated performance is that at the design condition, the sections of the propeller outboard of 0.70 radius were operating at Mach numbers between 0.90 and 1.0. The section data used in the performance calculations are of doubtful accuracy in this Mach number range, and recent section data presented in reference 18 have shown effects of camber contrary to the results given in reference 17.

In summary of this discussion of the propeller efficiency at the design condition, it can only be stated that losses due to compressibility effects began to rise at a lower Mach number than the calculated value. Aside from questioning the validity of the section data used in the performance calculations, no other reason for this discrepancy is known.

Comparison of the propeller characteristics for the optimum $\Delta\beta$ and a $\Delta\beta$ of 0.8° . - As shown in figure 22 for the six-blade dual-rotation propeller, and as would be anticipated, the effect of increasing the blade angle of the rear component (changing from optimum $\Delta\beta$ to $\Delta\beta = 0.8^\circ$) was to increase the power coefficient for the rear component at a given advance-diameter ratio, with a corresponding increase in thrust coefficient. Moreover, it is shown that there was no significant difference in the power absorbed by the front component with change in the rear blade angle. Figure 22 also shows, for $\beta_F = 65^\circ$ and Mach numbers from 0.60 to 0.80, that the front and rear components absorbed equal power at an advance-diameter ratio near that for maximum efficiency with the optimum $\Delta\beta$ setting. However, the rear blade angle used for the optimum setting with $\beta_F = 70^\circ$ appears to have been somewhat low for Mach numbers above 0.70 (see figs. 7, 13, and 15).

Comparisons of the data in figures 18 and 19 show that for both the six- and eight-blade, dual-rotation propellers, the maximum efficiency obtained with $\Delta\beta = 0.8^\circ$ was generally lower, by about 2 percent, than that with the optimum $\Delta\beta$ setting.

Effects of spinner length and of sealing the gaps at the platform propeller-spinner junctures. - The results of limited tests of the six-blade, dual-rotation propeller using spinner B are presented in figure 10 and summarized in figure 18(e). In general, the efficiency of the propeller with this spinner was about 2 percent lower (figs. 18(e) and 20(c)) than with spinner A. It is believed that this is due to the higher velocities over the inboard propeller-blade sections with the shorter spinner, similar to the results reported in reference 4.

As shown in figure 23, sealing the gaps between the propeller blades and the platform junctures had no significant effect on the propeller characteristics.

Negative Thrust

The effects of Mach number on the characteristics of the propellers when producing negative thrust are shown in figures 24 through 29 and in tables III and IV. Negative-thrust characteristics are shown, for Mach numbers above 0.15, on plots with tangent coordinates which enable coverage of the full range of test results.

Similar to results reported in reference 6, it can be shown from the data presented in figure 30 that there was practically no effect of compressibility on the negative-thrust and torque characteristics of the dual-rotation propeller for Mach numbers up to 0.60.

The basic negative-thrust characteristics of the six- and eight-blade propellers are in good agreement when compared on the basis of equal total activity factor. This is shown for Mach numbers of 0.15, 0.60, and 0.80 in figure 30. Also, comparison of the data presented in figure 31, again on the basis of equal activity factor, indicates good agreement between the negative-thrust characteristics of the two- and four-blade, single-rotation propellers. It can be shown that the negative-thrust data for the single-rotation propellers, after correction for activity factor, compare favorably with those for the dual-rotation propellers at a Mach number of 0.15 (data in fig. 31 compared with those in figs. 30(a) and (b)), but do not compare well for the higher Mach numbers (comparing corresponding data of figs. 28 and 24, for example).

Near Static Thrust

The characteristics of the six- and eight-blade propellers at low forward speeds are presented in figure 32 and table V. The velocity of the air in the test section for these tests was produced by the model propeller itself and thus varied with propeller rotational speed and blade angle as shown in figure 32.

The abrupt decrease in thrust coefficient and increase in power coefficient at values of nD below 60 (fig. 32) are similar to results reported in reference 6 for a three-blade propeller and are believed to be due to the effects of Reynolds number on the blade section characteristics.

The data in figure 32 were used to determine envelope curves for the variation of thrust per horsepower with power disc loading for the six- and

eight-blade, dual-rotation propellers. These are shown in figure 33, together with similar experimental results for the four-blade propeller (computed from fig. 8 of ref. 4) and the theoretical ideal curve for the static condition computed by the method of reference 19. For all power disc loadings, thrust per horsepower increased with increasing number of propeller blades. For the design power disc loading, approximately 21 horsepower per square foot, the dual propellers produced about 3 pounds of thrust per horsepower at near static conditions. The experimental thrusts per horsepower for the six- and eight-blade propellers were approximately 72 and 74 percent, respectively, of the theoretical ideal values. That the thrust-per-horsepower values for the dual-rotation propellers are higher than those reported for single-rotation propellers in references 4, 5, and 6 is probably due to lower rotational losses for the dual-rotation propellers. The extrapolation explained in the following paragraph indicates that the experimental thrust per horsepower would be about 20 percent higher if the data were for a true static condition.

The variations of thrust per horsepower with power coefficient for the six-blade dual-rotation propeller at near static conditions and at zero velocity (obtained by extrapolation) are compared in figure 34 with correlated static data (from ref. 11) for five other six-blade dual-rotation propellers having NACA 16-series sections. The values shown for the near static condition were calculated using the data in figure 32(a), and the values given for the zero-velocity condition were obtained by a straight-line extrapolation of the thrust and power coefficients as a function of test-section velocity using the data from figures 7(a) and 32(a). The power coefficient used in this figure was corrected for activity factor, integrated lift coefficient, and thickness ratio in accordance with the method of correlation of reference 11. These results show that the effect of small forward velocities on the thrust per horsepower was substantial, if the extrapolation procedure is valid. The agreement between the extrapolated results for zero velocity and the results presented in reference 11 is only fair.

CONCLUDING REMARKS

The following remarks may be made regarding the results of the subject investigation:

The highest Mach number at which the six- and eight-blade, dual-rotation propellers operated without marked compressibility losses was about 0.65 for a blade angle of 65° , at which condition the efficiency of both propellers was 85 percent. The effects of compressibility on maximum efficiency were similar to those reported in previous investigations, indicating that for Mach numbers above some value (for these propellers, about 0.80) higher efficiencies would be obtained by operation of the propellers at lower advance-diameter ratios and lower blade angles.

[REDACTED]

Increasing total solidity by increasing the number of blades from six to eight resulted in a nearly proportional increase in power absorption with an accompanying decrease in maximum efficiency of about 2 percent.

Lower efficiencies, by about 2 percent, were obtained for the propeller in combination with an NACA 1-series spinner as compared with those obtained for the propeller with the longer spinner. This result is attributable to the effects of the nonuniform flow field of the 1-series spinner and is similar to results reported for the NACA 4-(5)(05)-041 four-blade, single-rotation propeller with 1-series and extended cylindrical spinners.

There were no significant effects of compressibility on the negative-thrust characteristics of the dual-rotation propellers up to a Mach number of 0.60. When compared on the basis of equal total activity factor, the negative-thrust characteristics of the six- and eight-blade propellers were in good agreement.

The thrust per horsepower of the six- and eight-blade propellers at near static conditions varied with power disc loading as predicted by actuator-disc theory for the static condition, but the measured values were lower by about 28 and 26 percent, respectively. For the design power disc loading, approximately 21 horsepower per square foot, the dual propellers produced about three pounds of thrust per horsepower at near static conditions.

Ames Aeronautical Laboratory
National Advisory Committee for Aeronautics
Moffett Field, Calif., July 13, 1954

REFERENCES

1. Carmel, Melvin M., Morgan, Francis G., Jr., and Coppolino, Domenic A.: Effect of Compressibility and Camber as Determined from an Investigation of the NACA 4-(3)(08)-03 and 4-(5)(08)-03 Two-Blade Propellers up to Forward Mach Numbers of 0.925. NACA RM L50D28, 1950.
2. Delano, James B., and Harrison, Daniel E.: Investigation of the NACA 4-(4)(06)-04 Two-Blade Propeller at Forward Mach Numbers to 0.925. NACA RM L9I07, 1949.
3. Delano, James B., and Carmel, Melvin M.: Investigation of the NACA 4-(0)(03)-045 and NACA 4-(0)(08)-045 Two-Blade Propellers at Forward Mach Numbers to 0.925. NACA RM L9L06a, 1950.

[REDACTED]

4. Reynolds, Robert M., Buell, Donald A., and Walker, John H.: Investigation of an NACA 4-(5)(05)-041 Four-Blade Propeller with Several Spinners at Mach Numbers up to 0.90. NACA RM A52I19a, 1952.
5. Demele, Fred A., and Otey, William R.: Investigation of the NACA 1.167-(0)(03)-058 and NACA 1.167-(0)(05)-058 Three-Blade Propellers at Forward Mach Numbers to 0.92 Including Effects of Thrust-Axis Inclination. NACA RM A53F16, 1953.
6. Kenyon, George C., and Reynolds, Robert M.: Investigation of a Three-Blade Propeller in Combination With Two Different Spinners and an NACA D-Type Cowl at Mach Numbers up to 0.80. NACA RM A54B18a, 1954.
7. Evans, Albert John, and Liner, George: A Wind-Tunnel Investigation of the Aerodynamic Characteristics of a Full-Scale Supersonic-Type Three-Blade Propeller at Mach Numbers to 0.96. NACA RM L53F01, 1953.
8. Platt, Robert J., Jr., and Shumaker, Robert A.: Investigation of the NACA 3-(3)(05)-05 Eight-Blade Dual-Rotating Propeller at Forward Mach Numbers to 0.925. NACA RM L50D21, 1950.
9. Gray, W. H., and Gilman, Jean, Jr.: Characteristics of Several Single- and Dual-Rotating Propellers in Negative Thrust. NACA WR L-634, 1945. (Supersedes NACA MR L5C07)
10. Swihart, John M.: Experimental and Calculated Static Characteristics of a Two-Blade NACA 10-(3)(062)-045 Propeller. NACA RM L54A19, 1954.
11. Webb, Dana A., and Willer, Jack E.: Propeller Performance at Zero Forward Speed. WADC TR 52-152, Wright Air Development Center, July 1952.
12. Keith, Arvid L., Jr., Bingham, Gene J., and Rubin, Arnold J.: Effects of Propeller-Shank Geometry and Propeller-Spinner Juncture Configuration on Characteristics of an NACA 1-Series Cowling-Spinner Combination With an Eight-Blade Dual-Rotation Propeller. NACA RM L51F26, 1951.
13. Sammonds, Robert I., and Molk, Ashley J.: Effects of Propeller-Spinner Juncture on the Pressure-Recovery Characteristics of an NACA 1-Series D-Type Cowl in Combination with a Four-Blade Single-Rotation Propeller at Mach Numbers Up to 0.83 and at an Angle of Attack of 0°. NACA RM A52D01a, 1952.
14. Young, A. D.: Note on the Application of the Linear Perturbation Theory To Determine the Effect of Compressibility on the Wind Tunnel Constraint on a Propeller. R.A.E. TN No. Aero. 1539, British A.R.C., 1944.

15. Crigler, John L., and Talkin, Herbert W.: Charts for Determining Propeller Efficiency. NACA WR L-144, 1944. (Formerly NACA ACR L4I29)
16. Gilman, Jean, Jr.: Application of Theodorsen's Propeller Theory to the Calculation of the Performance of Dual-Rotating Propellers. NACA RM L51A17, 1951.
17. Enos, L. H., and Borst, H. V.: Propeller Performance Analysis. Aerodynamic Characteristics, NACA 16 Series Airfoils. Pt. II. Rep. No. C-2000, Curtiss-Wright Corp., Propeller Div. (Caldwell, N. J.), 1948.
18. Stivers, Louis S., Jr.: Effects of Subsonic Mach Number on the Forces and Pressure Distributions on Four NACA 64A-Series Airfoil Sections at Angles of Attack as High as 28° . NACA TN 3162, 1954.
19. Gilman, Jean, Jr.: Analytical Study of Static and Low-Speed Performance of Thin Propellers Using Two-Speed Gear Ratios to Obtain Optimum Rotational Speeds. NACA RM L52I09, 1952.

TABLE I.-- BLADE ANGLES AND MACH NUMBERS FOR TESTS OF VARIOUS PROPELLER CONFIGURATIONS

Mach number	Propeller blade angle, β or β_F , deg														
	70	65	60	55	50	40	30	25	20,15	10	5	0	-5,-10,-15	-20	
.20	--	--	--	--	--	--	--	--	a	ab	a	--	--	--	--
.15	--	--	--	--	--	--	--	afg	abfg	afg	afg	abfg	a	ab	
.20	--	--	--	--	--	ab	a	--	--	--	--	--	--	--	
.40	--	b	ab	ab	abf	ab	a	--	--	--	--	--	--	--	
.50	--	f	--	f	--	--	--	--	--	--	--	--	--	--	
.60	--	¹ abcde	abf	ab	abf	--	--	--	--	--	--	--	--	--	
.70	ace	¹ abcde	abf	ab	abf	--	--	--	--	--	--	--	--	--	
.75	ace	abcde	ab	ab	ab	--	--	--	--	--	--	--	--	--	
.80	ace	¹ abcde	abf	b	--	--	--	--	--	--	--	--	--	--	
.84	ace	abcde	ab	--	--	--	--	--	--	--	--	--	--	--	
.90	e	cde	--	--	--	--	--	--	--	--	--	--	--	--	

Configuration	Propeller	Spinner	$\Delta\beta$, deg	Thrust
a	6-blade dual-rotation	A	optimum	positive and negative
b	8-blade dual-rotation	A	optimum	positive and negative
c	6-blade dual-rotation	A	0.8	positive and negative
d	6-blade dual-rotation	B	0.8	positive thrust only
e	8-blade dual-rotation	A	0.8	positive and negative
f	2-blade single-rotation	C	--	positive and negative
g	4-blade single-rotation	C	--	negative thrust only

¹Repeat runs with the platform gaps sealed, configuration a only.



TABLE II.- INDEX OF DATA FIGURES

Figure number	Plot	Propeller	$\Delta\beta$, deg	Number of blades, B	Mach number, M	Front blade angle, β_F , deg	Spinner	Reynolds number per ft, $Rn \times 10^{-6}$
Positive thrust								
7	C_T, C_P, η, M_t vs. J	Dual	Optimum	6	0.15 to 0.84	15 to 70	A	1.0
8		Dual	Optimum	8	0.15 to 0.84	15 to 65	A	1.0
9		Dual	0.8	6	0.60 to 0.90	65, 70	A	1.0
10		Dual	0.8	6	0.60 to 0.90	65	B	1.0
11		Dual	0.8	8	0.60 to 0.90	65, 70	A	1.0
12		Single	---	2	0.50 to 0.80	60	C	1.5
13	C_{P_F}, C_{P_R} vs. J	Dual	Optimum	6	0.15 to 0.84	15 to 70	A	1.0
14		Dual	Optimum	8	0.15 to 0.84	15 to 65	A	1.0
15		Dual	0.8	6	0.60 to 0.90	65, 70	A	1.0
16		Dual	0.8	6	0.60 to 0.90	65	B	1.0
17		Dual	0.8	8	0.60 to 0.90	65, 70	A	1.0
18	η_{max} vs. M	Dual	Optimum	6, 8	0.15 to 0.84	15 to 70	A	1.0
18		Dual	0.8	6, 8	0.60 to 0.90	65, 70	A	1.0
18		Dual	0.8	6	0.60 to 0.90	65	B	1.0
18		Single	---	2	0.40 to 0.70	50, 60	C	1.5
19	η_{max} vs. J	Dual	Optimum	6, 8	0.15 to 0.84	15 to 70	A	1.0
19		Dual	0.8	6, 8	0.60 to 0.90	65, 70	A	1.0
20	η_{max} vs. M_t	Dual	Optimum	6, 8	----	15 to 70	A	1.0
20		Dual	0.8	6, 8	----	65, 70	A	1.0
20		Dual	0.8	6	----	65	B	1.0
a21	C_T, C_P, η vs. J	Dual	Optimum	6, 8	0.40 to 0.80	65	A	1.0
b22		Dual	0.8	6	0.60 to 0.80	65, 70	A	1.0
c23		Dual	Optimum	6	0.60 to 0.80	65	A	1.0
Negative thrust								
24	C_T, C_P vs. J	Dual	Optimum	6	0.15 to 0.84	-20 to 70	A	1.0
25		Dual	Optimum	8	0.15 to 0.84	-20 to 65	A	1.0
26		Dual	0.8	6	0.60 to 0.90	65, 70	A	1.0
27		Dual	0.8	8	0.60 to 0.90	65, 70	A	1.0
28		Single	---	2	0.15	0 to 25	C	1.0
28		Single	---	2	0.40 to 0.80	50, 60	C	1.5
29		Single	---	4	0.15	0 to 25	C	1.0
d30	C_T, C_P vs. β_F	Dual	Optimum	6, 8	0.15 to 0.84	-20 to 70	A	1.0
31		Single	---	2	0.15	0 to 25	C	1.0
31		Single	---	4	0.15	0 to 25	C	1.0
Near static thrust								
32	C_T, C_P, V vs. nD	Dual	Optimum	6	≈ 0	10 to 25	A	---
32		Dual	Optimum	8	≈ 0	15, 20	A	---
33	T/HP vs. HP/S	Dual	Optimum	6, 8	≈ 0	---	A	---
34	T/HP vs. C_P'	Dual	Optimum	6, 8	≈ 0	---	A	---

^aComparison of the 6- and 8-blade data for $\Delta\beta$ = optimum.^bComparison of the 6-blade data for $\Delta\beta$ = optimum and $\Delta\beta$ = 0.8°.^cEffect of sealing the juncture gap.^dData for B = 8 shown for M = 0.15, 0.60, and 0.80.

TABLE III.- NEGATIVE-THRUST CHARACTERISTICS OF THE NACA 4-(5)(05)-037
 SIX- AND EIGHT-BLADE, DUAL-ROTATION PROPELLERS, $\Delta\beta = \text{OPTIMUM}$
 (a) $B = 6$

M	β_F , deg	J	C_T	C_{P_F}	C_{P_R}	M	β_F , deg	J	C_T	C_{P_F}	C_{P_R}	M	β_F , deg	J	C_T	C_{P_F}	C_{P_R}
0.15	-20	1.43 1.48 1.55 1.61 1.70 1.79 1.80 1.88 1.98 2.09 2.16 2.25 2.34 2.43 2.52 2.72 2.94 3.13 3.42 3.70 4.09 4.48 4.98 5.36 7.03	-0.769 -0.834 -0.919 -0.973 -1.044 -1.132 -1.224 -1.299 -1.387 -1.463 -1.537 -1.578 -1.638 -1.686 -0.047 -0.211 -0.280 -0.328 -0.395 -0.463 -0.531 -0.600 -0.667 -0.734 -0.788 -0.843 -0.898 -0.953 -1.008 -1.063 -1.118 -1.173 -1.228 -1.283 -1.338 -1.393 -1.448 -1.498 -1.547 -1.596 -1.653 -1.708 -1.753 -1.798 -1.845 -1.890 -1.935 -1.980 -2.025 -2.070 -2.115 -2.160 -2.205 -2.250 -2.295 -2.340 -2.385 -2.430 -2.475 -2.520 -2.565 -2.610 -2.655 -2.700 -2.745 -2.780 -2.825 -2.860 -2.905 -2.940 -2.975 -3.010 -3.045 -3.080 -3.115 -3.150 -3.185 -3.220 -3.255 -3.290 -3.325 -3.360 -3.395 -3.430 -3.465 -3.500 -3.535 -3.570 -3.605 -3.640 -3.675 -3.710 -3.745 -3.780 -3.815 -3.850 -3.885 -3.920 -3.955 -3.990 -4.025 -4.060 -4.095 -4.130 -4.165 -4.200 -4.235 -4.270 -4.305 -4.340 -4.375 -4.410 -4.445 -4.480 -4.515 -4.550 -4.585 -4.620 -4.655 -4.690 -4.725 -4.760 -4.795 -4.830 -4.865 -4.900 -4.935 -4.970 -5.005 -5.040 -5.075 -5.110 -5.145 -5.180 -5.215 -5.250 -5.285 -5.320 -5.355 -5.390 -5.425 -5.460 -5.495 -5.530 -5.565 -5.600 -5.635 -5.670 -5.705 -5.740 -5.775 -5.810 -5.845 -5.880 -5.915 -5.950 -5.985 -6.020 -6.055 -6.090 -6.125 -6.160 -6.195 -6.230 -6.265 -6.300 -6.335 -6.370 -6.405 -6.440 -6.475 -6.510 -6.545 -6.580 -6.615 -6.650 -6.685 -6.720 -6.755 -6.790 -6.825 -6.860 -6.895 -6.930 -6.965 -7.000 -7.035 -7.070 -7.105 -7.140 -7.175 -7.210 -7.245 -7.280 -7.315 -7.350 -7.385 -7.420 -7.455 -7.490 -7.525 -7.560 -7.595 -7.630 -7.665 -7.700 -7.735 -7.770 -7.805 -7.840 -7.875 -7.910 -7.945 -7.980 -8.015 -8.050 -8.085 -8.120 -8.155 -8.190 -8.225 -8.260 -8.295 -8.330 -8.365 -8.400 -8.435 -8.470 -8.505 -8.540 -8.575 -8.610 -8.645 -8.680 -8.715 -8.750 -8.785 -8.820 -8.855 -8.890 -8.925 -8.960 -8.995 -9.030 -9.065 -9.100 -9.135 -9.170 -9.205 -9.240 -9.275 -9.310 -9.345 -9.380 -9.415 -9.450 -9.485 -9.520 -9.555 -9.590 -9.625 -9.660 -9.695 -9.730 -9.765 -9.800 -9.835 -9.870 -9.905 -9.940 -9.975 -10.010 -10.045 -10.080 -10.115 -10.150 -10.185 -10.220 -10.255 -10.290 -10.325 -10.360 -10.395 -10.430 -10.465 -10.500 -10.535 -10.570 -10.605 -10.640 -10.675 -10.710 -10.745 -10.780 -10.815 -10.850 -10.885 -10.920 -10.955 -10.990 -11.025 -11.060 -11.095 -11.130 -11.165 -11.200 -11.235 -11.270 -11.305 -11.340 -11.375 -11.410 -11.445 -11.480 -11.515 -11.550 -11.585 -11.620 -11.655 -11.690 -11.725 -11.760 -11.795 -11.830 -11.865 -11.900 -11.935 -11.970 -12.005 -12.040 -12.075 -12.110 -12.145 -12.180 -12.215 -12.250 -12.285 -12.320 -12.355 -12.390 -12.425 -12.460 -12.495 -12.530 -12.565 -12.600 -12.635 -12.670 -12.705 -12.740 -12.775 -12.810 -12.845 -12.880 -12.915 -12.950 -12.985 -13.020 -13.055 -13.090 -13.125 -13.160 -13.195 -13.230 -13.265 -13.300 -13.335 -13.370 -13.405 -13.440 -13.475 -13.510 -13.545 -13.580 -13.615 -13.650 -13.685 -13.720 -13.755 -13.790 -13.825 -13.860 -13.895 -13.930 -13.965 -14.000 -14.035 -14.070 -14.105 -14.140 -14.175 -14.210 -14.245 -14.280 -14.315 -14.350 -14.385 -14.420 -14.455 -14.490 -14.525 -14.560 -14.595 -14.630 -14.665 -14.700 -14.735 -14.770 -14.805 -14.840 -14.875 -14.910 -14.945 -14.980 -15.015 -15.050 -15.085 -15.120 -15.155 -15.190 -15.225 -15.260 -15.295 -15.330 -15.365 -15.400 -15.435 -15.470 -15.505 -15.540 -15.575 -15.610 -15.645 -15.680 -15.715 -15.750 -15.785 -15.820 -15.855 -15.890 -15.925 -15.960 -15.995 -16.030 -16.065 -16.100 -16.135 -16.170 -16.205 -16.240 -16.275 -16.310 -16.345 -16.380 -16.415 -16.450 -16.485 -16.520 -16.555 -16.590 -16.625 -16.660 -16.695 -16.730 -16.765 -16.800 -16.835 -16.870 -16.905 -16.940 -16.975 -17.010 -17.045 -17.080 -17.115 -17.150 -17.185 -17.220 -17.255 -17.290 -17.325 -17.360 -17.395 -17.430 -17.465 -17.500 -17.535 -17.570 -17.605 -17.640 -17.675 -17.710 -17.745 -17.780 -17.815 -17.850 -17.885 -17.920 -17.955 -17.990 -18.025 -18.060 -18.095 -18.130 -18.165 -18.200 -18.235 -18.270 -18.305 -18.340 -18.375 -18.410 -18.445 -18.480 -18.515 -18.550 -18.585 -18.620 -18.655 -18.690 -18.725 -18.760 -18.795 -18.830 -18.865 -18.900 -18.935 -18.970 -19.005 -19.040 -19.075 -19.110 -19.145 -19.180 -19.215 -19.250 -19.285 -19.320 -19.355 -19.390 -19.425 -19.460 -19.495 -19.530 -19.565 -19.600 -19.635 -19.670 -19.705 -19.740 -19.775 -19.810 -19.845 -19.880 -19.915 -19.950 -19.985 -20.020 -20.055 -20.090 -20.125 -20.160 -20.195 -20.230 -20.265 -20.300 -20.335 -20.370 -20.405 -20.440 -20.475 -20.510 -20.545 -20.580 -20.615 -20.650 -20.685 -20.720 -20.755 -20.790 -20.825 -20.860 -20.895 -20.930 -20.965 -21.000 -21.035 -21.070 -21.105 -21.140 -21.175 -21.210 -21.245 -21.280 -21.315 -21.350 -21.385 -21.420 -21.455 -21.490 -21.525 -21.560 -21.595 -21.630 -21.665 -21.700 -21.735 -21.770 -21.805 -21.840 -21.875 -21.910 -21.945 -21.980 -22.015 -22.050 -22.085 -22.120 -22.155 -22.190 -22.225 -22.260 -22.295 -22.330 -22.365 -22.400 -22.435 -22.470 -22.505 -22.540 -22.575 -22.610 -22.645 -22.680 -22.715 -22.750 -22.785 -22.820 -22.855 -22.890 -22.925 -22.960 -22.995 -23.030 -23.065 -23.100 -23.135 -23.170 -23.205 -23.240 -23.275 -23.310 -23.345 -23.380 -23.415 -23.450 -23.485 -23.520 -23.555 -23.590 -23.625 -23.660 -23.695 -23.730 -23.765 -23.800 -23.835 -23.870 -23.905 -23.940 -23.975 -24.010 -24.045 -24.080 -24.115 -24.150 -24.185 -24.220 -24.255 -24.290 -24.325 -24.360 -24.395 -24.430 -24.465 -24.500 -24.535 -24.570 -24.605 -24.640 -24.675 -24.710 -24.745 -24.780 -24.815 -24.850 -24.885 -24.920 -24.955 -25.000 -25.035 -25.070 -25.105 -25.140 -25.175 -25.210 -25.245 -25.280 -25.315 -25.350 -25.385 -25.420 -25.455 -25.490 -25.525 -25.560 -25.595 -25.630 -25.665 -25.700 -25.735 -25.770 -25.805 -25.840 -25.875 -25.910 -25.945 -25.980 -26.015 -26.050 -26.085 -26.120 -26.155 -26.190 -26.225 -26.260 -26.295 -26.330 -26.365 -26.400 -26.435 -26.470 -26.505 -26.540 -26.575 -26.610 -26.645 -26.680 -26.715 -26.750 -26.785 -26.820 -26.855 -26.890 -26.925 -26.960 -27.000 -27.035 -27.070 -27.105 -27.140 -27.175 -27.210 -27.245 -27.280 -27.315 -27.350 -27.385 -27.420 -27.455 -27.490 -27.525 -27.560 -27.595 -27.630 -27.665 -27.700 -27.735 -27.770 -27.805 -27.840 -27.875 -27.910 -27.945 -27.980 -28.015 -28.050 -28.085 -28.120 -28.155 -28.190 -28.225 -28.260 -28.295 -28.330 -28.365 -28.400 -28.435 -28.470 -28.505 -28.540 -28.575 -28.610 -28.645 -28.680 -28.715 -28.750 -28.785 -28.820 -28.855 -28.890 -28.925 -28.960 -29.000 -29.035 -29.070 -29.105 -29.140 -29.175 -29.210 -29.245 -29.280 -29.315 -29.350 -29.385 -29.420 -29.455 -29.490 -29.525 -29.560 -29.595 -29.630 -29.665 -29.700 -29.735 -29.770 -29.805 -29.840 -29.875 -29.910 -29.945 -29.980 -30.015 -30.050 -30.085 -30.120 -30.155 -30.190 -30.225 -30.260 -30.295 -30.330 -30.365 -30.400 -30.435 -30.470 -30.505 -30.540 -30.575 -30.610 -30.645 -30.680 -30.715 -30.750 -30.785 -30.820 -30.855 -30.890 -30.925 -30.960 -31.000 -31.035 -31.070 -31.105 -31.140 -31.175 -31.210 -31.245 -31.280 -31.315 -31.350 -31.385 -31.420 -31.455 -31.490 -31.525 -31.560 -31.595 -31.630 -31.665 -31.700 -31.735 -31.770 -31.805 -31.840 -31.875 -31.910 -31.945 -31.980 -32.015 -32.050 -32.085 -32.120 -32.155 -32.190 -32.225 -32.260 -32.295 -32.330 -32.365 -32.400 -32.435 -32.470 -32.505 -32.540 -32.575 -32.610 -32.645 -32.680 -32.715 -32.750 -32.785 -32.820 -32.855 -32.890 -32.925 -32.960 -33.000 -33.035 -33.070 -33.105 -33.140 -33.175 -33.210 -33.245 -33.280 -33.315 -33.350 -33.385 -33.420 -33.455 -33.490 -33.525 -33.560 -33.595 -33.630 -33.665 -33.700 -33.735 -33.770 -33.805 -33.840 -33.875 -33.910 -33.945 -33.980 -34.015 -34.050 -34.085 -34.120 -34.155 -34.190 -34.225 -34.260 -34.295 -34.330 -34.365 -34.400 -34.435 -34.470 -34.505 -34.540 -34.575 -34.610 -34.645 -34.680 -34.715 -34.750 -34.785 -34.820 -34.855 -34.890 -34.925 -34.960 -35.000 -35.035 -35.070 -35.105 -35.140 -35.175 -35.210 -35.245 -35.280 -35.315 -35.350 -35.385 -35.420 -35.455 -35.490 -35.525 -35.560 -35.595 -35.630 -35.665 -35.700 -35.735 -35.770 -35.805 -35.840 -35.875 -35.910 -35.945 -35.980 -36.015 -36.050 -36.085 -36.120 -36.155 -36.190 -36.225 -36.260 -36.295 -36.330 -36.365 -36.400 -36.435 -36.470 -36.505 -36.540 -36.575 -36.610 -36.645 -36.680 -36.715 -36.750 -36.785 -36.820 -36.855 -36.890 -36.925 -36.960 -37.000 -37.035 -37.070 -37.105 -37.140 -37.175 -37.210 -37.245 -37.280 -37.315 -37.350 -37.385 -37.420 -37.455 -37.490 -37.525 -37.560 -37.595 -37.630 -37.665 -37.700 -37.735 -37.770 -37.805 -37.840 -37.875 -37.910 -37.945 -37.980 -38.015 -38.050 -38.085 -38.120 -38.155 -38.190 -38.225 -38.260 -38.295 -38.330 -38.365 -38.400 -38.435 -38.470 -38.505 -38.540 -38.575 -38.610 -38.645 -38.680 -38.715 -38.750 -38.785 -38.820 -38.855 -38.890 -38.925 -38.960 -39.000 -39.035 -39.070 -39.105 -39.140 -39.175 -39.210 -39.245 -39.280 -39.315 -39.350 -39.385 -39.420 -39.455 -39.490 -39.525 -39.560 -39.595 -39.630 -39.665 -39.700 -39.735 -39.770 -39.805 -39.840 -39.875 -39.910 -39.945 -39.980 -40.015 -40.050 -40.085 -40.120 -40.155 -40.190 -40.225 -40.260 -40.295 -40.330 -40.365 -40.400 -40.435 -40.470 -40.505 -40.540 -40.575 -40.610 -40.645 -40.680 -40.715 -40.750 -40.785 -40.820 -40.855 -40.890 -40.925 -40.960 -41.000 -41.035 -41.070 -41.105 -41.140 -41.175 -41.210 -41.245 -41.280 -41.315 -41.350 -41.385 -41.420 -41.455 -41.490 -41.525 -41.560 -41.595 -41.630 -41.665 -41.700 -41.735 -41.770 -41.805 -41.840 -41.875 -41.910 -41.945 -41.980 -42.015 -42.050 -42.085 -42.120 -42.155 -42.190 -42.225 -42.260 -42.295 -42.330 -42.365 -42.400 -42.435 -42.470 -42.505 -42.540 -42.575 -42.610 -42.645 -42.680 -42.715 -42.750 -42.785 -42.820 -42.855 -42.890 -42.925 -42.960 -43.000 -43.035 -43.070 -43.105 -43.140 -43.175 -43.210 -43.245 -43.280 -43.315 -43.350 -43.385 -43.420 -43.455 -43.490 -43.525 -43.560 -43.595 -43.630 -43.66														

TABLE III.- NEGATIVE-THRUST CHARACTERISTICS OF THE NACA 4-(5)(05)-037 SIX-
AND EIGHT-BLADE, DUAL-ROTATION PROPELLERS, $\Delta\theta = \text{OPTIMUM}$ - Continued
(a) $B = 6$ - Continued

M	β_T , deg	J	C_T	C_{T_F}	C_{P_R}	M	β_T , deg	J	C_T	C_{T_F}	C_{P_R}	M	β_T , deg	J	C_T	C_{T_F}	C_{P_R}	
0.40	30	1.69	-0.241	-0.11	-0.13	0.60	30	3.40	-1.453	-1.16	-1.16	0.70	50	6.65	-2.382	-2.17	-2.36	
	1.74	-0.246	-0.11	-0.15			30	1.60	-1.530	-1.26	-1.26		50	7.51	-3.065	-2.93	-3.08	
	1.83	-0.318	-0.17	-0.19			30	1.89	-1.648	-1.61	-1.69		50	8.21	-3.783	-3.63	-3.82	
	1.93	-0.405	-0.20	-0.21			30	1.19	-1.714	-1.67	-1.82		50	9.09	-4.700	-4.51	-4.72	
	2.05	-0.454	-0.22	-0.24			30	1.27	-1.930	-1.81	-1.95		50	9.86	-5.553	-5.44	-5.60	
	2.14	-0.504	-0.25	-0.27			30	1.06	-1.187	-1.04	-1.24		50	10.92	-6.911	-6.76	-7.04	
	2.24	-0.556	-0.27	-0.30			30	1.85	-1.690	-1.47	-1.70		50	14.92	-13.093	-12.80	-13.49	
	2.34	-0.609	-0.30	-0.33			30	6.82	-2.352	-2.16	-2.43		50	19.81	-22.935	-22.14	-22.99	
	2.44	-0.668	-0.33	-0.35			30	7.84	-3.285	-3.04	-3.29		50	24.86	-36.244	-37.07	-35.11	
	2.54	-0.715	-0.35	-0.37			30	5.79	-1.176	-1.87	-2.45							
	2.63	-0.769	-0.38	-0.40			30	9.73	-1.176	-1.87	-2.45							
	2.83	-0.868	-0.43	-0.44			30	10.68	-1.625	-5.91	-6.20							
	3.03	-0.951	-0.49	-0.49			30	11.59	-11.94	-11.39	-12.62							
	3.23	-1.103	-0.56	-0.54			30	19.59	-21.61	-21.36	-22.80							
	3.42	-1.276	-0.63	-0.68			30	24.71	-24.13	-24.36	-24.23							
	3.71	-1.498	-0.73	-0.70			30	29.37	-47.68	-47.61	-37.47							
	4.01	-1.673	-0.86	-0.80		50	32.4	-0.945	.09	-.09		50	3.20	-.066	.08	-.10		
	4.39	-1.996	-1.05	-0.94			30	4.16	-1.943	-1.26	-1.73		50	3.29	-.124	0	-.20	
	4.89	-2.474	-1.29	-1.17			30	3.34	-1.07	.01	-.19		50	3.39	-.181	-.07	-.89	
	5.39	-3.235	-1.67	-1.67			30	3.45	-1.172	-.06	-.31		50	3.49	-.251	-.16	-.40	
	6.83	-4.822	-0.63	-0.27			30	3.23	-1.239	-.15	-.48		50	3.59	-.307	-.23	-.47	
	7.80	-5.319	-1.33	-3.07			30	3.65	-1.904	-.24	-.51		50	3.79	-.362	-.35	-.58	
	8.79	-7.983	-1.19	-1.91			30	3.73	-1.962	-.33	-.56		50	3.81	-.418	-.47	-.55	
	9.80	-9.818	-5.12	1.84			30	3.87	-1.43	-.61	-.61		50	3.90	-.460	-.57	-.58	
	40	1.94	-0.44	.01	-.03	50	3.93	-1.959	-.24	-.59	50	4.00	-.500	-.68	-.61			
	2.04	-1.112	-.04	-.15			30	4.35	-1.613	-.73	-.88	50	4.09	-.536	-.66	-.66		
	2.13	-1.179	-.10	-.15			30	4.73	-1.681	-.79	-.91	50	4.20	-.576	-.69	-.71		
	2.24	-1.248	-.16	-.21			30	4.74	-1.78	-.84	-.98	50	4.30	-.615	-.73	-.76		
	2.34	-1.309	-.22	-.25			30	5.56	-1.103	-.18	-.47	50	4.38	-.652	-.78	-.88		
	2.44	-1.360	-.27	-.38			30	6.13	-1.369	-.14	-.82	50	4.78	-.941	-.87	-.99		
	2.63	-1.468	-.34	-.36			30	6.71	-1.737	-.17	-.85	50	4.90	-.974	-.98	-.10		
	2.83	-1.566	-.40	-.46			30	6.77	-1.737	-.17	-.85	50	5.29	-1.018	-.109	-.130		
	3.12	-1.677	-.46	-.48			30	7.38	-1.673	-.07	-.85	50	5.69	-1.209	-.199	-.153		
	3.13	-1.851	-.54	-.65			30	7.98	-1.805	-.70	-.93	50	6.11	-1.436	-.153	-.182		
	3.71	-1.977	-.69	-.74			30	8.90	-1.266	-.36	-.42	50	6.45	-1.598	-.177	-.08		
	3.82	-1.297	-.91	-.93			30	9.91	-1.153	-.23	-.30	50	7.09	-2.033	-.14	-.51		
	4.70	-1.633	-.15	-.18			30	10.86	-1.087	-.71	-.40	50	7.68	-2.495	-.66	-.31		
	5.16	-1.826	-.19	-.18			30	11.83	-1.986	-.97	-.27	50	8.26	-3.904	-.17	-.37		
	7.16	-1.199	-.08	-.08		60	3.96	-1.085	-.19	-.09	60	3.85	-.006	.22	-.08			
	8.42	-2.317	-.93	-.91			30	4.03	-1.082	-.19	-.08	60	3.95	-.070	.12	-.16		
	9.90	-7.669	-.51	-.57			30	4.15	-1.133	-.03	-.38	60	4.05	-.132	.03	-.28		
	30	2.79	-.055	.05	-.08		30	4.34	-1.945	-.11	-.27	60	4.15	-.190	-.03	-.24		
	2.89	-1.110	0	-.15			30	4.73	-1.670	-.28	-.91	60	4.25	-.256	-.12	-.27		
	3.07	-1.237	-.18	-.32			30	4.94	-1.263	-.70	-.03	60	4.36	-.316	-.22	-.28		
	3.26	-1.370	-.28	-.56			30	5.54	-1.793	-.03	-.35	60	4.77	-.580	-.70	-.88		
	3.47	-1.593	-.32	-.57			30	6.16	-1.006	-.30	-.68	60	5.36	-.806	-.11	-.27		
	3.78	-1.825	-.35	-.72			30	6.74	-1.247	-.17	-.06	60	6.19	-1.026	-.38	-.66		
	4.09	-1.749	-.32	-.87			30	7.31	-1.153	-.92	-.14	60	6.93	-1.389	-.73	-.17		
	4.49	-1.911	-.33	-.93			30	7.92	-1.833	-.33	-.95	60	7.96	-1.936	-.45	-.96		
	5.00	-1.156	-.34	-.88			30	8.89	-2.375	-.06	-.71	60	8.97	-2.530	-.28	-.81		
	6.00	-1.787	-.11	-.87			30	9.87	-3.005	-.87	-.67	60	9.81	-3.121	-.07	-.66		
	6.99	-1.558	-.07	-.86			30	10.86	-5.710	-.81	-.76	60	10.98	-3.978	-.13	-.89		
	7.36	-1.389	-.13	-.73			30	11.82	-7.430	-.98	-.16	60	12.93	-5.773	-.68	-.51		
	8.93	-1.213	-.13	-.56			30	12.80	-13.792	-.00	-.61	60	14.92	-7.902	-.45	-.69		
	9.96	-1.270	-.11	-.70			30	13.78	-21.724	-.00	-.15	60	19.81	-14.361	-.26	-.82		
	13.43	-1.704	-.23	-.60			30	14.76	-21.577	-.00	-.00	60	27.98	-28.880	-.88	-.17		
	16.39	-14.917	-.16	-.17			30	14.90	-24.90	-.00	-.00	60	29.77	-33.098	-.37	-.56		
50	3.71	-.003	.14	-.01		60	4.93	-.011	.37	-.06	60	4.90	-.040	.36	-.14			
	3.77	-1.996	-.19	-.21			40	4.99	-.042	.30	-.17	60	5.00	-.091	.23	-.26		
	4.98	-1.418	-.36	-.67			40	5.20	-.233	-.01	-.73	60	5.40	-.211	.07	-.88		
	5.96	-1.776	-.21	-.84			40	5.61	-.363	-.22	-.00	60	5.60	-.117	.36	-.07		
	6.80	-1.848	-.09	-.93			40	5.80	-.711	-.53	-.36	60	5.81	-.243	.27	-.24		
	7.88	-1.184	-.19	-.71			40	6.03	-.967	-.84	-.53	60	6.00	-.600	.88	-.36		
	8.80	-1.677	-.13	-.63			40	6.21	-.260	-.08	-.83	60	6.22	-.692	.98	-.53		
	9.88	-1.320	-.08	-.11			40	6.63	-.802	-.10	-.83	60	6.41	-.793	-.14	-.60		
	10.98	-1.126	-.11	-.56			40	6.84	-.892	-.21	-.96	60	6.63	-.890	-.26	-.73		
	15.39	-7.872	-.16	-.63			40	7.01	-.977	-.17	-.06	60	7.09	-.251	.88	-.05		
	16.61	-12.199	-.12	-.69	-.02		40	7.98	-.260	-.17	-.06	60	7.66	-.604	-.15	-.88		
	4.15	-.056	.13	-.16			40	8.02	-.382	-.26	-.16	60	8.28	-.851	-.16	-.28		
	4.71	-1.328	-.01	-.04			40	8.12	-.381	-.36	-.16	60	9.09	-1.174	-.188	-.06		
	5.06	-1.405	-.23	-.03			40	8.23	-.389	-.44	-.16	60	9.88	-1.133	-.233	-.18		
	5.72	-1.805	-.10	-.56			40	8.33	-.503	-.53	-.00	60	13.76	-3.823	-.576	-.83		

TABLE III.- NEGATIVE-THRUST CHARACTERISTICS OF THE NACA 4-(5)(05)-037 SIX-
AND EIGHT-BLADE, DUAL-ROTATION PROPELLERS, $\Delta\beta$ = OPTIMUM - Continued
(a) $B = 6$ - Concluded

X	β_p , deg	J	α_T	C_{T_p}	C_{PR}	X	β_p , deg	J	α_T	C_{T_p}	C_{PR}	X	β_p , deg	J	α_T	C_{T_p}	C_{PR}	
0.75	50	4.20	-0.883	-0.81	-0.91	0.75	65	5.80	-0.532	-0.61	-1.28	0.80	65	5.17	-0.323	-0.09	-0.90	
	4.46	-0.977	-0.90	-1.01			6.02	-0.640	-0.89	-1.41	5.37		6.75	-0.386	-0.22	-1.27		
	4.60	-1.079	-0.97	-1.18			6.21	-0.718	-1.07	-1.53	5.58		7.15	-0.455	-0.33	-1.45		
	4.79	-1.169	-1.04	-1.22			6.42	-0.787	-1.21	-1.66	5.81		7.56	-0.549	-0.44	-1.70		
	5.08	-1.332	-1.19	-1.37			6.61	-0.872	-1.35	-1.80	6.02		8.12	-0.648	-0.71	-2.10		
	5.28	-1.404	-1.13	-1.46			6.84	-0.939	-1.46	-1.89	6.31		8.58	-0.893	-0.93	-2.30		
	5.48	-1.840	-1.67	-1.88							6.21		8.96	-1.33	-1.33	-1.74		
	6.47	-2.288	-2.11	-2.31									70	6.37	-0.129	.48	-0.29	
	7.09	-2.629	-2.63	-2.87										7.07	-0.368	-0.23	-0.93	
	7.69	-3.361	-3.14	-3.44										7.87	-0.703	-0.81	-1.98	
	8.28	-3.981	-3.74	-4.08										8.70	-1.034	-1.60	-2.74	
	8.89	-4.638	-4.41	-4.72										9.45	-1.319	-2.13	-3.36	
	9.88	-5.211	-5.28	-5.63										11.81	-0.887	-4.04	-5.72	
	10.70	-6.810	-6.52	-7.00										16.84	-2.910	-9.76	-12.70	
	11.76	-8.283	-8.03	-8.58										21.92	-9.382	-18.17	-21.88	
	14.62	-12.985	-12.57	-13.44										25.80	-13.291	-26.64	-30.73	
	20.29	-24.844	-25.34	-29.39										29.80	-18.115	-36.20	-40.88	
	24.32	-35.358	-36.65	-38.54														
55	3.14	-0.90	.10	-1.16			0.75	3.33	-0.289	-0.17	-0.47	0.80	65	3.57	-0.026	.28	-0.09	
	3.23	-1.136	.03	-2.24				3.42	-0.366	-0.24	-0.54			3.63	-0.079	.22	-0.16	
	3.32	-2.213	.06	-0.38				3.51	-0.389	-0.34	-0.63			3.76	-0.132	.12	-0.31	
	3.42	-2.280	.14	-0.49				3.61	-0.469	-0.43	-0.70			3.86	-0.220	.08	-0.44	
	3.53	-3.360	.25	-0.68				3.70	-0.501	-0.50	-0.76			4.06	-0.343	.21	-0.68	
	3.60	-3.390	.38	-0.88				3.80	-0.582	-0.64	-0.81			4.16	-0.405	.30	-0.78	
	3.73	-4.477	.46	-0.95				3.93	-0.645	-0.77	-0.93			4.27	-0.469	.44	-0.89	
	3.83	-5.004	.58	-0.87				4.12	-0.742	-0.96	-0.90			4.38	-0.544	.56	-0.99	
	3.94	-5.24	.71	-0.66				4.21	-0.792	-1.06	-0.93			4.48	-0.597	.67	-1.07	
	4.14	-6.66	.93	-0.73				4.31	-0.840	-1.13	-0.97			4.58	-0.665	.79	-1.17	
	4.34	-6.81	.88	-0.84				4.50	-0.938	-1.38	-1.03			4.68	-0.725	.91	-1.27	
	4.50	-7.73	.85	-0.94				4.72	-0.929	-1.04	-1.20			4.79	-0.797	1.02	-1.36	
	4.74	-8.32	.98	-1.05				4.91	-1.009	-1.10	-1.27			5.07	-0.927	1.36	-1.59	
	4.90	-9.08	.96	-1.14				5.30	-1.189	-1.27	-1.51			5.49	-1.164	1.81	-1.71	
	5.31	-1.097	-1.14	-1.41				5.70	-1.361	-1.45	-1.74			5.89	-1.369	2.26	-1.98	
	5.72	-1.306	-1.33	-1.65				6.07	-1.598	-1.68	-2.01			6.26	-1.431	2.00	-2.22	
	6.36	-1.692	-1.74	-2.03				7.09	-2.266	-2.43	-2.83			7.72	-2.731	-3.00	-3.47	
	6.92	-2.007	-2.16	-2.47				8.23	-3.152	-3.46	-4.00			8.85	-2.997	-3.07	-3.54	
	7.91	-2.732	-2.94	-3.34				9.45	-4.299	-4.72	-5.36			9.85	-3.995	-3.96	-4.62	
	8.31	-3.058	-3.29	-3.72				10.91	-5.870	-6.56	-7.33			10.33	-4.168	-5.60	-6.35	
	9.13	-3.784	-4.11	-4.66				12.39	-7.696	-8.70	-9.63			12.86	-5.625	-6.90	-7.70	
	9.93	-4.575	-5.05	-5.68				13.98	-9.801	-11.12	-12.17			14.39	-6.768	-11.17	-13.18	
	10.97	-5.674	-6.30	-6.97				16.89	-11.631	-16.74	-18.11			17.35	-12.091	-18.04	-19.12	
	13.10	-8.320	-9.44	-10.17				21.82	-24.401	-28.61	-29.92			22.93	-21.962	-30.99	-31.99	
	16.06	-12.783	-14.43	-15.66														
	21.61	-23.073	-26.64	-27.69														
60	3.84	-0.048	.18	-0.06			60	3.69	-0.035	.24	-0.07	65	4.50	-0.043	.44	-0.09		
	3.94	-1.108	.09	-0.23				3.80	-0.104	.19	-0.23			4.60	-0.118	.34	-0.28	
	4.04	-1.173	.08	-0.36				3.89	-0.170	.07	-0.38			4.71	-0.174	.27	-0.45	
	4.19	-2.245	.08	-0.42				3.99	-0.253	-0.03	-0.58			4.81	-0.250	.16	-0.68	
	4.24	-3.304	.16	-0.67				4.22	-0.399	-0.24	-0.89			4.91	-0.300	.06	-0.82	
	4.36	-3.860	.26	-0.84				4.31	-0.472	-0.35	-1.02			5.13	-0.439	-0.27	-1.18	
	4.45	-4.442	.35	-0.97				4.43	-0.543	-0.49	-1.14			5.33	-0.562	-0.41	-1.47	
	4.65	-5.033	.60	-0.89				4.54	-0.612	-0.68	-1.22			5.46	-0.707	-0.69	-1.82	
	4.85	-5.911	.85	-0.94				4.63	-0.662	-0.75	-1.27			5.73	-0.816	-0.96	-1.94	
	5.16	-7.712	-1.03	-1.08				4.74	-0.718	-0.87	-1.34			6.16	-1.042	-1.49	-2.34	
	5.25	-8.848	-1.18	-1.33				4.92	-0.770	-1.17	-1.19			6.29	-1.209	-2.08	-2.30	
	5.94	-1.006	-1.34	-1.57				5.33	-0.965	-1.69	-1.29			6.98	-1.394	-2.58	-2.45	
	6.73	-1.372	-1.79	-2.12				5.70	-0.997	-1.41	-1.47			7.38	-1.492	-2.48	-2.73	
	7.34	-1.659	-2.16	-2.57				6.10	-1.188	-1.59	-1.76							
	7.92	-2.027	-2.59	-3.11				6.71	-1.461	-1.91	-2.20							
	8.55	-2.624	-3.43	-4.03				7.31	-1.893	-2.35	-2.73							
	9.93	-3.341	-4.41	-5.03				7.98	-2.160	-2.79	-3.25							
	10.91	-4.127	-5.43	-6.20				8.88	-2.806	-3.68	-3.86							
	12.95	-6.042	-8.14	-9.98				9.91	-3.283	-4.74	-5.36							
	15.90	-9.489	-18.87	-13.93				10.81	-3.317	-5.73	-6.45							
	20.95	-16.729	-22.98	-24.15				12.31	-5.726	-7.66	-8.48							
	24.83	-23.859	-33.19	-34.46				13.92	-7.496	-10.13	-11.09							
	29.83	-34.271	-48.94	-48.73				16.72	-11.084	-15.18	-16.23							
								21.63	-18.956	-26.46	-27.51							
65	4.89	-0.047	.31	-0.14			65	4.66	-0.038	.35	-0.09	65	5.78	-0.028	.72	-0.15		
	4.98	-0.093	.24	-0.27				4.75	-0.073	.30	-0.18			5.98	-0.106	.59	-0.18	
	5.18	-0.212	.06	-0.58				4.87	-0.135	.21	-0.36			6.37	-0.298	.30	-0.80	
	5.40	-0.353	-1.25	-0.96				4.96	-0.193	.13	-0.54			6.76	-0.467	0	-1.31	
	5.59	-0.443	-1.33	-1.15									7.19	-0.734	-0.40	-2.36		
													7.77	-0.963	-0.88	-3.05		
													8.75	-1.332	-2.33	-3.25		
													9.73	-1.710	-2.02	-4.23		
													10.19	-1.934	-3.30	-4.69		
													11.18	-2.393	-4.15	-5.63		
													12.66	-3.162	-5.60	-7.34		
													14.31	-4.311	-7.80	-10.06		
													17.33	-6.391	-11.83	-14.61		
													22.69	-11.502	-21.73	-25.68		

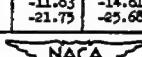


TABLE III.- NEGATIVE-THRUST CHARACTERISTICS OF THE NACA 4-(5)(05)-037 SIX-
AND EIGHT-BLADE, DUAL-ROTATION PROPELLERS, $\Delta\beta = \text{OPTIMUM}$ - Continued
(b) $B = 8$

K	β_T , deg	J	C_T	C_{T_P}	C_{T_R}	K	β_T , deg	J	C_T	C_{T_P}	C_{T_R}	K	β_T , deg	J	C_T	C_{T_P}	C_{T_R}
0.15	-80	1.76	-1.188	0.44	0.38	0.20	40	3.22	-2.669	-1.72	-1.87	0.60	50	7.39	-3.843	-3.71	-4.08
	1.83	-1.301	.47	.41				6.08	-3.839	-2.93	-2.69	8.43	5.342	5.19	5.23		
	1.91	-1.352	.50	.44				6.90	-3.021	-3.36	-3.41	8.96	5.847	5.71	5.09		
	1.96	-1.446	.53	.47				7.85	-6.530	-1.10	-4.40	9.96	7.352	7.17	7.68		
	2.12	-1.670	.57	.53								10.92	8.519	8.78	9.27		
	2.32	-1.889	.64	.61								14.91	17.209	16.96	15.27		
	2.50	-2.131	.71	.70								19.80	30.891	31.01	30.61		
	2.72	-2.396	.77	.76								25.01	46.891	49.78	50.15		
	2.89	-2.581	.84	.84								29.61	57.830	70.67	68.24		
	3.06	-2.773	.93	.90													
	3.23	-2.939	1.00	.98													
	3.46	-3.337	1.13	.99													
	3.73	-3.795	1.26	1.00													
	4.06	-4.079	1.40	1.21													
	4.35	-4.577	1.54	1.26													
	4.68	-5.080	1.68	1.42													
	5.00	-5.692	1.93	1.64													
	6.04	-7.733	2.65	2.18													
	6.97	-9.792	3.51	2.37													
0	-73	-1.159	.08	.01													
	.74	-1.173	.08	.01													
	.88	-1.204	.08	.01													
	.91	-1.251	.08	.01													
	.95	-1.273	.08	.01													
	1.08	-1.346	.01	.01													
	1.08	-1.346	.01	.01													
	1.13	-1.459	.01	.01													
	1.15	-1.480	0	.01													
	1.26	-1.607	0	.01													
	1.35	-1.696	.01	.01													
	1.43	-1.763	.01	.01													
	1.50	-1.894	.02	.01													
	1.68	-2.018	.02	.01													
	1.86	-2.172	.03	.01													
	2.06	-2.361	.04	.02													
	2.27	-2.601	.03	.03													
	2.45	-2.803	.03	.03													
	2.93	-3.308	.06	.08													
	3.14	-2.956	.07	.08													
	4.13	-3.785	.10	.05													
	4.88	-5.001	.13	.06													
	6.13	-7.619	.17	.13													
15	-73	-1.063	.01	.01													
	.79	-1.066	0	.01													
	.84	-1.074	.01	.01													
	.88	-1.138	.02	.02													
	.93	-1.176	.04	.03													
	1.08	-2.216	.05	.04													
	1.11	-3.303	.06	.06													
	1.20	-3.737	.10	.08													
	1.31	-4.666	.14	.10													
	1.42	-5.948	.16	.12													
	1.68	-7.074	.20	.16													
	2.03	-1.034	.26	.25													
	2.32	-1.194	.37	.35													
	3.01	-2.007	.53	.44													
	3.51	-2.806	.68	.58													
	4.08	-3.190	.78	.68													
	4.98	-3.947	.94	.88													
	5.00	-4.680	1.09	.93													
	6.24	-7.077	1.61	1.49													
	.98	-.011	.02	.01													
	.97	-1.013	0	.01													
	1.07	-1.174	.03	.03													
	1.18	-1.266	.07	.08													
	1.27	-1.306	.10	.08													
	1.38	-1.398	.14	.12													
	1.50	-1.571	.20	.17													
	1.79	-1.718	.25	.23													
	2.00	-1.896	.28	.26													
	2.38	-1.923	.35	.39													
	2.87	-1.596	.34	.49													
	3.41	-1.173	.72	.56													
	3.98	-4.778	.89	1.13													
	4.31	-3.318	1.04	1.08													
	4.98	-1.340	1.38	1.15													
	6.36	-6.837	1.87	1.82													
0.20	40	1.99	-.093	.08	-.04												
	2.18	-.199	.19	.17													
	2.40	-.398	.26	.34													
	2.63	-.604	.36	.48													
	2.80	-.725	.45	.58													
	3.01	-.883	.56	.72													
	3.22	-.1038	.63	.85													
	3.46	-.1196	.70	.98													
	3.74	-.1400	.88	1.18													
	3.99	-.1631	.96	1.03													
	4.33	-.1903	1.19	1.45													
	4.74	-.287	1.14	1.67													
	0.60	30	2.76	-1.200	.08	-.11											
		2.85	-1.189	.07	-.04												
		2.95	-1.273	.15	-.35												
		3.07	-1.369	.27	-.29												
		3.26	-1.521	.49	-.60												
		3.46	-1.621	.69	-.88												
		3.66	-1.744	.74	-.74												
		3.87	-1.870	.83	-.93												
		4.15	-1.040	.96	-.96												
		4.49	-1.232	1.11	-.35												
		4.75	-1.412	1.27	-.21												
		5.17	-1.786	1.58	-.08												
		5.78	-2.186	2.03	-.28												
		6.60	-6.939	2.78	-.12												

NACA

TABLE III.- NEGATIVE-THRUST CHARACTERISTICS OF THE NACA 4-(5)(05)-037 SIX-
AND EIGHT-BLADE, DUAL-ROTATION PROPELLERS, $\Delta\beta = \text{OPTIMUM}$ - Concluded
(b) $B = 8$ - Concluded

M	β_F , deg	J	O_T	C_{PF}	C_{PR}	M	β_F , deg	J	O_T	C_{PF}	C_{PR}	M	β_F , deg	J	O_T	C_{PF}	C_{PR}
0.70	55	3.15	-0.026	0.17	-0.02	0.75	55	3.96	-0.746	-0.86	-0.99	0.80	60	3.72	-0.080	0.87	-0.11
		3.26	-1.12	.07	-1.17			4.07	-1.79	-1.99	-1.02			3.83	-1.160	.18	-1.34
		3.36	-1.193	.03	-1.31			4.18	-1.877	-1.13	-1.07			3.94	-1.251	.06	-1.58
		3.47	-1.285	.14	-1.46			4.28	-1.914	-1.06	-1.13			4.04	-1.344	-0.03	-1.78
		3.57	-1.366	.24	-1.58			4.49	-1.998	-1.14	-1.29			4.13	-1.429	-1.14	-1.99
		3.68	-1.458	.38	-1.69			4.70	-1.102	-1.23	-1.43			4.25	-1.535	-2.26	-1.21
		3.77	-1.509	.49	-1.75			4.89	-1.219	-1.33	-1.60			4.34	-1.609	-1.39	-1.38
		3.87	-1.598	.62	-1.81			5.38	-1.526	-1.66	-1.99			4.52	-1.791	-1.67	-1.72
		3.98	-1.691	.76	-1.86			6.00	-1.981	-1.13	-1.60			4.76	-1.950	-1.99	-1.95
		4.09	-1.723	.86	-1.93			6.59	-2.150	-2.68	-3.19			4.96	-1.992	-1.38	-1.63
		4.28	-1.823	.98	-1.06			7.22	-3.042	-3.33	-3.93			5.37	-1.284	-0.00	-1.87
		4.50	-1.946	1.13	-1.21			7.85	-3.625	-4.05	-4.67			5.76	-1.403	-1.86	-2.28
		4.70	-1.057	1.25	-1.36			8.42	-4.231	-4.82	-5.50			6.16	-1.634	-0.13	-2.62
		4.87	-1.167	1.37	-1.51			9.10	-5.122	-5.79	-6.63			6.56	-1.899	-0.15	-3.09
		5.39	-1.498	1.68	-1.97			10.03	-6.378	-7.29	-8.20			6.99	-2.220	-2.84	-3.34
		6.00	-1.984	2.10	-2.52			11.06	-7.926	-9.15	-10.20			7.60	-2.691	-3.47	-4.30
		6.61	-2.374	2.61	-3.06			13.08	-11.311	-13.26	-14.49			8.17	-3.180	-4.09	-5.07
		7.20	-2.869	3.26	-3.63			15.04	-15.227	-17.99	-19.48			9.77	-3.732	-4.88	-5.97
		8.00	-3.673	4.16	-4.72			20.23	-28.063	-33.66	-37.73			10.97	-4.219	-5.93	-7.13
		8.99	-4.786	5.44	-6.01			25.18	-43.710	-53.83	-54.73			12.43	-5.083	-10.61	-12.63
		10.03	-6.096	6.98	-7.64			30.13	-58.207	-77.79	-76.24			14.08	-10.468	-11.15	-16.36
		11.03	-7.547	8.71	-9.56									16.97	-15.632	-21.59	-24.47
		13.24	-11.194	13.28	-14.06									21.93	-26.703	-37.46	-41.13
		15.13	-14.827	17.76	-18.66												
		20.05	-26.380	31.60	-33.42												
		25.03	-51.471	50.53	-52.34												
		30.14	-63.636	74.66	-72.19												
	60	3.91	-0.070	.19	-1.12			3.86	-0.065	.22	-1.11			4.75	-0.076	.39	-1.12
		4.00	-1.156	.09	-1.31			4.96	-1.141	.12	-1.28			4.93	-1.215	.19	-1.51
		4.20	-1.300	.15	-1.64			4.06	-1.221	.03	-1.16			5.31	-1.484	-1.18	-1.28
		4.40	-1.455	.32	-1.93			4.17	-1.309	-1.09	-1.67			5.74	-1.890	-1.74	-2.43
		4.62	-1.589	.66	-1.10			4.27	-1.392	-1.18	-1.85			6.14	-1.015	-1.44	-2.25
		4.81	-1.710	.87	-1.23			4.37	-1.428	-1.31	-1.05			6.56	-1.821	-1.87	-2.60
		5.15	-1.893	1.18	-1.90			4.47	-1.562	-1.2	-1.23			6.95	-1.448	-1.25	-2.94
		5.47	-1.110	1.49	-1.81			4.69	-1.713	-1.74	-1.23			7.33	-1.792	-2.16	-3.37
		5.80	-1.332	2.16	-2.16			4.88	-1.780	-1.08	-1.29			7.53	-2.138	-3.32	-4.22
		6.33	-1.584	2.06	-2.65			5.19	-1.953	-1.32	-1.58			8.71	-2.942	-3.94	-5.00
		6.73	-1.803	2.32	-2.95			5.30	-1.180	-1.29	-1.88			9.55	-3.181	-1.98	-2.90
		7.36	-2.214	2.83	-3.55			5.49	-1.400	-1.83	-2.27			10.61	-4.213	-6.48	-8.10
		7.89	-2.592	3.30	-4.12			5.60	-1.789	-2.32	-2.87			12.39	-5.792	-8.92	-10.91
		8.69	-3.198	4.13	-5.01			5.71	-2.207	-2.02	-3.53			14.29	-7.918	-12.67	-14.82
		9.54	-4.040	5.23	-6.25			5.81	-4.660	-1.41	-1.43			16.94	-11.355	-18.26	-21.16
		10.96	-5.465	7.14	-8.45			6.42	-3.160	-1.09	-1.88			21.98	-19.763	-32.63	-36.39
		15.27	-11.226	15.07	-17.13			6.42	-1.784	-1.27	-1.52			28.56	-34.362	-58.20	-62.48
		19.41	-19.011	23.86	-29.02			6.51	-1.692	-1.31	-1.50						
		25.68	-33.928	17.09	-30.84			6.59	-1.704	-1.02	-1.70						
		33.77	-59.486	84.77	-86.82			6.61	-1.662	-6.12	-7.13						
	65	4.94	-0.088	.35	-2.20			4.81	-0.039	.39	-0.06			3.60	-0.071	.31	-1.11
		5.33	-1.365	.08	-1.95			5.12	-2.34	.10	-1.57			3.74	-1.399	.19	-1.38
		5.76	-1.654	.69	-1.53			5.58	-2.666	.43	-1.48			3.84	-2.76	.08	-1.54
		6.15	-1.874	1.25	-1.93			5.95	-1.805	-1.04	-1.88			3.94	-1.353	-0.03	-1.71
		6.79	-1.199	1.87	-2.55			6.58	-1.137	-1.74	-2.37			4.06	-1.431	-1.16	-1.87
		7.14	-1.371	2.13	-2.85			7.17	-1.761	-2.72	-3.61			4.17	-1.929	-1.32	-1.04
		7.96	-1.817	2.81	-3.69			8.38	-1.192	-3.29	-4.30			4.28	-1.619	-1.47	-1.18
		8.75	-2.274	3.38	-4.61			8.98	-2.944	-3.92	-5.03			4.38	-1.710	-1.62	-1.33
		9.57	-2.869	4.32	-5.69			9.79	-3.101	-1.71	-6.05			4.49	-1.796	-1.79	-1.50
		10.98	-3.896	6.02	-7.50			11.03	-4.107	-6.41	-7.98			4.71	-1.961	-1.03	-1.80
		14.31	-7.060	11.37	-13.38			12.05	-5.997	-9.51	-11.27			4.90	-1.123	-1.32	-2.05
		19.86	-14.416	23.56	-26.71			13.02	-1.474	-15.22	-17.78			5.32	-1.451	-1.94	-2.45
		25.31	-24.140	10.27	-43.98			14.06	-9.474	-15.22	-17.78			5.71	-1.678	-2.52	-2.60
		34.64	-46.004	78.61	-81.84			15.98	-15.263	-24.86	-27.70			6.13	-1.839	-2.24	-3.08
								25.90	-26.686	-33.71	-37.47			6.51	-1.111	-2.74	-3.46
								31.77	-40.278	-57.90	-71.99			6.96	-1.460	-3.13	-4.07
	80	3.83	-1.653	.63	-1.72			3.82	-1.348	.12	-1.60			10.40	-5.762	-7.24	-9.66
		3.35	-1.736	.75	-1.78			3.42	-1.436	.23	-1.73			11.47	-7.271	-9.46	-12.03
		4.73	-1.562	1.45	-1.63			3.51	-1.203	.32	-1.05			13.04	-9.530	-12.77	-15.63
		5.09	-1.837	1.69	-1.94			3.61	-1.598	.45	-1.98			14.73	-12.431	-16.65	-20.31
		5.61	-2.285	2.09	-2.46			3.73	-1.773	.57	-1.09			17.71	-18.296	-25.11	-29.46
		6.27	-3.560	3.34	-3.76			3.85	-1.774	.78	-1.16			22.83	-31.303	-43.49	-49.90
		7.68	-4.526	4.32	-4.79			4.06	-1.943	.91	-1.22						
		8.47	-5.675	5.45	-5.90			4.25	-1.054	-1.30	-1.37						
		9.47	-7.475	7.17	-7.61			4.45	-1.181	-1.55	-1.48						
		10.64	-9.291	9.02	-10.15			4.68	-1.317	-1.76	-1.62						
		13.12	-14.342	14.09	-15.19			5.16	-1.508	-1.66	-2.04						
		15.99	-21.506	21.13	-22.08			5.32	-1.776	-1.94	-2.39						
		20.59	-35.693	35.68	-37.18			6.16	-2.269	-2.49	-3.07						
		25.08	-52.724	51.72	-54.49			6.68	-2.635	-2.89	-3.27						
		29.48	-72.371	75.67	-73.94			6.78	-2.835	-3.12	-3.81						
								7.39	-3.413	-3.77	-4.75						
		3.15	-1.114	.12	-1.19			8.08	-4.073	-4.26	-5.42						
		3.24	-1.179	.03	-1.31			8.80	-3.004	-5.65	-6.70						
		3.34	-2.274	-0.06	-1.30			9.61	-6.114	-6.95	-8.14						
		3.44	-3.655	-1.17	-1.66												

TABLE IV.- NEGATIVE-THRUST CHARACTERISTICS OF THE NACA 4-(5)(05)-037 SIX-
AND EIGHT-BLADE, DUAL-ROTATION PROPELLERS, $\Delta\theta = 0.8^\circ$
(a) $B = 6$

K	δ_p , deg	J	c_T	c_{T_p}	c_{T_R}	K	δ_p , deg	J	c_T	c_{T_p}	c_{T_R}	K	δ_p , deg	J	c_T	c_{T_p}	c_{T_R}
0.60	65	5.37	-1.33	-0.02	-0.01	0.75	65	8.95	-1.79	-0.06	-0.04	0.80	65	5.70	-0.67	-0.17	-0.03
		5.75	-0.67	-0.36	-0.05			9.99	-2.20	-0.14	-0.05			5.90	-0.73	-0.15	-0.04
		6.18	-0.68	-1.35	-0.05			10.97	-2.47	-0.17	-0.05			6.15	-0.54	-0.04	-0.07
		6.58	-1.75	-1.15	-0.05			11.96	-2.74	-0.20	-0.05			6.31	-0.80	-1.20	-1.00
		6.95	-1.37	-1.09	-0.05			20.63	-20.70	-1.34	-0.05			6.35	-1.20	-2.14	-2.16
		7.35	-1.08	-1.71	-0.11			24.96	-17.97	-2.91	-0.05			6.74	-1.17	-2.41	-2.16
		7.82	-1.19	-1.95	-0.16			30.16	-21.30	-4.11	-0.11			7.13	-1.312	-2.53	-2.39
		8.02	-1.99	-0.09	-0.05									7.75	-1.495	-2.48	-2.67
		9.00	-1.68	-2.71	-1.43									8.31	-1.745	-3.93	-3.11
		10.04	-2.18	-3.22	-1.35									9.18	-2.123	-3.66	-3.80
		10.93	-2.64	-4.32	-2.16									9.71	-2.518	-4.23	-4.43
		11.95	-3.28	-8.67	-10.28									10.61	-3.051	-5.06	-5.37
		19.96	-9.84	-16.39	-18.69									12.15	-1.146	-7.00	-7.30
		24.87	-15.63	-86.30	-89.37									13.75	-2.822	-9.42	-9.71
		30.08	-23.183	-39.28	-43.05									15.98	-1.267	-12.00	-12.66
														19.05	-11.067	-19.08	-19.95
														24.00	-17.017	-31.03	-30.31
0.70	65	5.16	-0.63	.06	-0.06	0.80	65	6.99	-1.47	-0.18	-0.06	0.80	65	5.70	-0.67	.37	-0.03
		5.56	-1.35	-1.15	-0.06			9.99	-2.20	-1.74	-0.06			5.90	-0.73	-1.15	-0.24
		5.96	-1.25	-1.78	-1.15			10.97	-2.47	-2.07	-0.06			6.15	-0.54	-1.20	-1.00
		6.36	-0.91	-1.09	-1.14			11.96	-2.74	-2.63	-0.06			6.35	-1.20	-2.14	-2.16
		6.75	-0.87	-1.33	-1.71			20.63	-21.30	-4.11	-0.11			6.74	-1.17	-2.41	-2.16
		7.13	-0.98	-1.25	-1.96			24.96	-17.97	-2.91	-0.05			7.13	-1.312	-2.53	-2.39
		7.58	-1.129	-1.89	-2.20			30.16	-21.30	-4.11	-0.11			7.75	-1.495	-2.48	-2.67
		7.96	-1.271	-2.10	-2.23									8.31	-1.745	-3.93	-3.11
		8.96	-1.713	-2.78	-3.32									9.18	-2.123	-3.66	-3.80
		9.96	-1.68	-3.22	-1.51									9.71	-2.518	-4.23	-4.43
		10.93	-2.783	-1.57	-2.24									10.61	-3.051	-5.06	-5.37
		14.93	-5.261	-9.19	-10.20									12.15	-1.146	-7.00	-7.30
		19.88	-10.209	-17.07	-18.65									13.75	-2.822	-9.42	-9.71
		28.03	-21.009	-35.71	-37.39									15.98	-1.267	-12.00	-12.66
		49.89	-24.023	-11.06	-11.68									19.05	-11.067	-19.08	-19.95
														24.00	-17.017	-31.03	-30.31
70	65	7.13	-1.66	.04	-0.18	0.80	65	6.99	-1.21	.01	-0.15	0.80	65	6.37	-1.10	.28	.04
		7.65	-1.473	-1.02	-1.08			9.99	-2.20	-1.74	-0.06			6.79	-0.80	-1.07	-1.34
		8.35	-1.271	-1.25	-1.78			10.97	-2.47	-2.07	-0.06			7.16	-1.461	-1.43	-1.93
		9.13	-0.87	-1.33	-1.71			11.96	-2.74	-2.63	-0.06			7.59	-1.06	-1.94	-1.93
		9.90	-1.296	-2.47	-3.23			20.63	-21.30	-4.11	-0.11			7.97	-1.882	-1.41	-2.61
		10.93	-1.649	-3.19	-3.28			24.96	-17.97	-2.91	-0.05			8.68	-1.284	-2.36	-3.03
		14.87	-1.429	-7.12	-9.16			30.16	-21.30	-4.11	-0.11			9.71	-1.331	-2.53	-3.71
		19.88	-6.788	-14.09	-17.42									11.23	-2.974	-5.71	-7.06
		24.74	-11.001	-23.31	-27.17									14.70	-3.039	-7.97	-9.26
		29.56	-15.922	-33.96	-36.03									17.70	-6.005	-11.89	-13.98
0.75	65	5.15	-1.06	.08	-0.11	0.80	65	6.83	-1.14	.18	-0.10	0.80	65	4.37	-0.078	.23	.04
		5.55	-1.473	-1.02	-1.08			9.99	-2.20	-1.74	-0.06			4.80	-1.192	-1.04	-1.38
		6.18	-1.271	-1.25	-1.78			10.97	-2.47	-2.07	-0.06			5.06	-1.364	-1.21	-1.51
		6.86	-1.296	-2.47	-3.23			11.96	-2.74	-2.63	-0.06			5.30	-1.579	-1.63	-1.11
		10.93	-1.649	-3.19	-3.28			20.63	-21.30	-4.11	-0.11			5.92	-1.832	-1.10	-2.15
		14.87	-1.429	-7.12	-9.16			24.96	-17.97	-2.91	-0.05			6.33	-1.100	-1.99	-2.15
		19.88	-6.788	-14.09	-17.42			30.16	-21.30	-4.11	-0.11			6.74	-1.374	-2.11	-2.73
		24.74	-11.001	-23.31	-27.17									7.12	-1.630	-2.08	-3.21
		29.56	-15.922	-33.96	-36.03									7.76	-2.107	-3.43	-1.21
														8.40	-2.347	-1.08	-3.16
														9.04	-4.973	-4.61	-6.12
														9.61	-1.364	-2.11	-7.16
														10.37	-3.590	-5.61	-5.43
														11.15	-1.268	-6.76	-5.71
														11.70	-2.353	-7.05	-5.12
														13.45	-2.053	-9.26	-5.27
														13.11	-8.050	-1.03	-19.88
														17.28	-19.118	-17.46	-27.35
														20.81	-17.001	-26.12	-1.78

(b) $B = 8$

K	δ_p , deg	J	c_T	c_{T_p}	c_{T_R}	K	δ_p , deg	J	c_T	c_{T_p}	c_{T_R}	K	δ_p , deg	J	c_T	c_{T_p}	c_{T_R}
0.60	65	5.19	-0.036	0.21	0.06	0.70	70	8.66	-1.115	-1.09	-0.01	0.80	65	4.77	-0.033	.28	.02
		5.60	-1.09	-0.27	-0.06			9.00	-1.295	-2.29	-3.36			4.90	-0.093	.16	.03
		5.99	-1.59	-0.73	-1.36			9.42	-1.514	-2.73	-3.51			5.33	-0.368	-0.35	-0.71
		6.38	-1.81	-1.32	-1.08			9.81	-1.708	-3.15	-4.05			5.71	-0.727	-0.59	-1.59
		6.77	-1.061	-1.77	-2.35			11.79	-2.739	-5.34	-7.20			6.18	-1.092	-1.53	-2.21
		7.18	-1.270	-4.21	-4.85			6.06	-1.008	.27	.27			6.56	-1.321	-1.36	-2.57
		7.58	-1.465	-2.85	-3.85			9.42	-1.516	-2.73	-3.51			7.04	-1.782	-2.36	-2.99
		8.01	-1.928	-3.24	-3.85			9.81	-1.708	-3.15	-4.05			7.42	-1.821	-2.08	-2.99
		8.42	-1.928	-3.24	-3.85			10.36	-1.378	-2.22	-3.17			7.80	-1.905	-2.36	-3.14
		8.80	-2.123	-3.26	-4.61			11.18	-1.407	-2.87	-3.67			8.19	-2.290	-1.98	-4.56
		9.21	-2.369	-3.97	-3.13			12.43	-1.476	-3.29	-3.88			9.18	-4.654	-1.47	-5.33
		9.60	-2.638	-4.37	-3.61			12.88	-1.521	-3.82	-4.08			9.76	-1.314	-5.40	-5.80
		10.02	-2.918	-4.39	-3.64			6.82	-1.067	.33	.06			10.29	-1.605	-6.03	-7.16
		10.43	-3.191	-5.33	-6.71			8.21	-1.933	-1.39	-0.27			11.03	-1.238	-7.02	-8.36
		5.19	-1.111	.08	-0.08			8.62	-1.067	.33	.06			11.93	-5.003	-8.49	-9.98
		5.58	-1.417	-1.45	-1.52			9.08	-1.265	.08	.06			12.80	-6.000	-10.15	-11.79
		5.96	-1.677	-1.01	-1.23			9.48	-1.348	-1.24	-0.28			13.73	-6.977	-11.88	-13.82
		6.38	-1.499	-1.57	-1.39			10.22	-1.348	-1.47	-0.30			6.11	-0.287	.63	.97
		6.78	-1.316	-4.82</													

TABLE IV.- NEGATIVE-THRUST CHARACTERISTICS OF THE NACA 4-(5)(05)-037 SIX-
AND EIGHT-BLADE, DUAL-ROTATION PROPELLERS, $\Delta\beta = 0.8^\circ$ - Concluded
(b) $B = 8$ - Concluded

M	β_F , deg	J	C_T	C_{T_F}	C_{P_R}	M	β_F , deg	J	C_T	C_{T_F}	C_{P_R}	M	β_F , deg	J	C_T	C_{T_F}	C_{P_R}
0.84	65	4.63	-0.033	0.36	0.26	0.84	70	6.90	-0.463	-0.35	-0.87	0.90	65	6.03	-1.194	-1.42	-2.36
	47.72	-0.099	.26	.06			7.33	-0.821	-1.01	-2.12			62	-1.358	-1.71	-2.70	
	4.86	-0.192	.11	-.26			7.74	-1.099	-1.60	-3.17			64	-1.753	-2.04	-3.16	
	5.07	-0.369	-.17	-.80			8.12	-1.433	-2.29	-4.16			66	-1.732	-2.36	-3.57	
	5.23	-0.499	-.42	-1.20			8.53	-1.225	-3.20	-3.88			68	-1.986	-2.72	-4.03	
	5.48	-0.721	-.76	-1.82			8.94	-1.813	-3.79	-4.23			71	-2.124	-3.06	-4.47	
	5.65	-0.893	-.08	-2.23			9.33	-1.869	-3.48	-4.73			73	-2.321	-3.38	-4.98	
	5.89	-1.066	-1.44	-2.63			9.77	-2.124	-3.97	-5.40			75	-2.726	-1.07	-5.86	
	6.07	-1.200	-1.78	-2.89			10.14	-2.315	-4.33	-5.90			7.88	-2.900	-4.38	-6.32	
	6.29	-1.348	-2.15	-3.09			10.51	-2.674	-5.03	-6.66			7D	5.76	-0.011	0.80	0.79
	6.38	-1.554	-2.61	-3.31			11.01	-2.940	-5.61	-7.24			5.98	-1.170	.56	.32	.32
	6.70	-1.616	-2.89	-3.42			11.17	-3.056	-5.85	-7.59			6.20	-1.300	.32		
	7.10	-1.857	-3.57	-5.63			12.21	-3.891	-7.80	-9.73			6.60	-1.986	-2.22	-1.06	
	7.28	-1.913	-3.19	-4.74			14.14	-5.213	-10.19	-12.74			6.97	-2.857	-3.84	-1.81	
	7.30	-2.128	-3.22	-4.38			24.29	-5.397	-10.66	-13.07			7.40	-1.131	-1.44	-2.59	
	9.46	-3.294	-5.29	-6.92		0.90	65	4.48	-0.069	0.36	0.26	0.90	65	7.90	-1.488	-2.17	-3.51
	10.17	-3.834	-6.09	-7.57			4.59	-1.162	.26	0			8.26	-1.775	-2.81	-4.33	
	11.11	-4.715	-7.43	-9.33			4.71	-2.223	.14	-1.17			8.77	-2.168	-3.61	-5.43	
	12.21	-5.807	-9.38	-11.51			4.80	-2.61	.05	-3.33			9.09	-2.463	-4.30	-6.26	
	13.24	-7.077	-11.19	-13.88			4.94	-3.75	-0.9	-5.55			9.35	-2.842	-5.15	-7.34	
	14.36	-8.438	-13.44	-16.54			5.14	-5.17	-.31	-8.89			9.97	-3.222	-5.96	-8.47	
	6.10	-0.032	0.63	0.66			5.39	-7.06	-.60	-1.26			10.46	-3.721	-7.02	-9.97	
	6.30	-0.138	.36	.29			5.58	-8.87	-.85	-1.59			11.25	-4.247	-7.46	-12.11	
	6.51	-0.245	.18	-.01			5.78	-9.91	-1.10	-1.93							



TABLE V.- NEAR-STATIC-THRUST CHARACTERISTICS OF THE NACA 4-(5)(05)-037 SIX-
AND EIGHT-BLADE, DUAL-ROTATION PROPELLERS, $\Delta\beta = \text{OPTIMUM}$
(a) $B = 6$

β_F , deg	V, ft/sec	nD	C_T	C_{T_F}	C_{P_R}	β_F , deg	V, ft/sec	nD	C_T	C_{T_F}	C_{P_R}	β_F , deg	V, ft/sec	nD	C_T	C_{T_F}	C_{P_R}
10	14	26.7	0.098	0.267	0.221	15	30	119.9	0.188	0.061	0.098	20	65	213.4	0.271	0.097	0.096
	40.0	.095	.086	.114	34	132.9	.193	.056	.056	68	226.6	.274	.097	.097			
	53.3	.094	.064	.072	39	146.3	.189	.058	.056	72	240.1	.281	.098	.098			
	66.5	.101	.052	.053	41	159.6	.194	.059	.055	76	253.4	.287	.101	.100			
	80.0	.103	.043	.040	44	172.9	.195	.059	.054	81	267.0	.287	.102	.100			
	93.3	.111	.040	.036	47	186.7	.200	.058	.055	25	8	26.7	0.246	0.404	0.362		
	106.5	.123	.037	.030	50	199.7	.199	.059	.054	18	40.1	.306	.223	.244			
	120.0	.126	.036	.031	53	213.1	.192	.056	.055	15	53.2	.316	.185	.200			
	133.3	.120	.034	.029	56	226.9	.192	.056	.055	27	66.7	.322	.175	.188			
	146.7	.120	.034	.028	62	240.4	.196	.059	.055	28	80.0	.329	.164	.167			
	160.0	.125	.035	.028	66	252.8	.200	.056	.056	32	93.3	.339	.158	.162			
	173.3	.123	.033	.028	71	266.7	.203	.051	.057	34	106.9	.339	.161	.136			
	186.7	.123	.034	.028	74	289.7	.208	.059	.056	39	120.0	.334	.154	.156			
	200.0	.123	.033	.028	77	303.7	.212	.150	.170	41	133.1	.344	.154	.155			
	213.4	.125	.034	.028	81	313.1	.223	.119	.134	49	146.7	.345	.152	.155			
	226.6	.124	.033	.027	84	326.7	.229	.110	.121	53	159.9	.345	.158	.156			
	240.0	.127	.034	.028	87	339.7	.244	.104	.106	57	173.1	.344	.154	.156			
	253.3	.129	.033	.028	91	353.7	.248	.099	.106	62	186.7	.350	.153	.158			
	266.7	.131	.036	.028	95	367.7	.252	.100	.100	66	199.9	.359	.154	.158			
	8	26.7	0.165	0.303	0.253	109	381.7	.254	.093	.098	71	213.4	.357	.152	.158		
	40.0	.186	.135	.145		113	395.7	.259	.096	.096	76	229.2	.349	.152	.156		
	53.1	.178	.093	.091		117	409.7	.259	.097	.094	81	240.0	.361	.158	.163		
	66.5	.183	.076	.076		121	423.7	.261	.093	.095	86	253.8	.362	.159	.165		
	80.0	.173	.072	.068		125	437.7	.265	.094	.095	90	266.7	.371	.163	.167		
	93.1	.189	.059	.063		129	451.7	.271	.096	.096							
	106.5	.189	.060	.069		133.9	465.7	.269	.097	.097							

(b) $B = 8$

β_F , deg	V, ft/sec	nD	C_T	C_{T_F}	C_{P_R}	β_F , deg	V, ft/sec	nD	C_T	C_{T_F}	C_{P_R}	β_F , deg	V, ft/sec	nD	C_T	C_{T_F}	C_{P_R}
15	16	26.7	0.178	0.402	0.147	15	68	240.0	0.222	0.071	0.063	20	34	120.0	0.306	0.115	0.110
	40.0	.172	.156	.084	71	253.4	.224	.075	.064	41	133.1	.307	.118	.109			
	53.3	.192	.093	.065	76	266.7	.228	.073	.064	47	146.6	.308	.115	.110			
	66.5	.192	.098	.071	80	280.1	.229	.076	.065	52	160.1	.308	.114	.110			
	80.0	.202	.079	.062	83	293.4	.230	.077	.066	55	173.3	.310	.116	.111			
	93.4	.206	.074	.060	87	306.7	.233	.078	.067	61	186.6	.312	.113	.111			
	106.7	.210	.069	.063	90	320.1	.236	.079	.068	67	200.0	.314	.115	.112			
	120.0	.211	.068	.062	94	333.9	.239	.081	.071	71	213.4	.318	.115	.112			
	133.3	.214	.068	.062	98	347.7	.243	.082	.072	74	226.9	.320	.117	.113			
	146.4	.212	.067	.061	20	26.8	0.246	0.480	0.148	79	240.1	.322	.117	.113			
	159.9	.216	.068	.062	20	40.1	.288	.258	.129	83	253.5	.323	.118	.118			
	173.3	.218	.068	.062	20	53.5	.282	.170	.119	89	266.7	.329	.120	.120			
	186.6	.218	.069	.066	22	66.7	.299	.135	.112	91	280.0	.330	.122	.122			
	200.3	.219	.070	.063	22	80.0	.298	.129	.115	94	296.0	.335	.126	.			

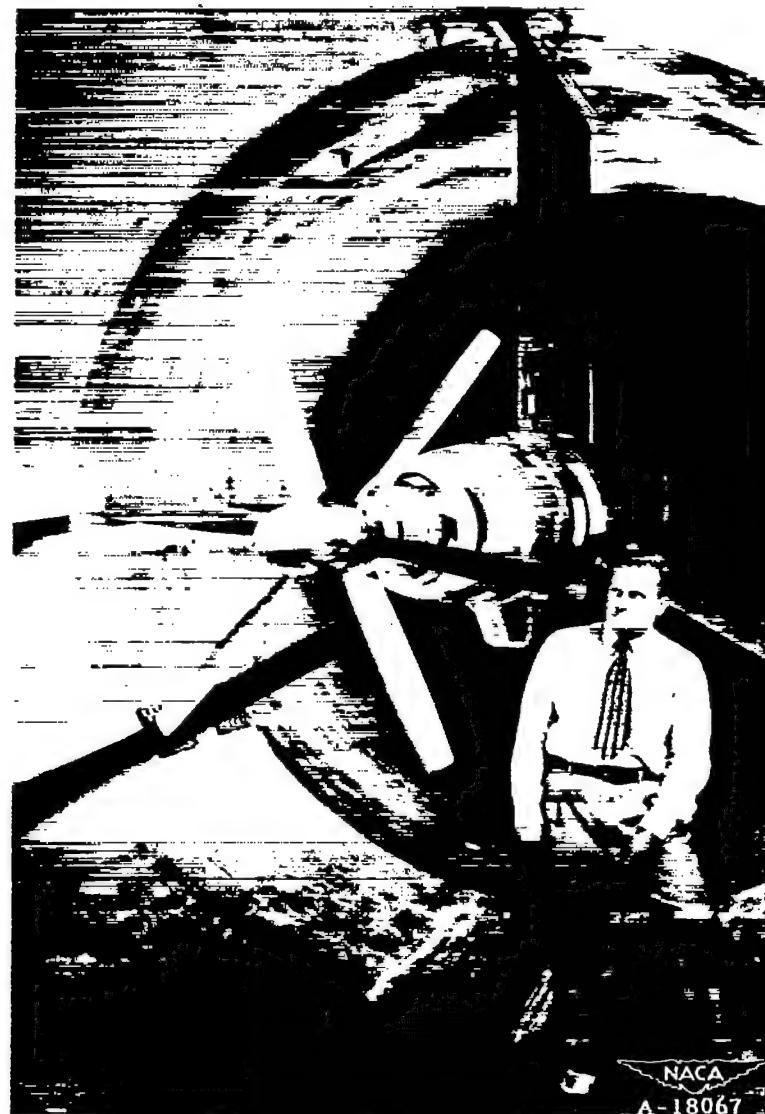
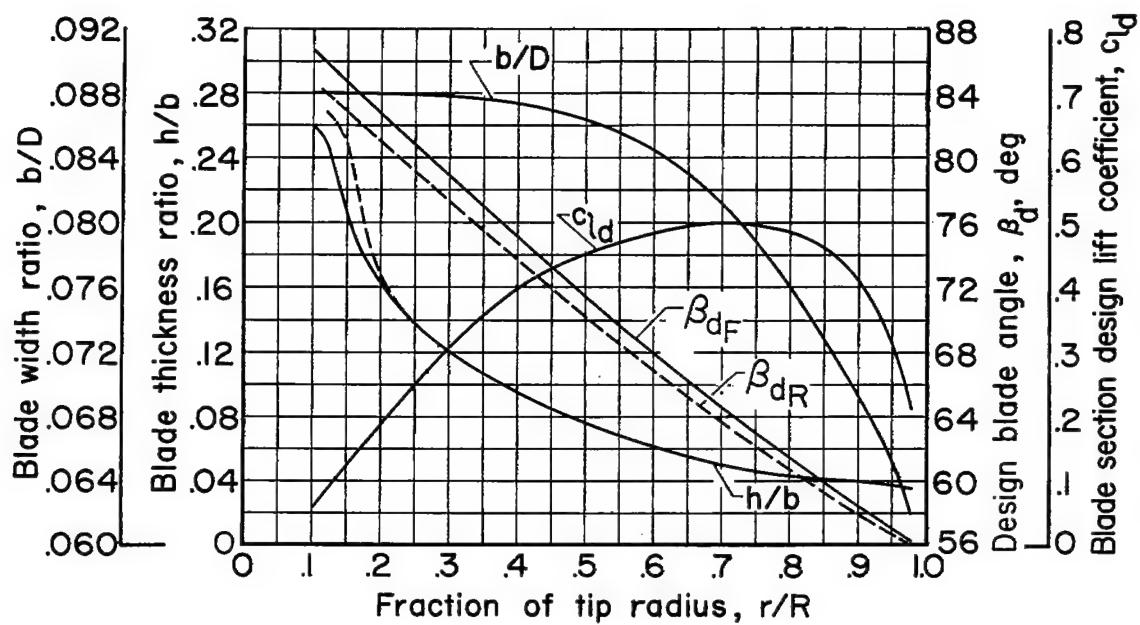


Figure 1.- Photograph of the 1000-horsepower dynamometer with the NACA 4-(5)(05)-037 six-blade, dual-rotation propeller.



(a) NACA 4-(5)(05)-037 six- and eight-blade, dual-rotation propellers.

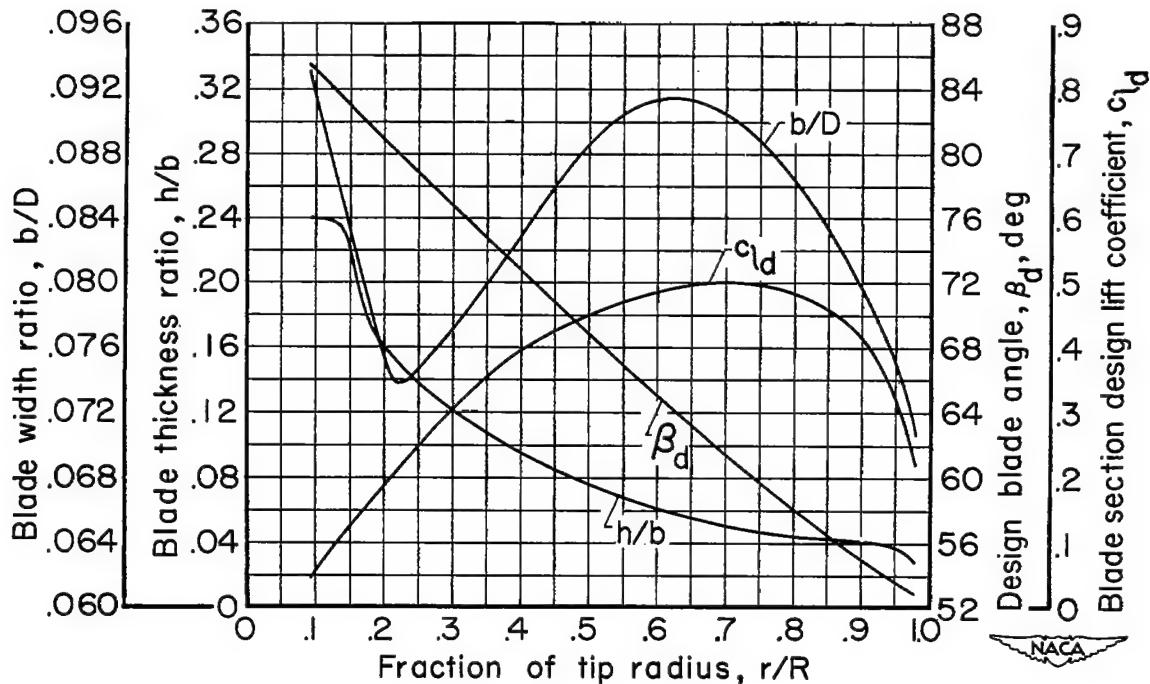
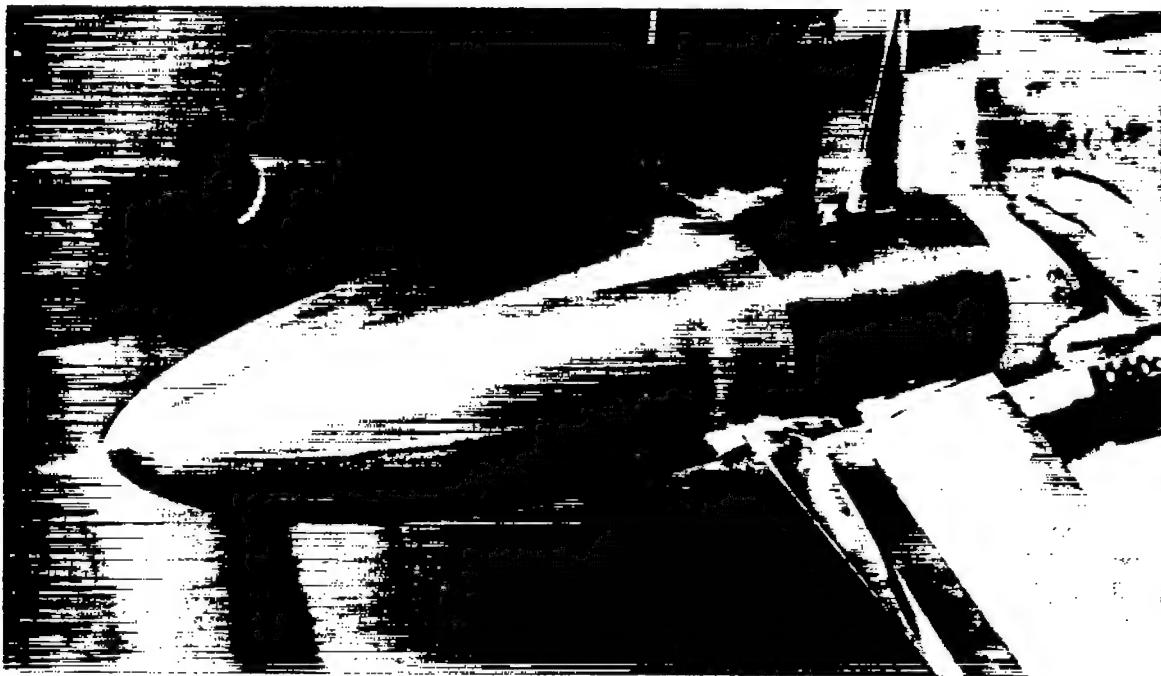
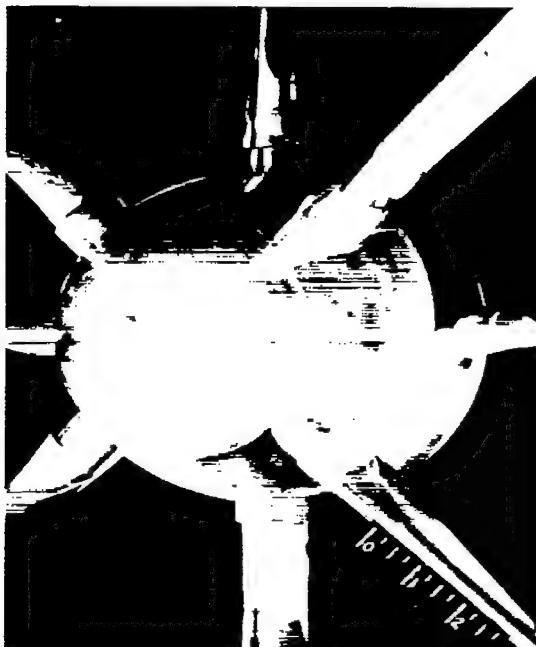


Figure 2.- Propeller blade-form curves.



(a) Spinner A.



(b) Spinner B.



(c) Spinner C.

A-19070

Figure 3.- Photograph of the spinners and platform propeller-spinner junctures.

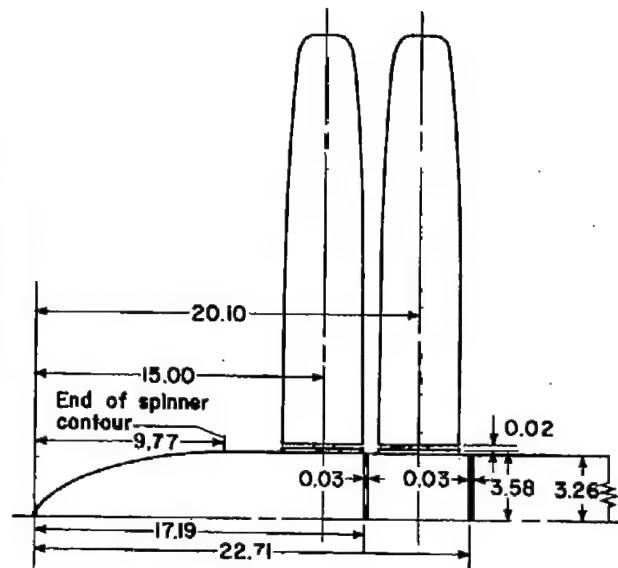
All dimensions in inches

Propeller blades shown in developed plan form

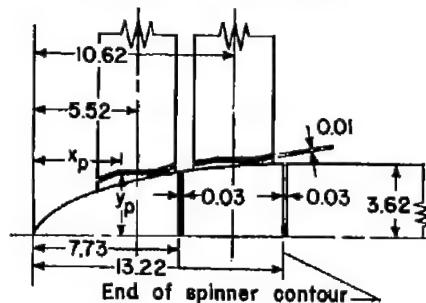
Spinners are contoured to the NACA I-series profile (reference 12)

Platforms align with blades when $\beta_F = 65^\circ$ and $\beta_R = 64.2^\circ$ ($\beta = 60^\circ$ for single)

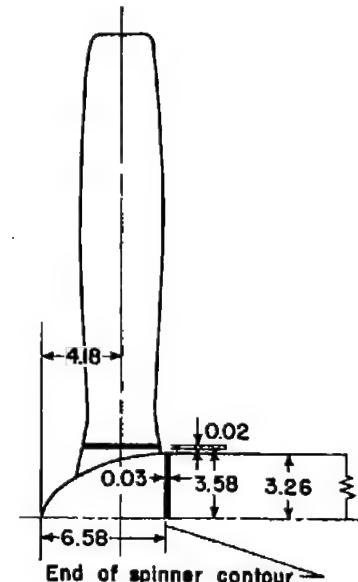
Platform coordinates			
Front		Rear	
x_p	y_p	x_p	y_p
3.482	2.890	8.582	3.655
3.720	2.924	8.820	3.695
3.920	2.992	9.220	3.760
4.320	3.167	9.620	3.825
4.720	3.220	10.020	3.860
6.520	3.220	11.420	3.860
6.920	3.317	11.820	3.890
7.320	3.411	12.220	3.950
7.706	3.502	12.606	4.040



(a) Spinner A.



(b) Spinner B.



(c) Spinner C.

Figure 4.- Details of the spinners and platform propeller-spinner junctures.

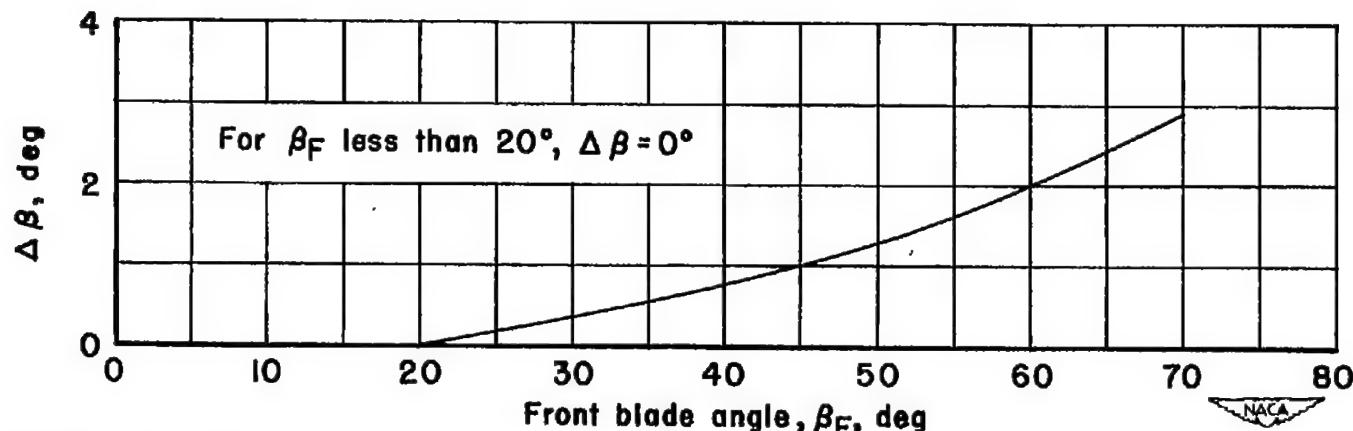


Figure 5.- The difference between the front and rear blade angles used for the optimum setting of the dual-rotation propellers.

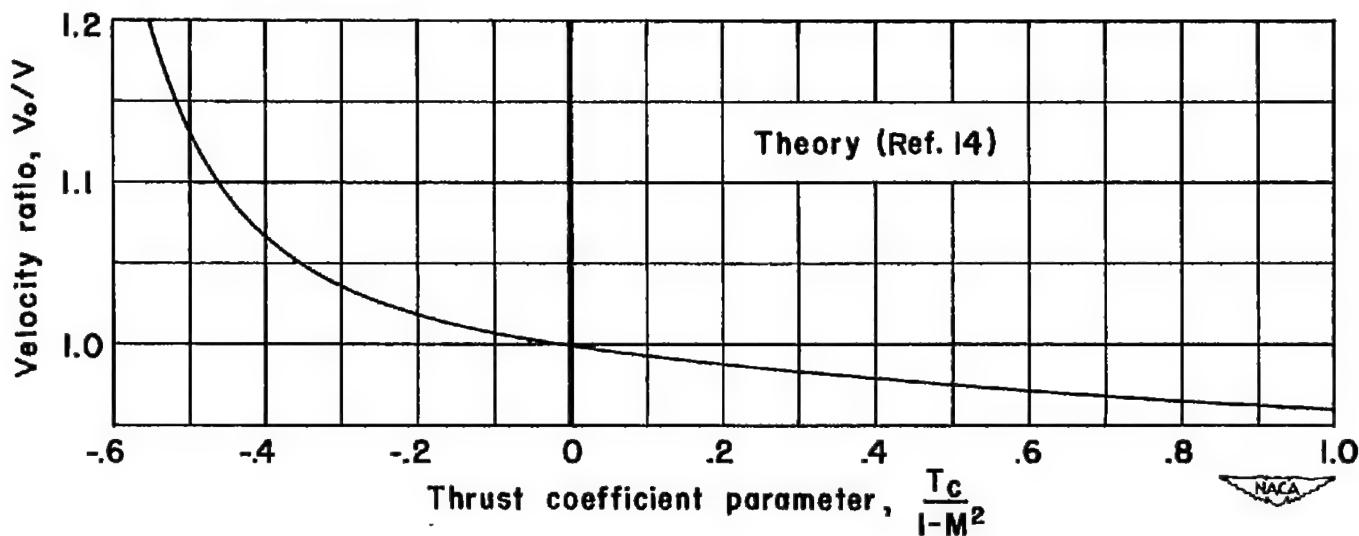


Figure 6.- Tunnel-wall-interference correction for a 4-foot-diameter propeller in the Ames 12-foot pressure wind tunnel.

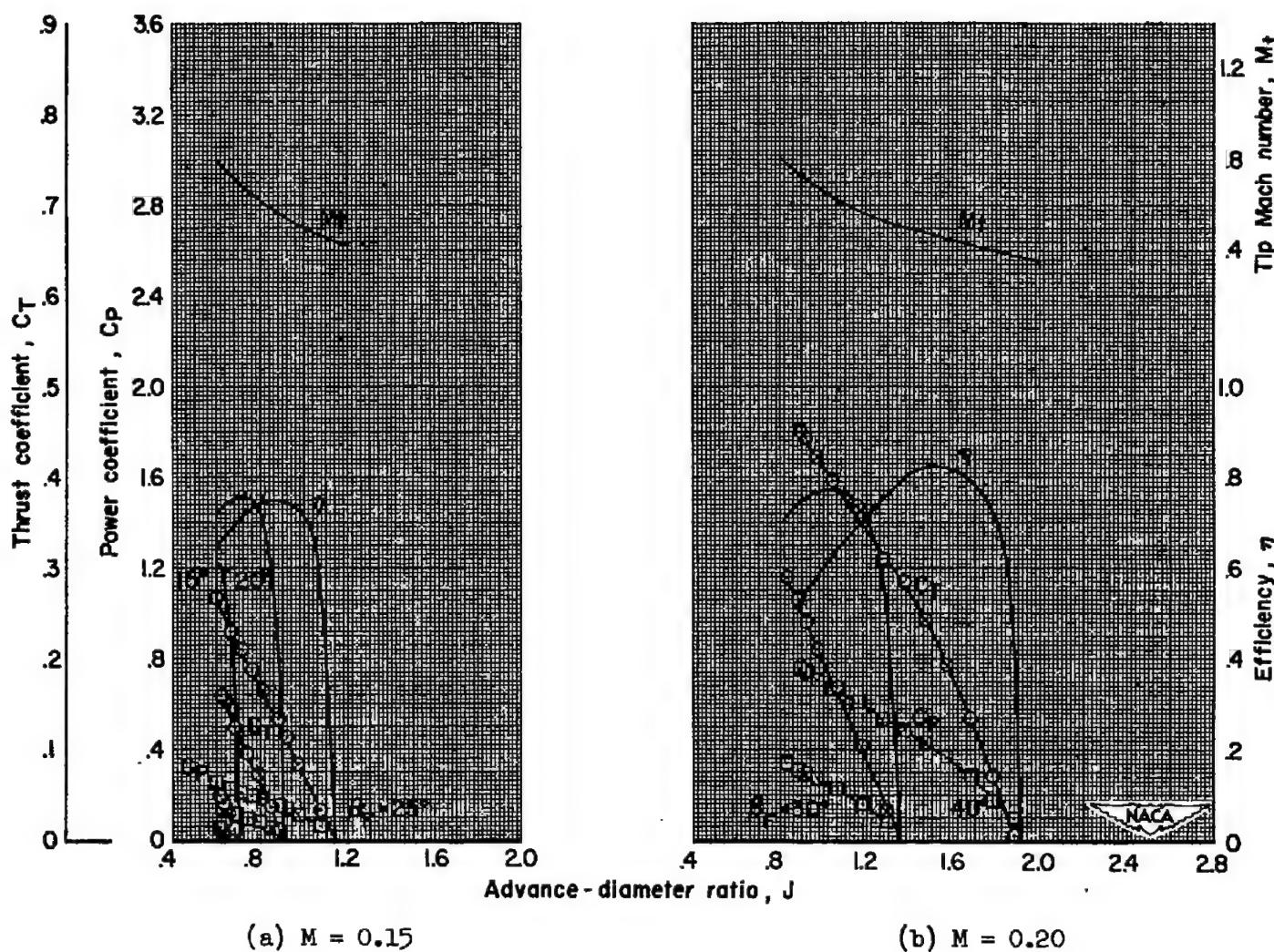


Figure 7.- Positive-thrust characteristics; NACA 4-(5)(05)-037 six-blade, dual-rotation propeller,
 $\Delta\beta$ = optimum, spinner A.

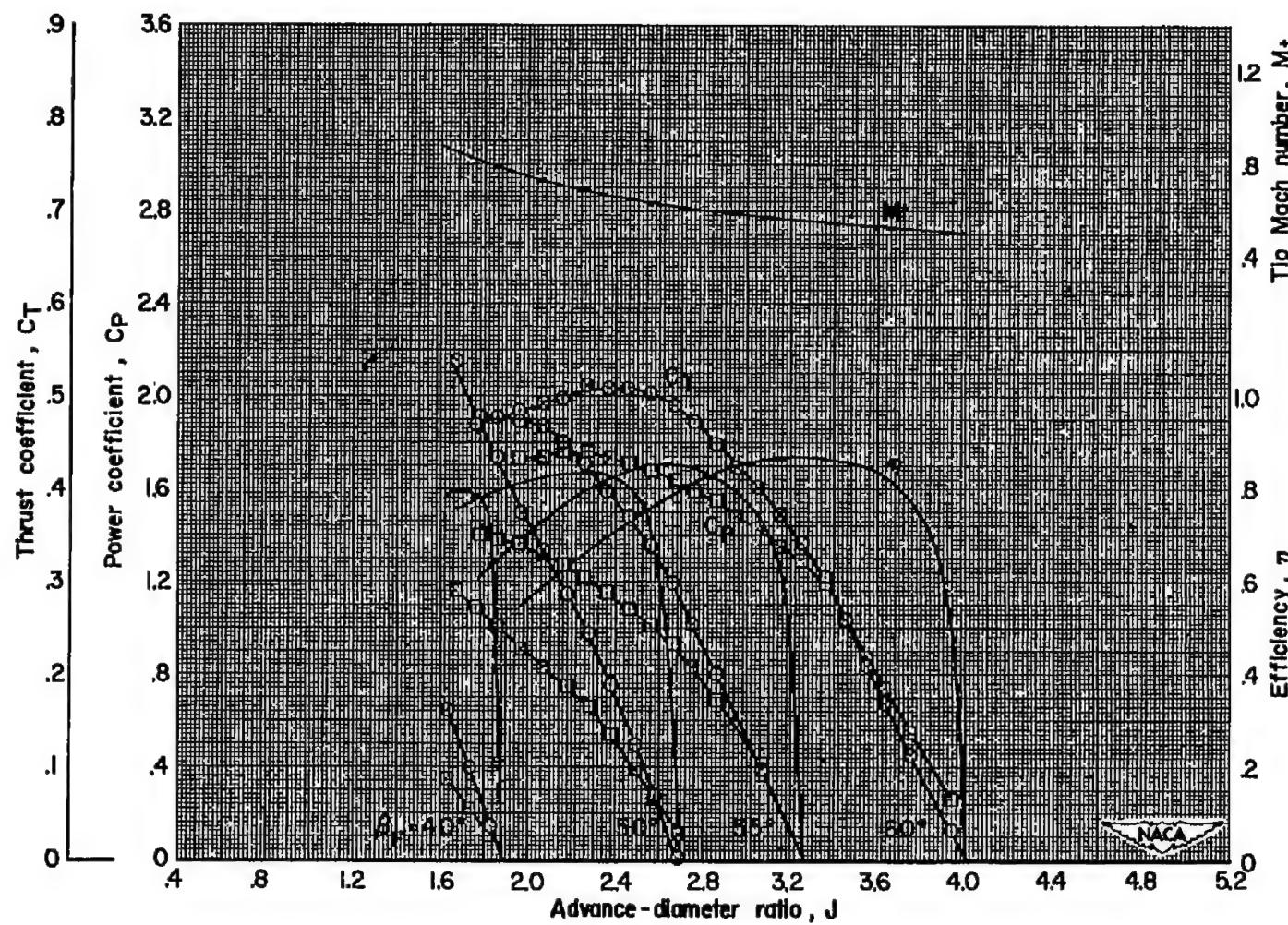
(c) $M = 0.40$

Figure 7.- Continued.

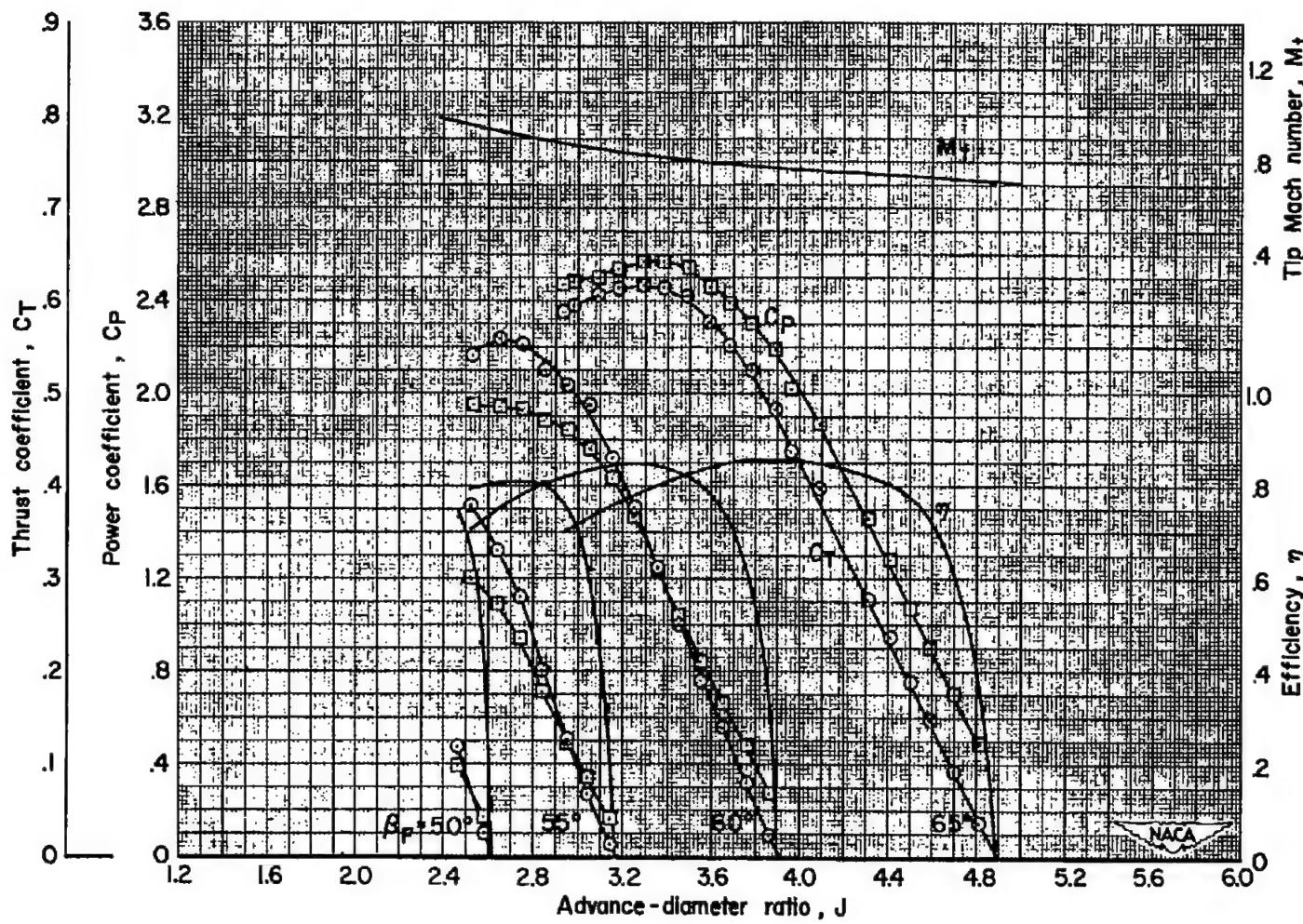
(d) $M = 0.60$

Figure 7.- Continued.

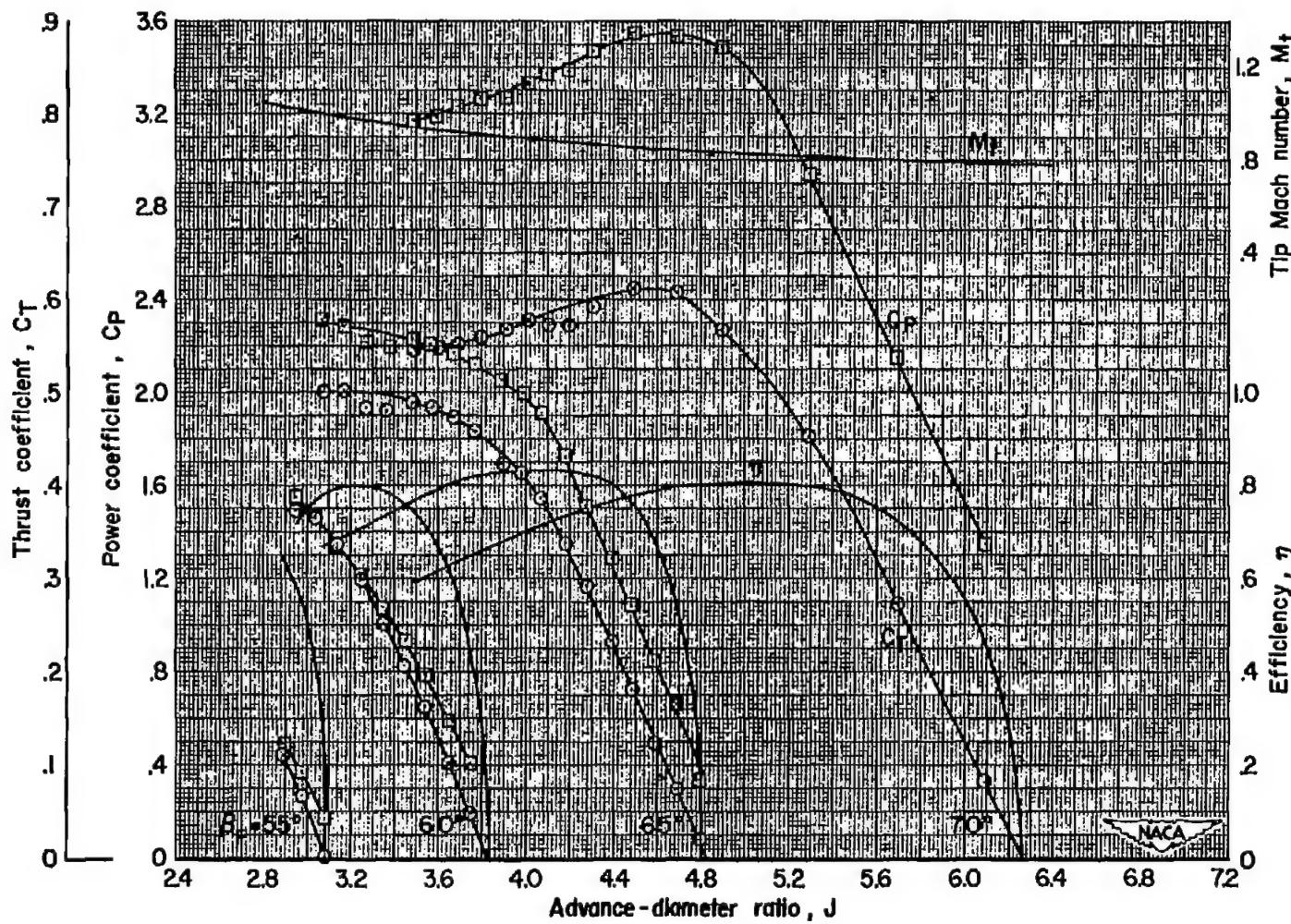
(e) $M = 0.70$

Figure 7.- Continued.

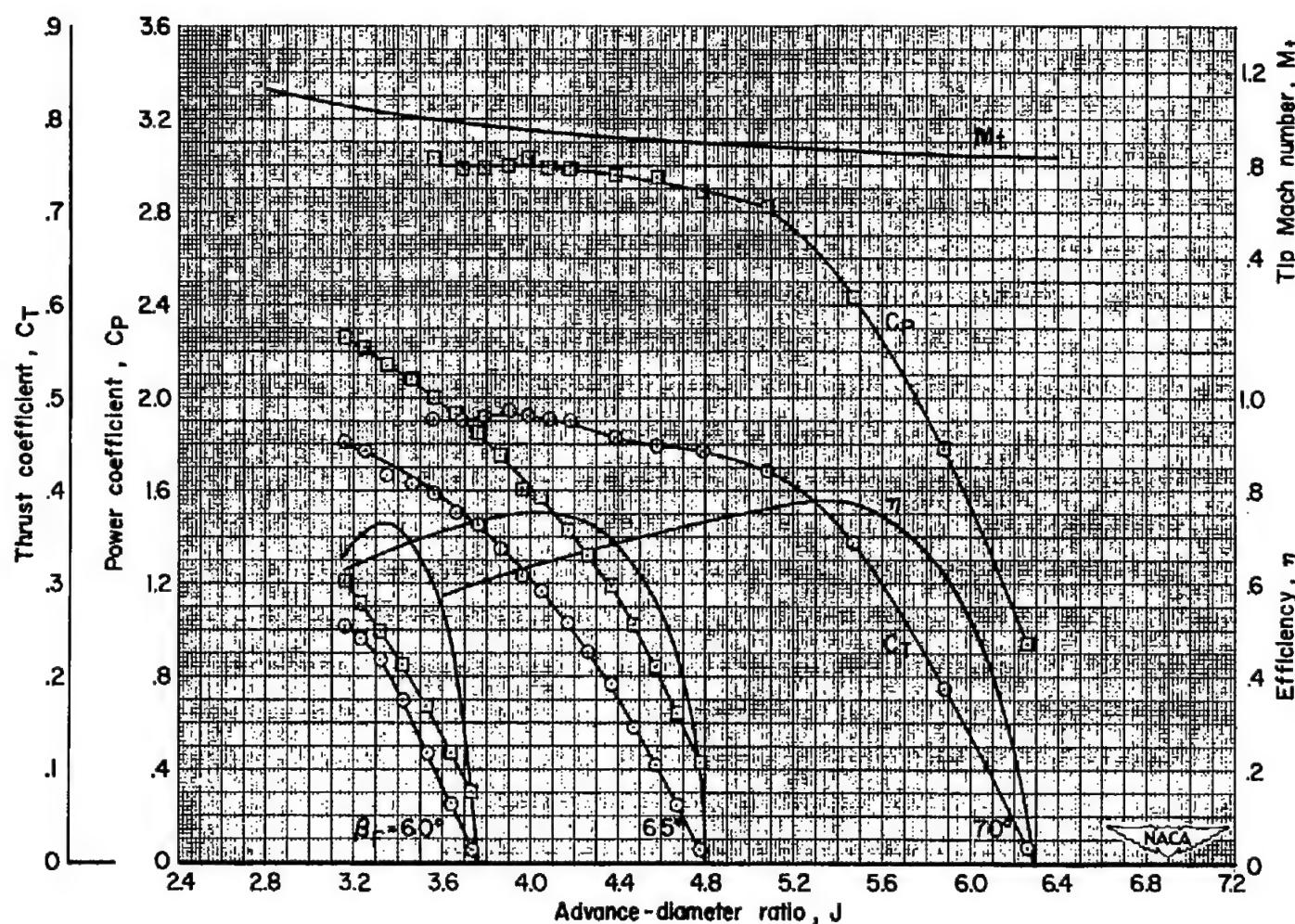
(f) $M = 0.75$

Figure 7.- Continued.

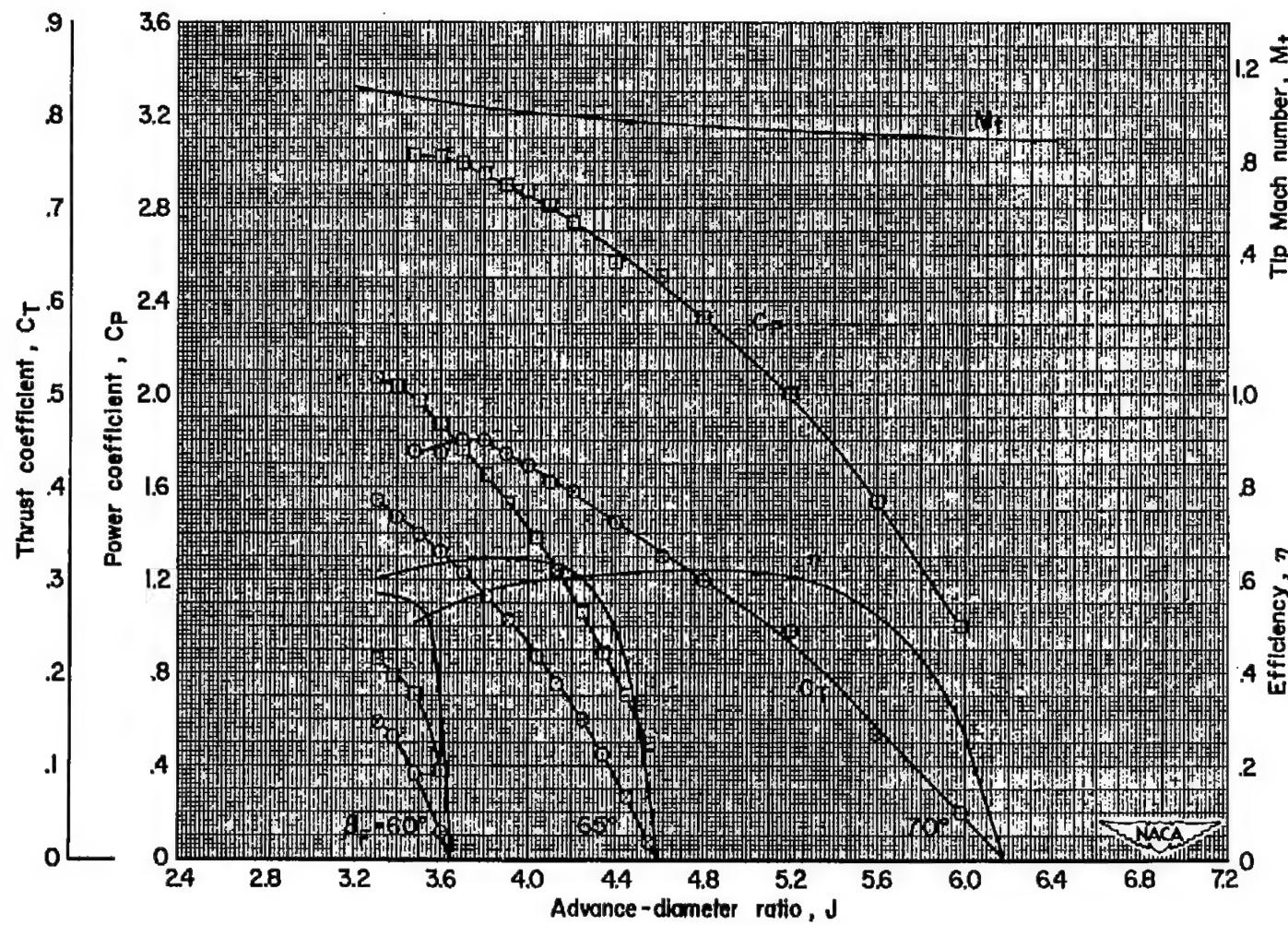
(g) $M = 0.80$

Figure 7.- Continued.

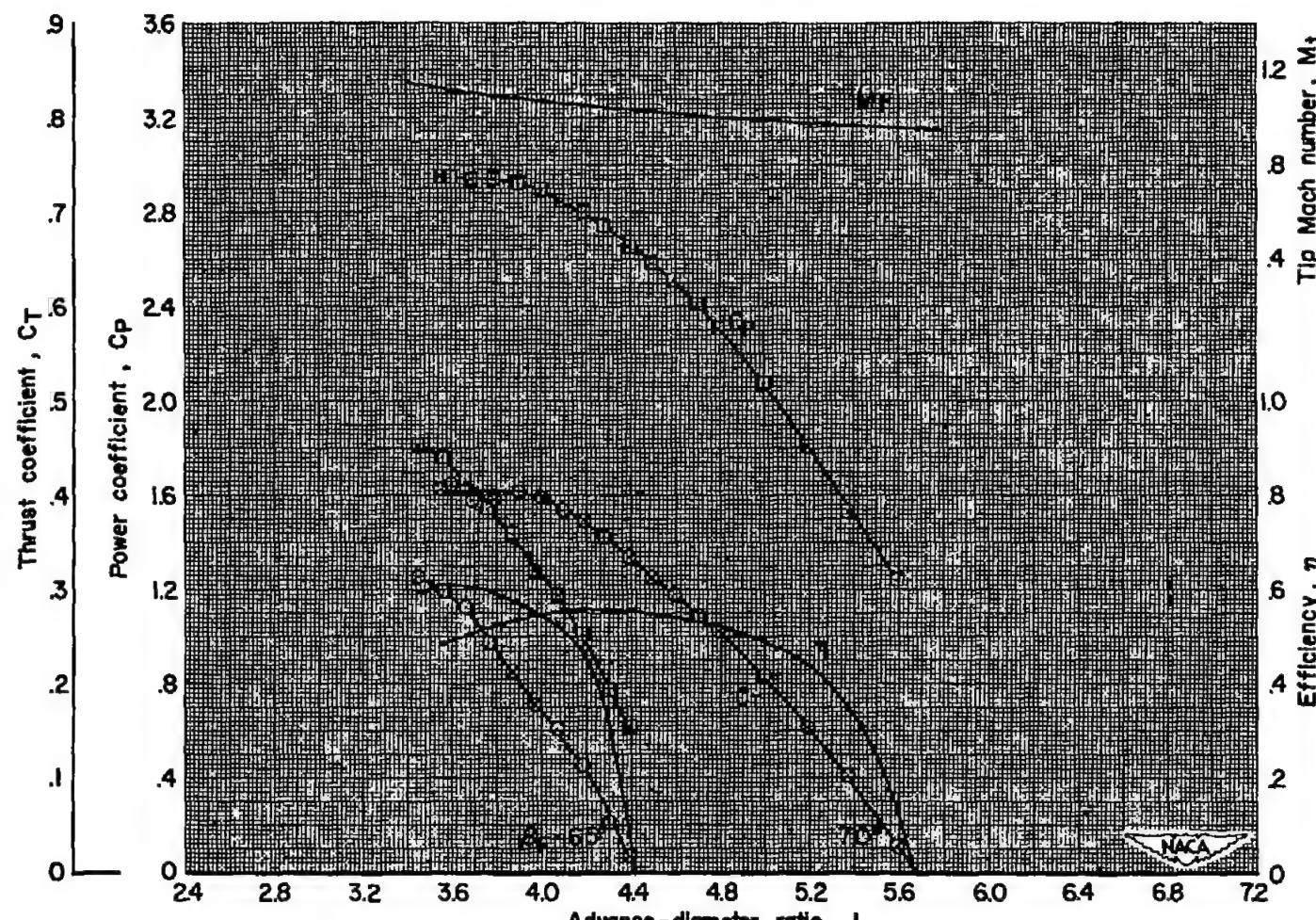
(b) $M = 0.84$

Figure 7.- Concluded.

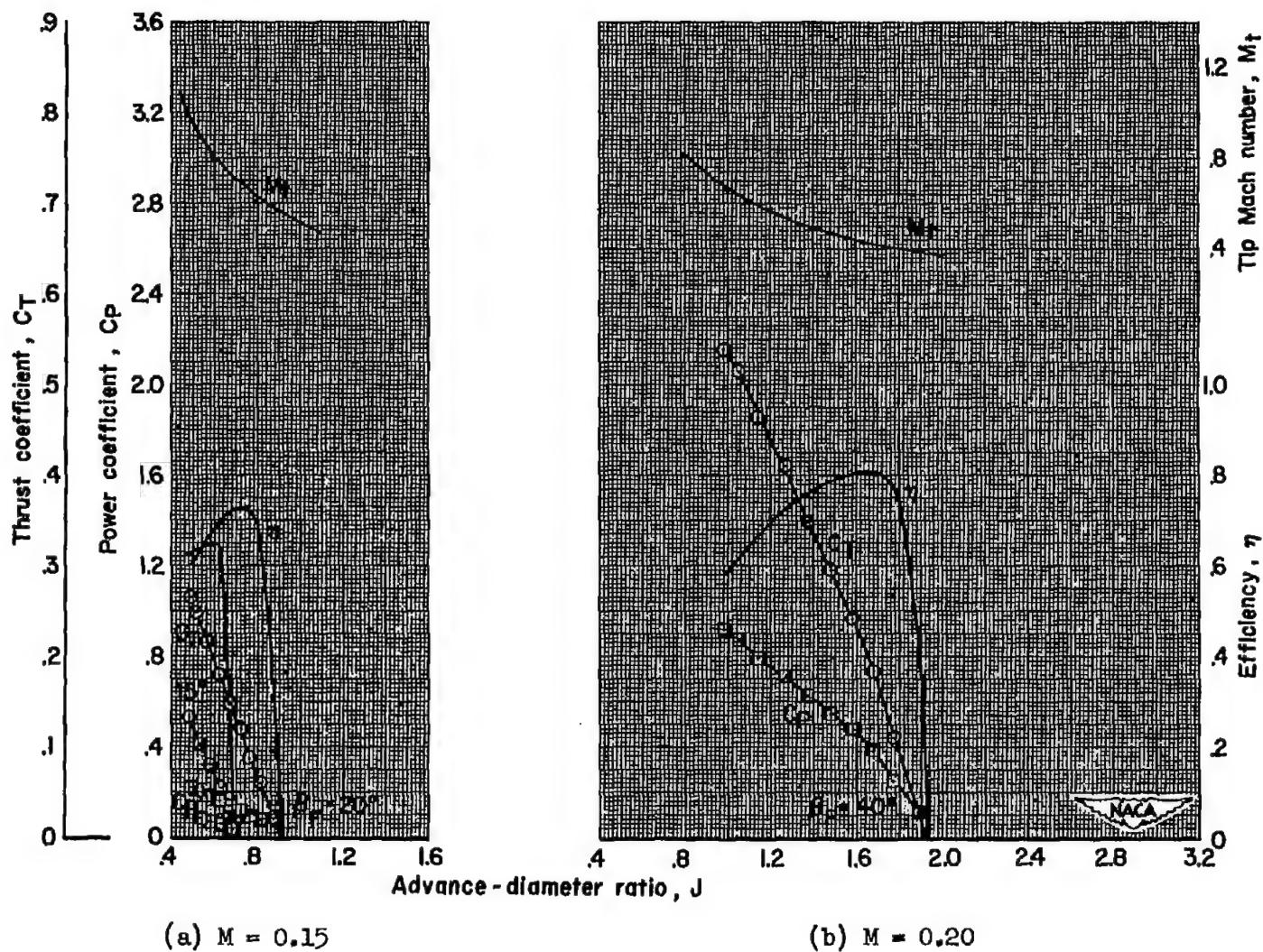


Figure 8.- Positive-thrust characteristics; NACA 4-(5)(05)-037 eight-blade, dual-rotation propeller,
 $\Delta\beta$ = optimum, spinner A.

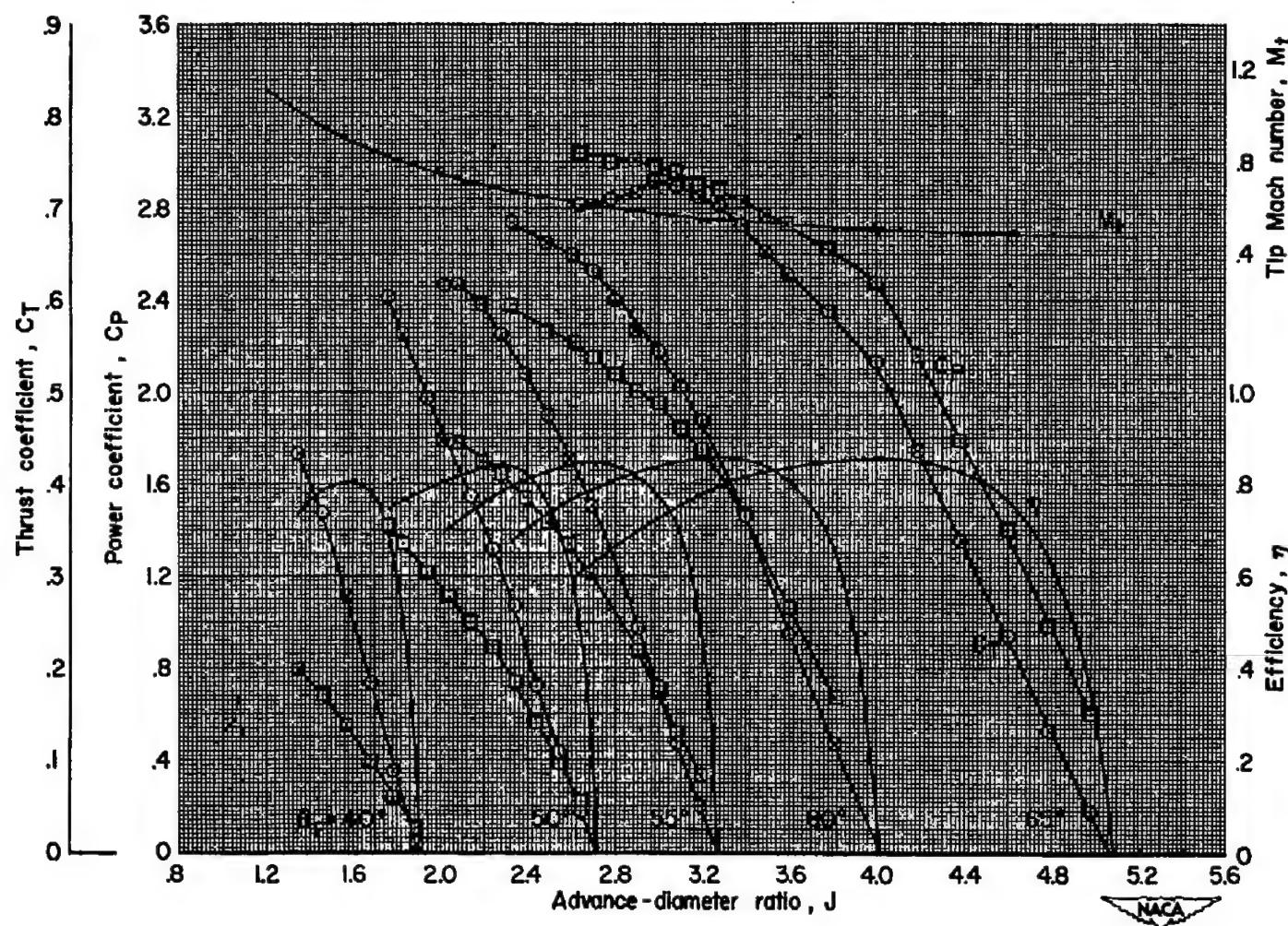
(c) $M = 0.40$

Figure 8.- Continued.

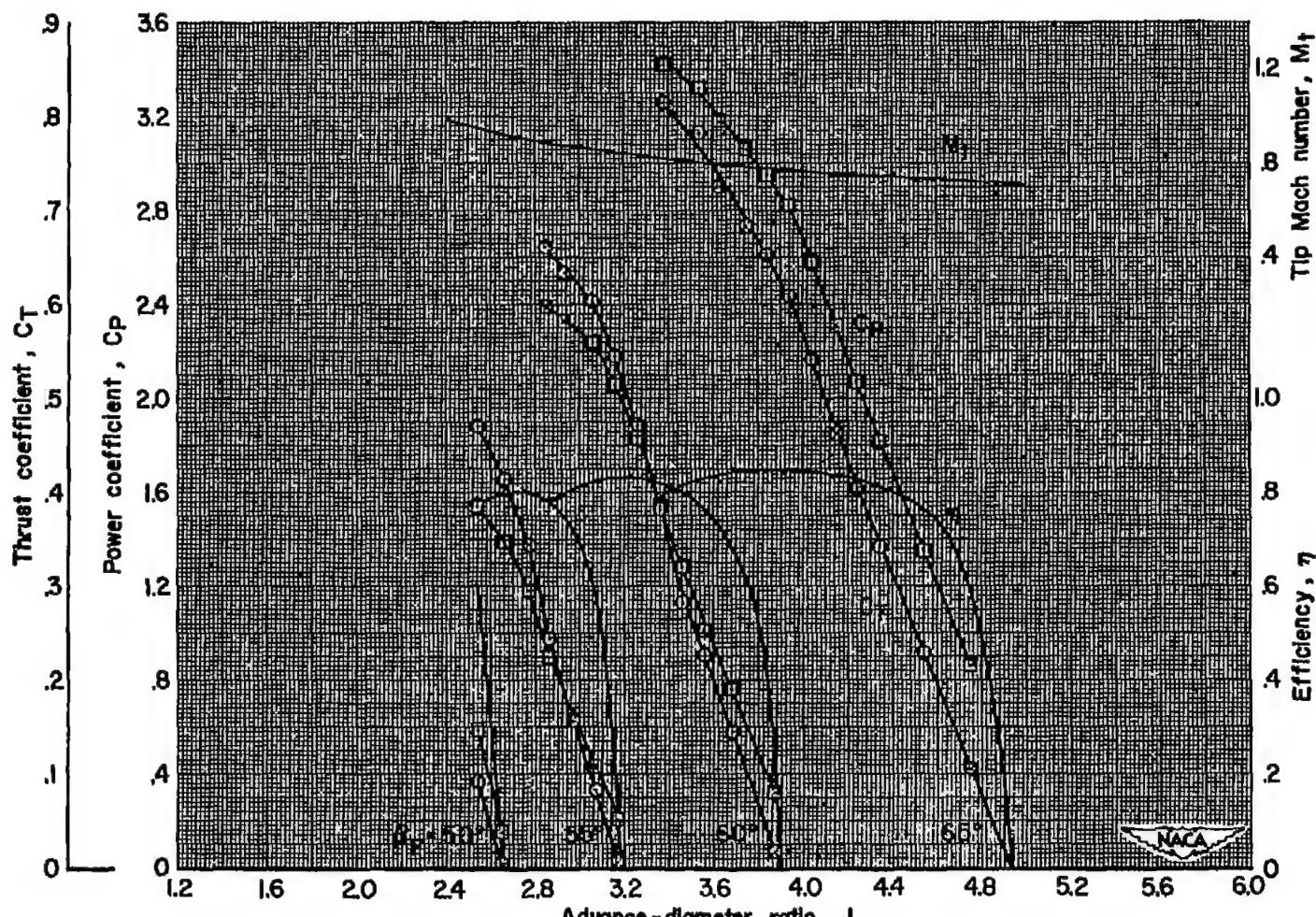
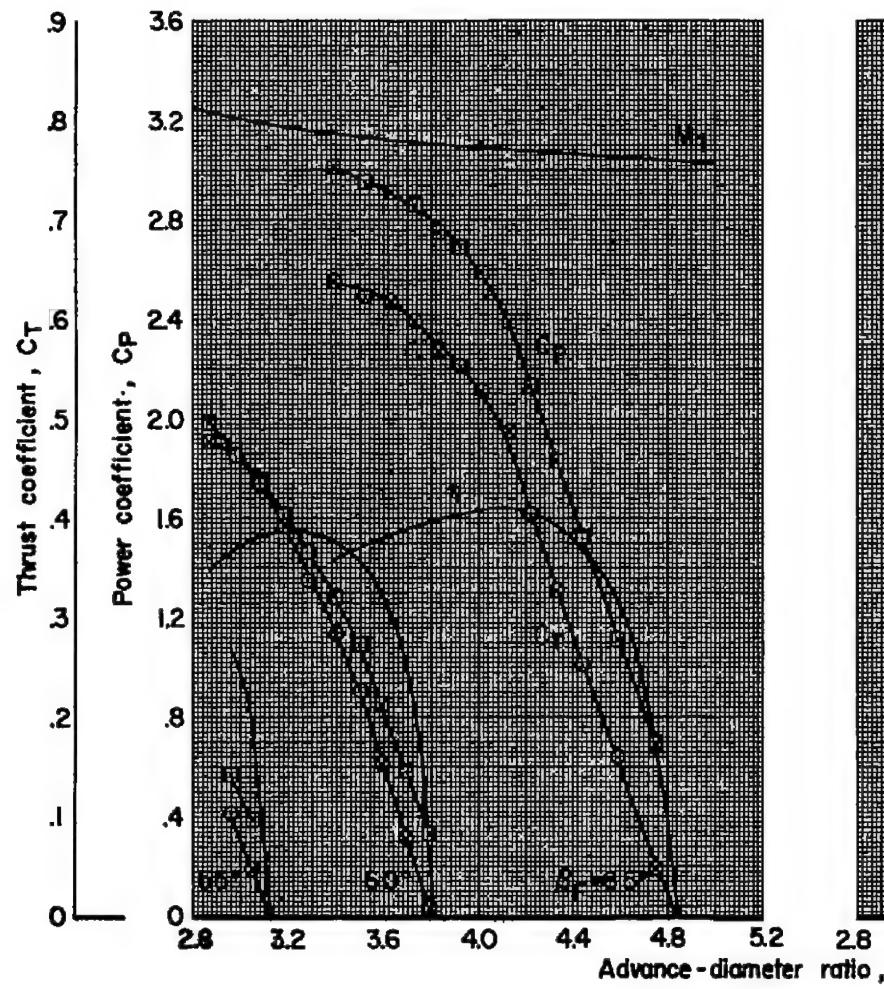
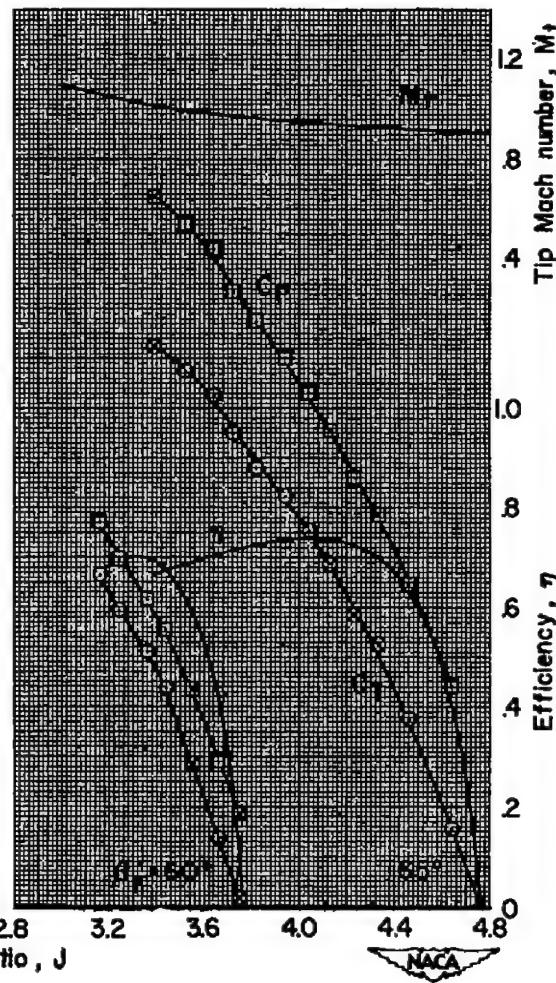
(d) $M = 0.60$

Figure 8.- Continued.



(e) $M = 0.70$



(f) $M = 0.75$

Figure 8.- Continued.

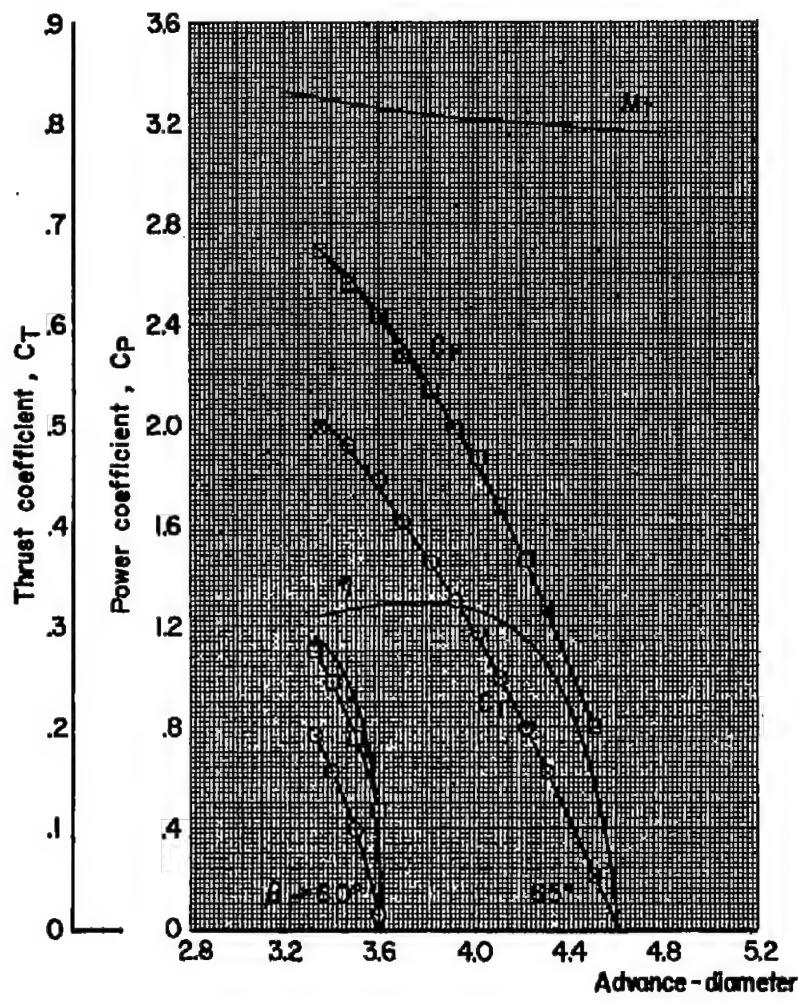
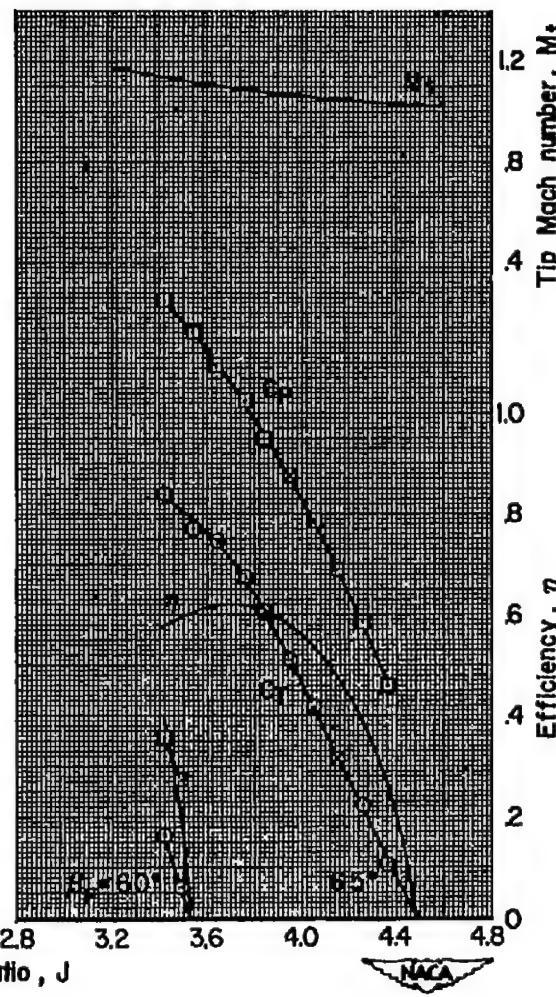
(g) $M = 0.80$ (h) $M = 0.84$

Figure 8.- Concluded.

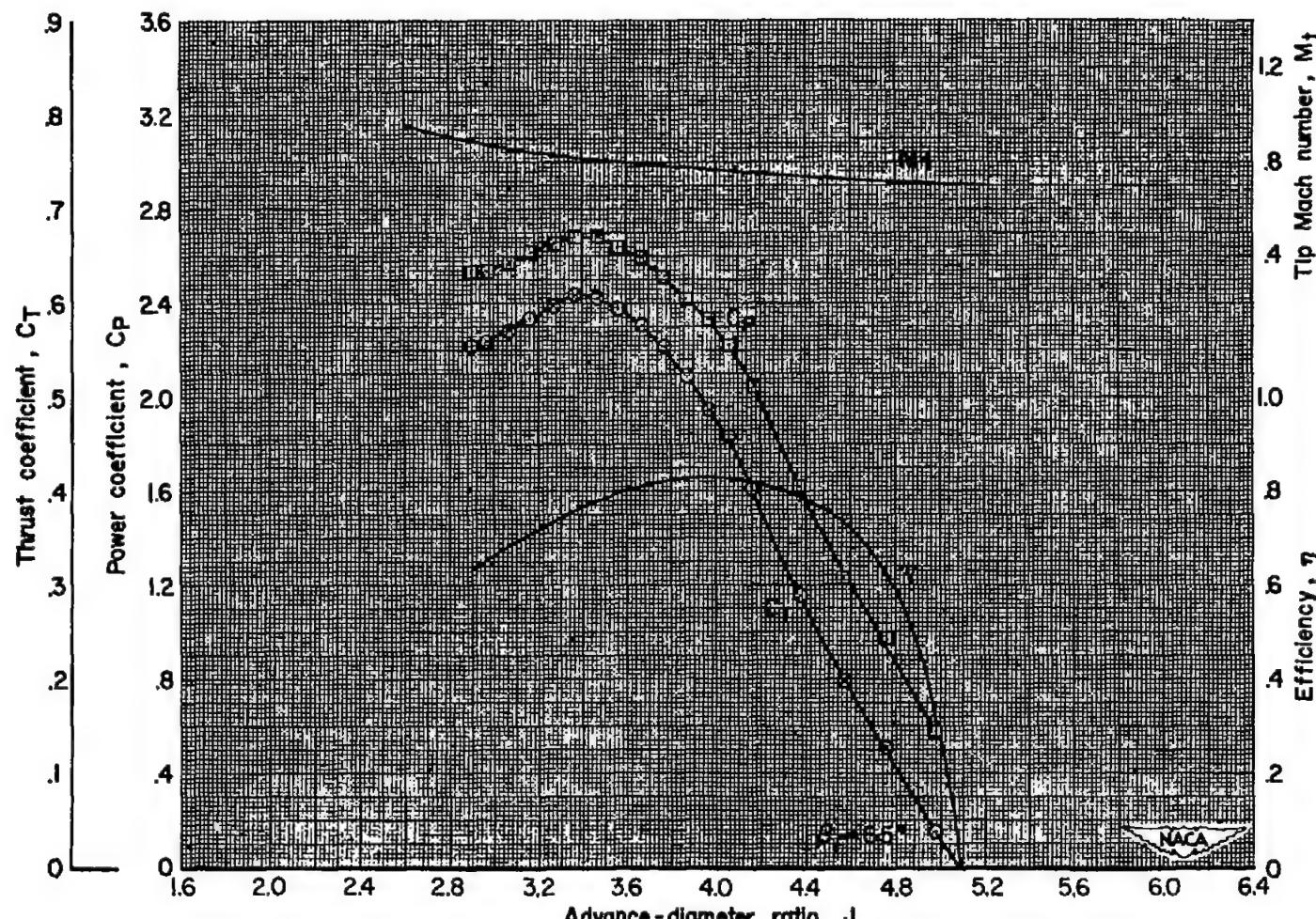
(a) $M = 0.60$

Figure 9.- Positive-thrust characteristics; NACA 4-(5)(05)-037 six-blade, dual-rotation propeller,
 $\Delta\beta = 0.8^\circ$, spinner A.

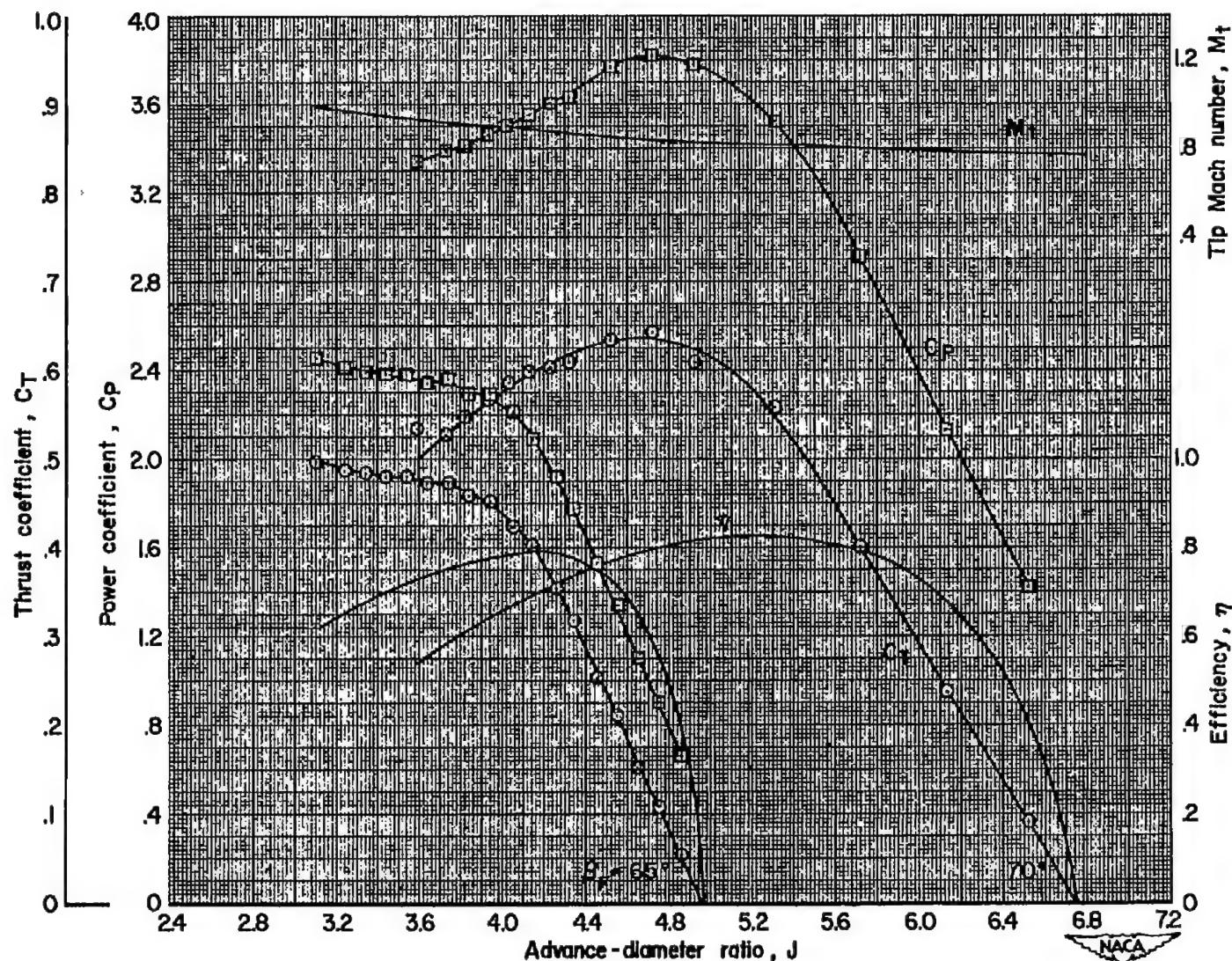
(b) $M = 0.70$

Figure 9.- Continued.

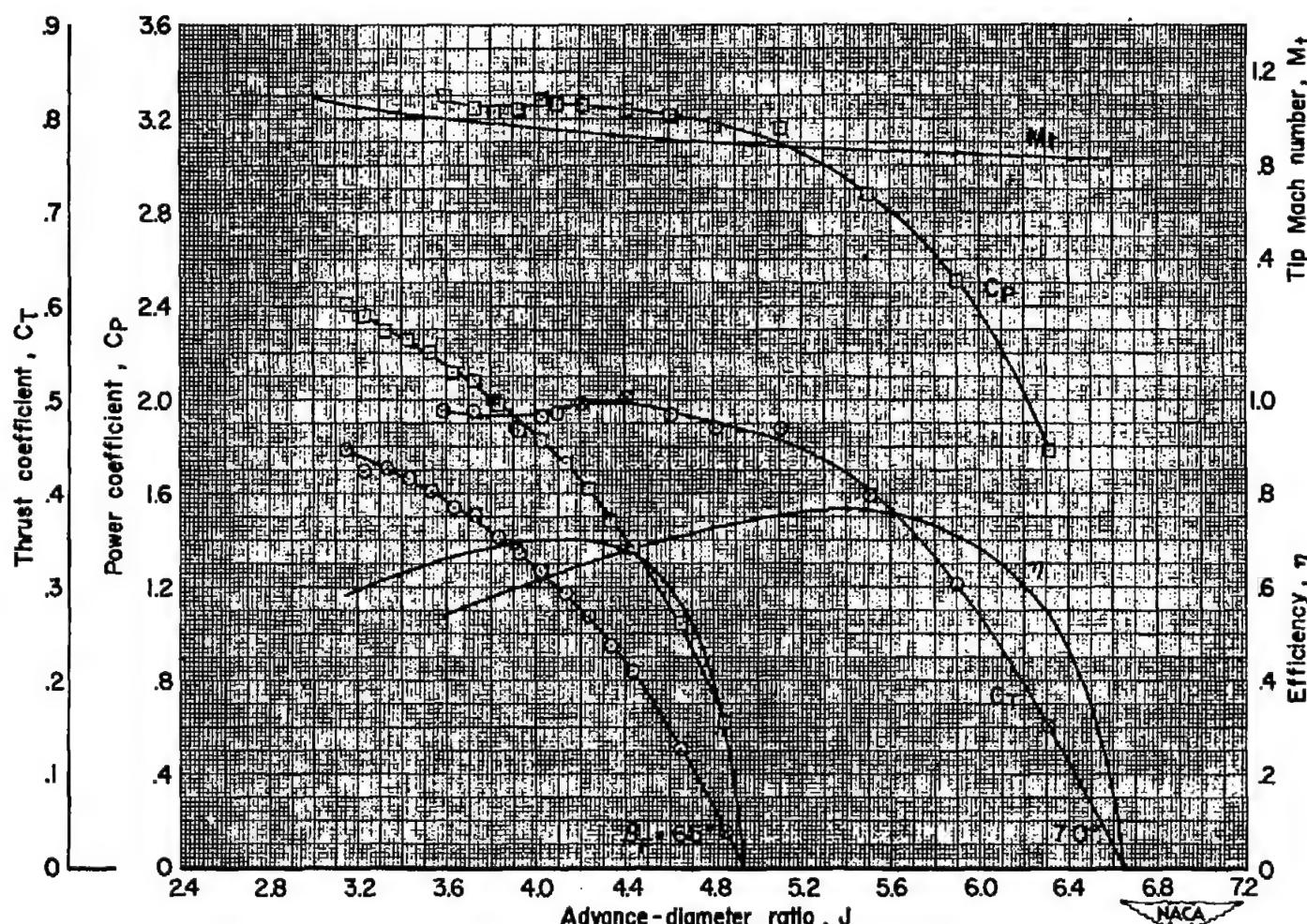
(c) $M = 0.75$

Figure 9.- Continued.

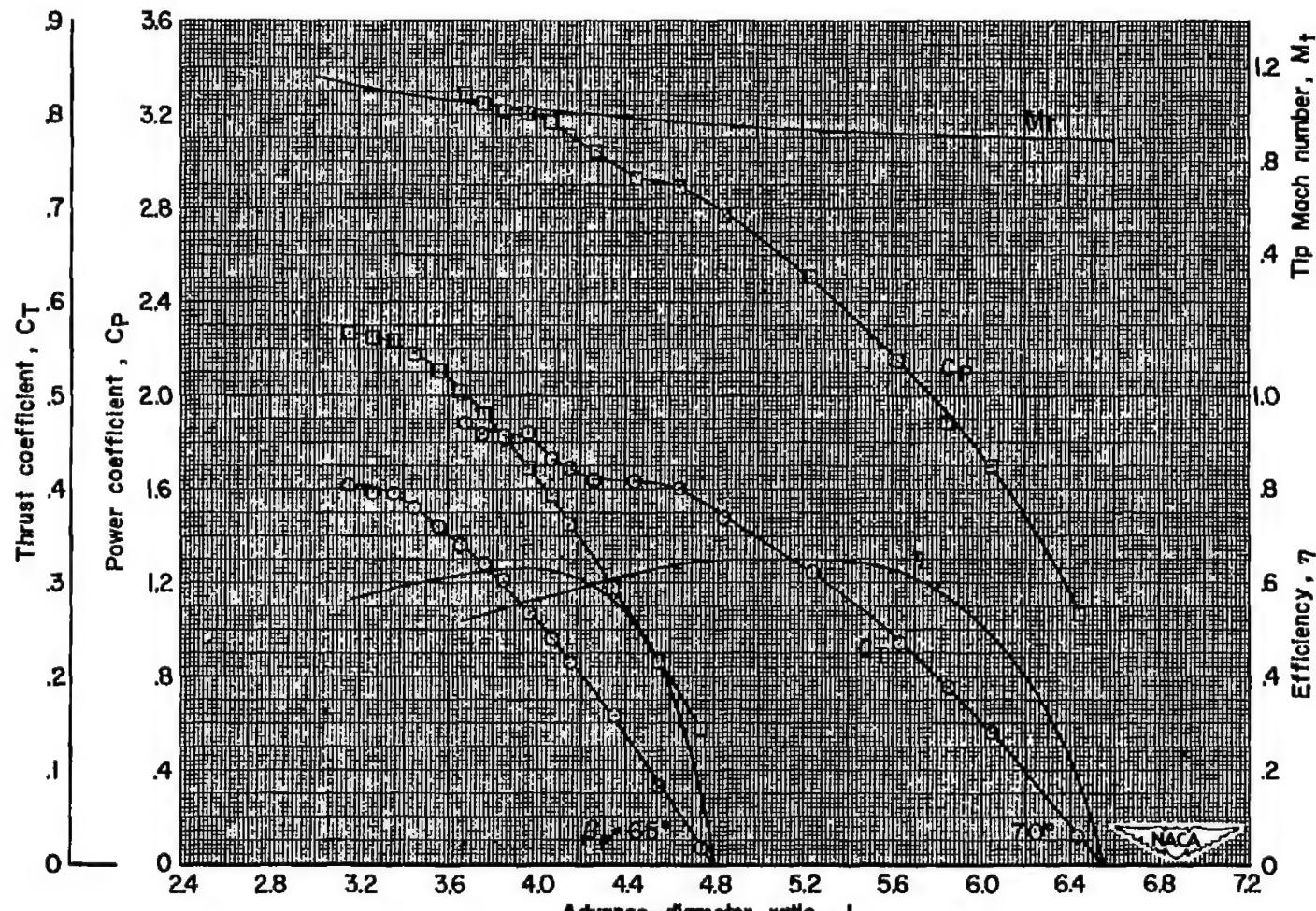
(d) $M = 0.80$

Figure 9.- Continued.

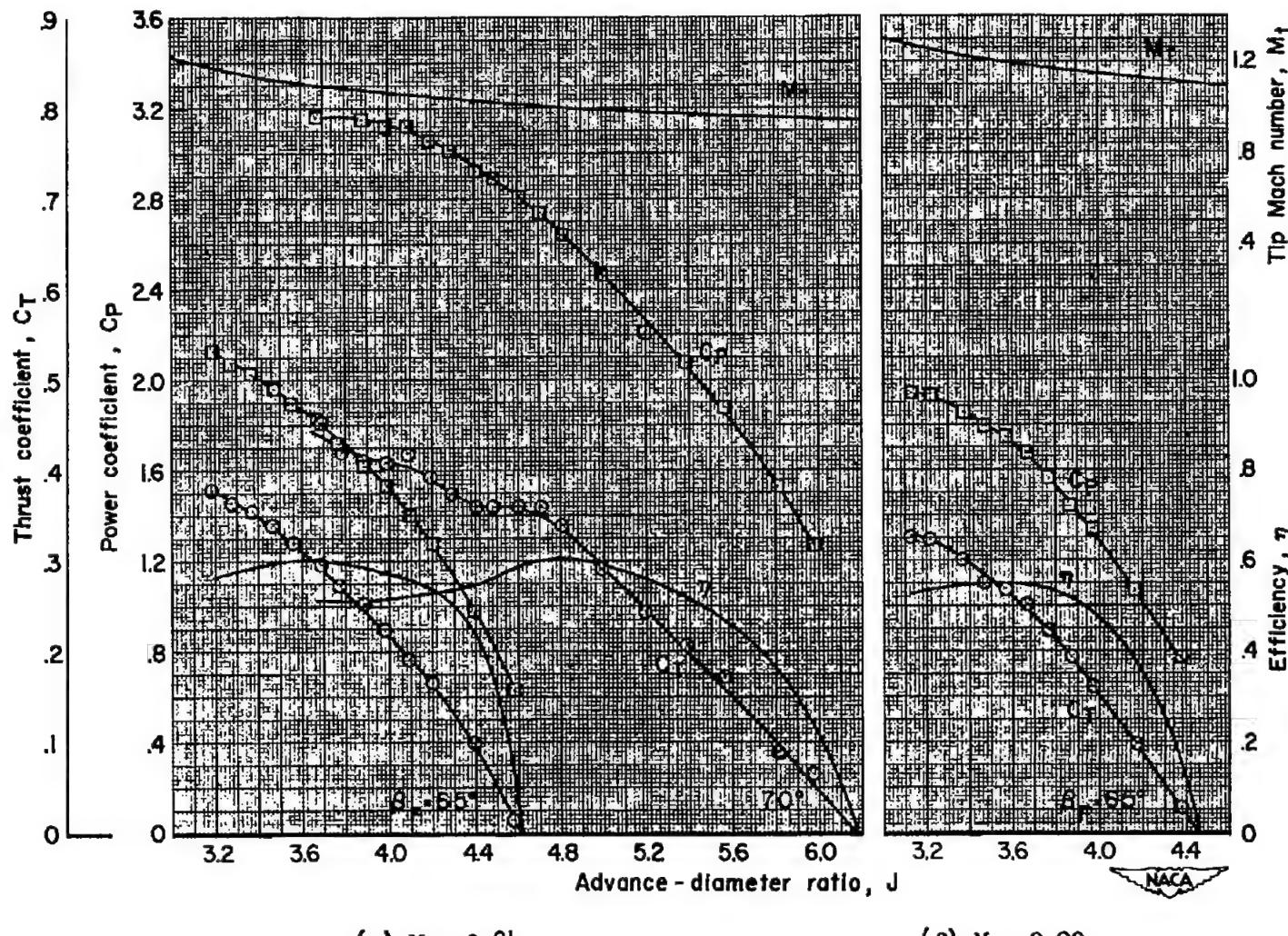
(e) $M = 0.84$ (f) $M = 0.90$

Figure 9.- Concluded.

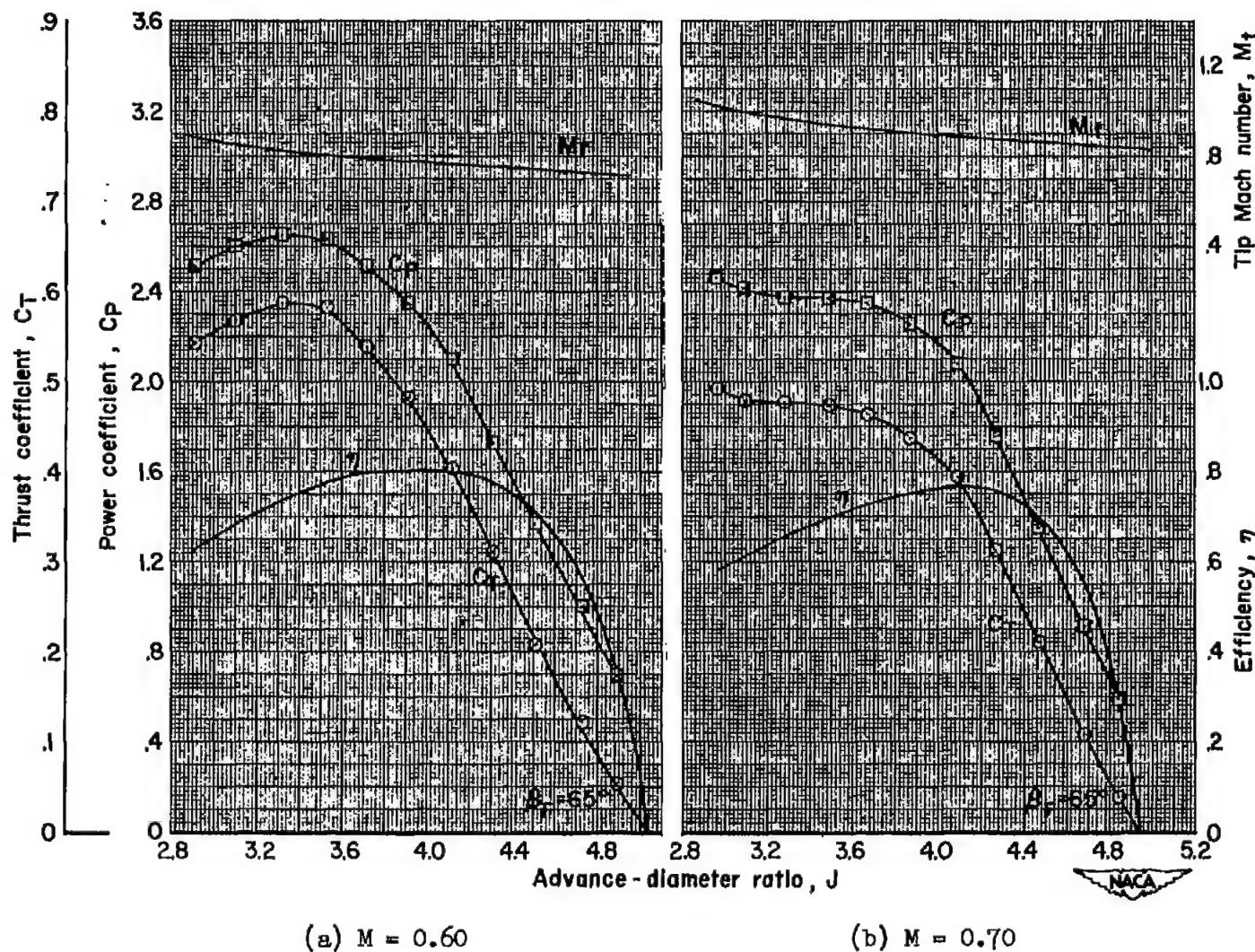


Figure 10.- Positive-thrust characteristics; NACA 4-(5)(05)-037 six-blade, dual-rotation propeller,
 $\Delta\beta = 0.8^\circ$, spinner B.

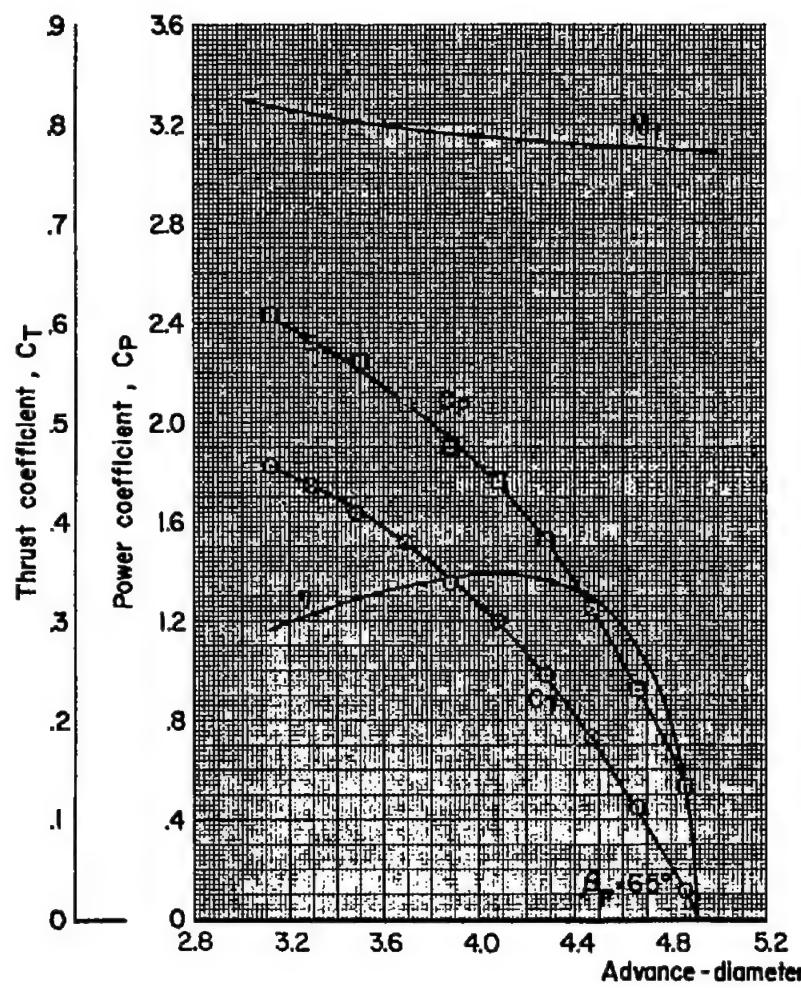
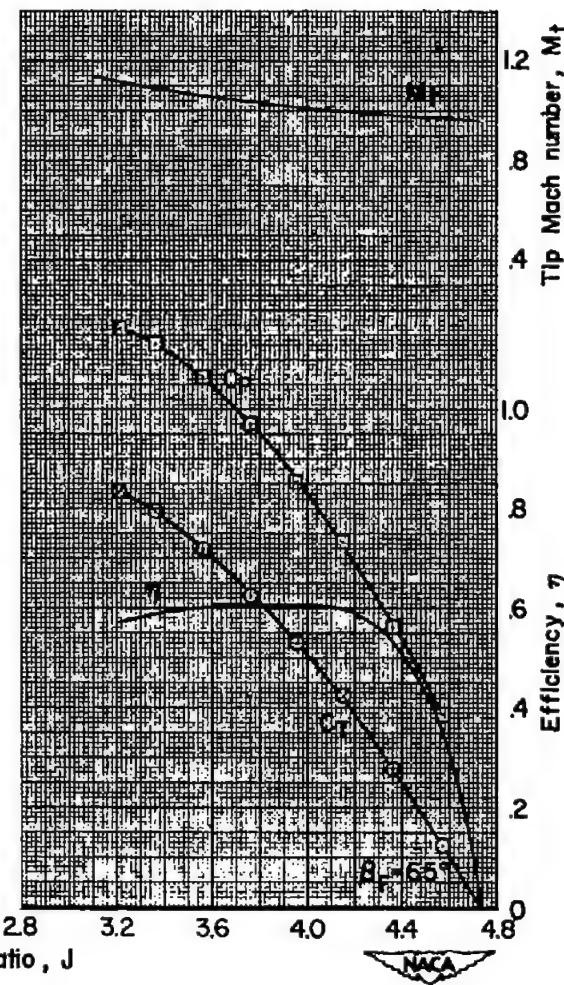
(c) $M = 0.75$ (d) $M = 0.80$

Figure 10.- Continued.

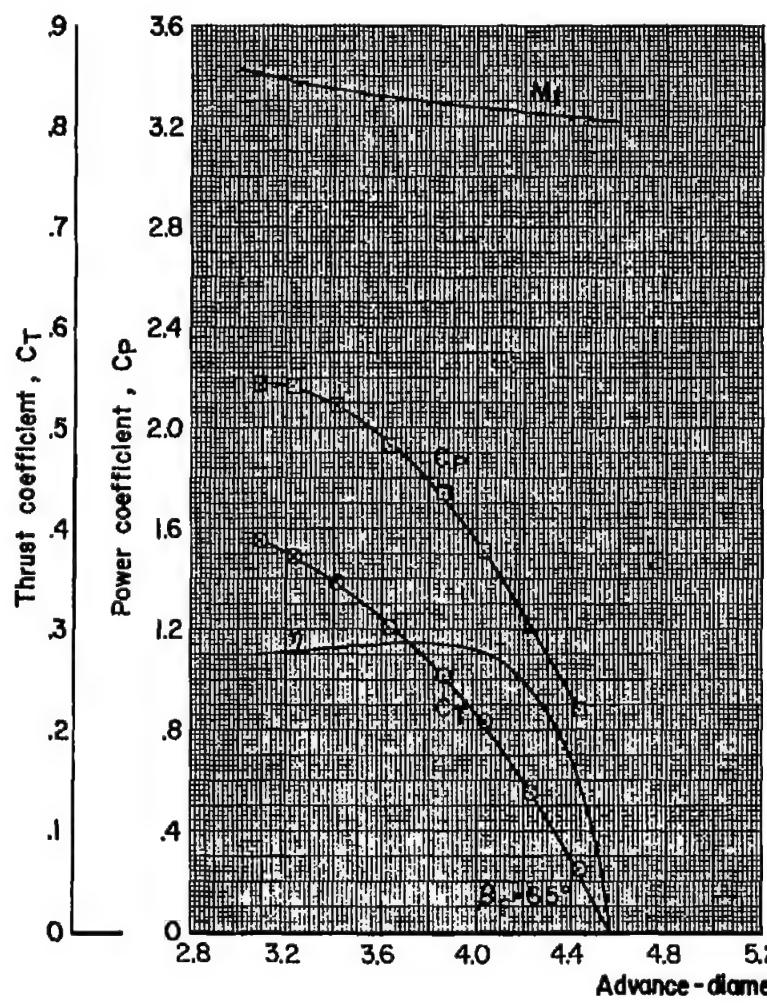
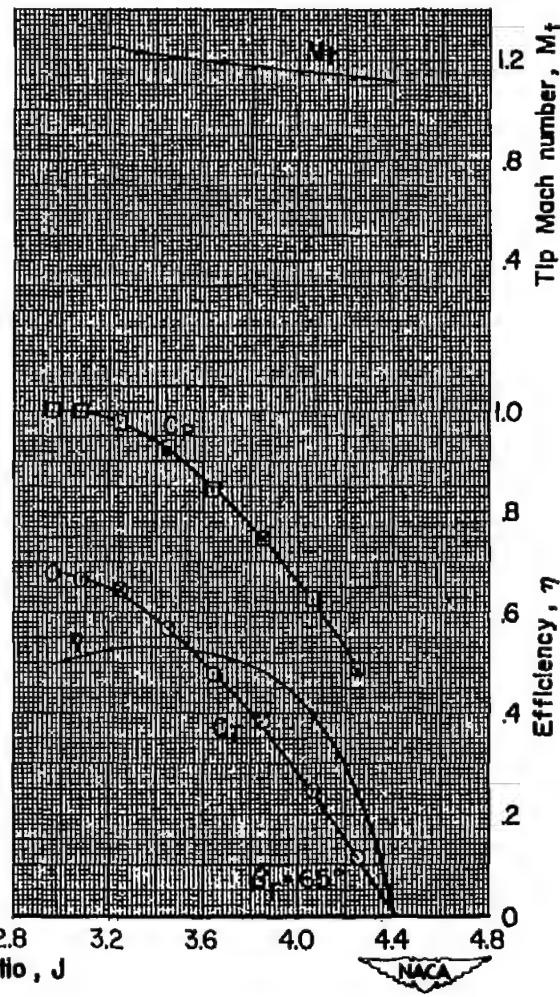
(e) $M = 0.84$ (f) $M = 0.90$

Figure 10.- Concluded.

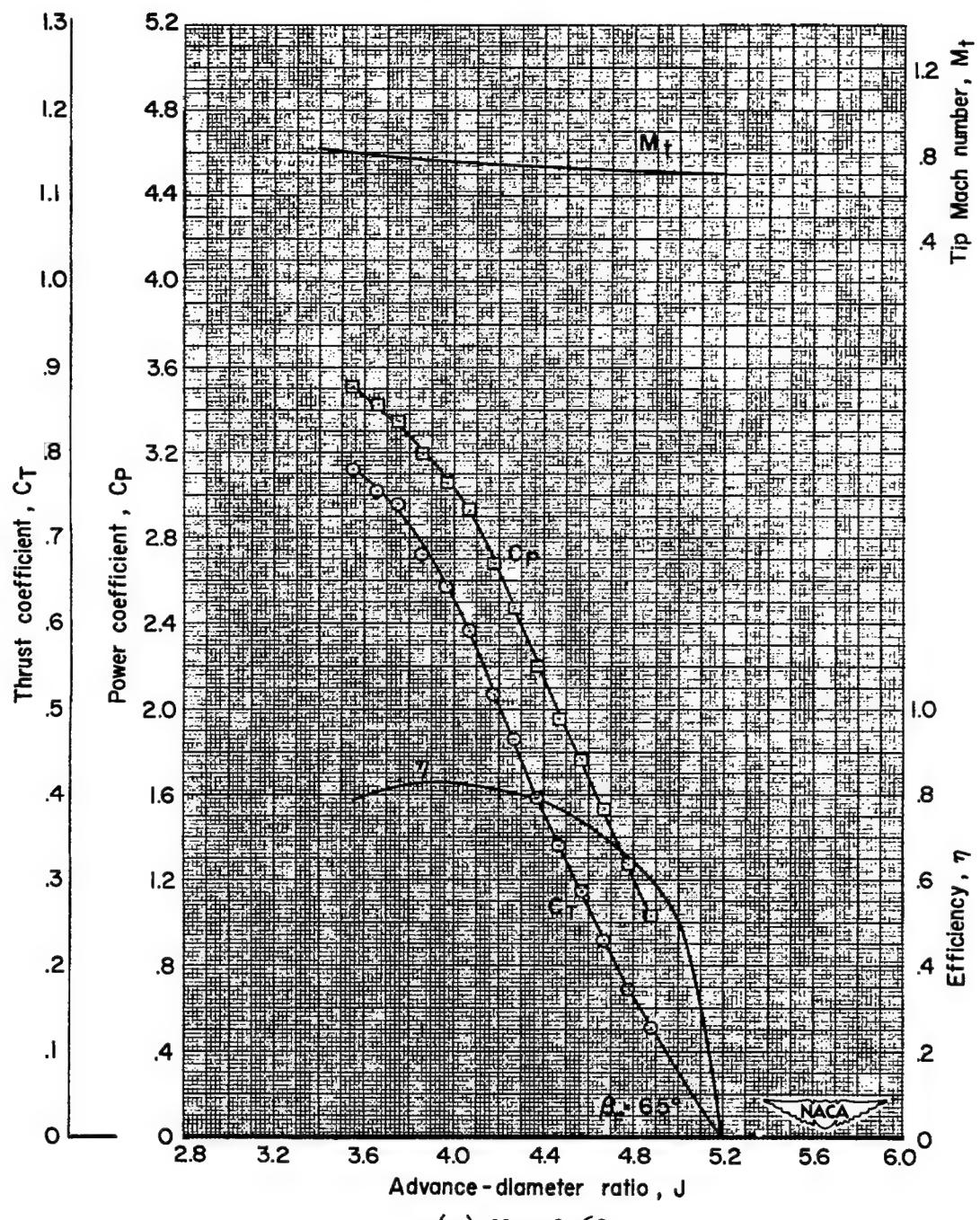
(a) $M = 0.60$

Figure 11.- Positive-thrust characteristics; NACA 4-(5)(05)-037 eight-blade, dual-rotation propeller, $\Delta\beta = 0.8^\circ$, spinner A.

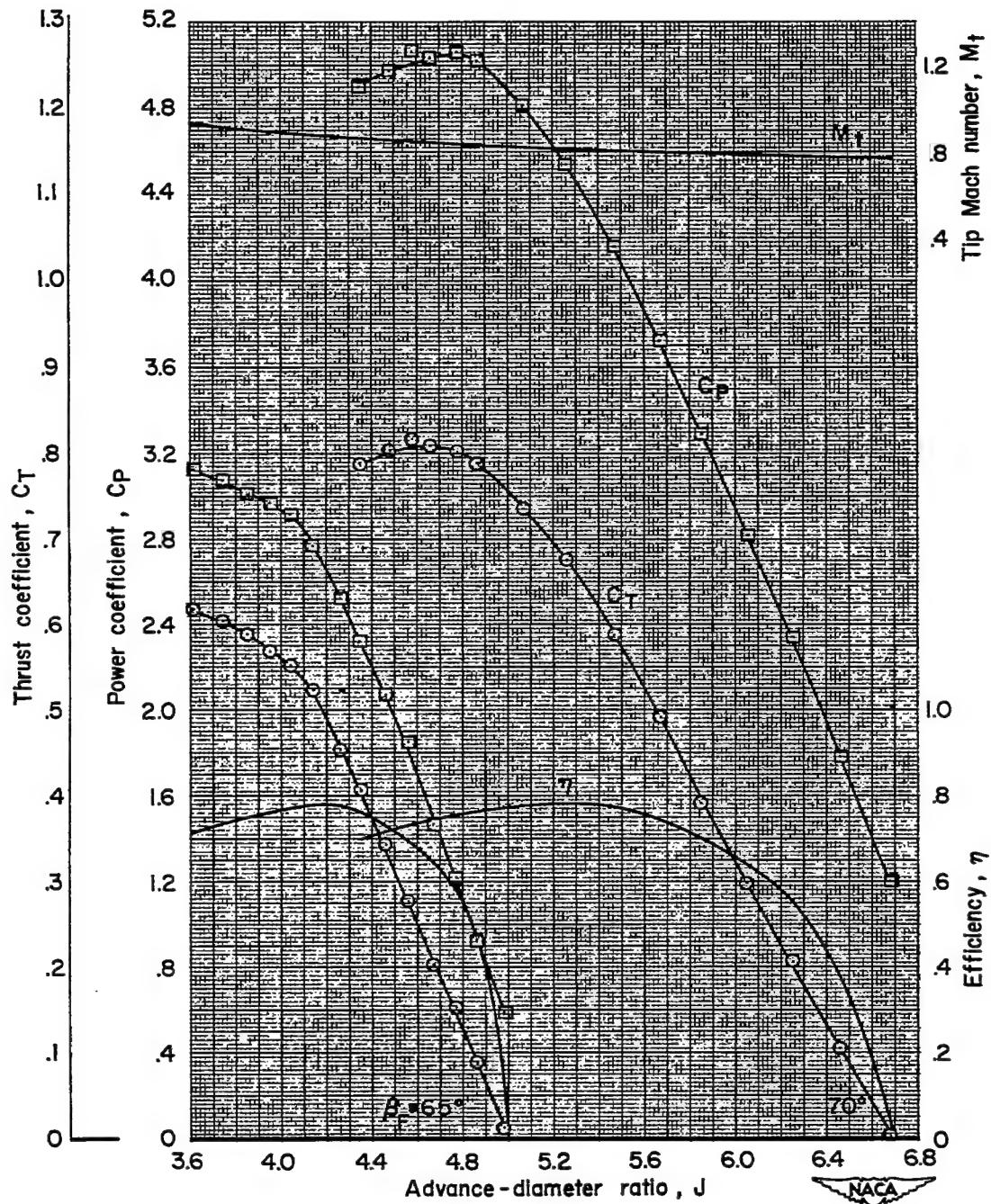
(b) $M = 0.70$

Figure 11.- Continued.

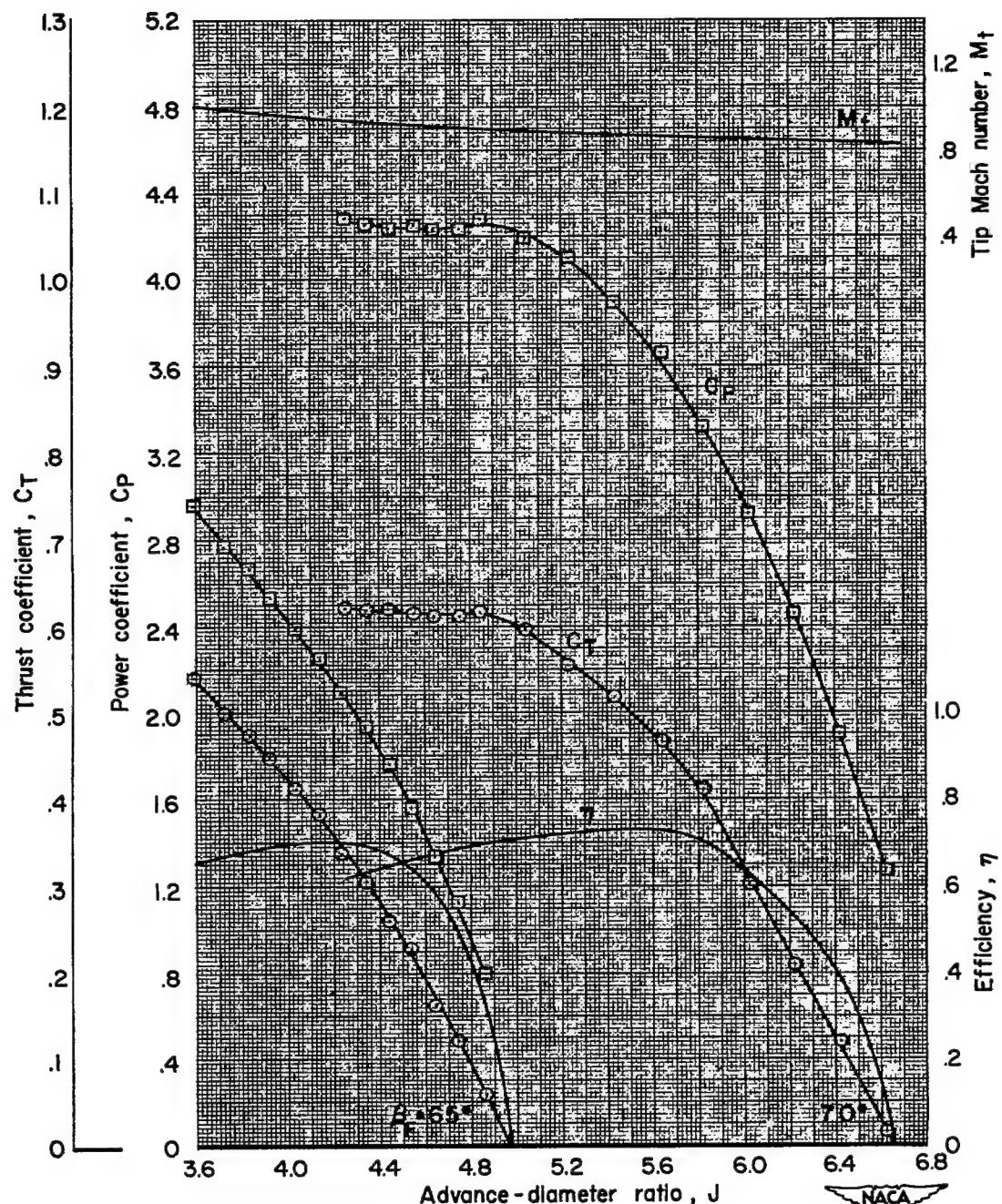
(c) $M = 0.75$

Figure 11.- Continued.

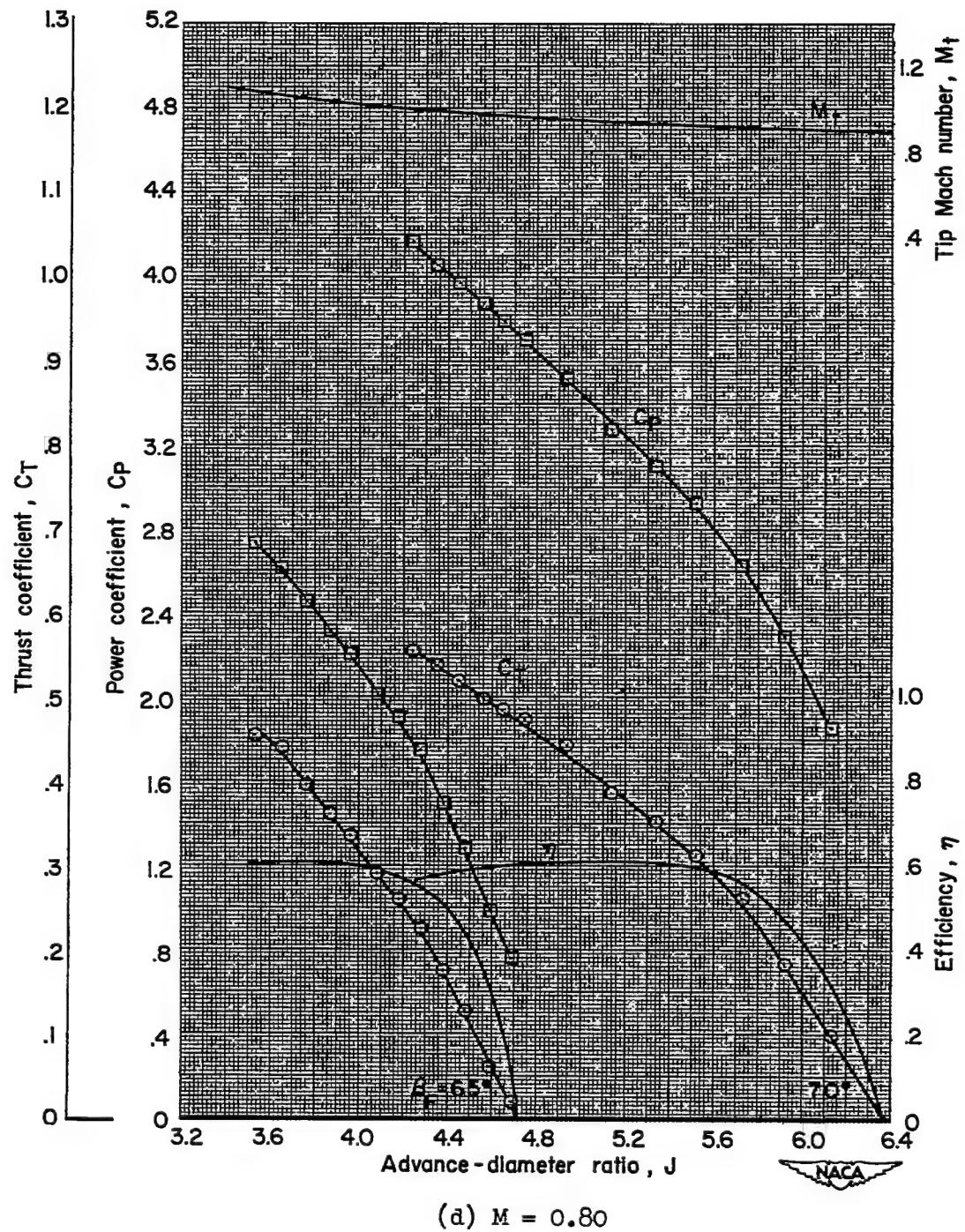


Figure 11.- Continued.

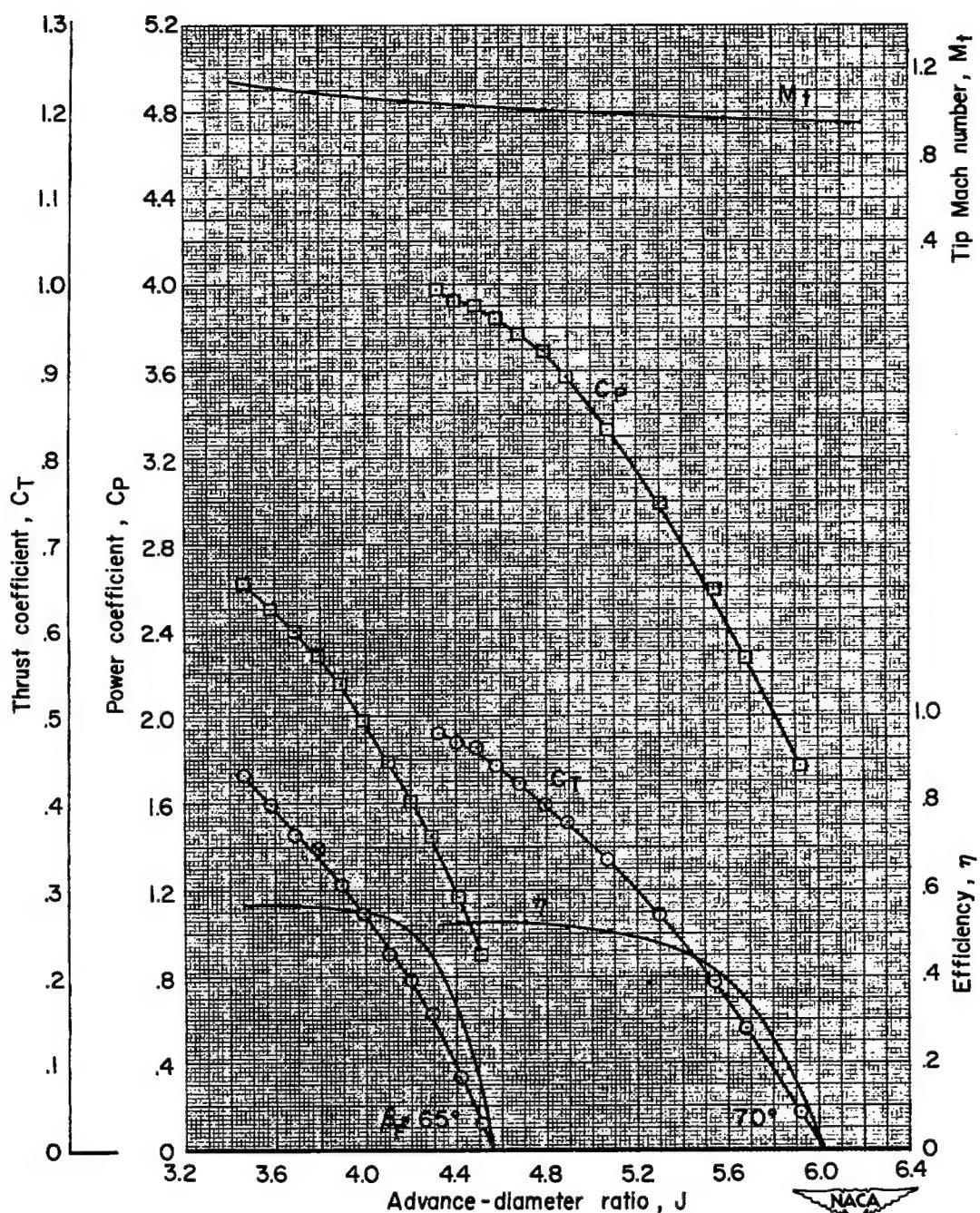
(e) $M = 0.84$

Figure 11.- Continued.

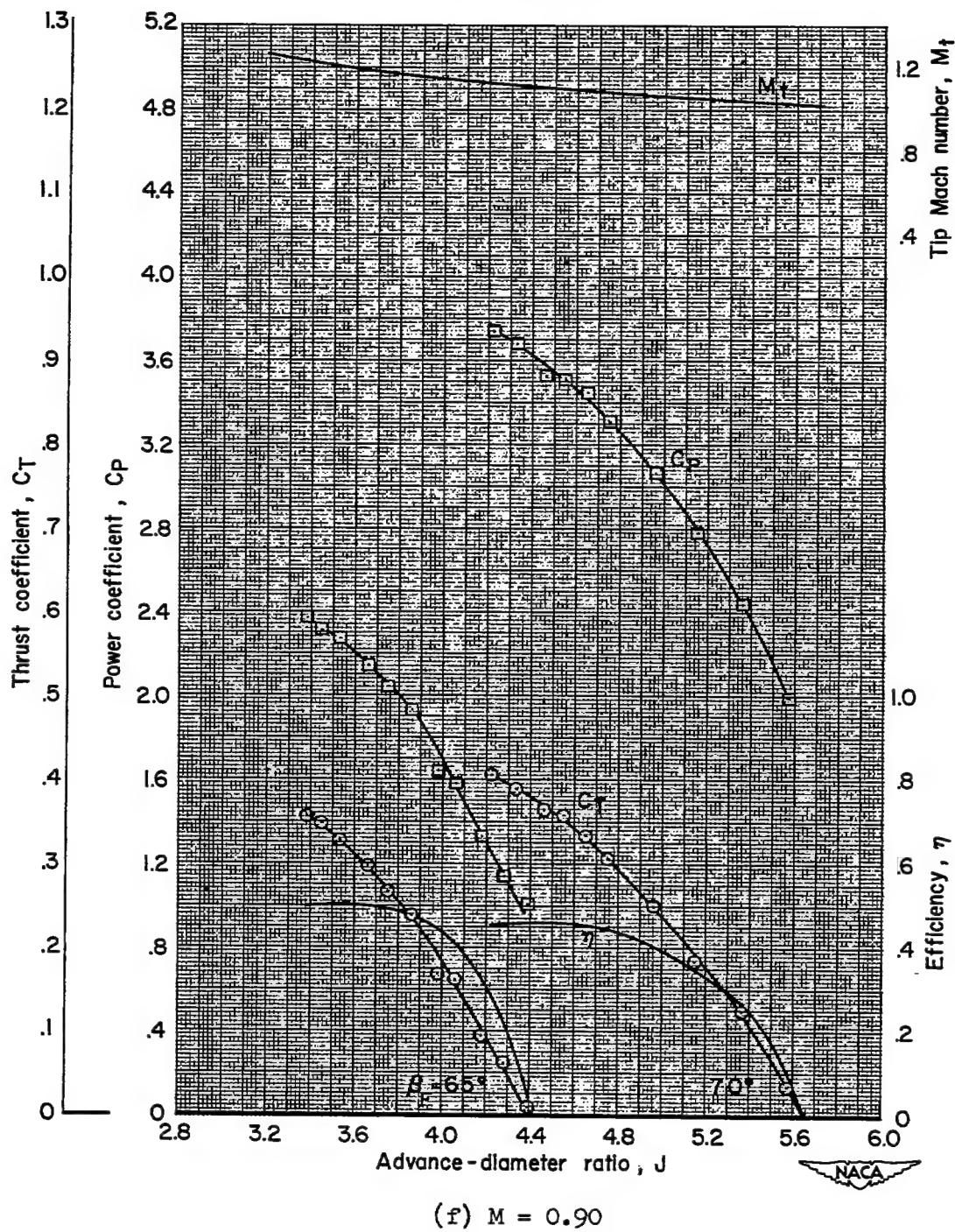


Figure 11.- Concluded.

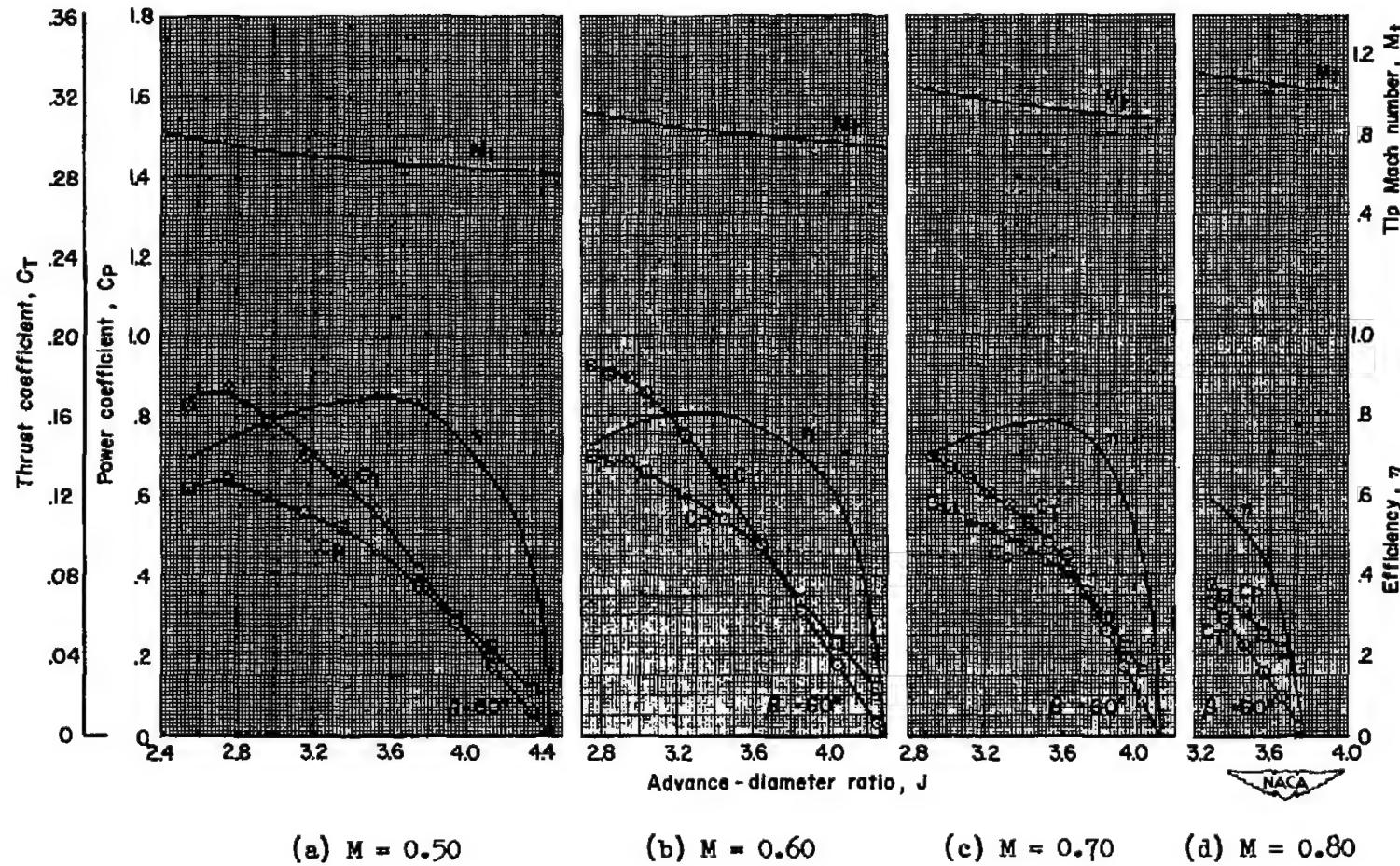


Figure 12.- Positive-thrust characteristics; NACA 4-(5)(05)-041 two-blade, single-rotation propeller, spinner C.

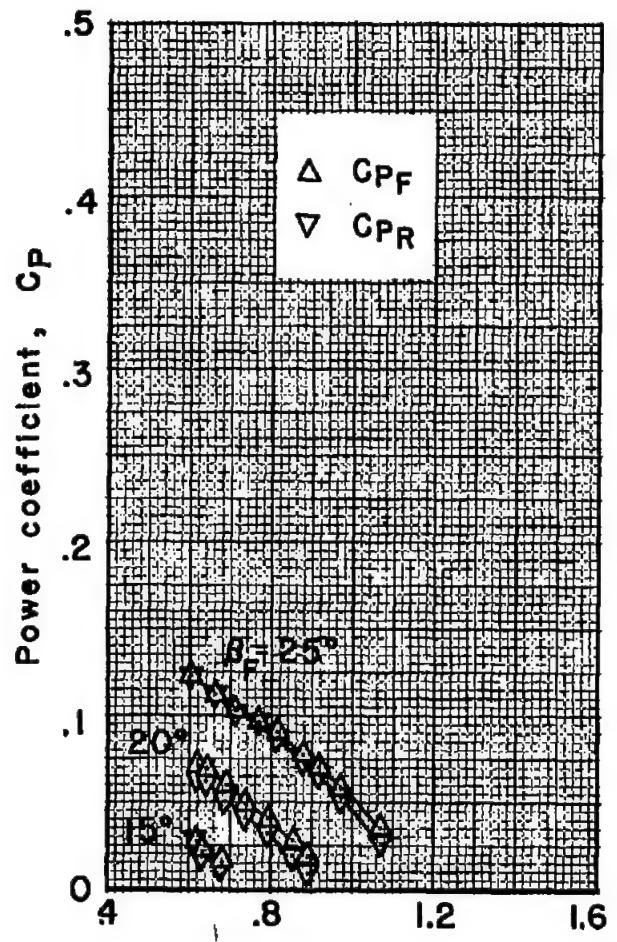
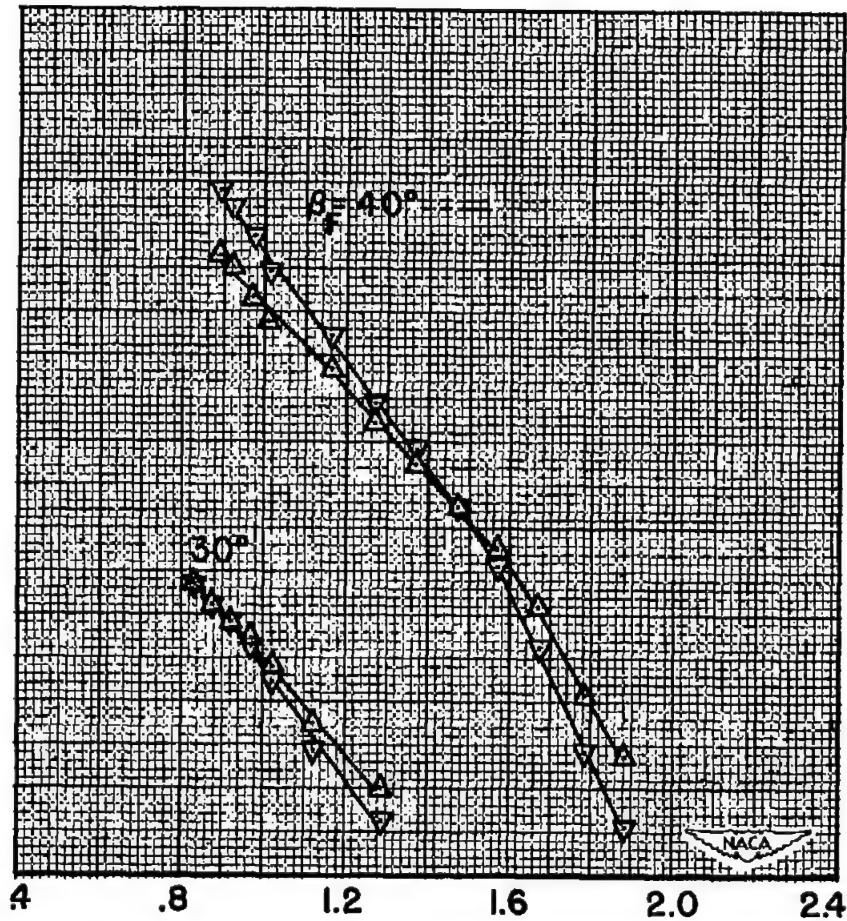
(a) $M = 0.15$ (b) $M = 0.20$

Figure 13.- Variation of power coefficients of the front and rear components with advance-diameter ratio for positive thrust; NACA 4-(5)(05)-037 six-blade, dual-rotation propeller, $\Delta\beta$ = optimum, spinner A.

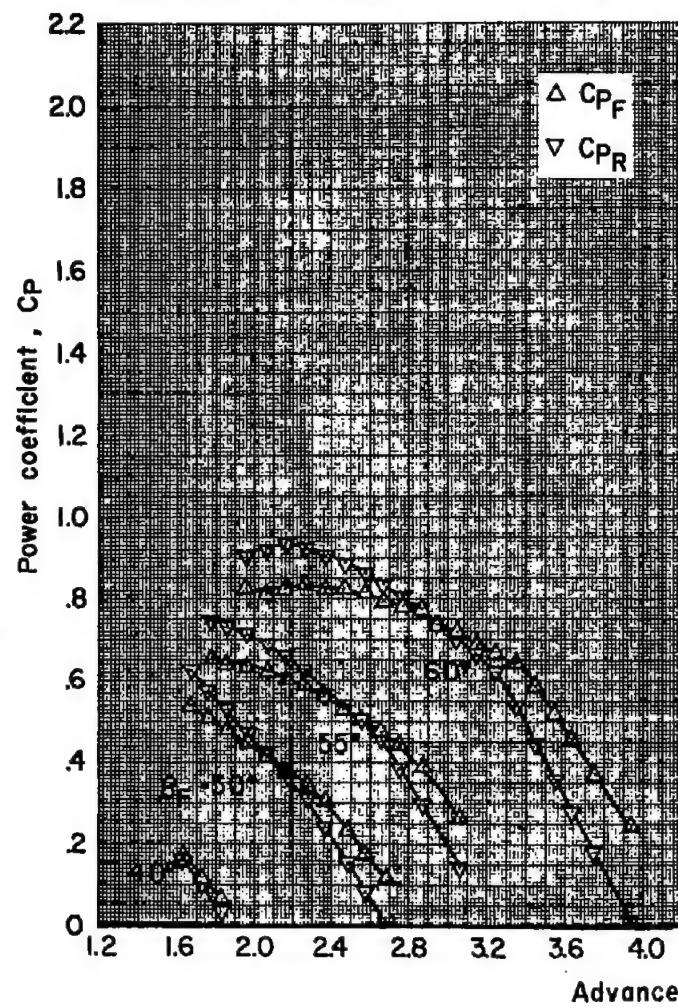
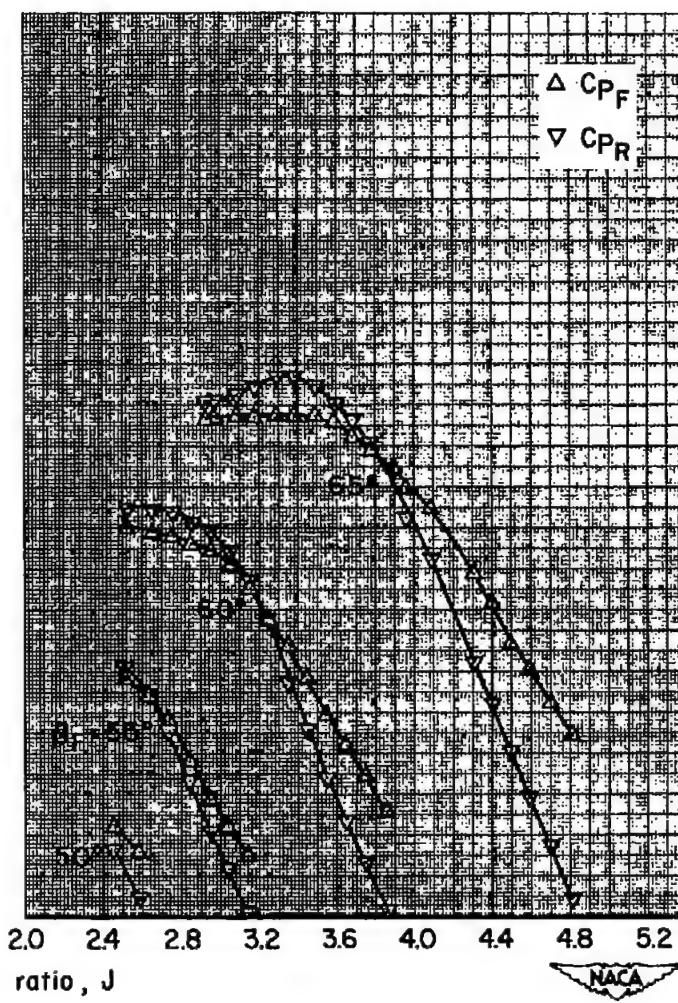
(c) $M = 0.40$ (d) $M = 0.60$

Figure 13.- Continued.

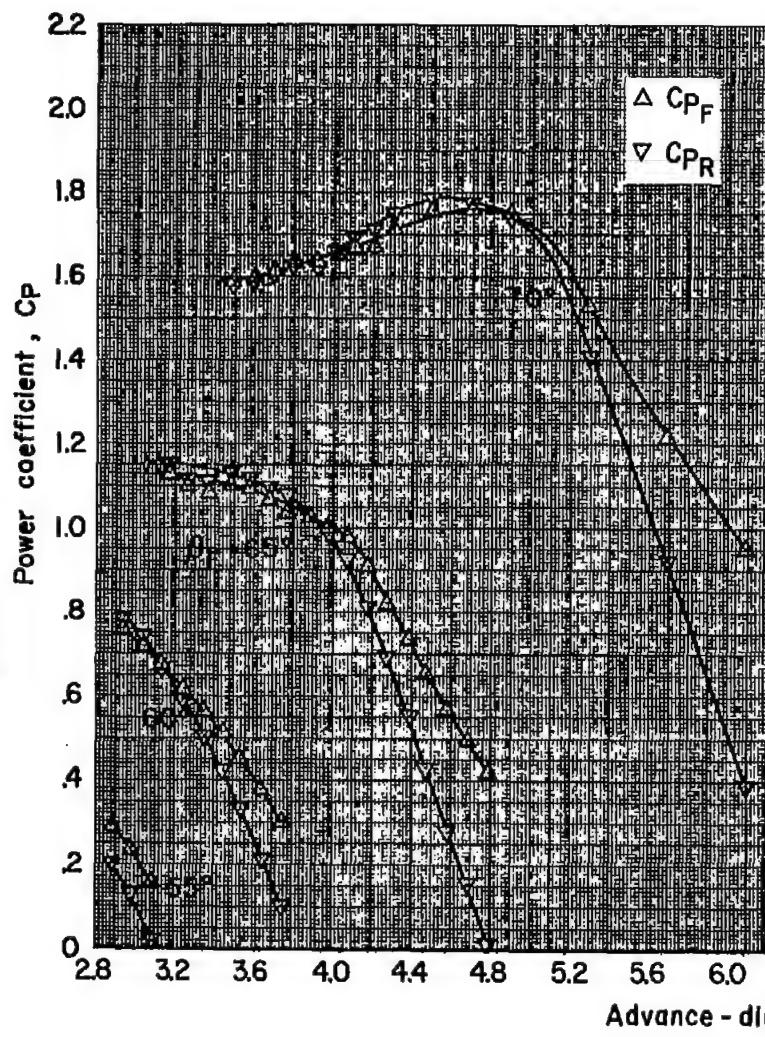
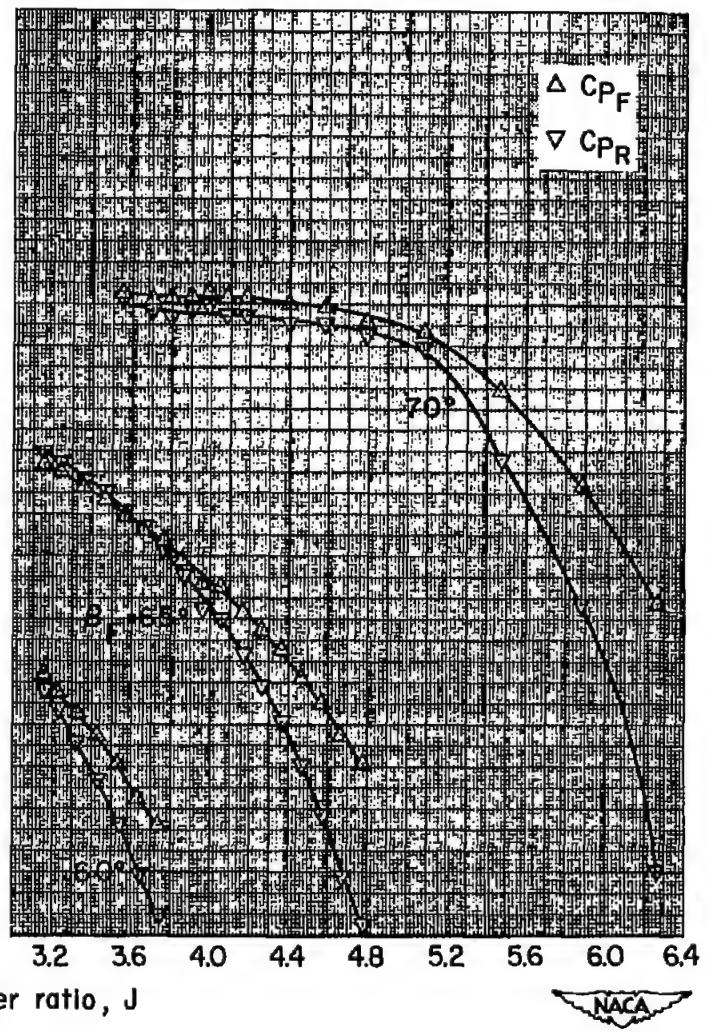
(e) $M = 0.70$ (f) $M = 0.75$

Figure 13.- Continued.

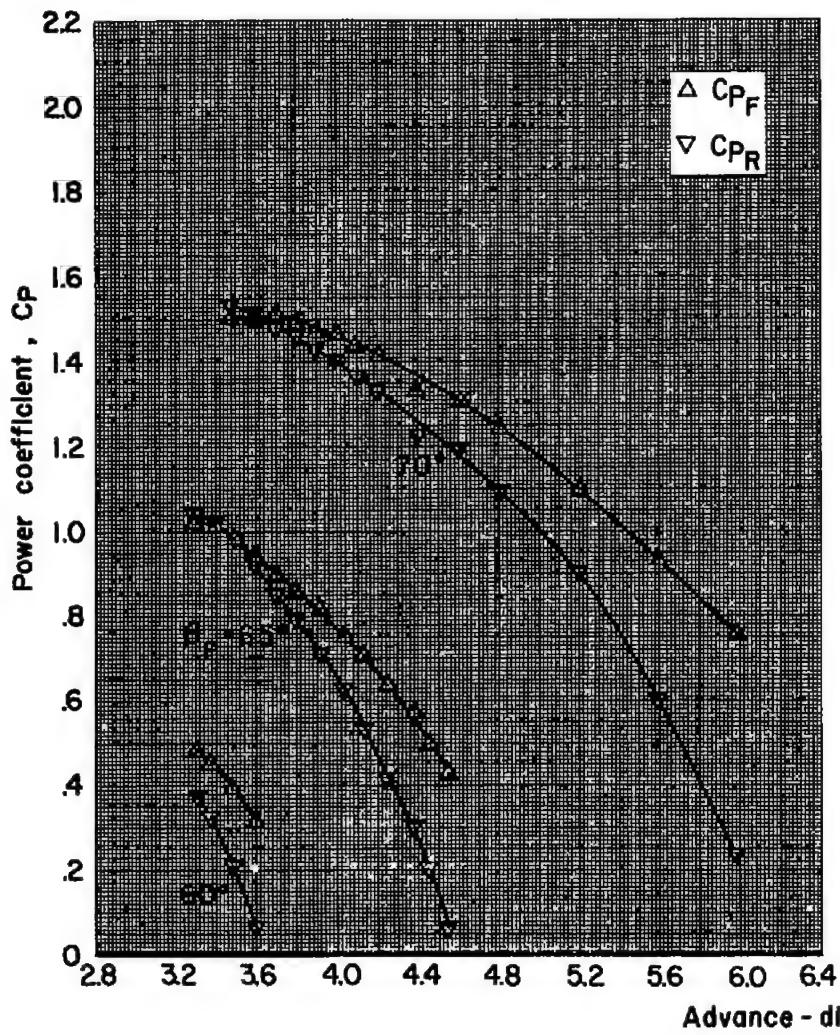
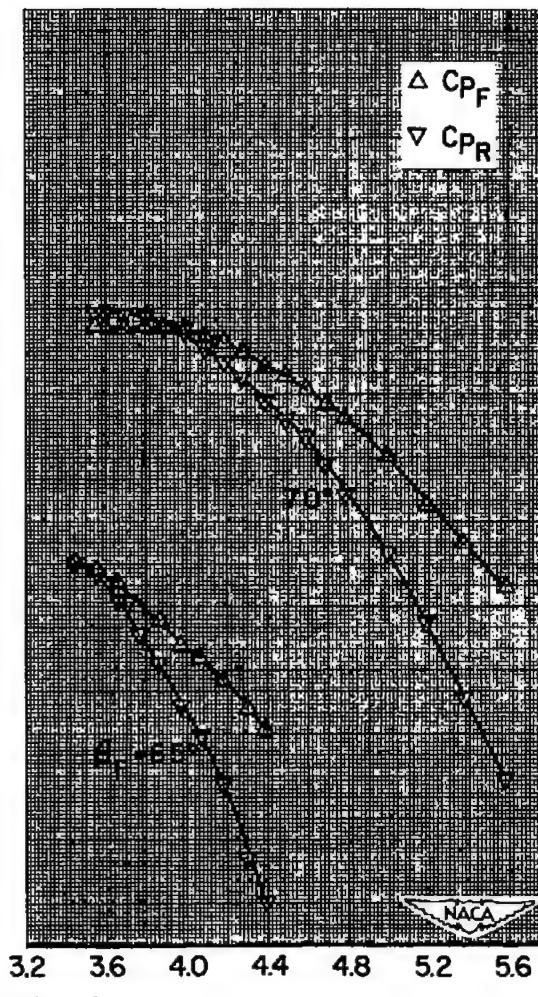
(g) $M = 0.80$ (h) $M = 0.84$

Figure 13.- Concluded.

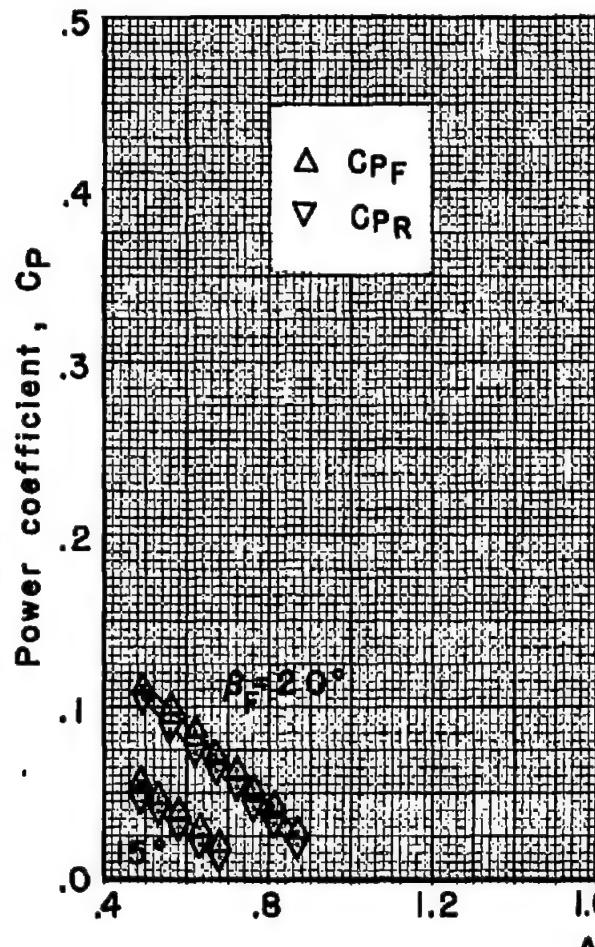
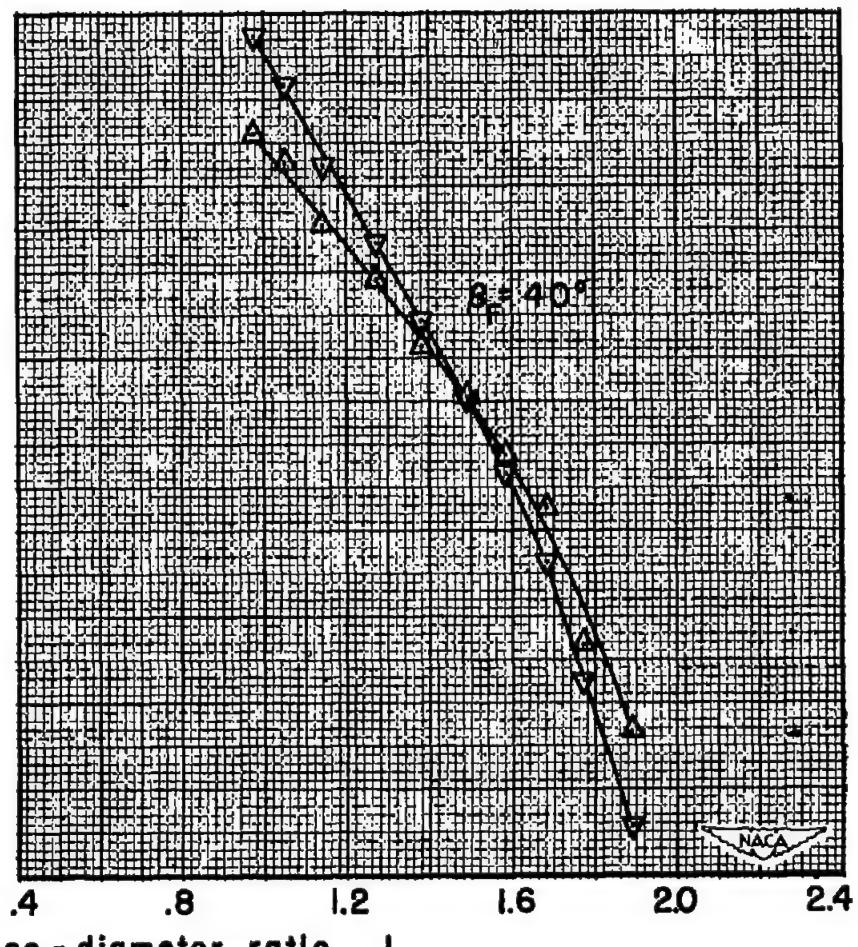
(a) $M = 0.15$ (b) $M = 0.20$

Figure 14.- Variation of power coefficients of the front and rear components with advance-diameter ratio for positive thrust; NACA 4-(5)(05)-037 eight-blade, dual-rotation propeller, $\Delta\beta$ = optimum, spinner A.

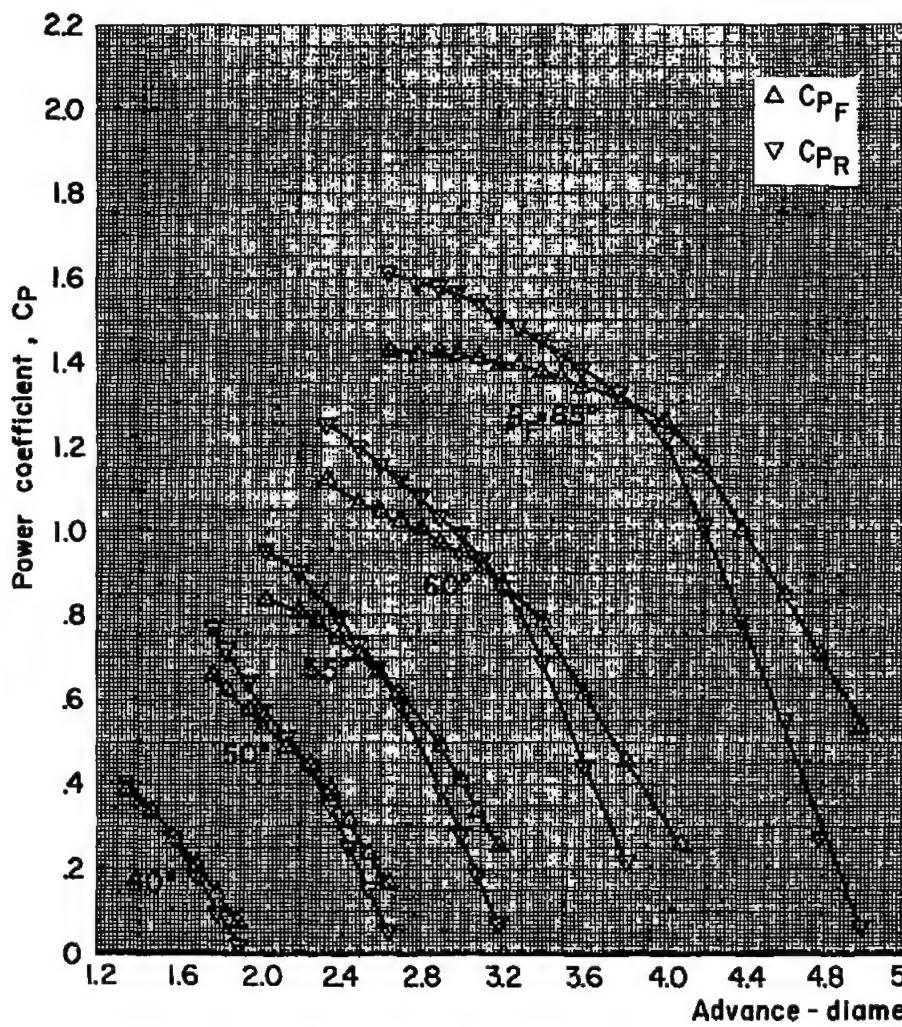
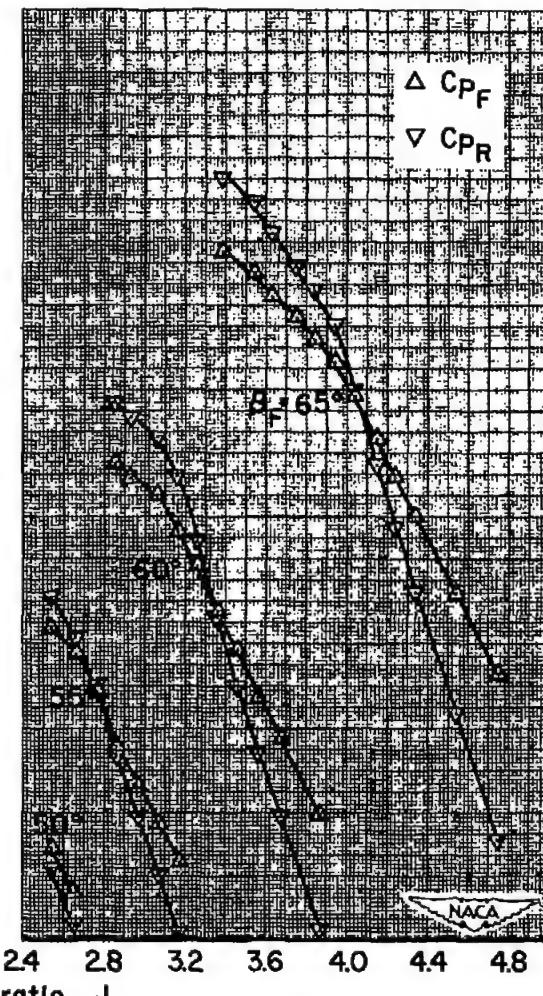
(c) $M = 0.40$ (d) $M = 0.60$

Figure 14.- Continued.

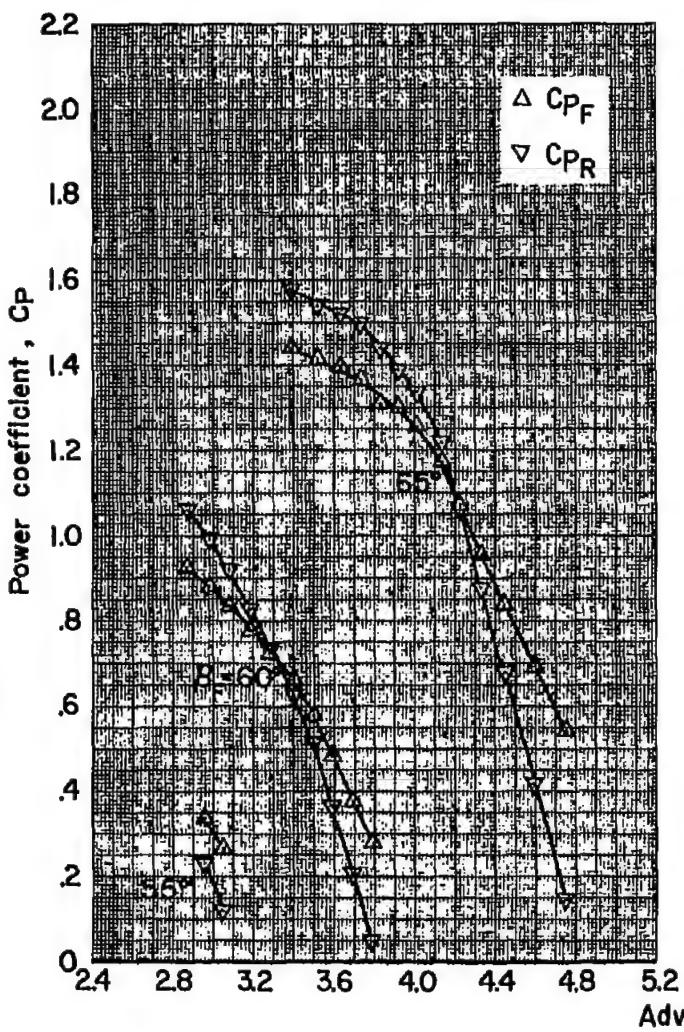
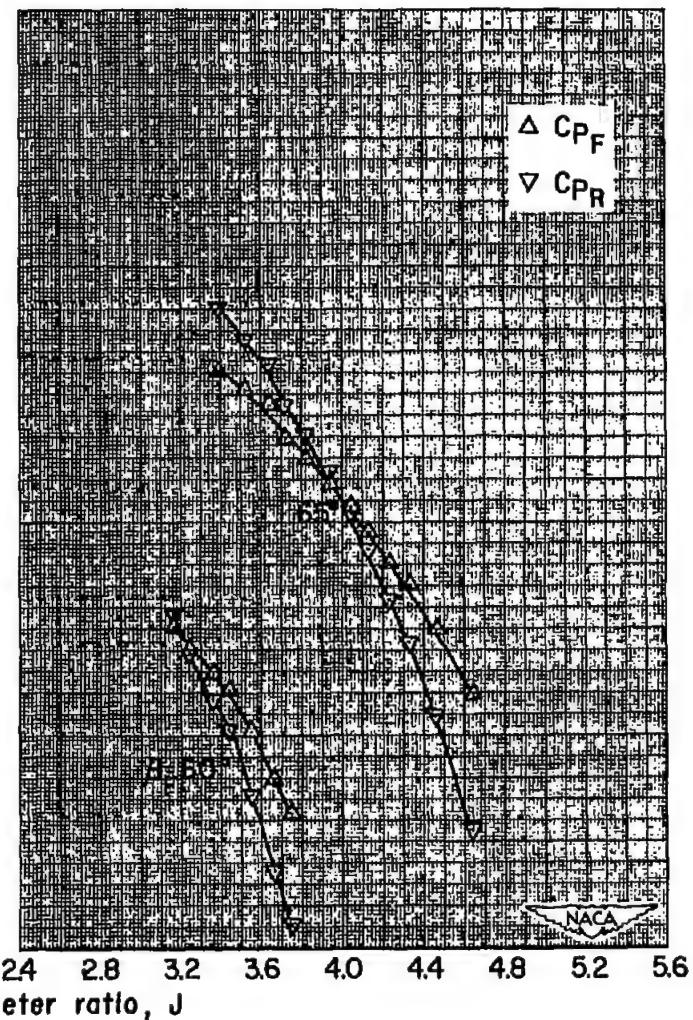
(e) $M = 0.70$ (f) $M = 0.75$

Figure 14.- Continued.

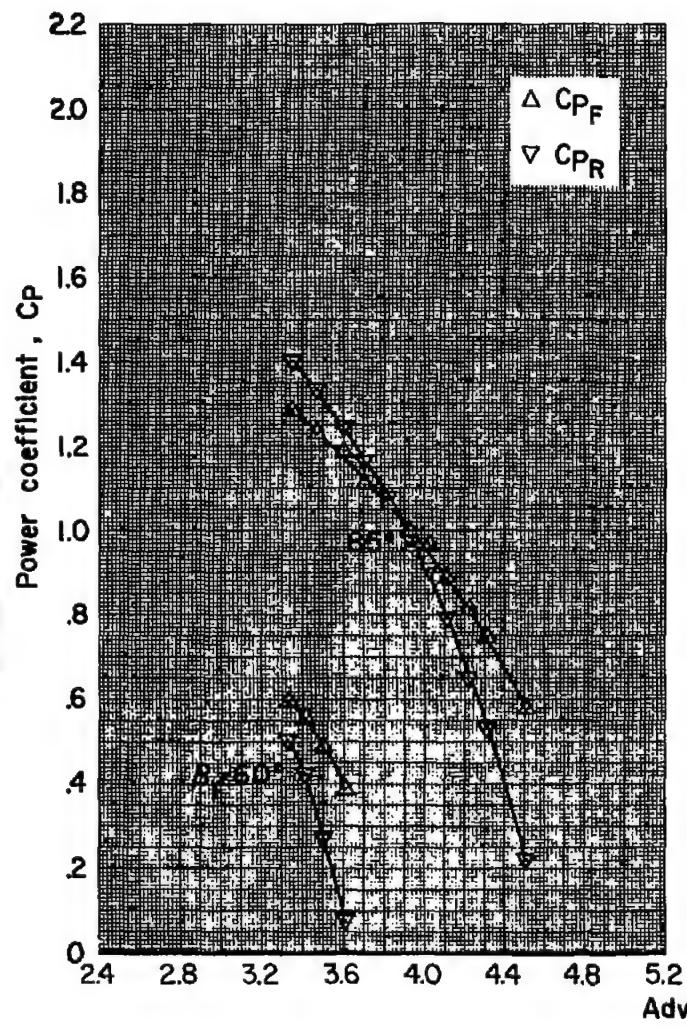
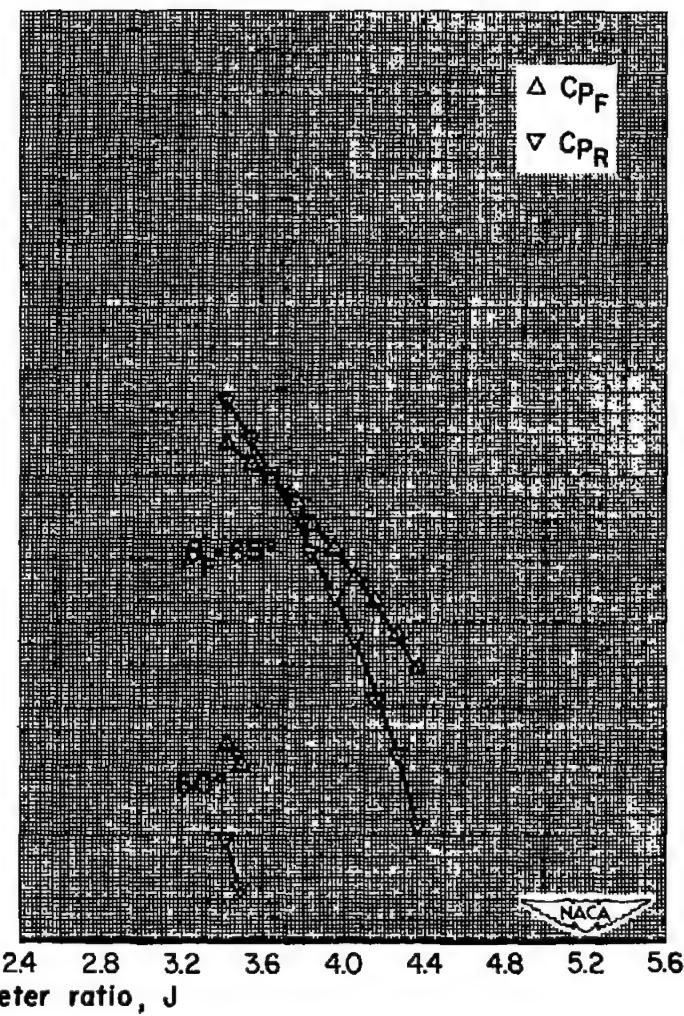
(g) $M = 0.80$ (h) $M = 0.84$

Figure 14.- Concluded.

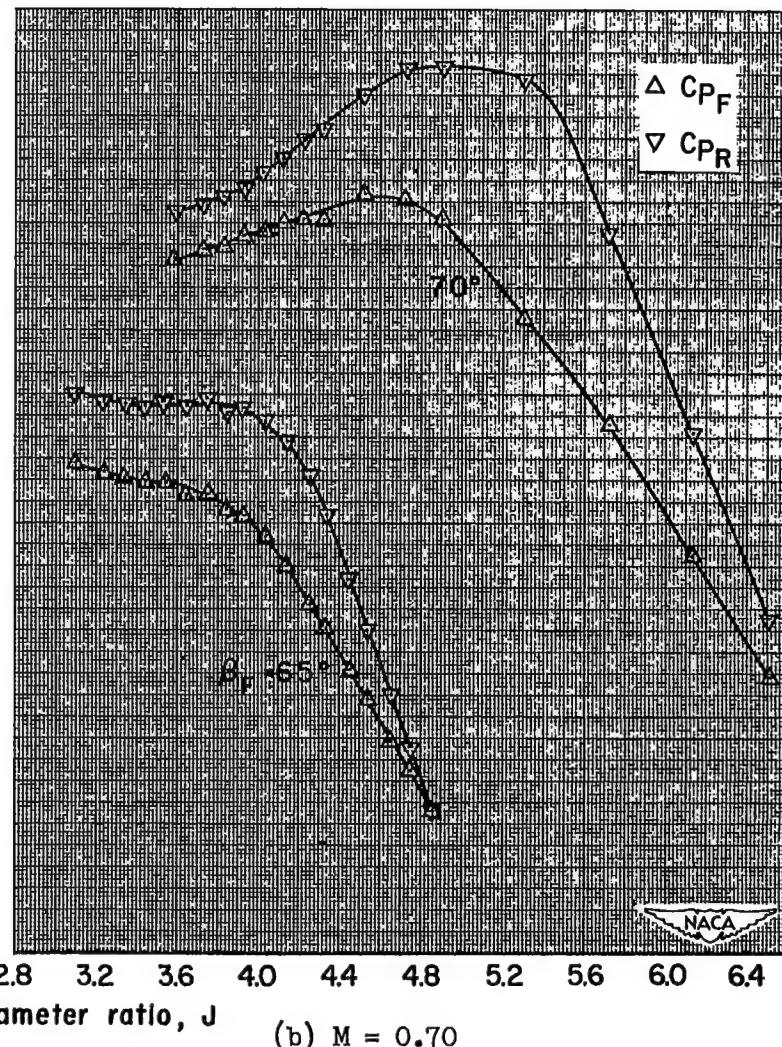
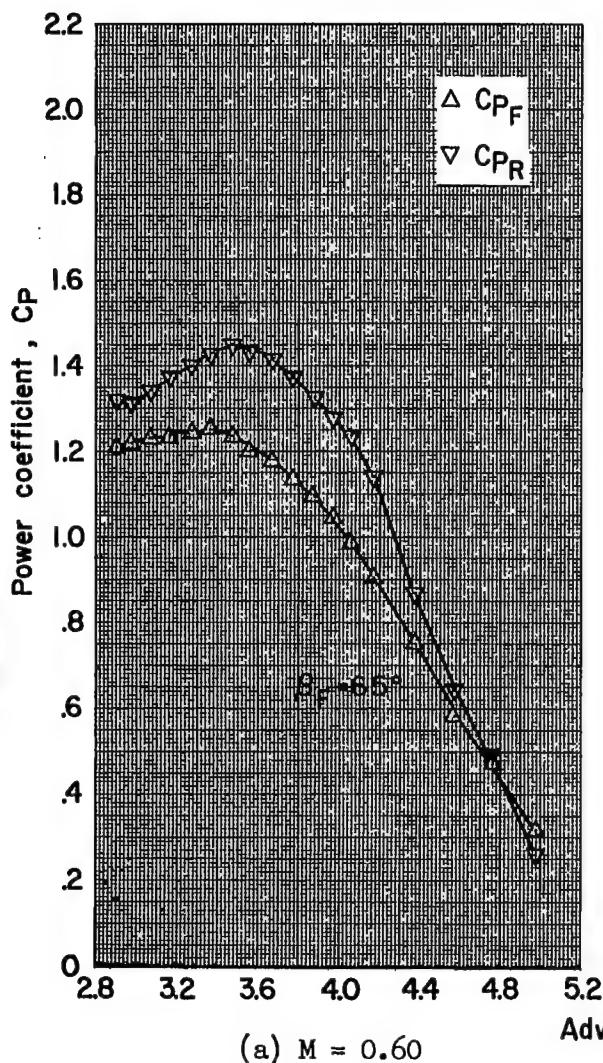


Figure 15.- Variation of power coefficients of the front and rear components with advance-diameter ratio for positive thrust; NACA 4-(5)(05)-037 six-blade, dual-rotation propeller, $\Delta\beta = 0.8^\circ$, spinner A.

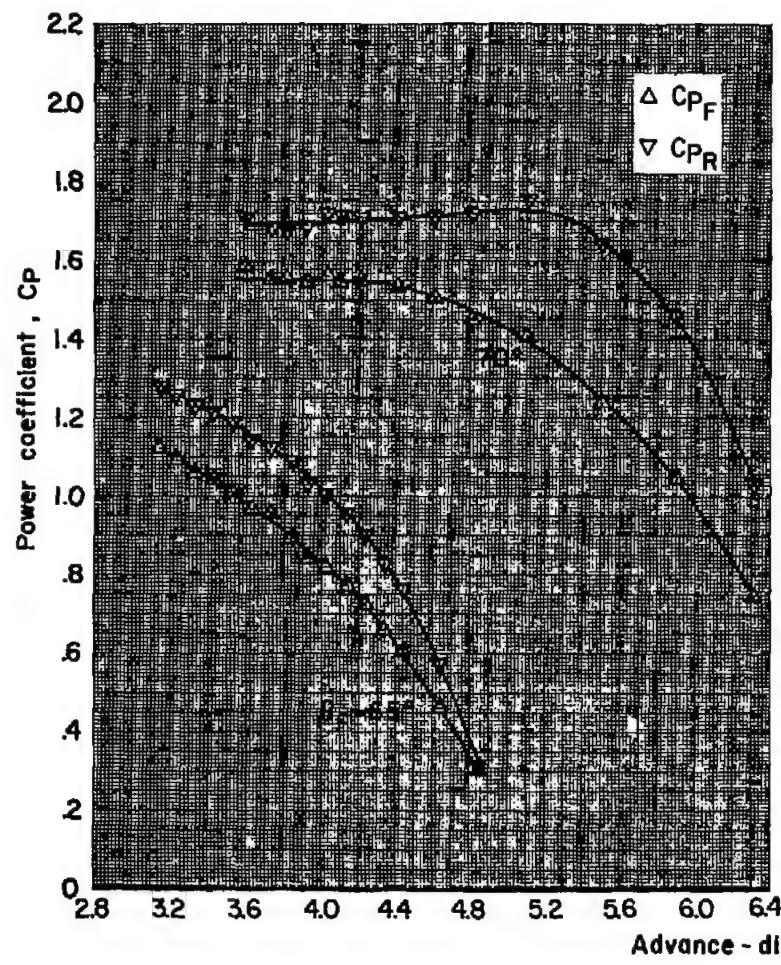
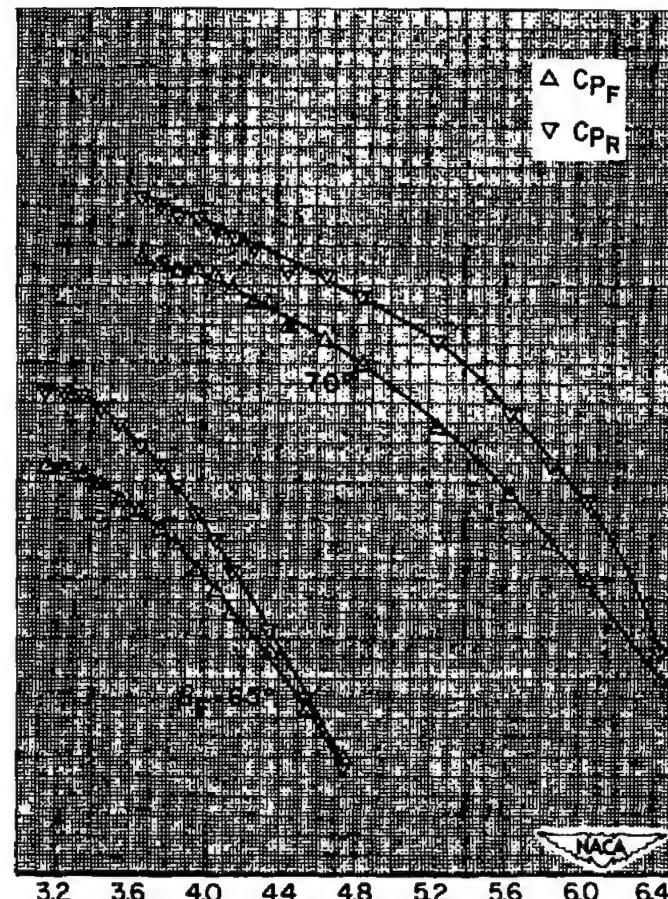
(c) $M = 0.75$ (d) $M = 0.80$

Figure 15.- Continued.

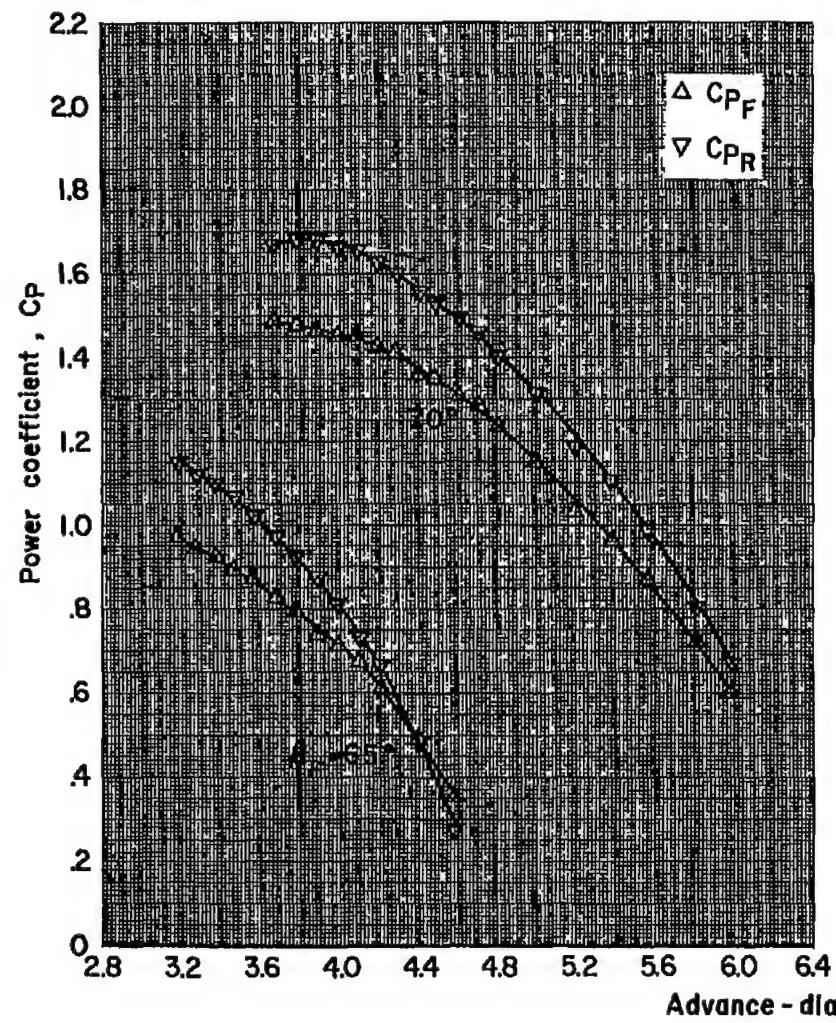
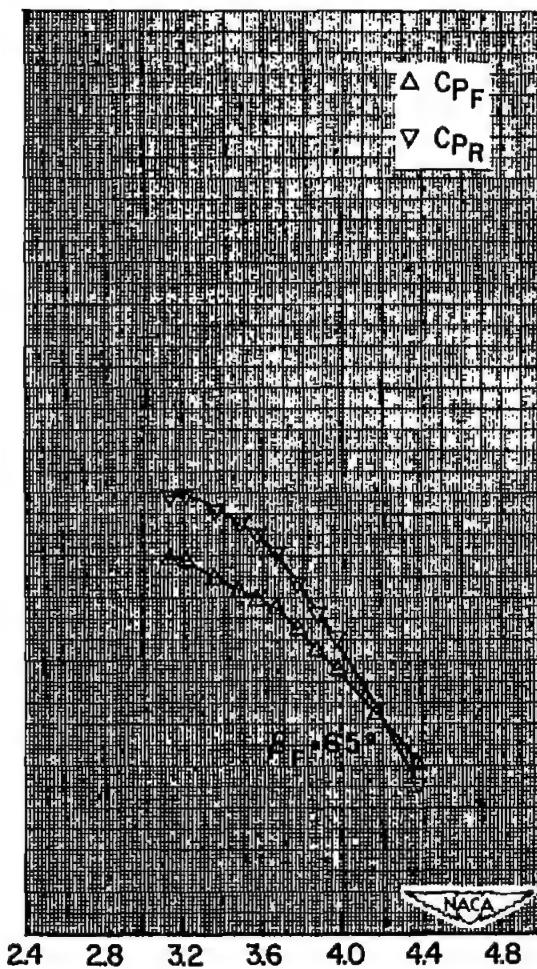
(e) $M = 0.84$ (f) $M = 0.90$

Figure 15.- Concluded.

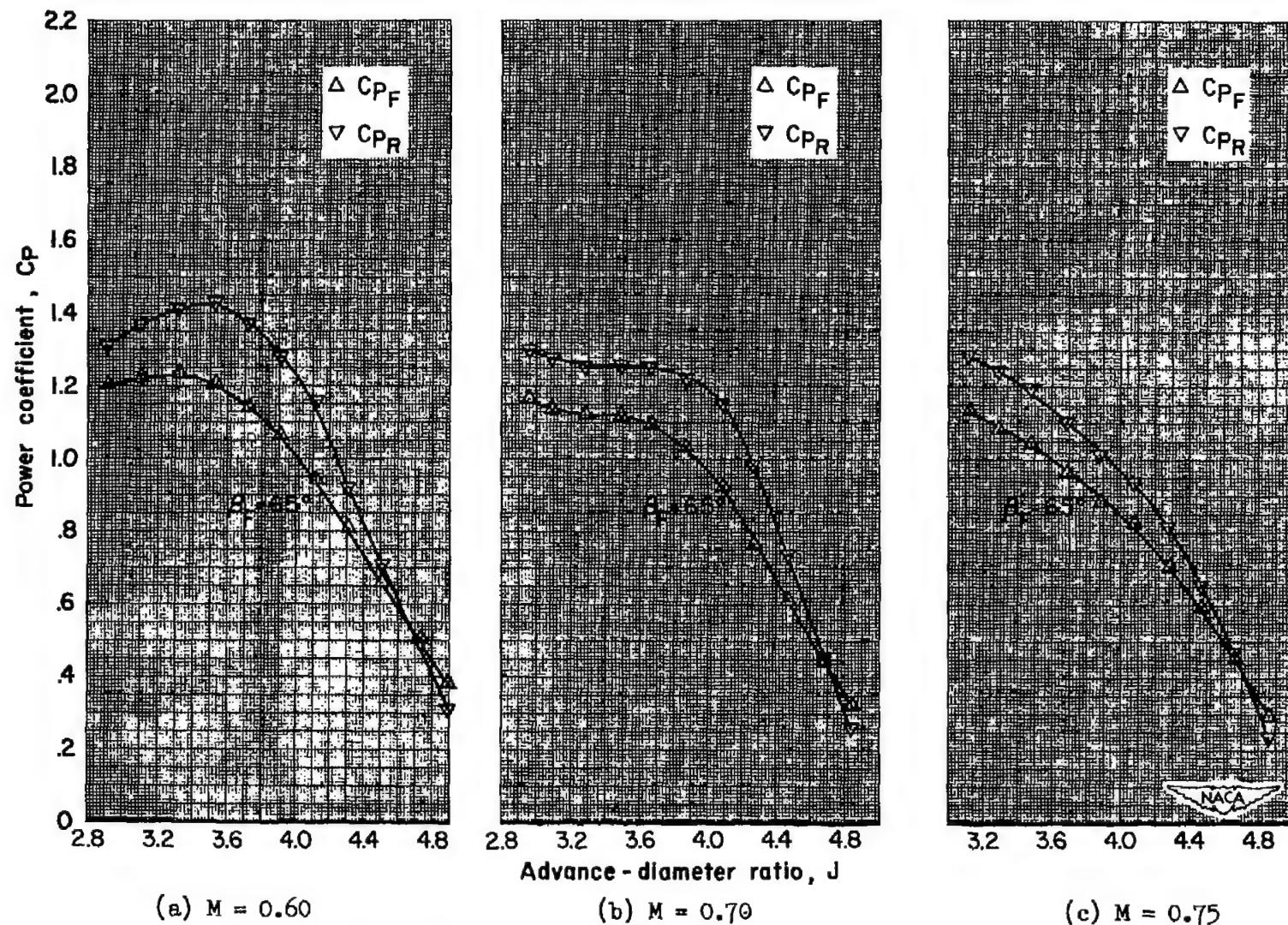


Figure 16.- Variation of power coefficients of the front and rear components with advance-diameter ratio for positive thrust; NACA 4-(5)(05)-037 six-blade, dual-rotation propeller, $\Delta\beta = 0.8^\circ$, spinner B.

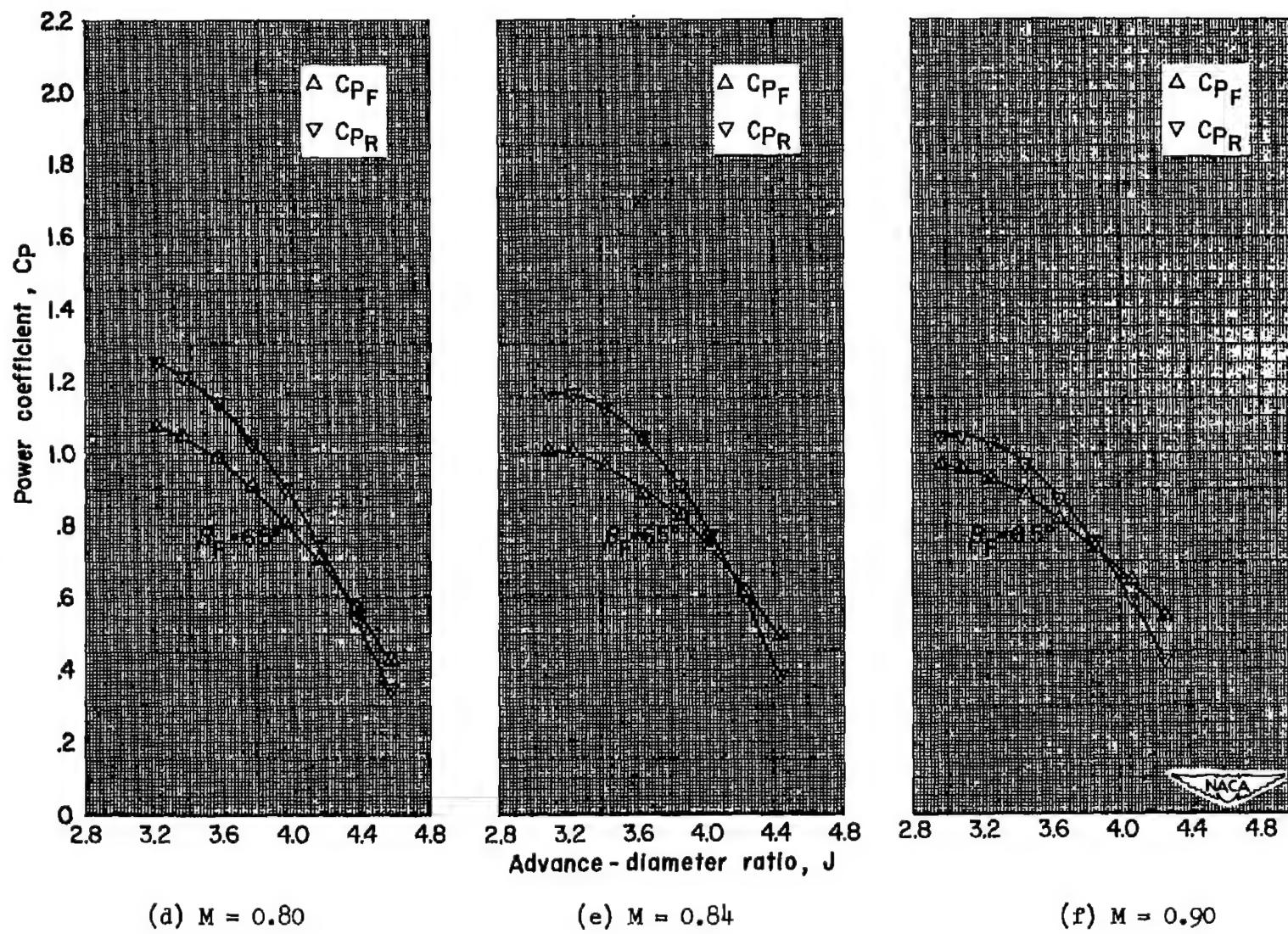


Figure 16.- Concluded.

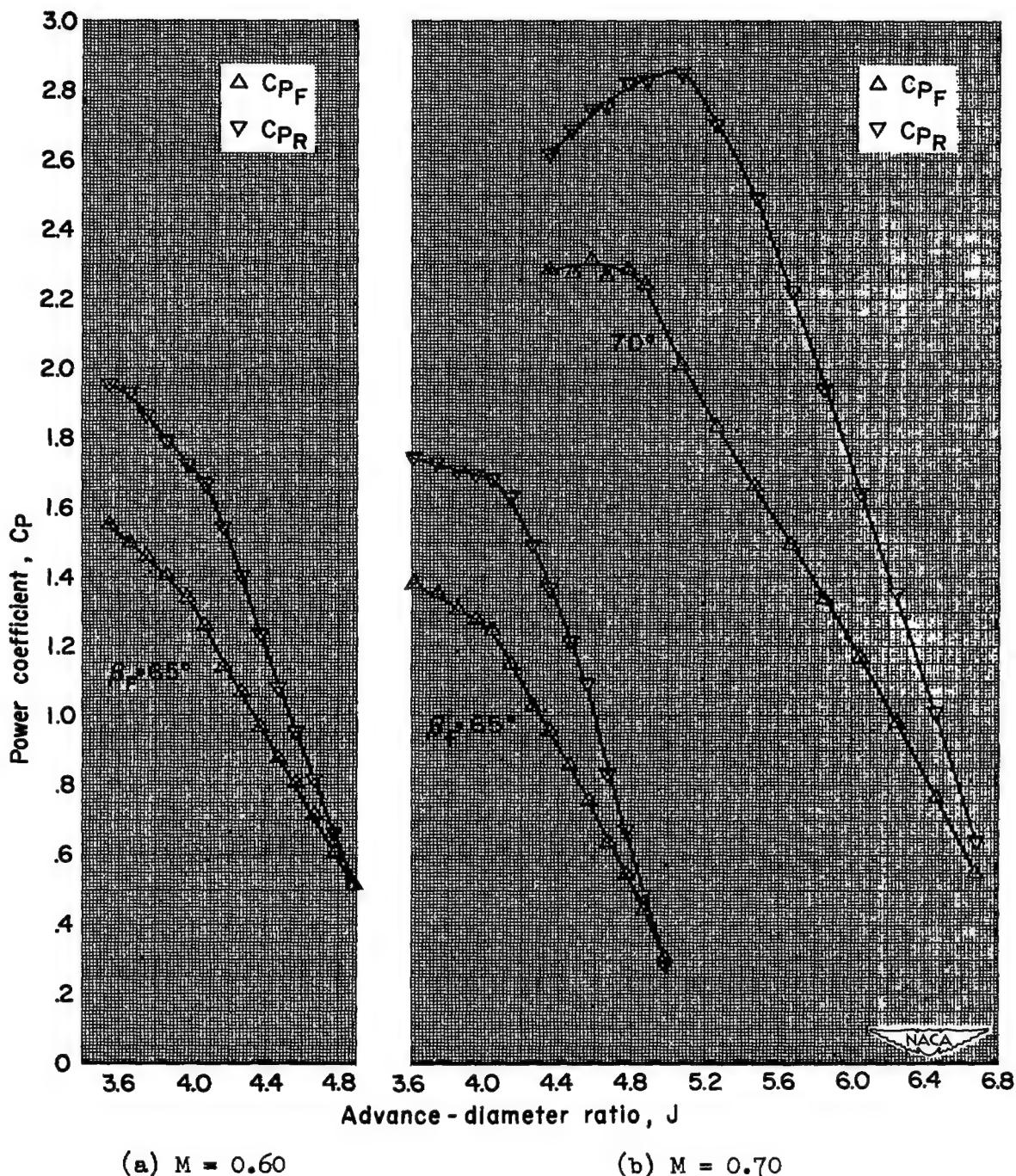


Figure 17.- Variation of power coefficients of the front and rear components with advance-diameter ratio for positive thrust; NACA 4-(5)(05)-037 eight-blade, dual-rotation propeller, $\Delta\beta = 0.8^\circ$, spinner A.

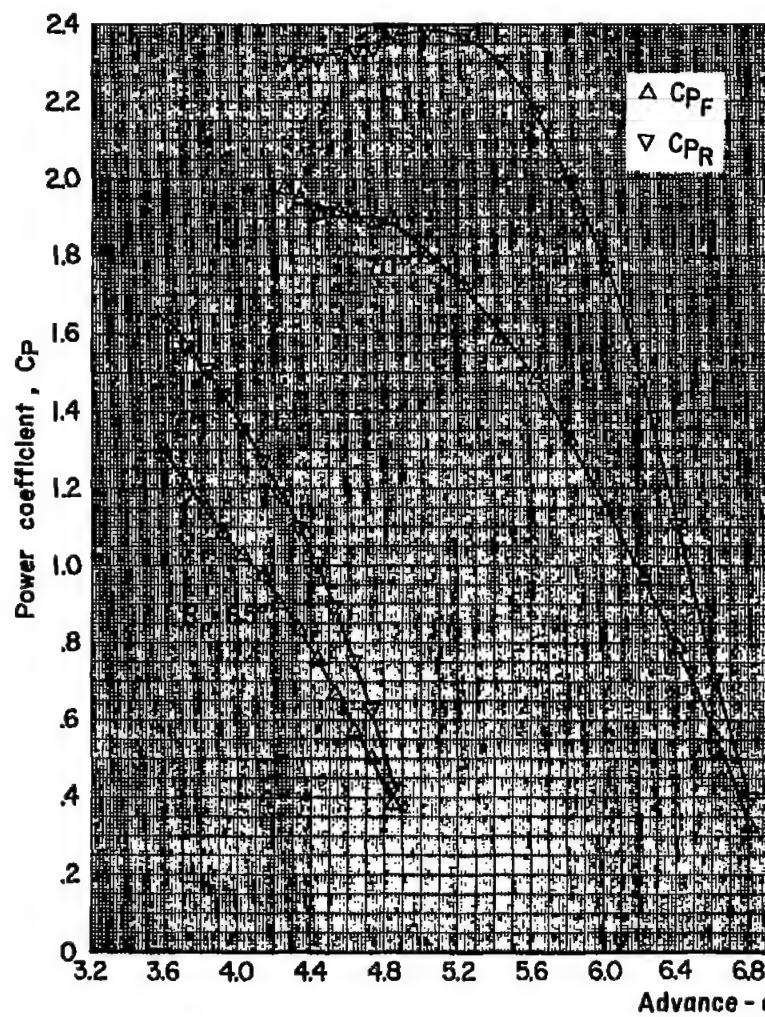
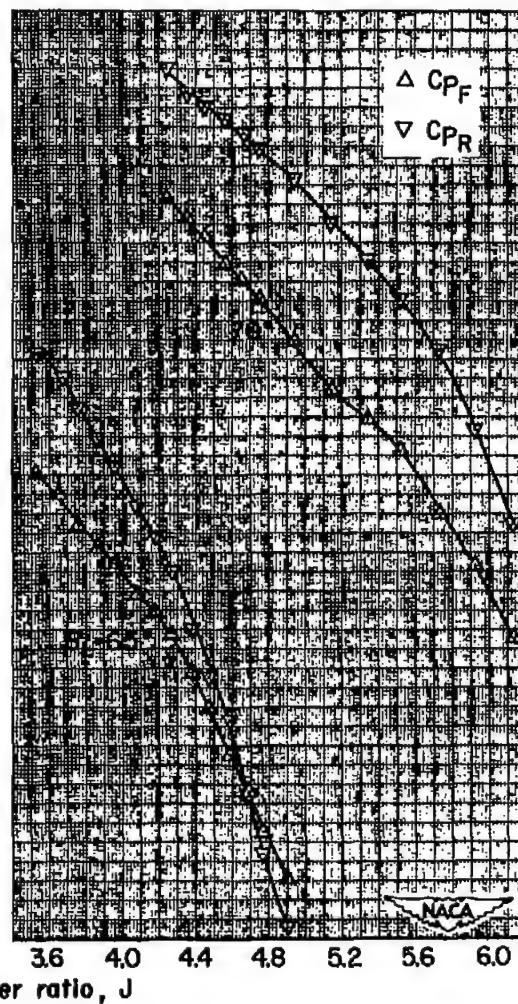
(c) $M = 0.75$ (d) $M = 0.80$

Figure 17.- Continued.

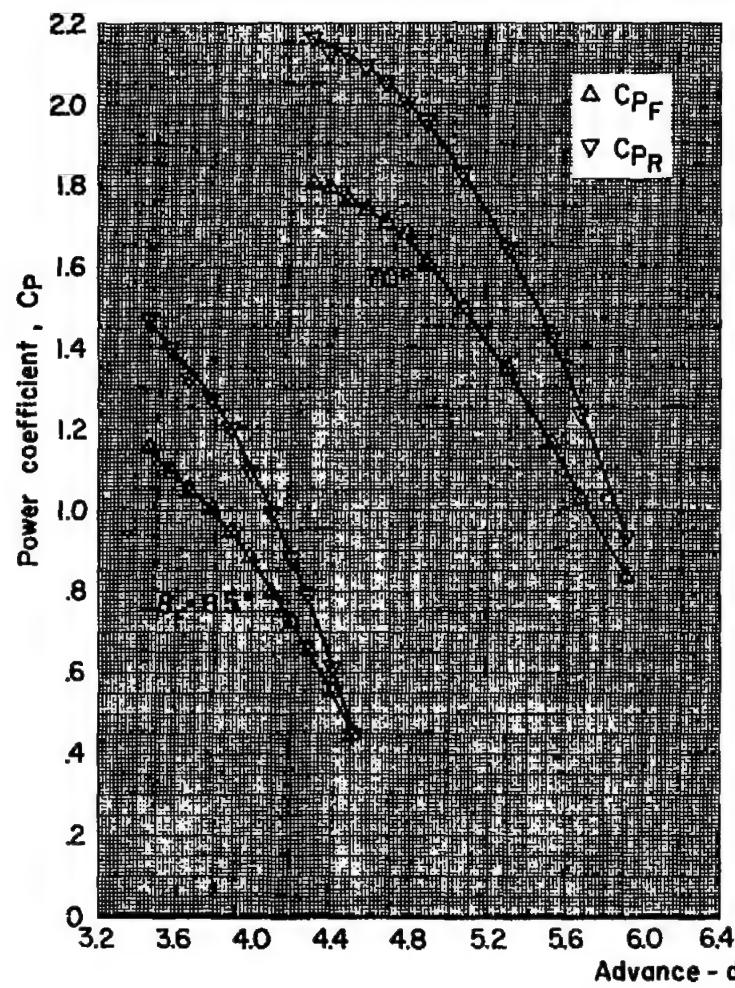
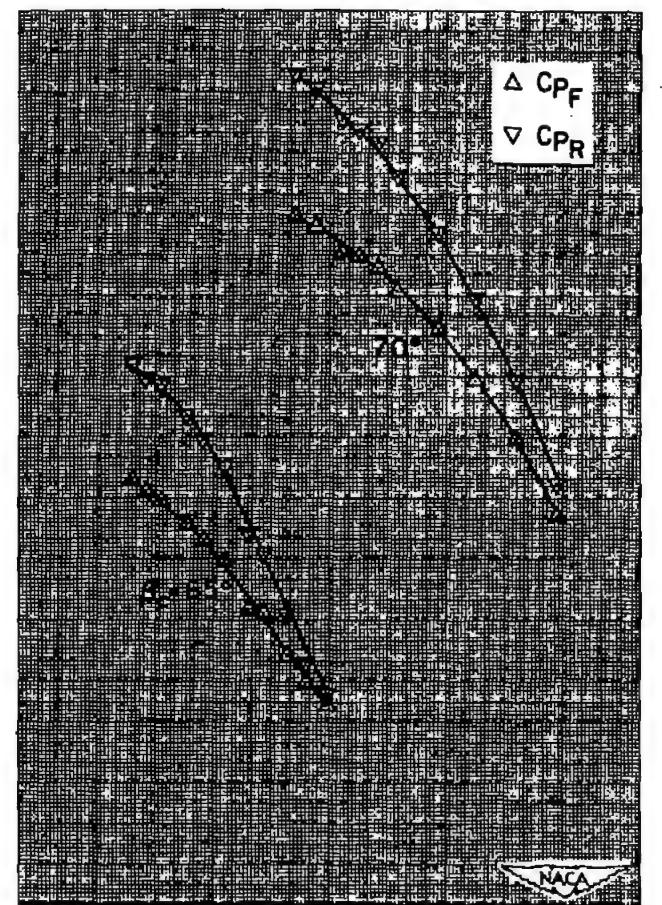
(e) $M = 0.84$ (f) $M = 0.90$

Figure 17.- Concluded.

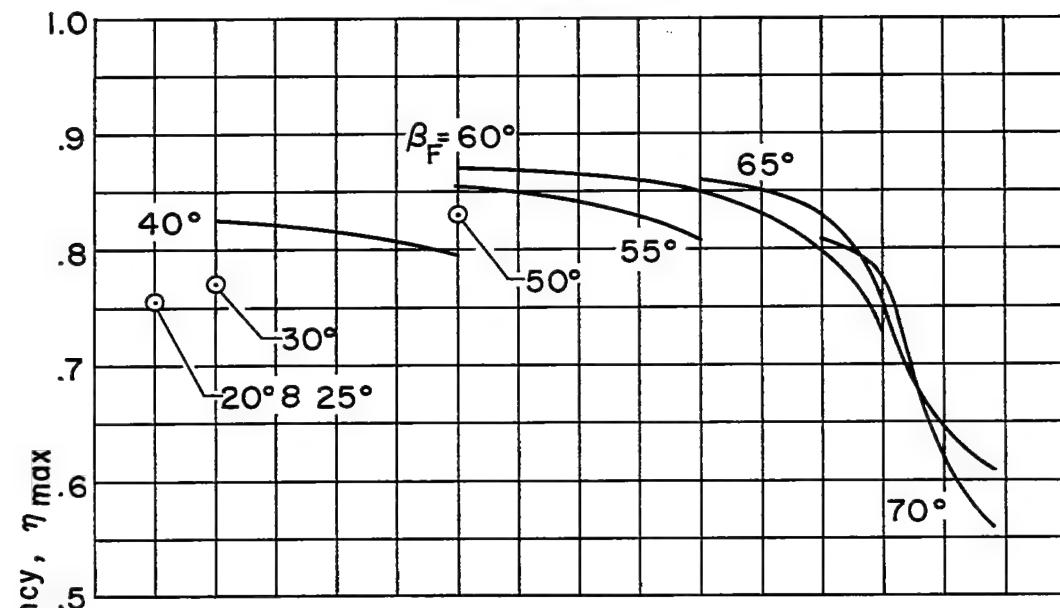
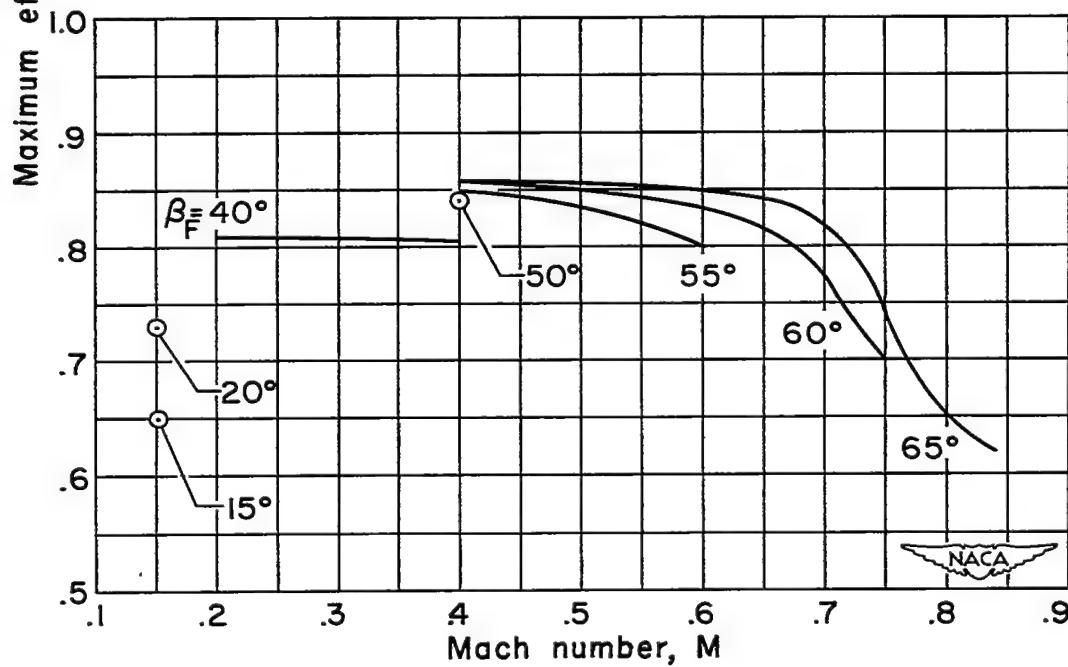
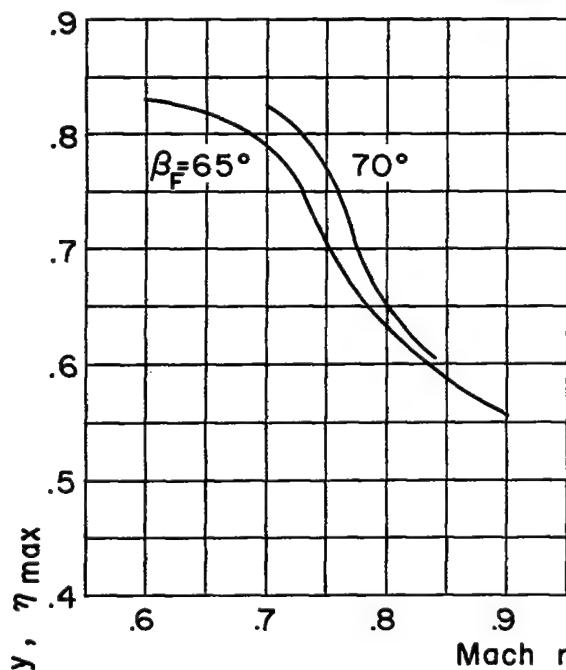
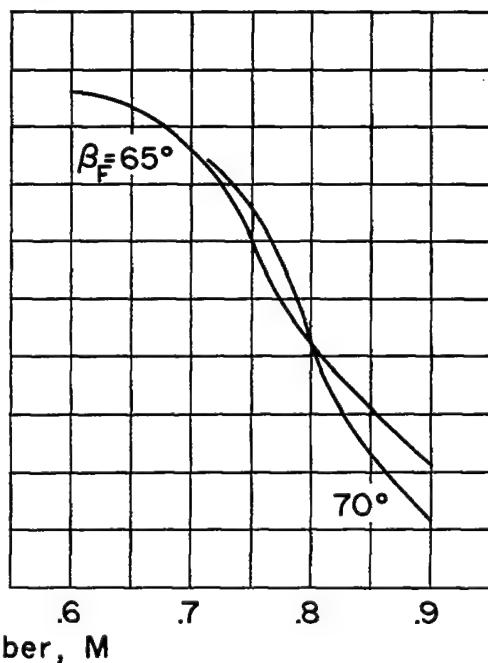
(a) $B = 6$, $\Delta\beta$ = optimum, spinner A.(b) $B = 8$, $\Delta\beta$ = optimum, spinner A.

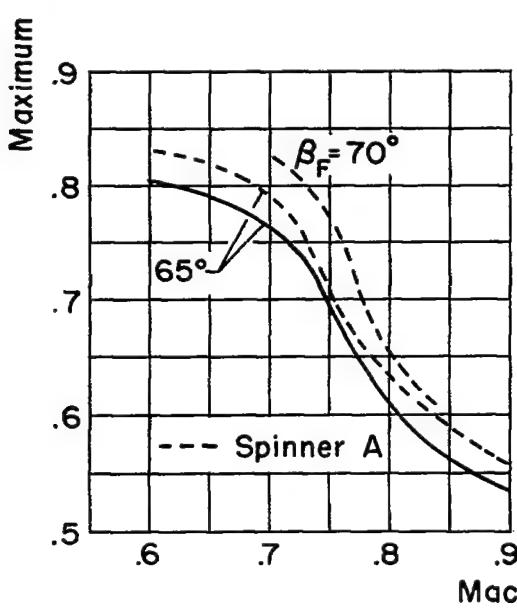
Figure 18.- The effect of Mach number on maximum efficiency; NACA 4-(5)(05)-037 six- and eight-blade, dual-rotation propellers and the NACA 4-(5)(05)-041 two-blade, single-rotation propeller.



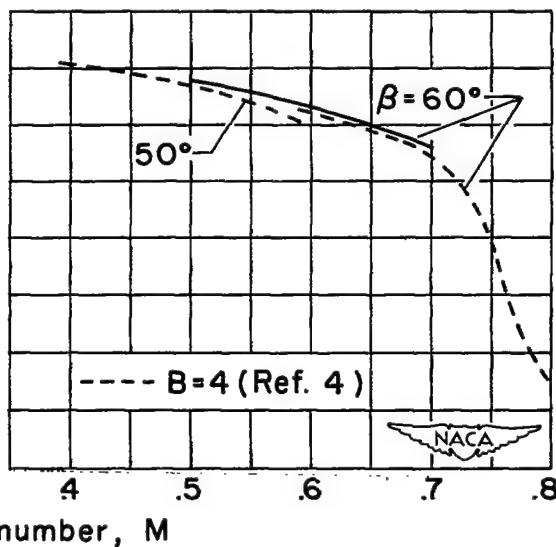
(c) $B = 6$, $\Delta\beta = 0.8^\circ$,
spinner A.



(d) $B = 8$, $\Delta\beta = 0.8^\circ$,
spinner A.



(e) $B = 6$, $\Delta\beta = 0.8^\circ$,
spinner B.



(f) $B = 2$, spinner C.

Figure 18.- Concluded.

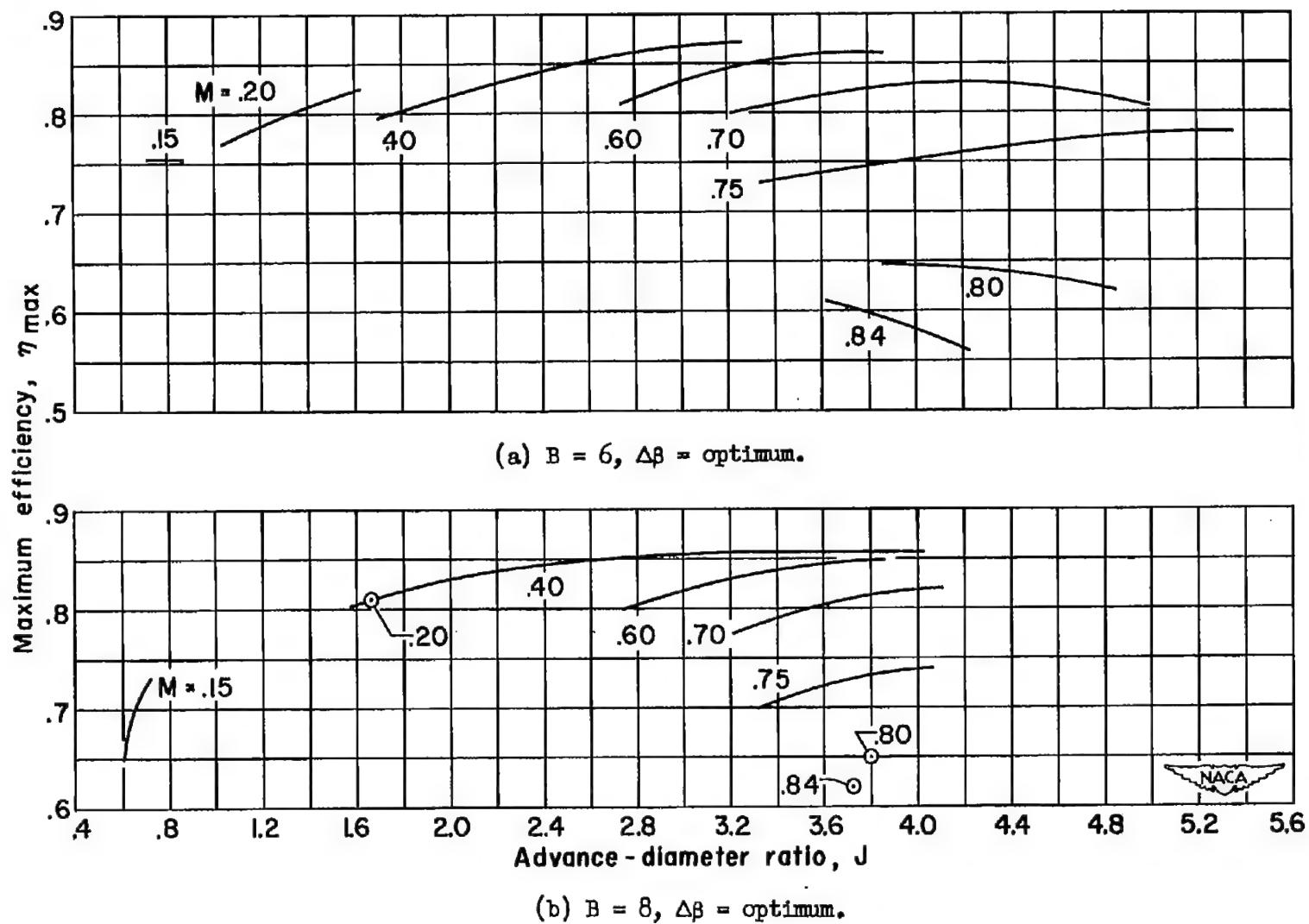


Figure 19.- The effect of advance-diameter ratio on maximum efficiency; NACA 4-(5)(05)-037 six- and eight-blade, dual-rotation propellers, spinner A.

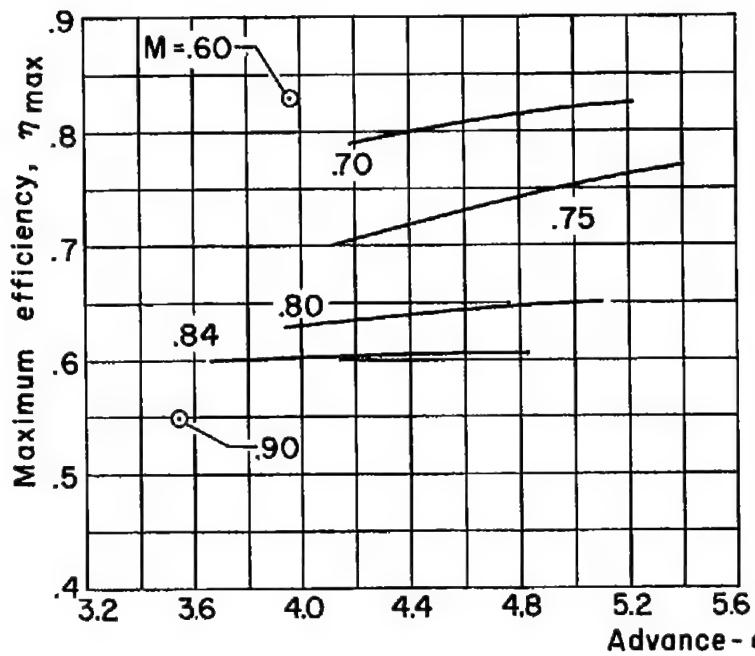
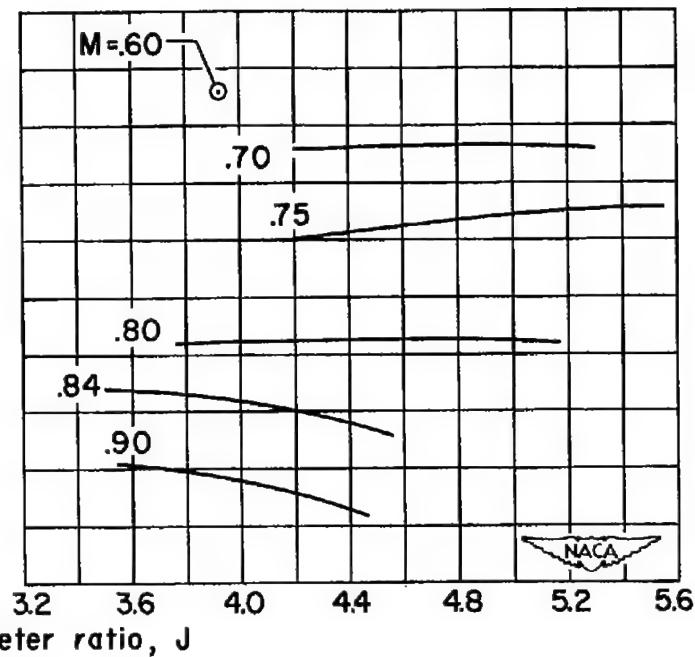
(c) $B = 6, \Delta\beta = 0.8^\circ$ (d) $B = 8, \Delta\beta = 0.8^\circ$

Figure 19.- Concluded.

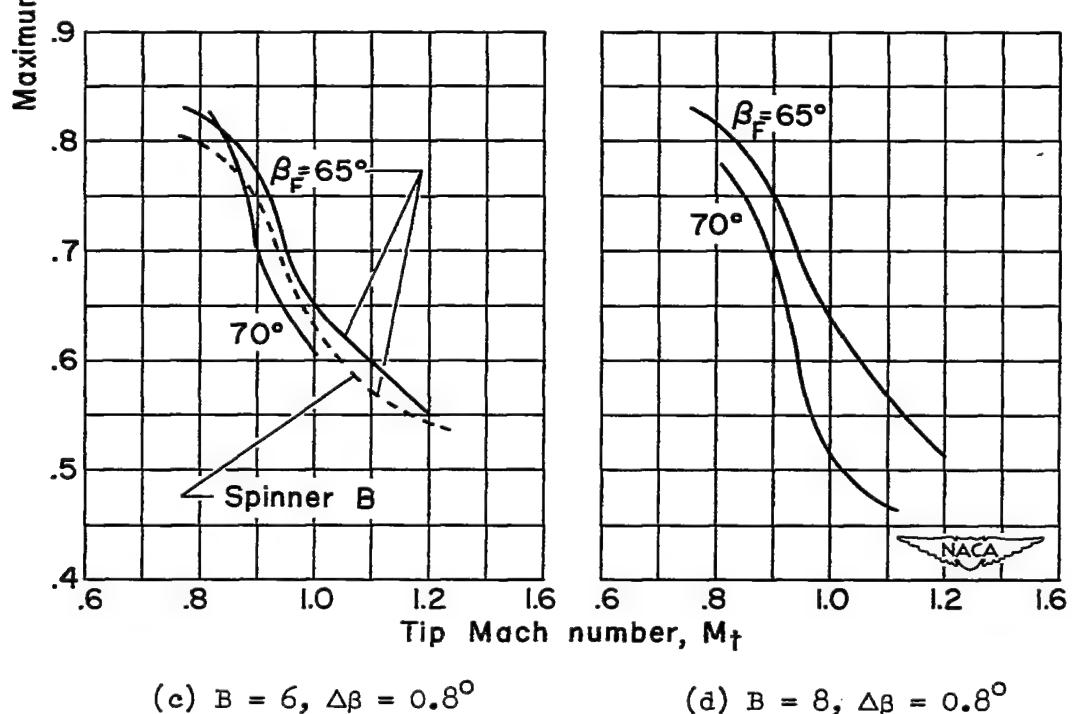
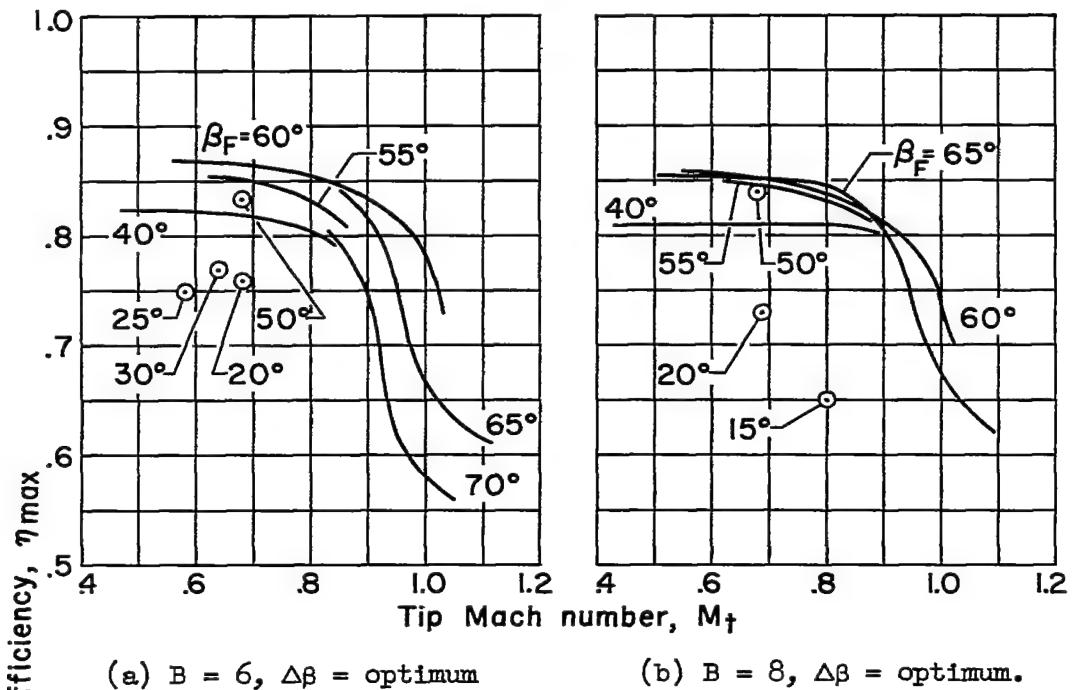


Figure 20.- The effect of tip Mach number on maximum efficiency; NACA 4-(5)(05)-037 six- and eight-blade, dual-rotation propellers, spinner A.

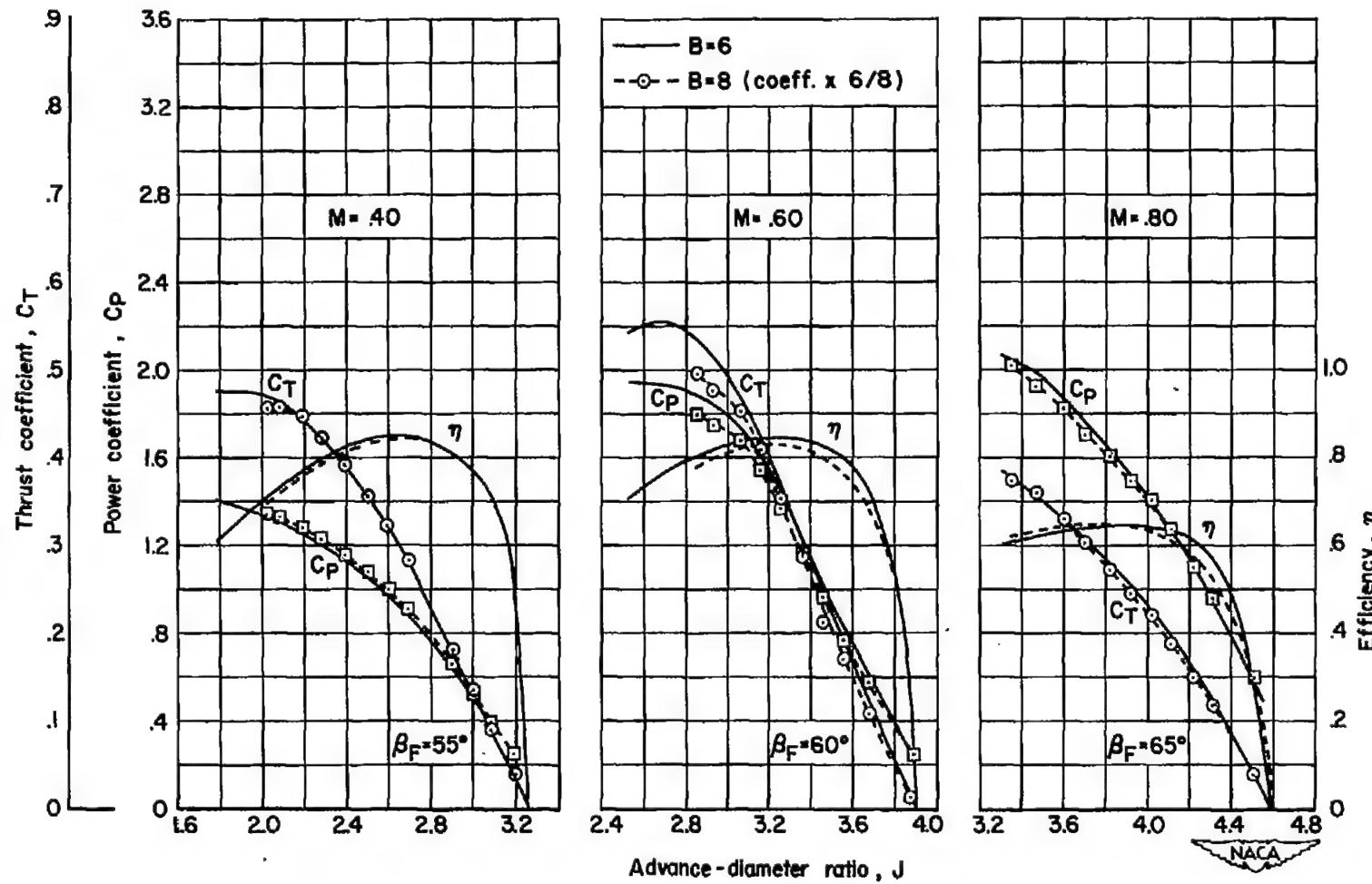


Figure 21.- Comparison of the positive-thrust characteristics of the NACA 4-(5)(05)-037 six- and eight-blade, dual-rotation propellers; $\Delta\beta$ = optimum, spinner A.

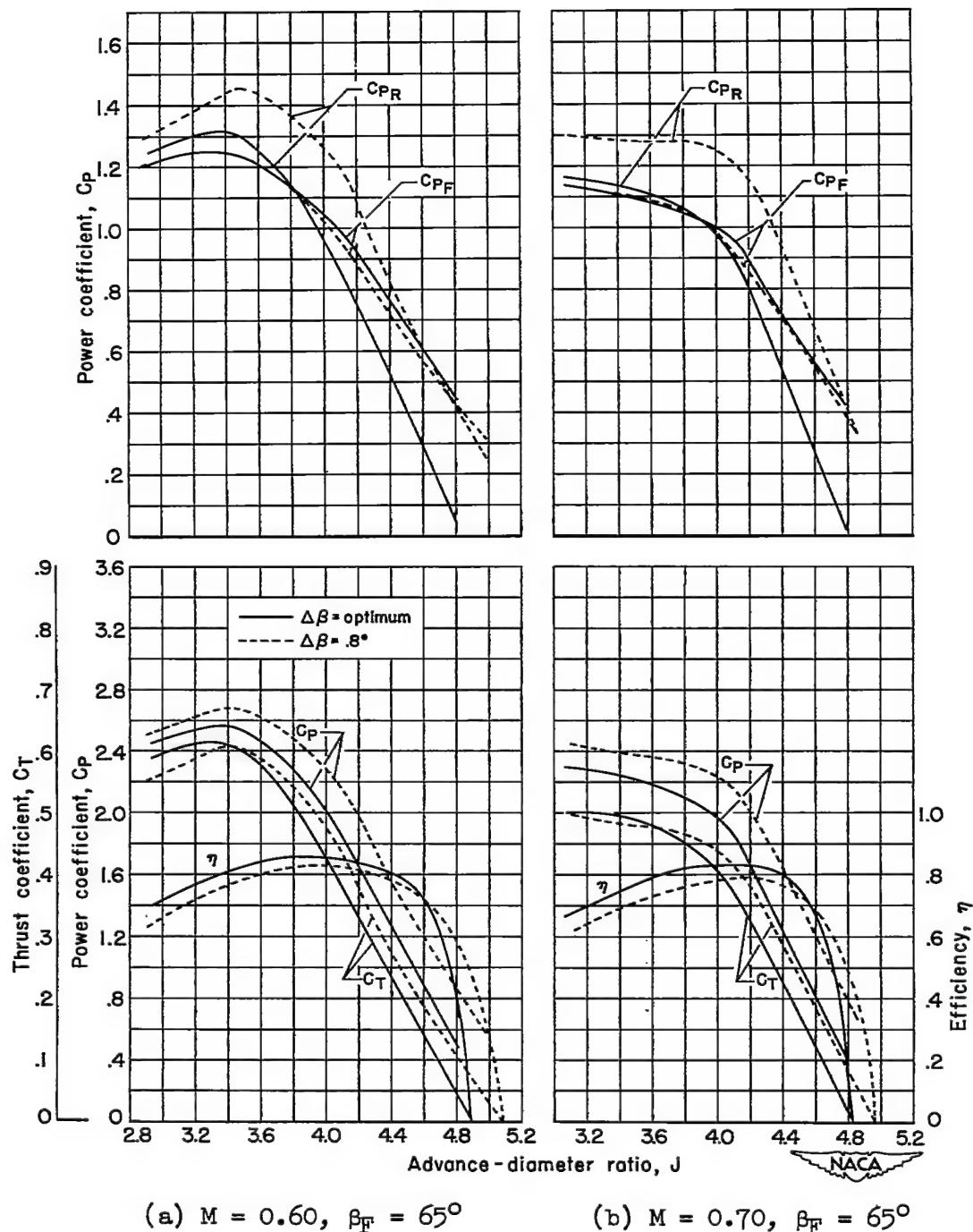


Figure 22.- Comparison of the positive-thrust characteristics of the NACA 4-(5)(05)-037 six-blade, dual-rotation propeller with $\Delta\beta = \text{optimum}$ and $\Delta\beta = 0.8^\circ$, spinner A.

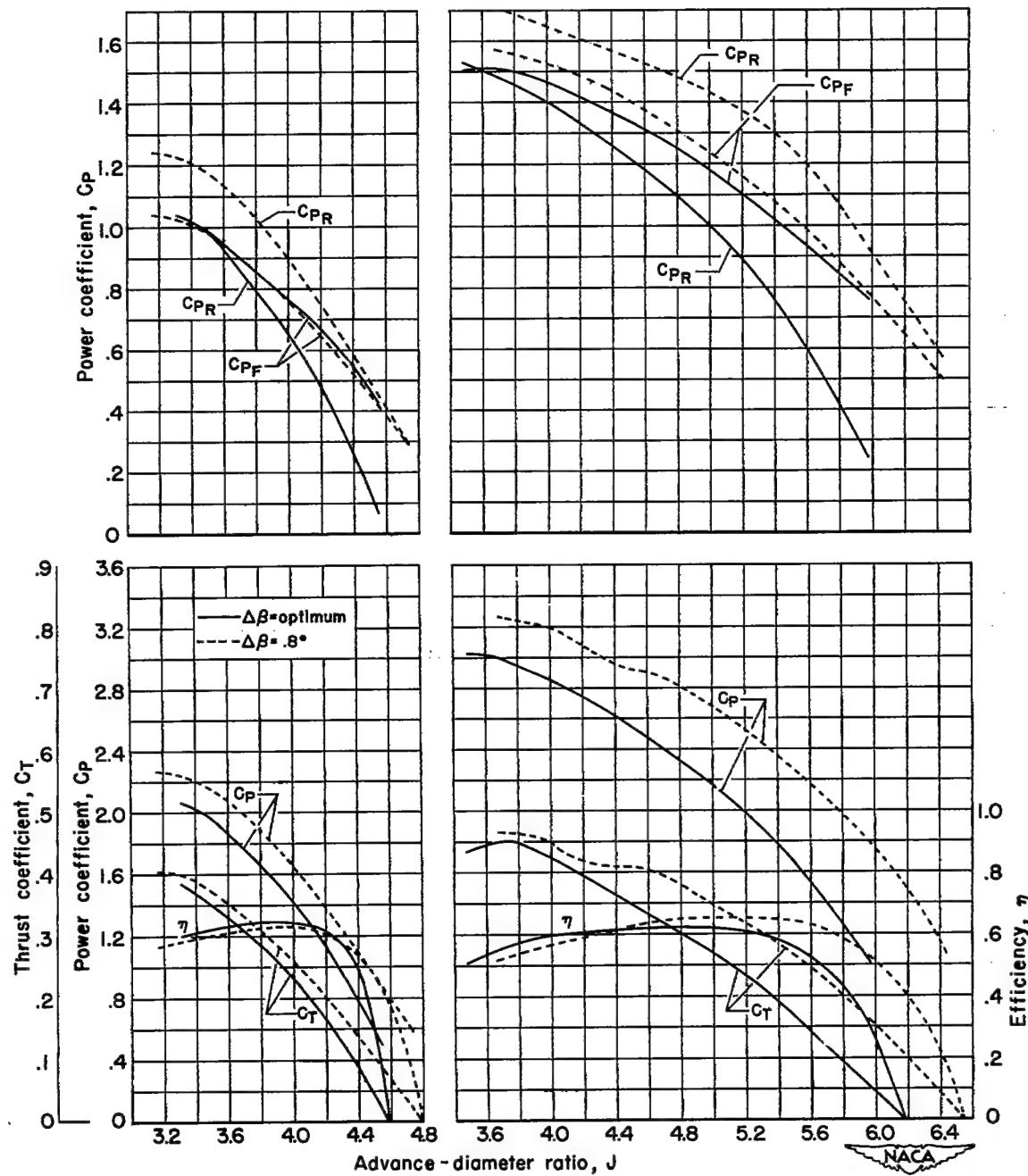
(c) $M = 0.80, \beta_F = 65^\circ$ (d) $M = 0.80, \beta_F = 70^\circ$

Figure 22.- Concluded.

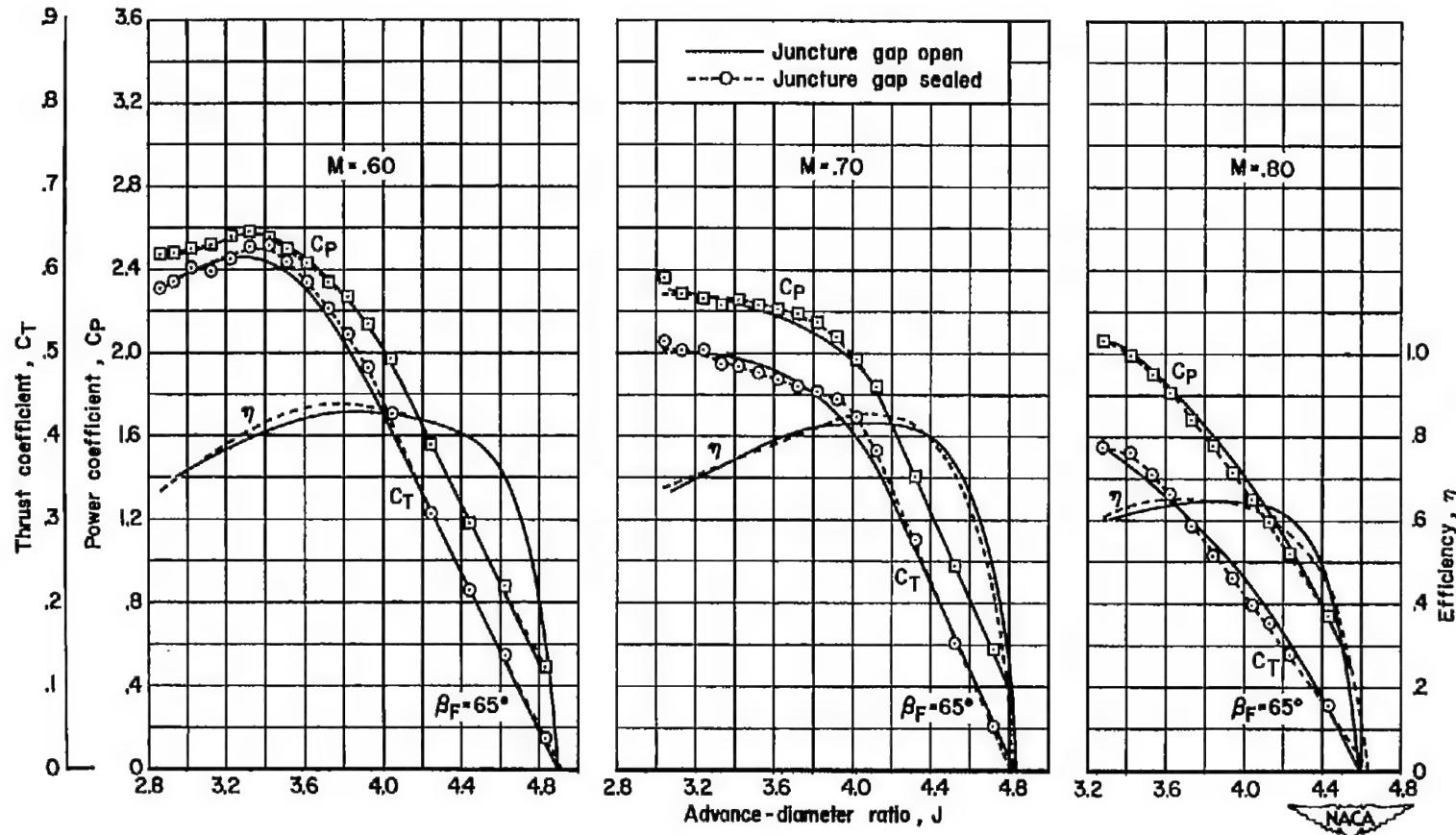


Figure 23.-- Comparison of the positive-thrust characteristics of the NACA 4-(5)(05)-037 six-blade, dual-rotation propeller with the platform-juncture gaps open and sealed; $\Delta\beta$ = optimum, spinner A.

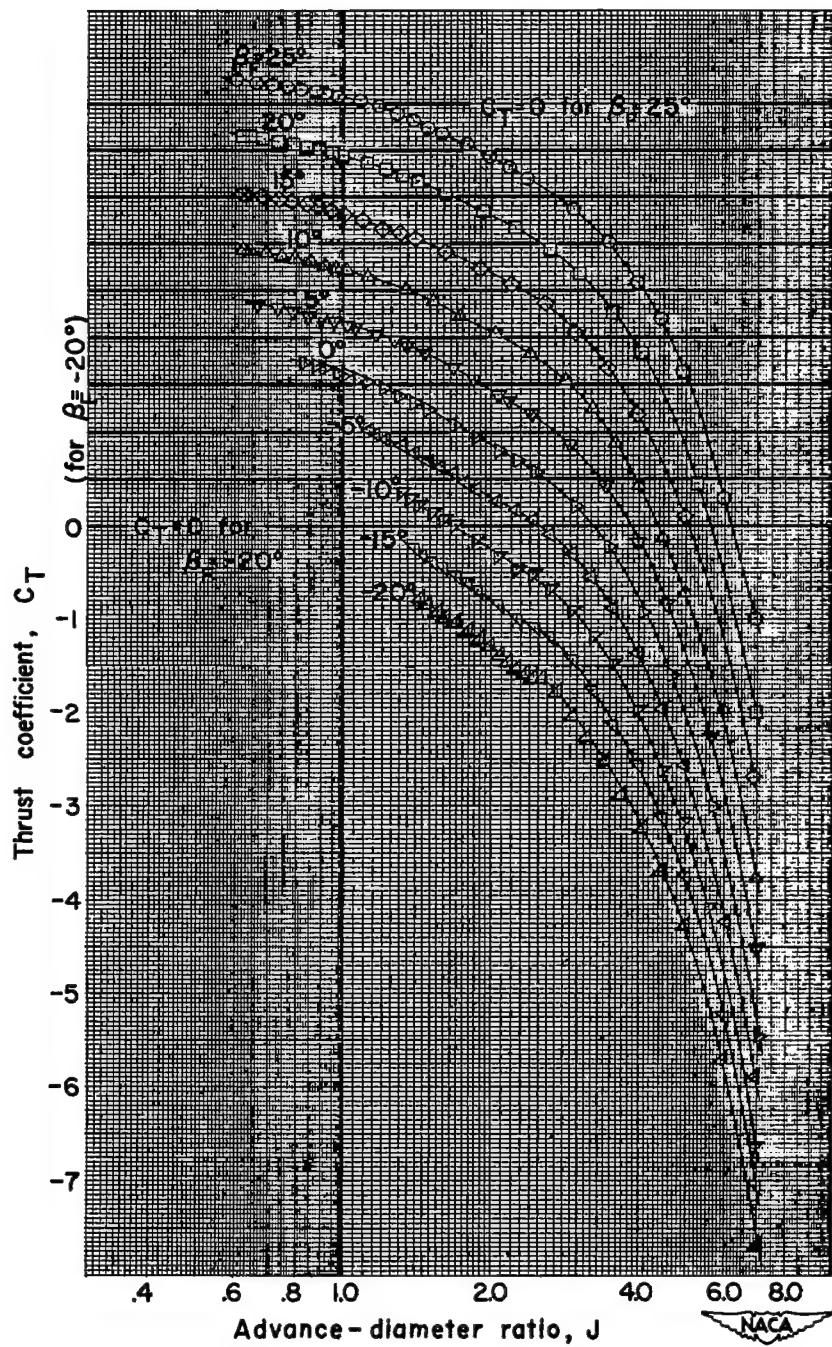


Figure 24.- Negative-thrust characteristics; NACA 4-(5)(05)-037 six-blade, dual-rotation propeller, $\Delta\beta$ = optimum, spinner A.

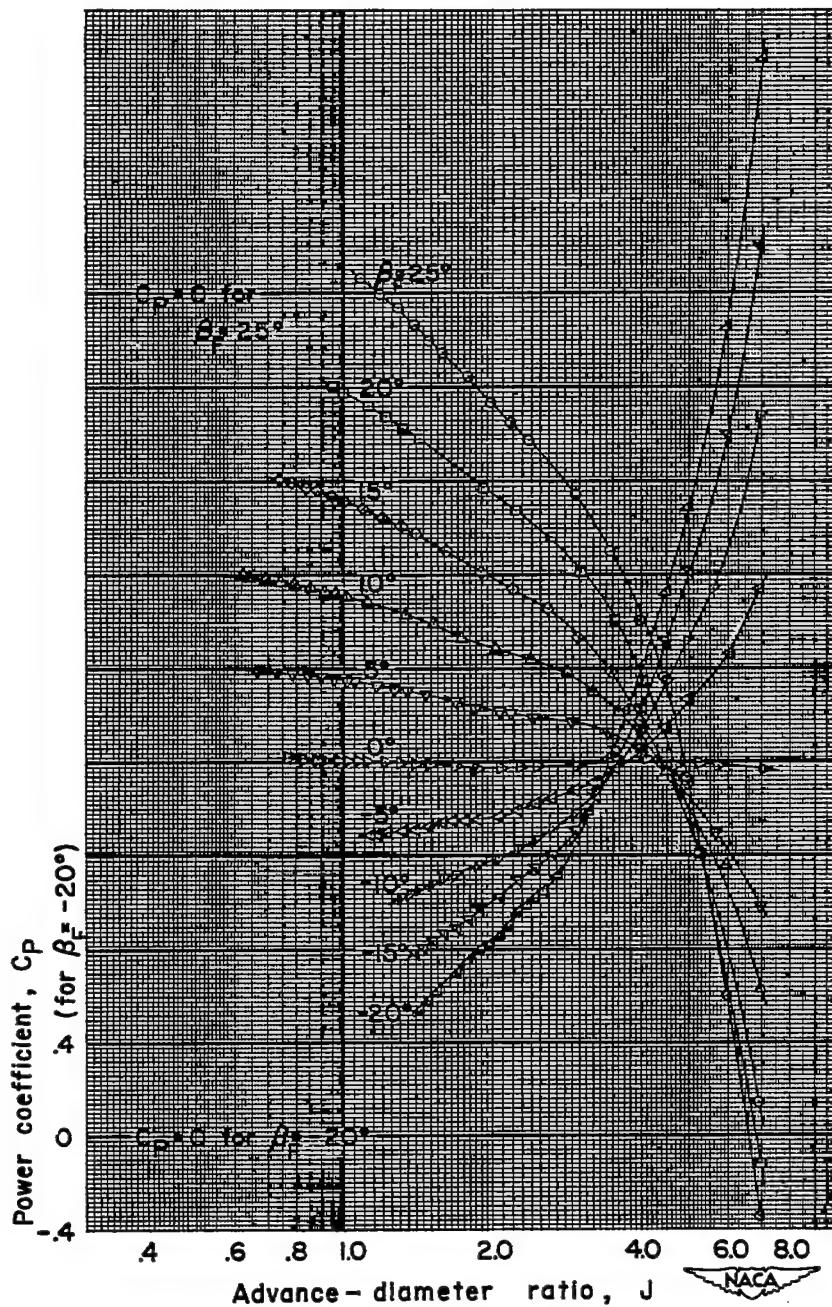
(b) $M = 0.15$, C_P vs. J

Figure 24.- Continued.

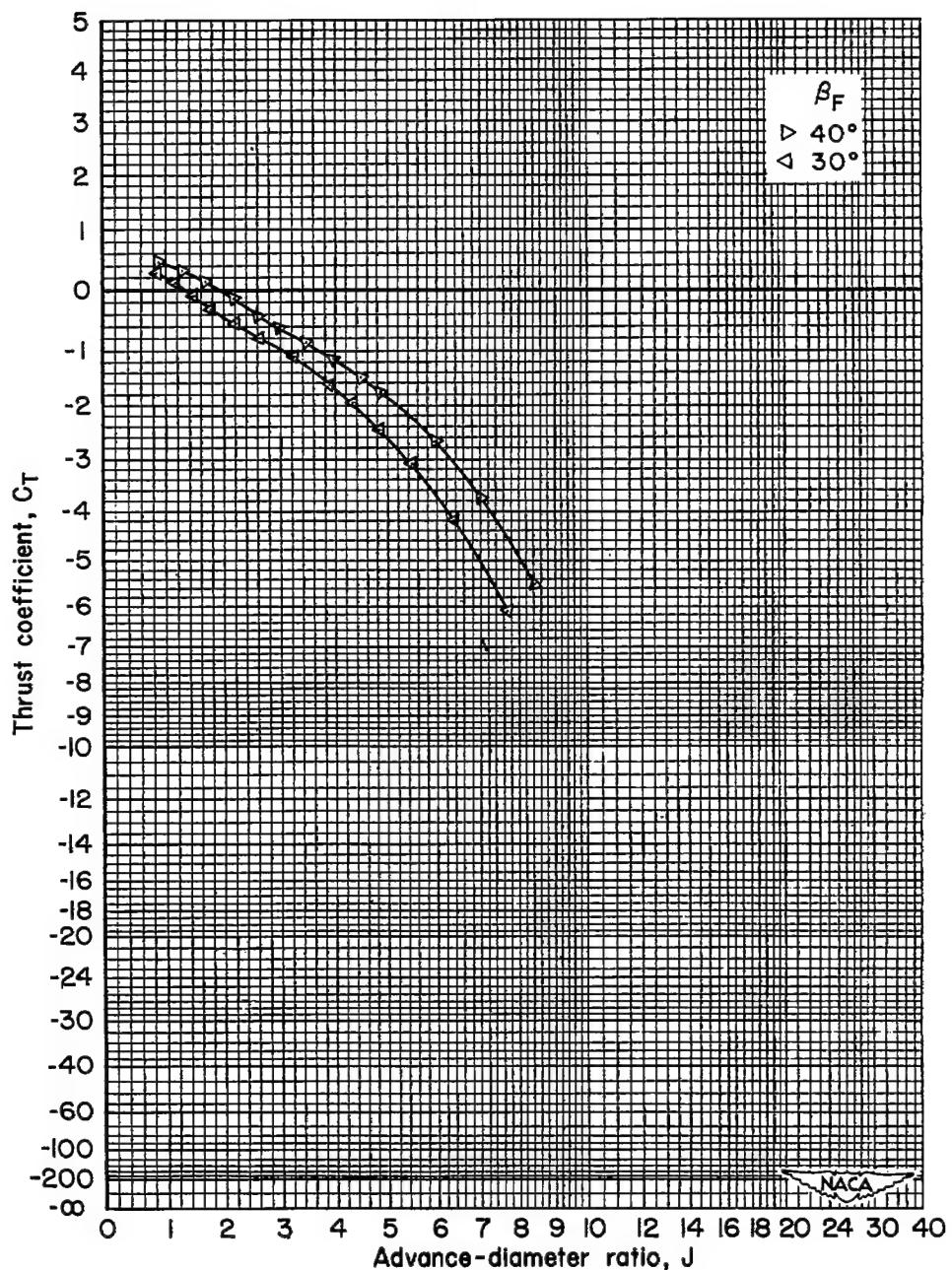
(c) $M = 0.20$, C_T vs. J

Figure 24.- Continued.

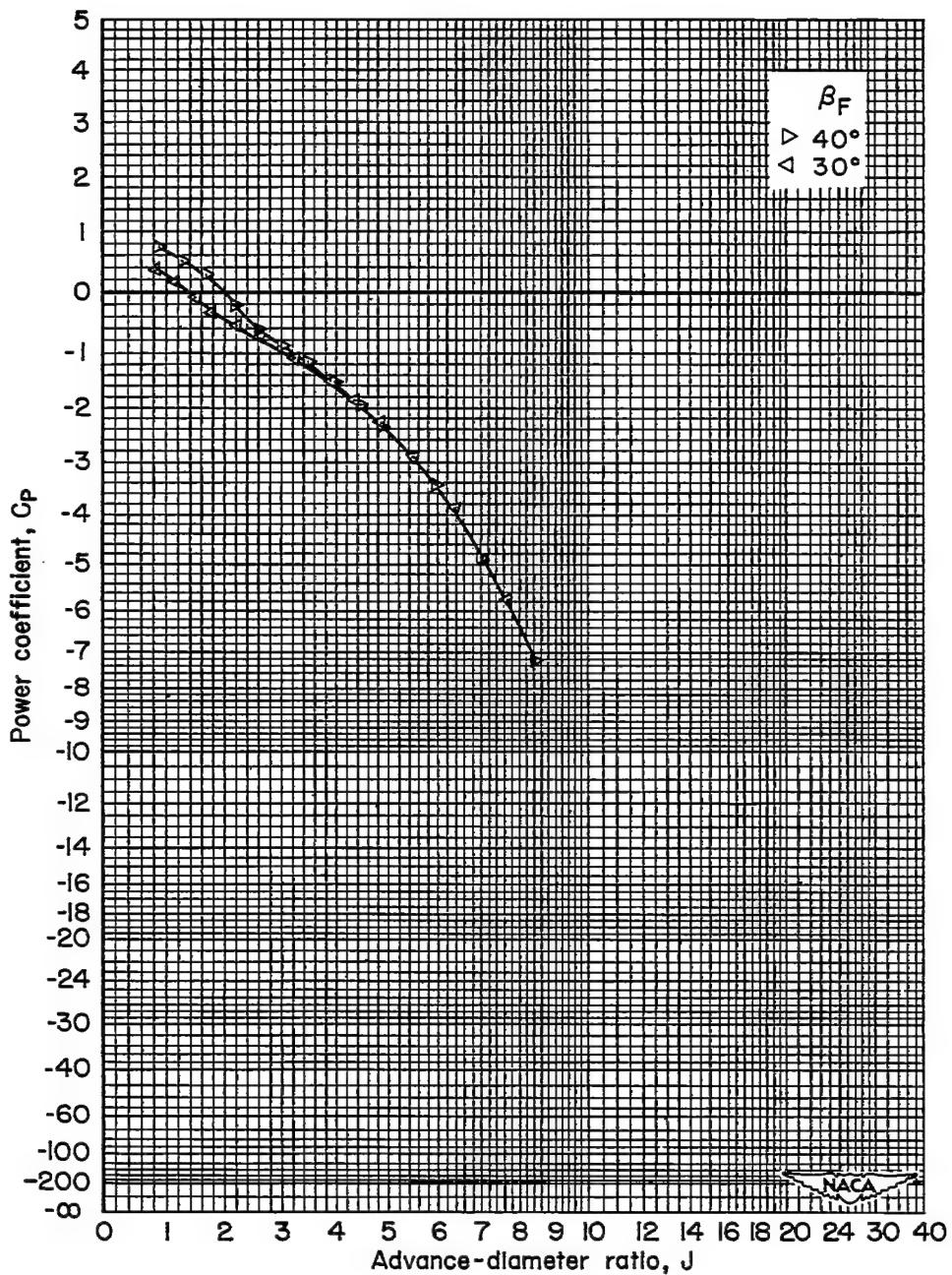
(d) $M = 0.20$, C_p vs. J

Figure 24.- Continued.

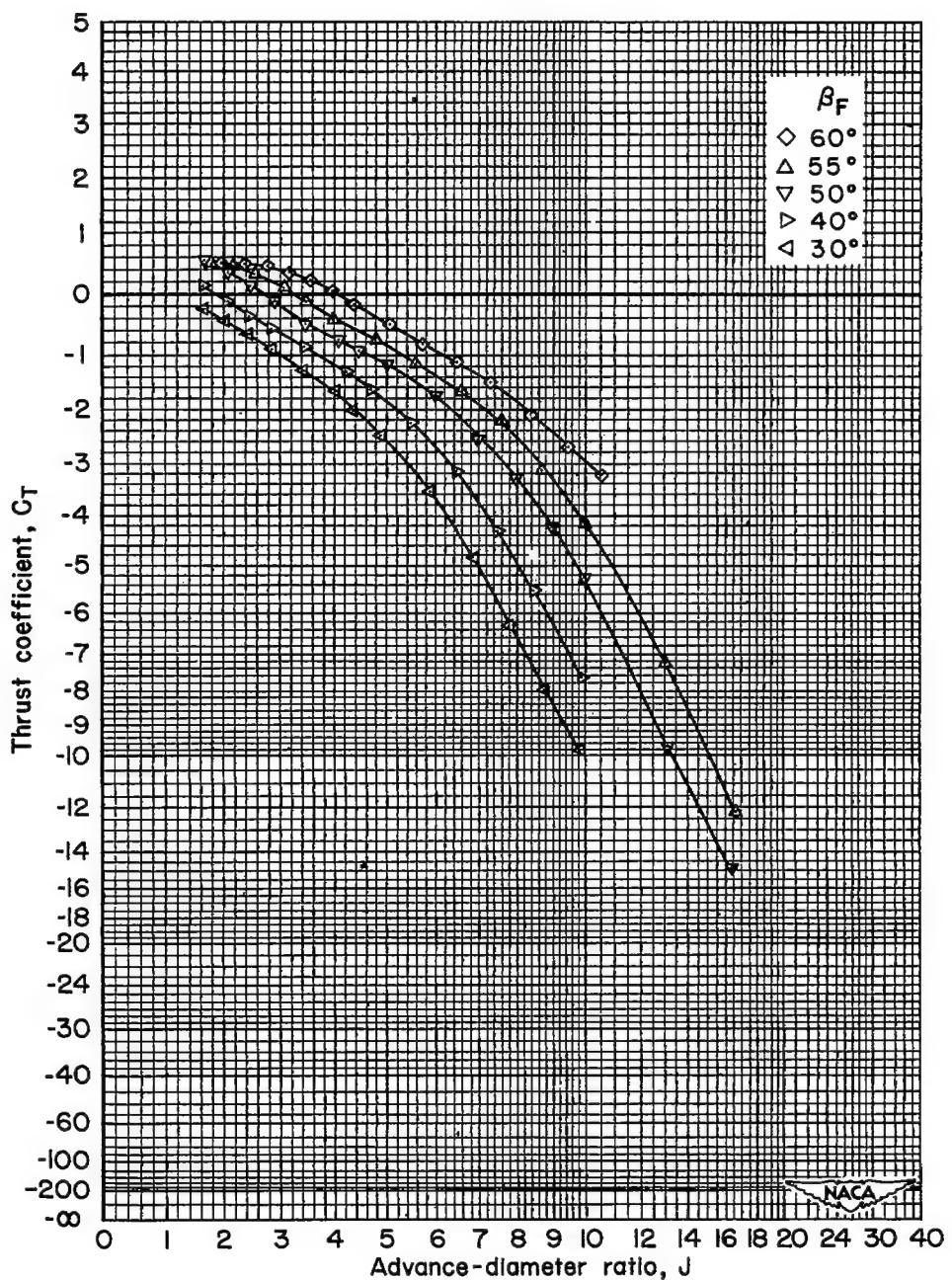
(e) $M = 0.40$, C_T vs. J

Figure 24.- Continued.

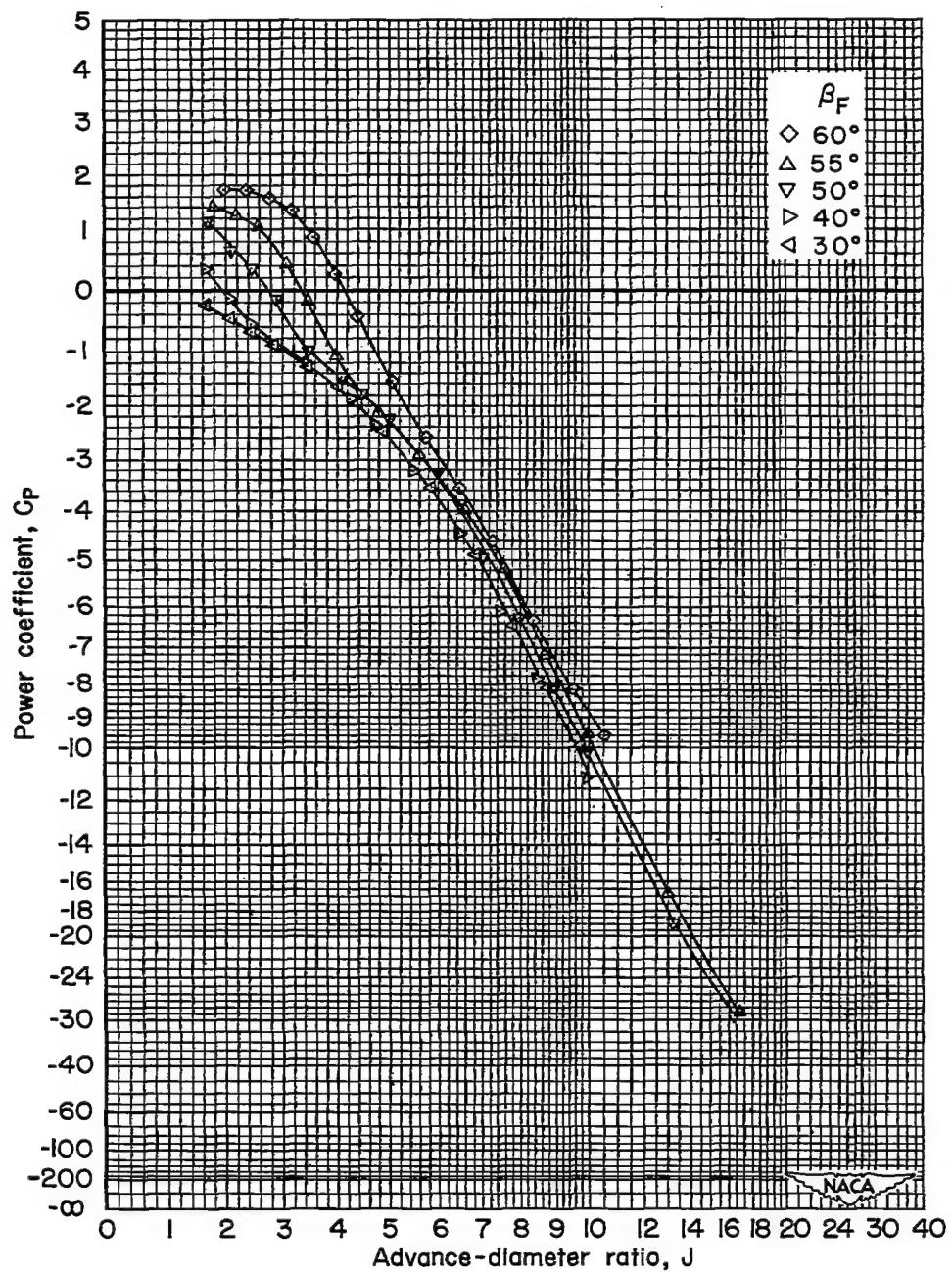
(f) $M = 0.40$, C_p vs. J

Figure 24.- Continued.

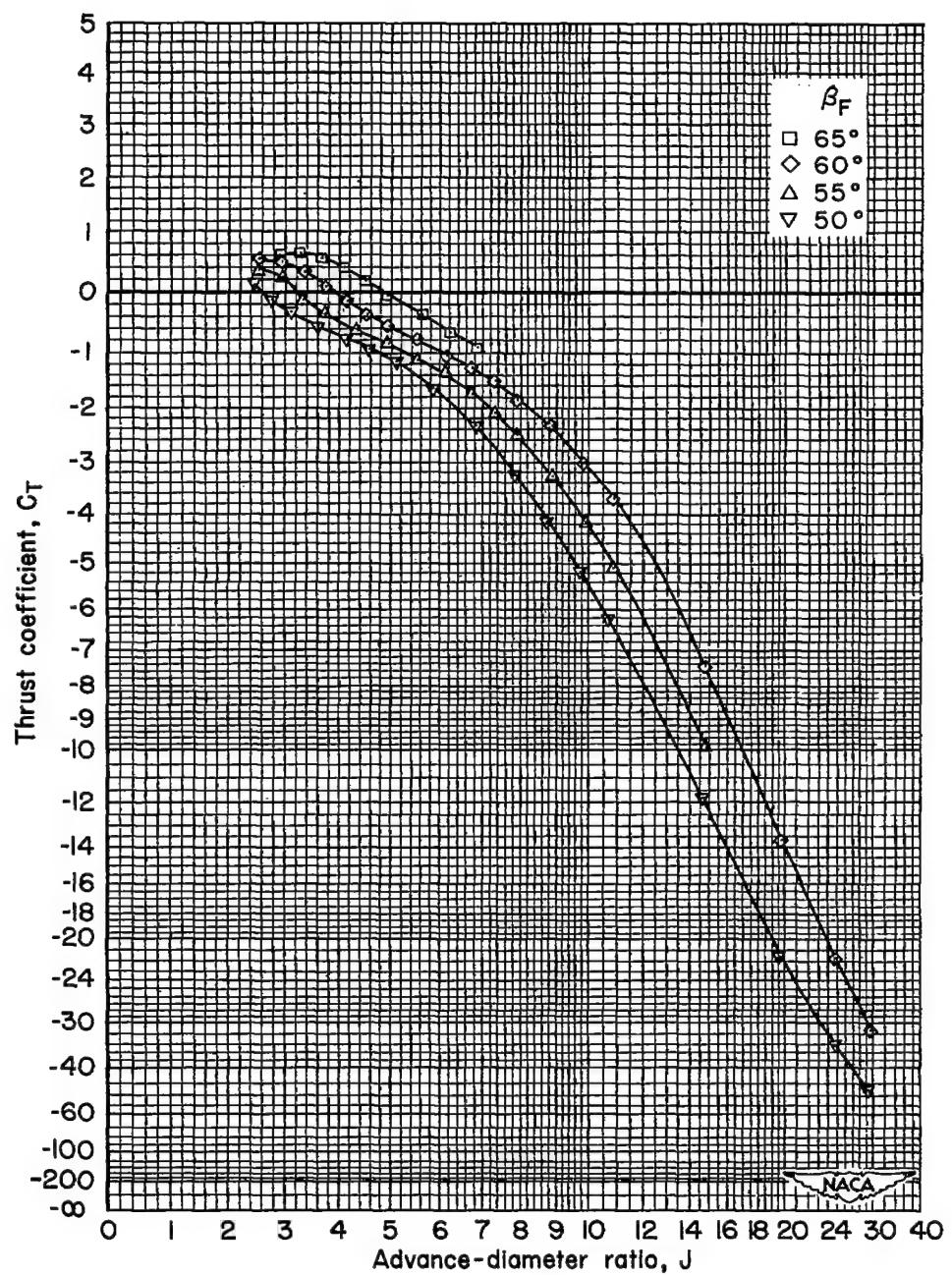
(g) $M = 0.60$, C_T vs. J

Figure 24.- Continued.

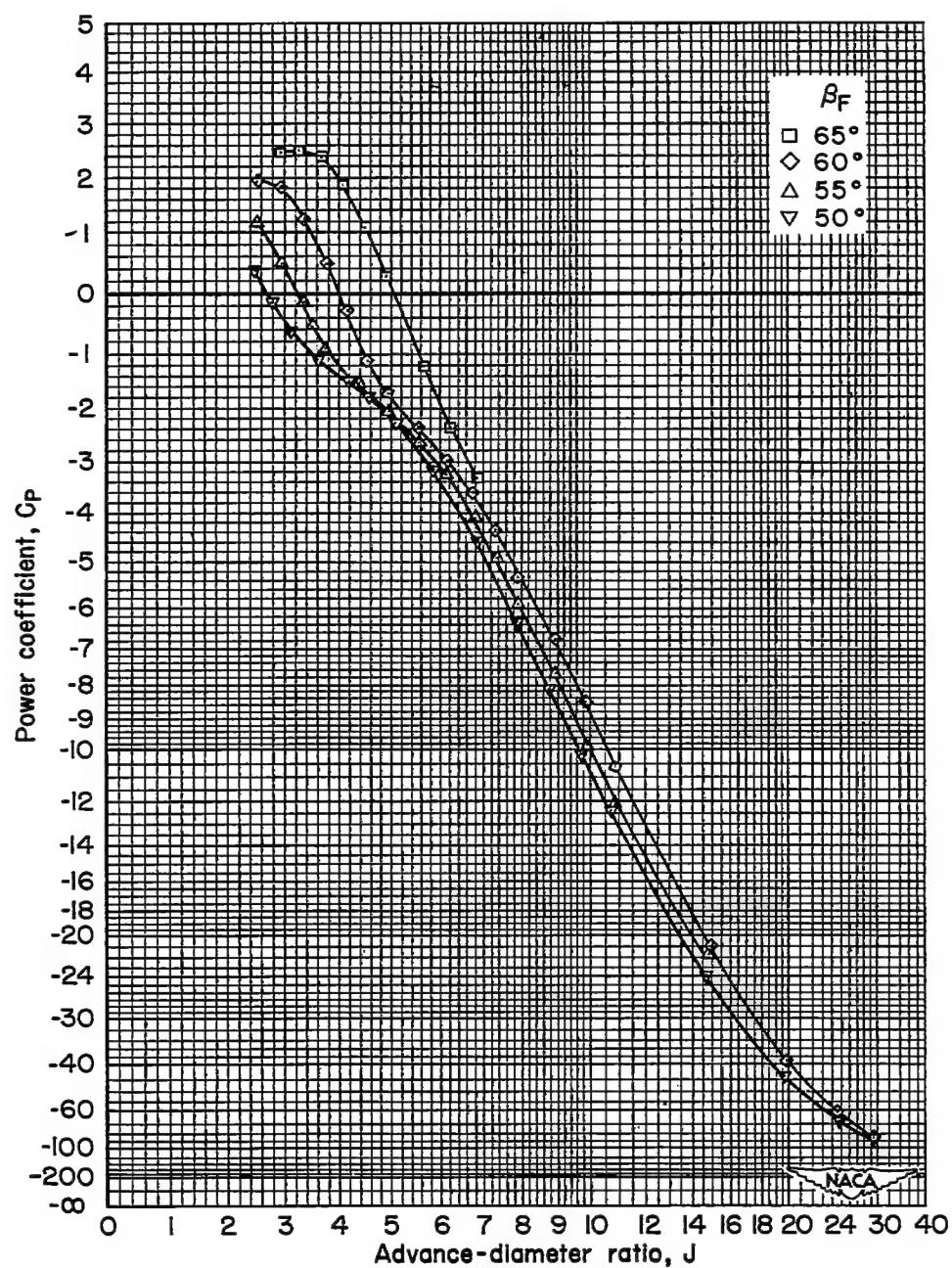
(h) $M = 0.60$, C_P vs. J

Figure 24.- Continued.

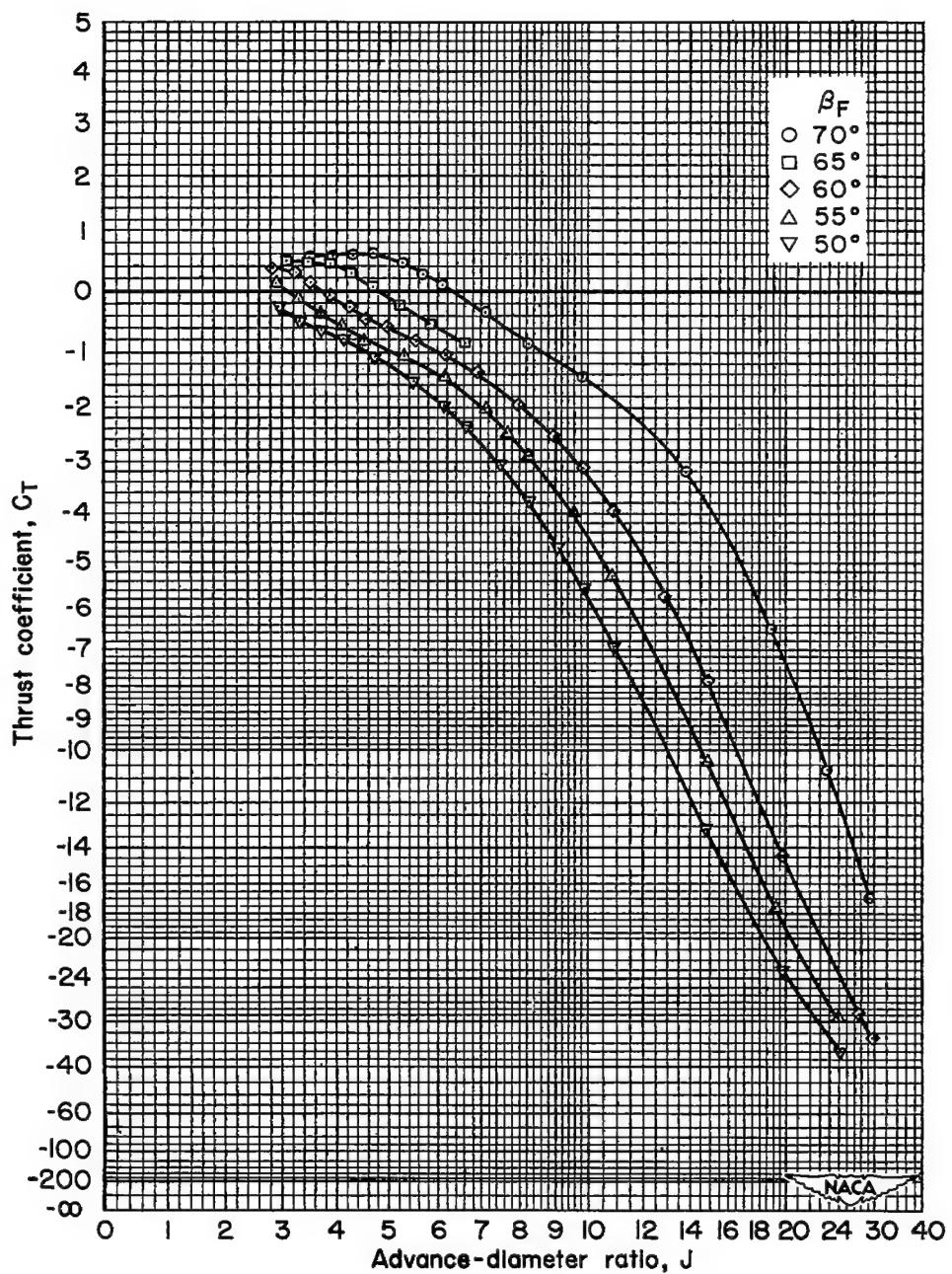
(i) $M = 0.70$, C_T vs. J

Figure 24.- Continued.

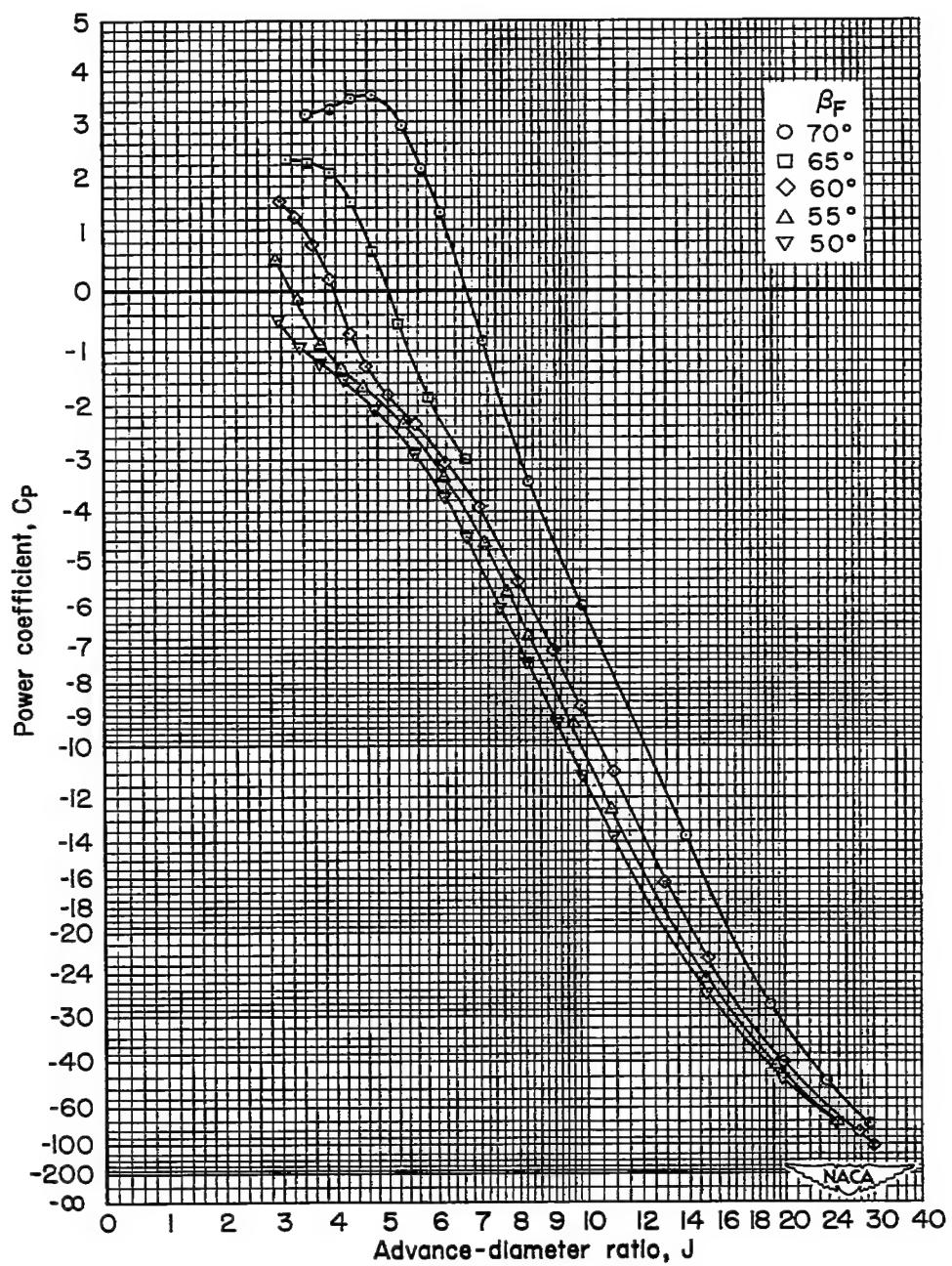
(j) $M = 0.70$, C_p vs. J

Figure 24.- Continued.

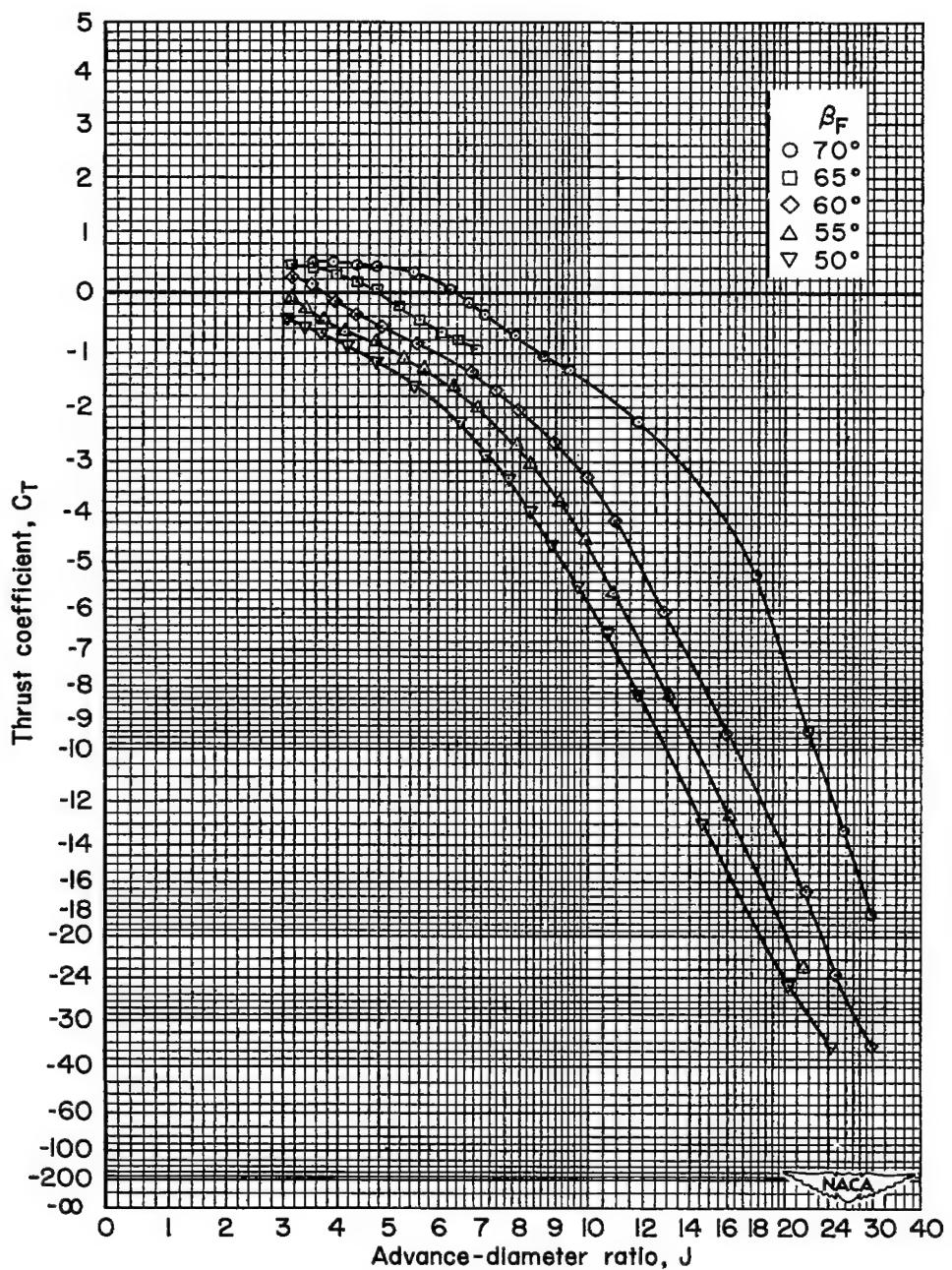
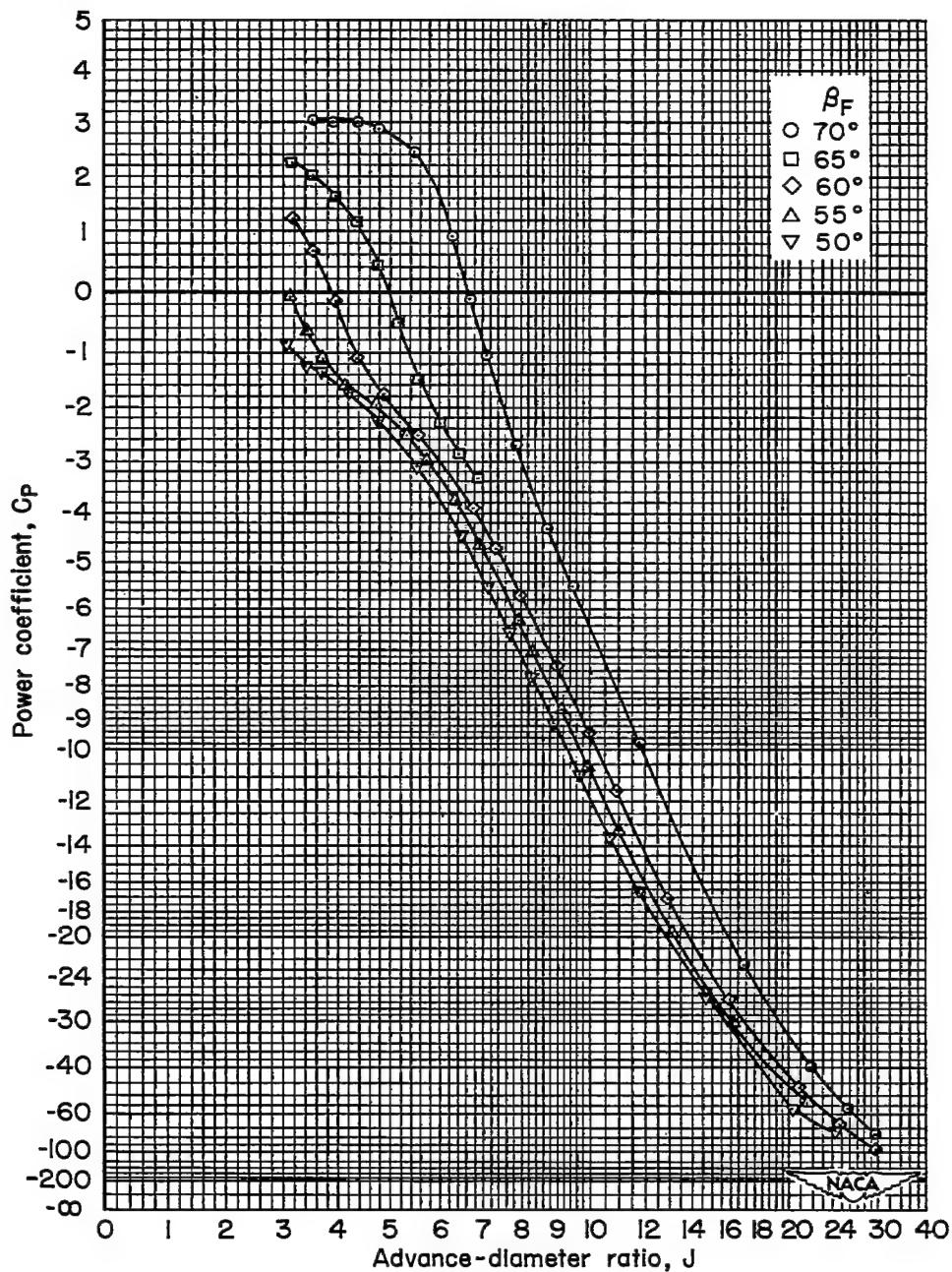
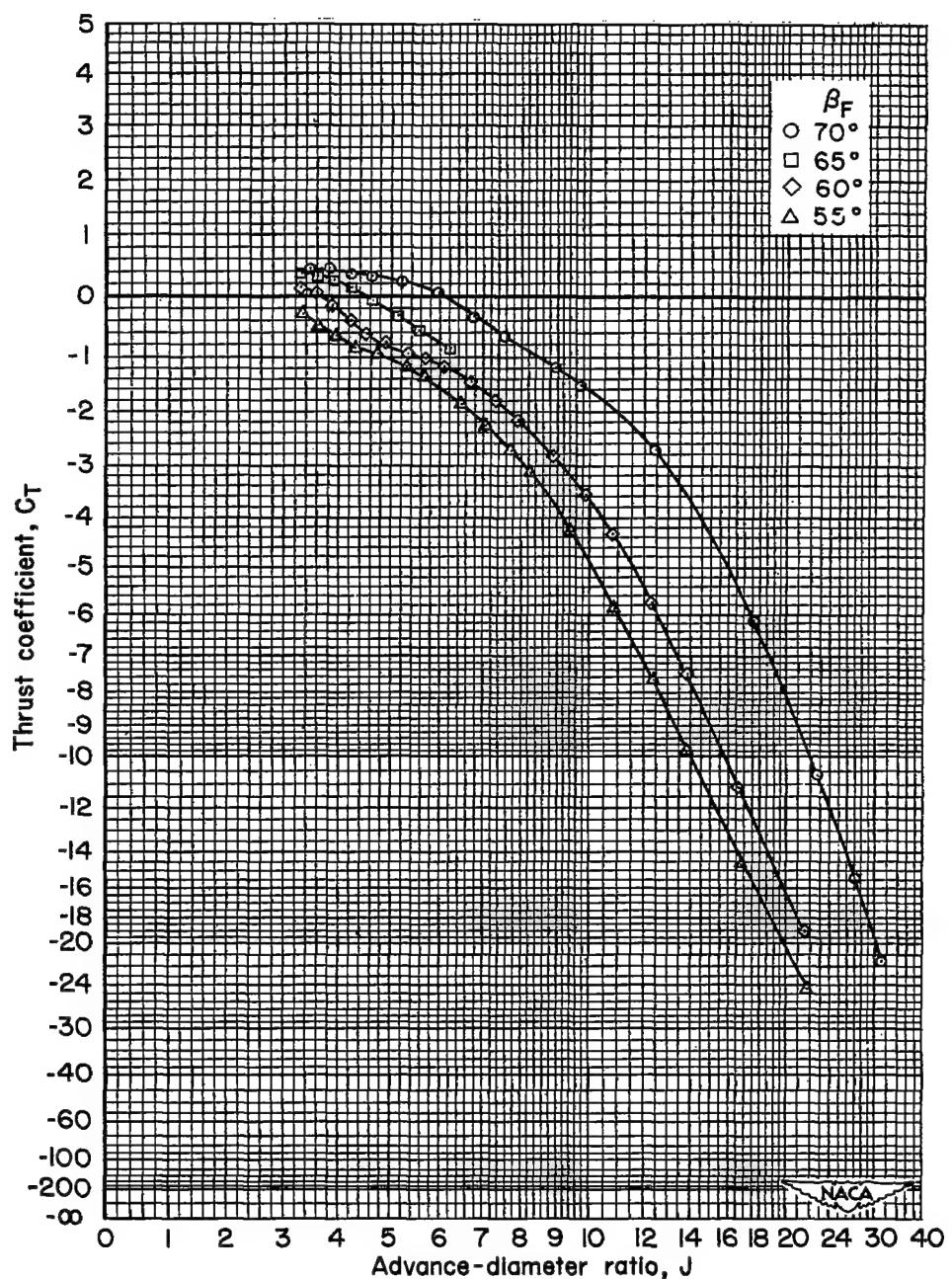
(k) $M = 0.75$, C_T vs. J

Figure 24.- Continued.



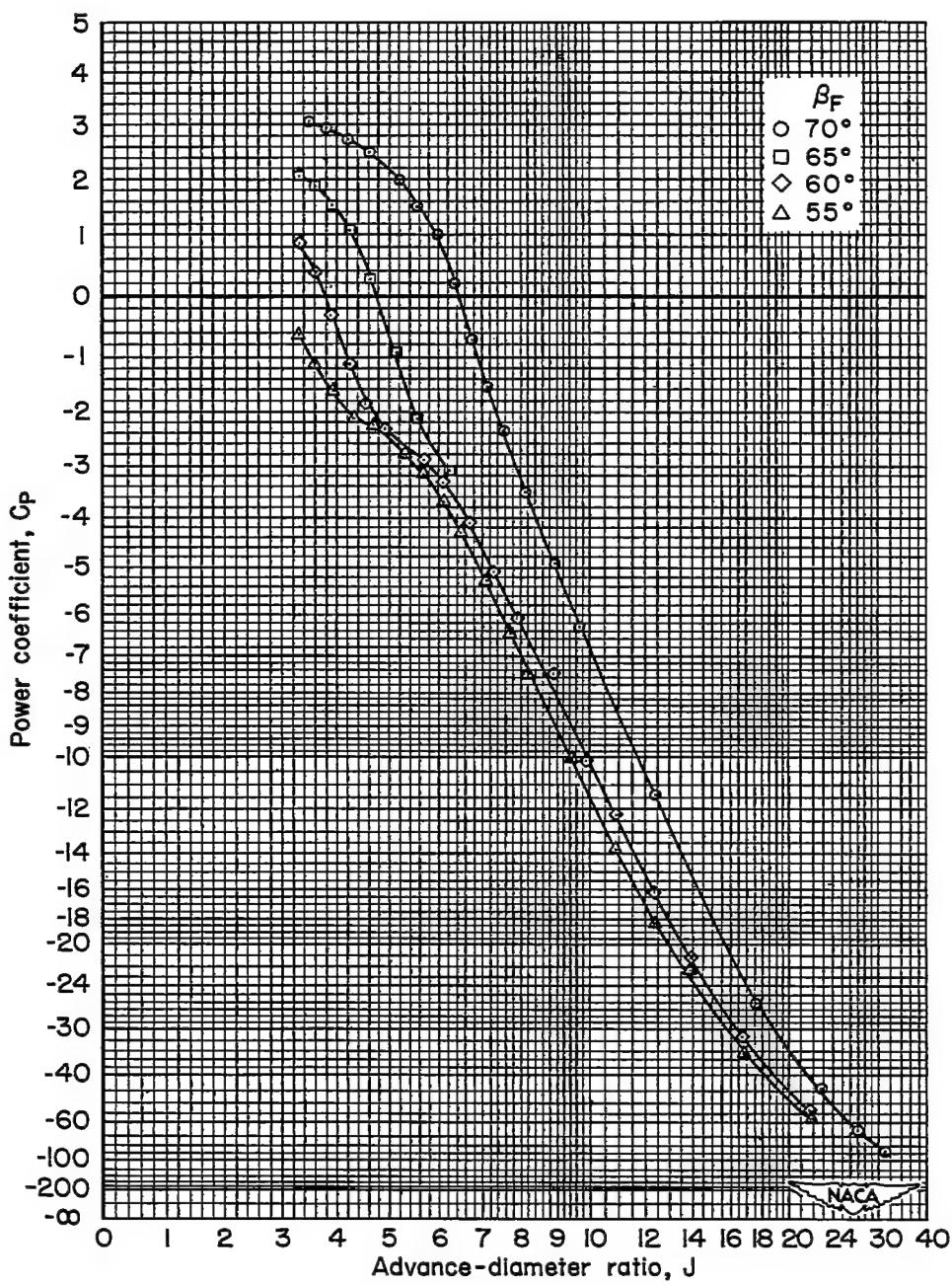
(1) $M = 0.75$, C_p vs. J

Figure 24.- Continued.



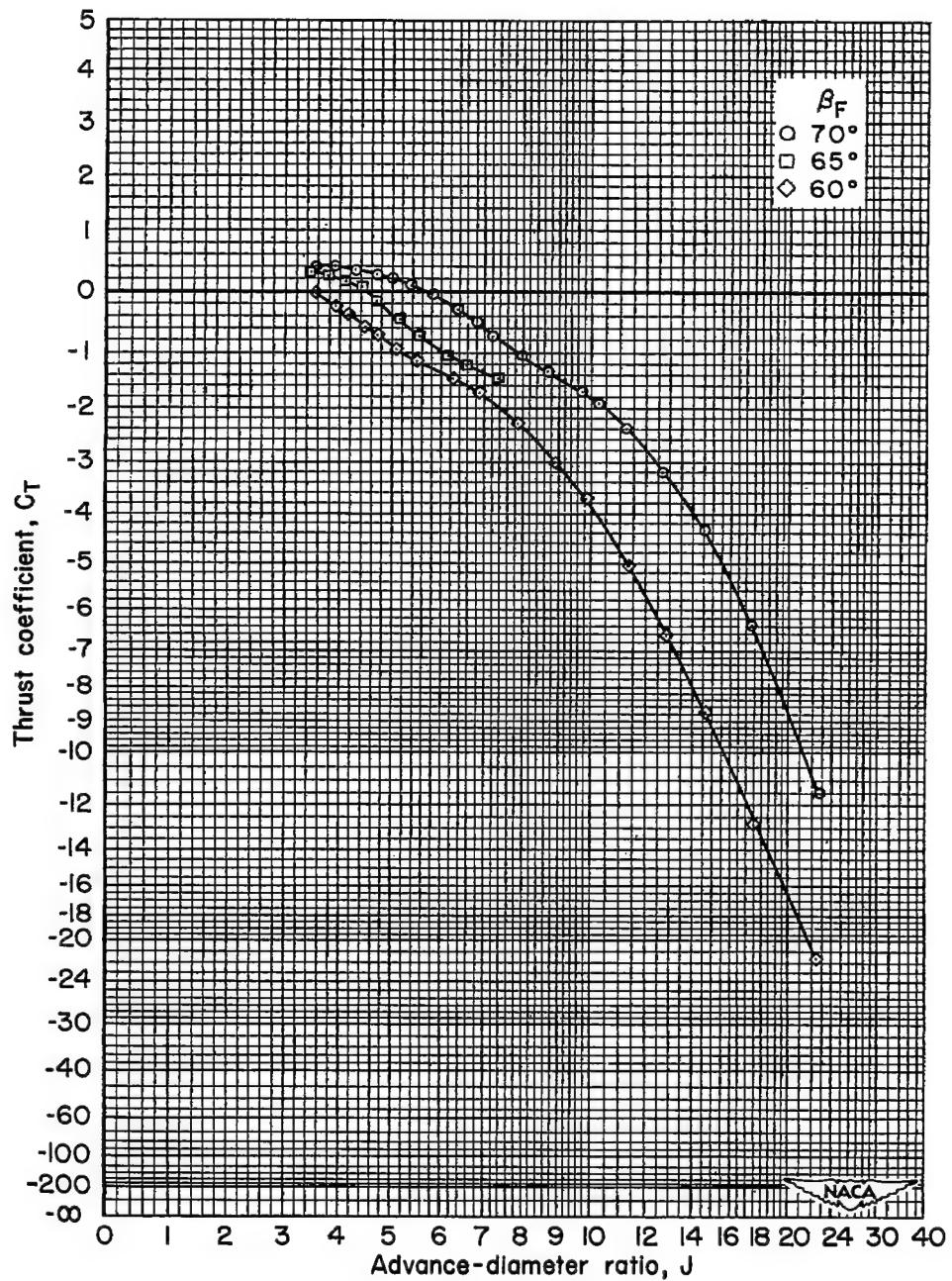
(m) $M = 0.80$, C_T vs. J

Figure 24.- Continued.



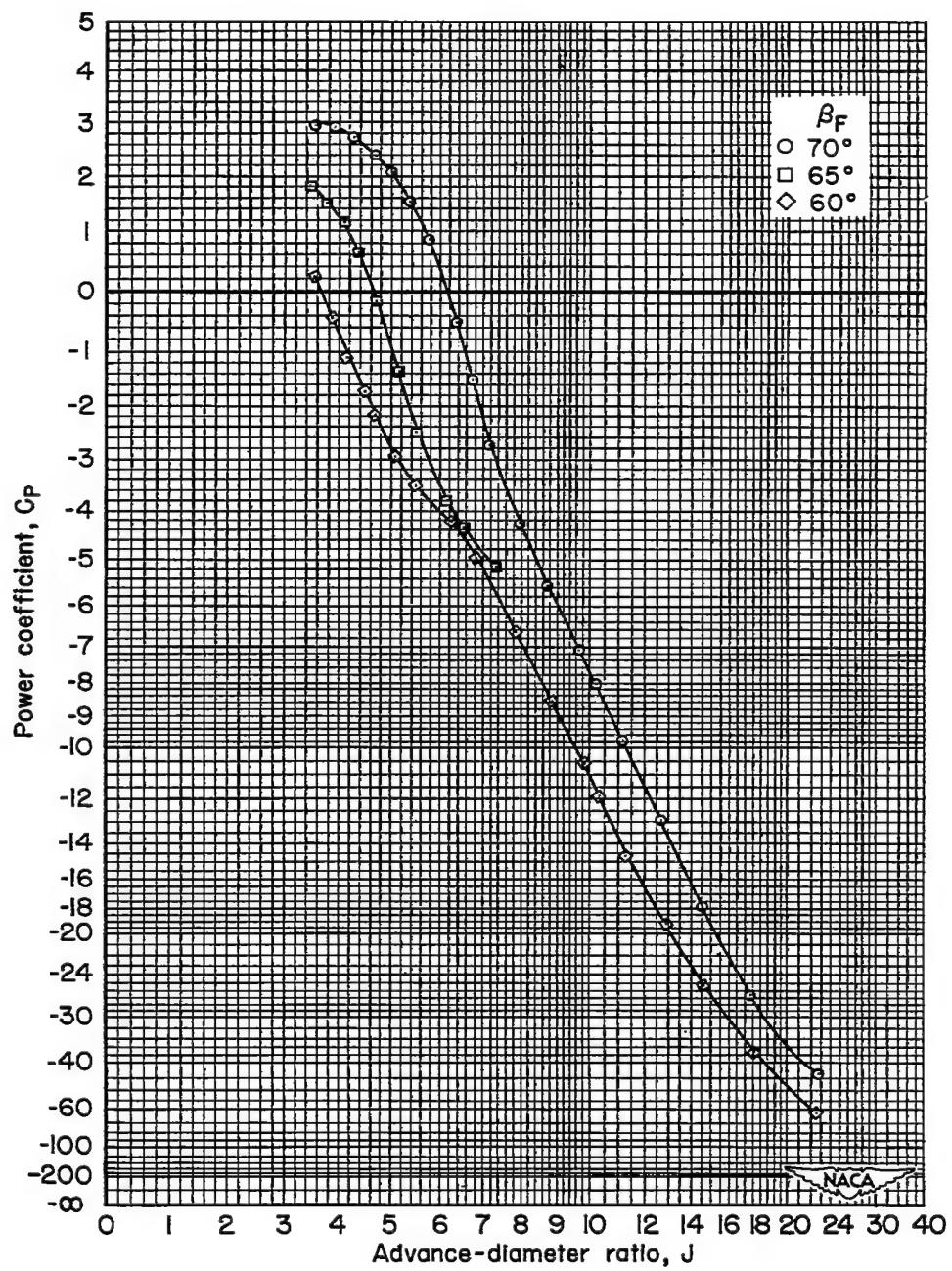
(n) $M = 0.80$, C_p vs. J

Figure 24.- Continued.



(o) $M = 0.84$, C_T vs. J

Figure 24.- Continued.



(p) $M = 0.84$, C_p vs. J

Figure 24.- Concluded.

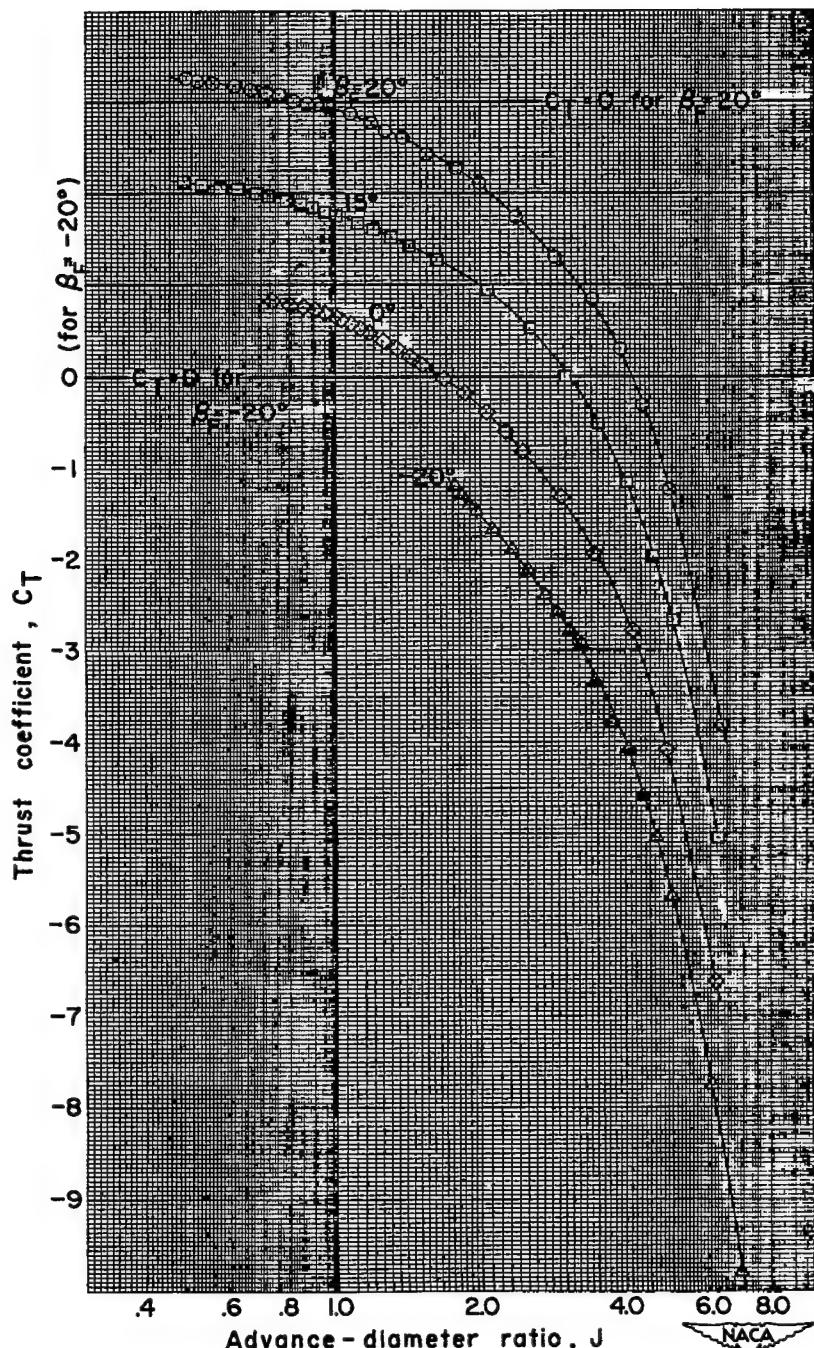
(a) $M = 0.15$, C_T vs. J

Figure 25.- Negative-thrust characteristics; NACA 4-(5)(05)-037 eight-blade, dual-rotation propeller, $\Delta\beta$ = optimum, spinner A.

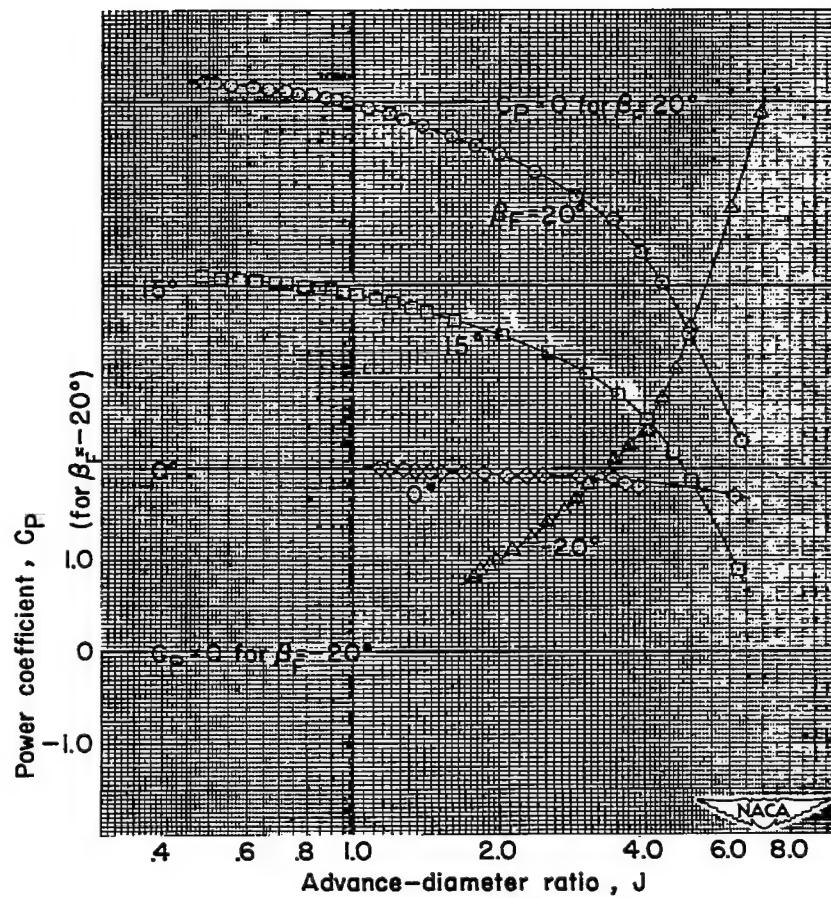
(b) $M = 0.15$, C_P vs. J

Figure 25.- Continued.

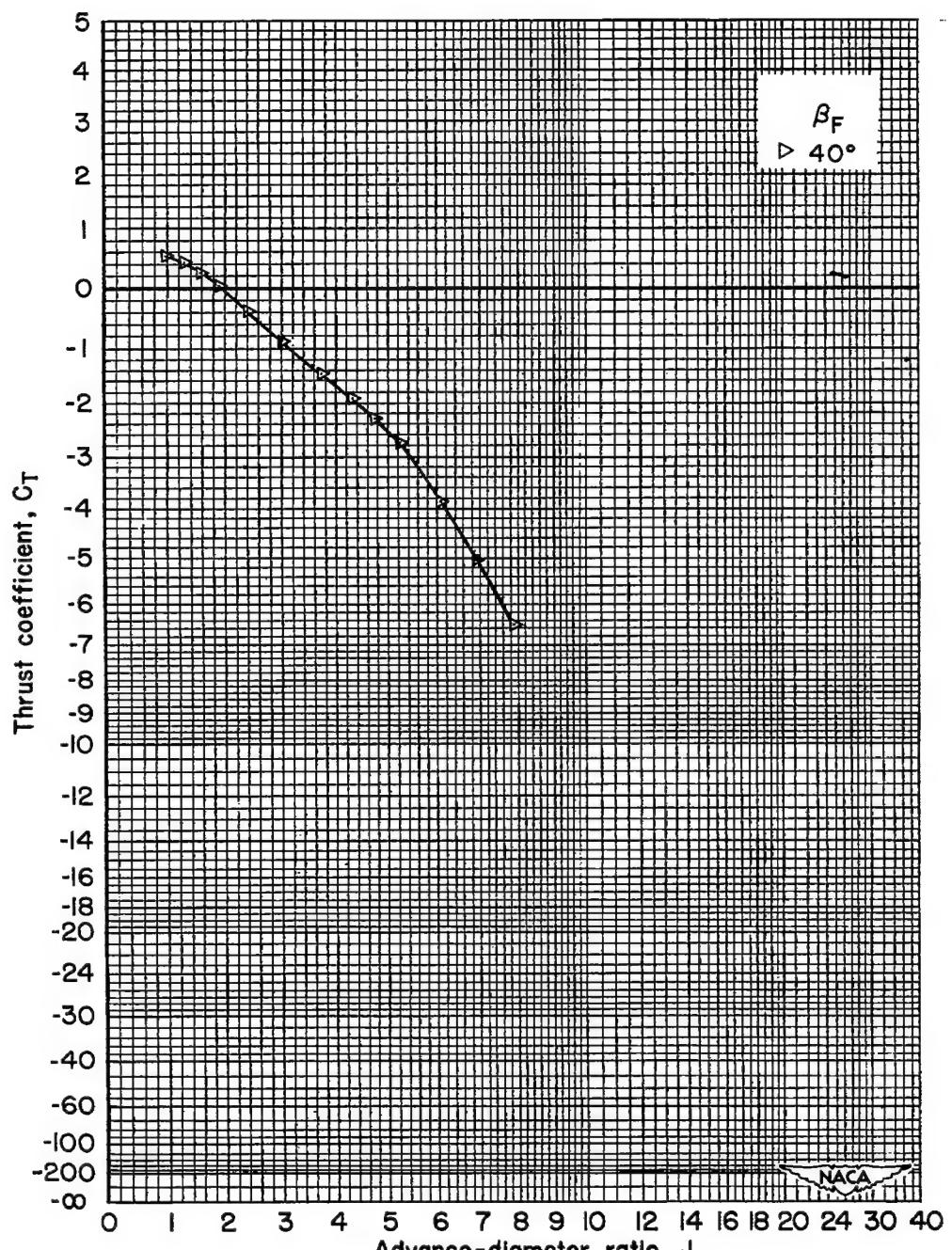
(c) $M = 0.20$, C_T vs. J

Figure 25.- Continued.

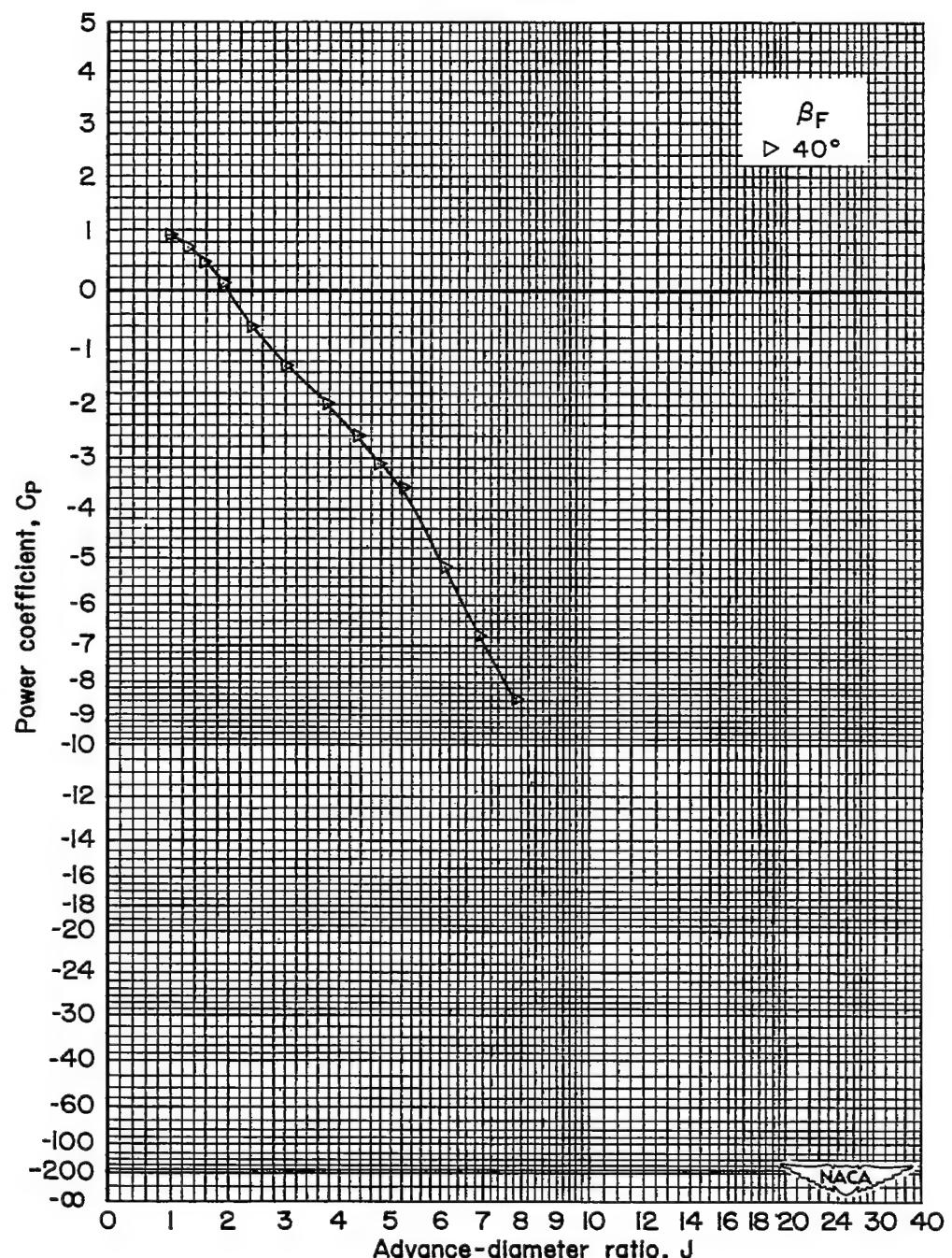
(a) $M = 0.20$, C_P vs. J

Figure 25.- Continued.

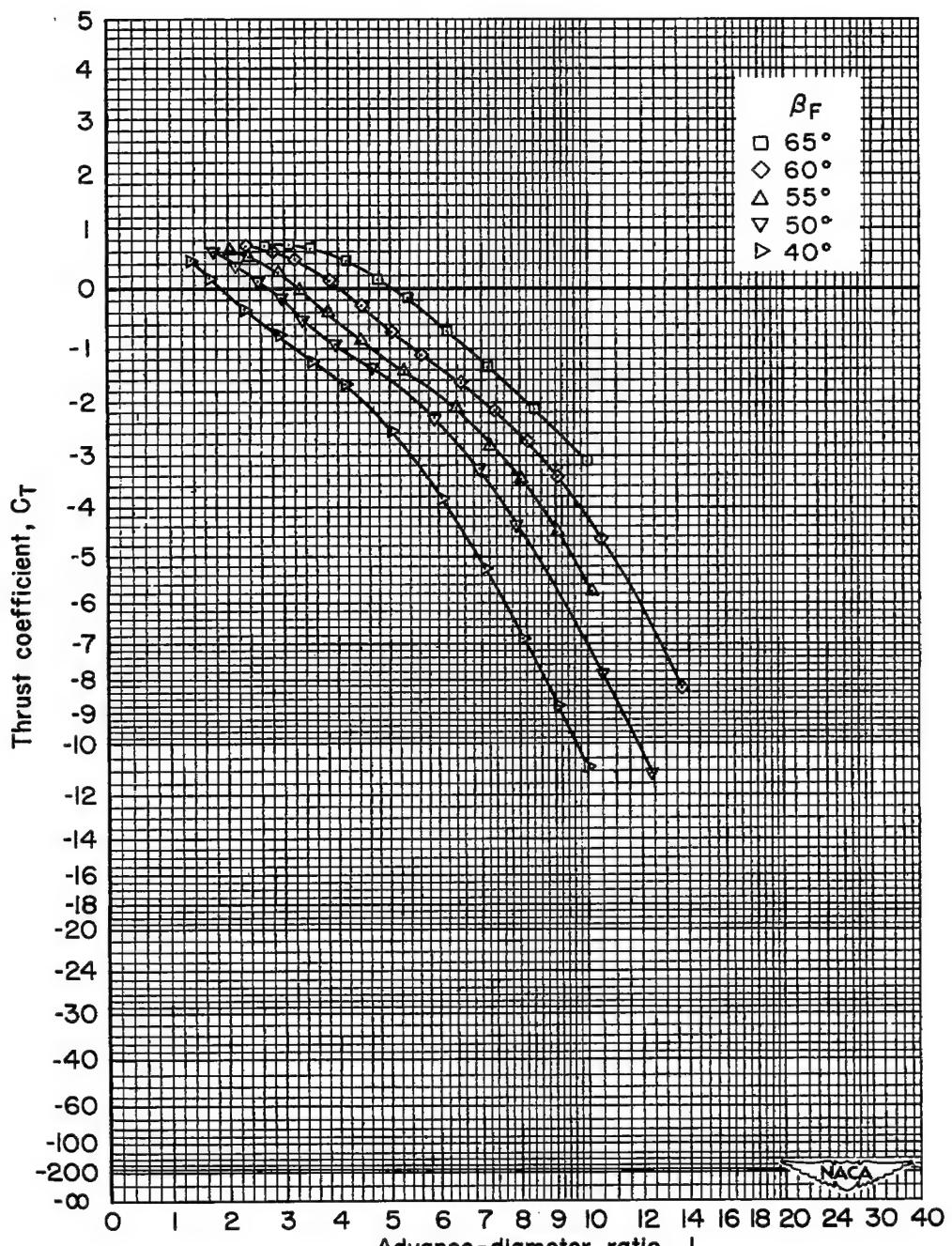
(e) $M = 0.40$, C_T vs. J

Figure 25.- Continued.

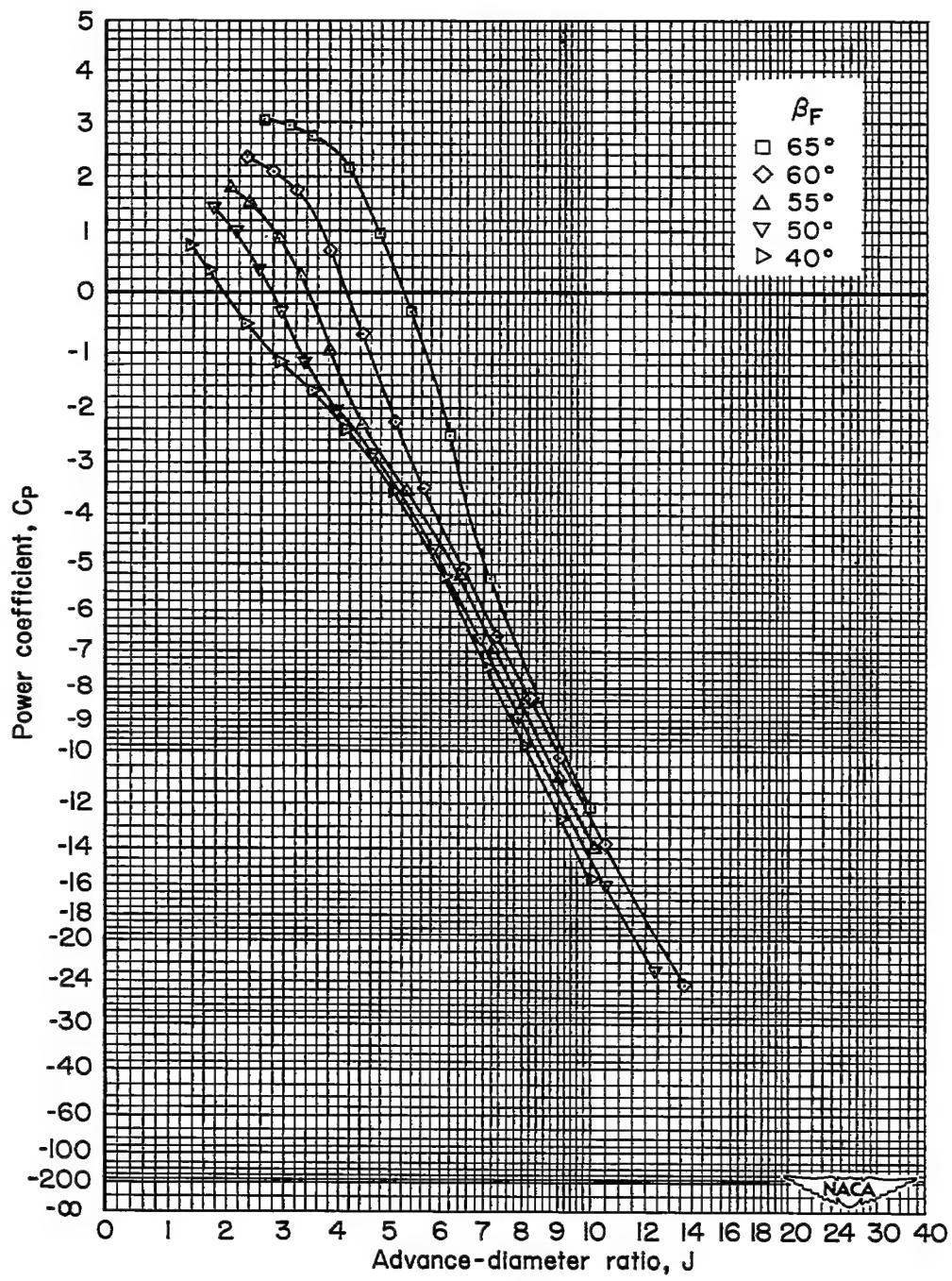
(f) $M = 0.40$, C_p vs. J

Figure 25.- Continued.

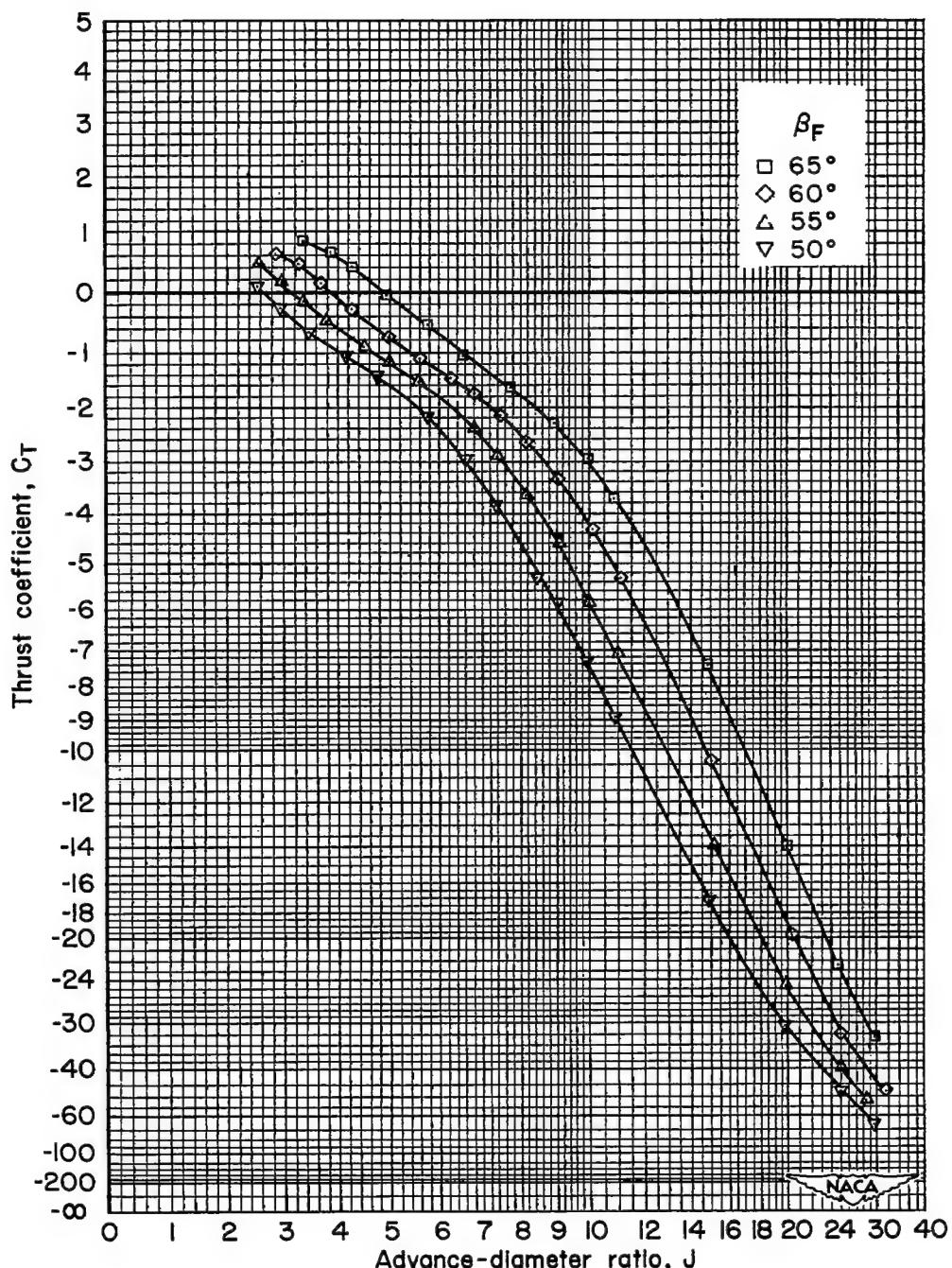
(g) $M = 0.60$, C_T vs. J

Figure 25.- Continued.

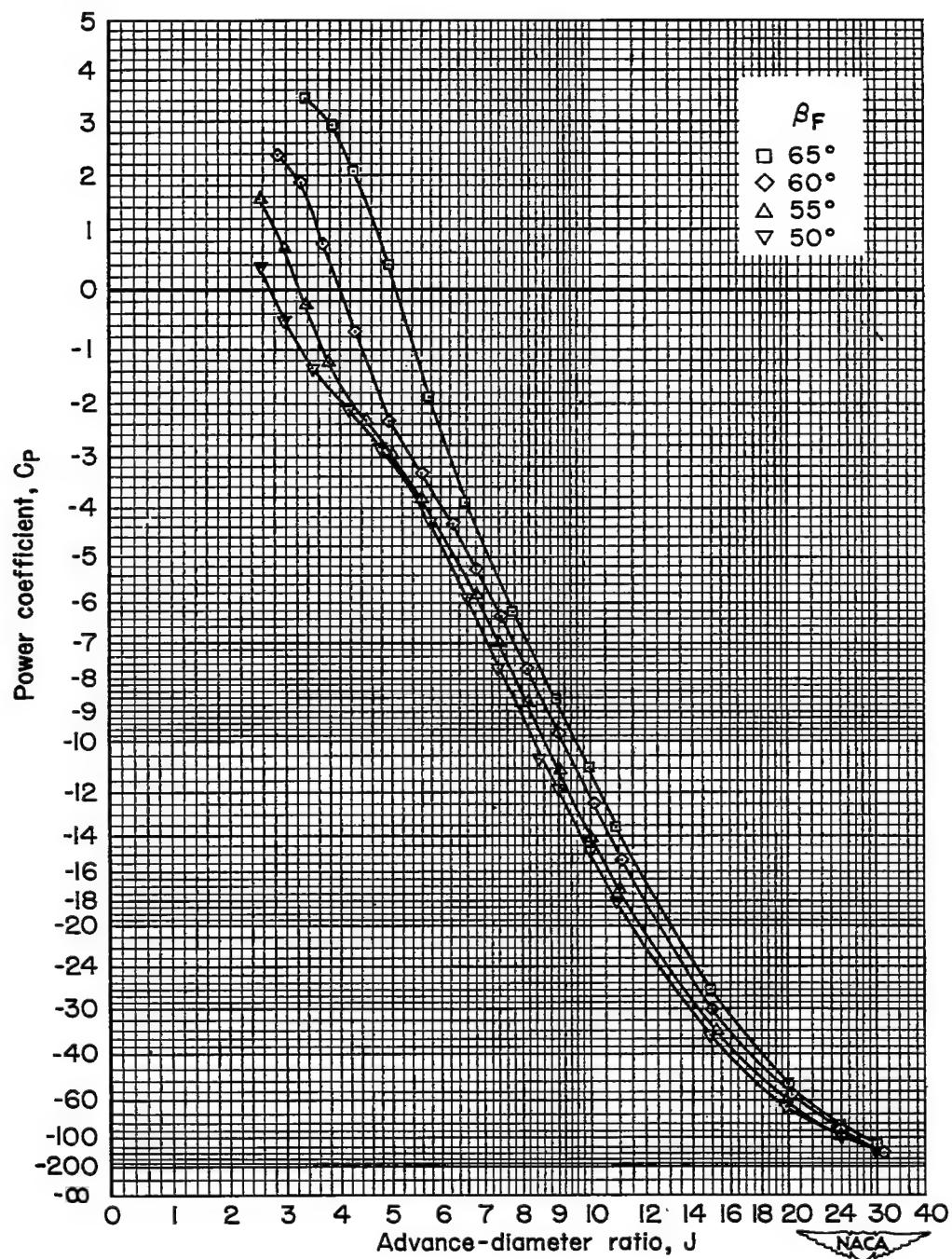
(h) $M = 0.60$, C_P vs. J

Figure 25.- Continued.

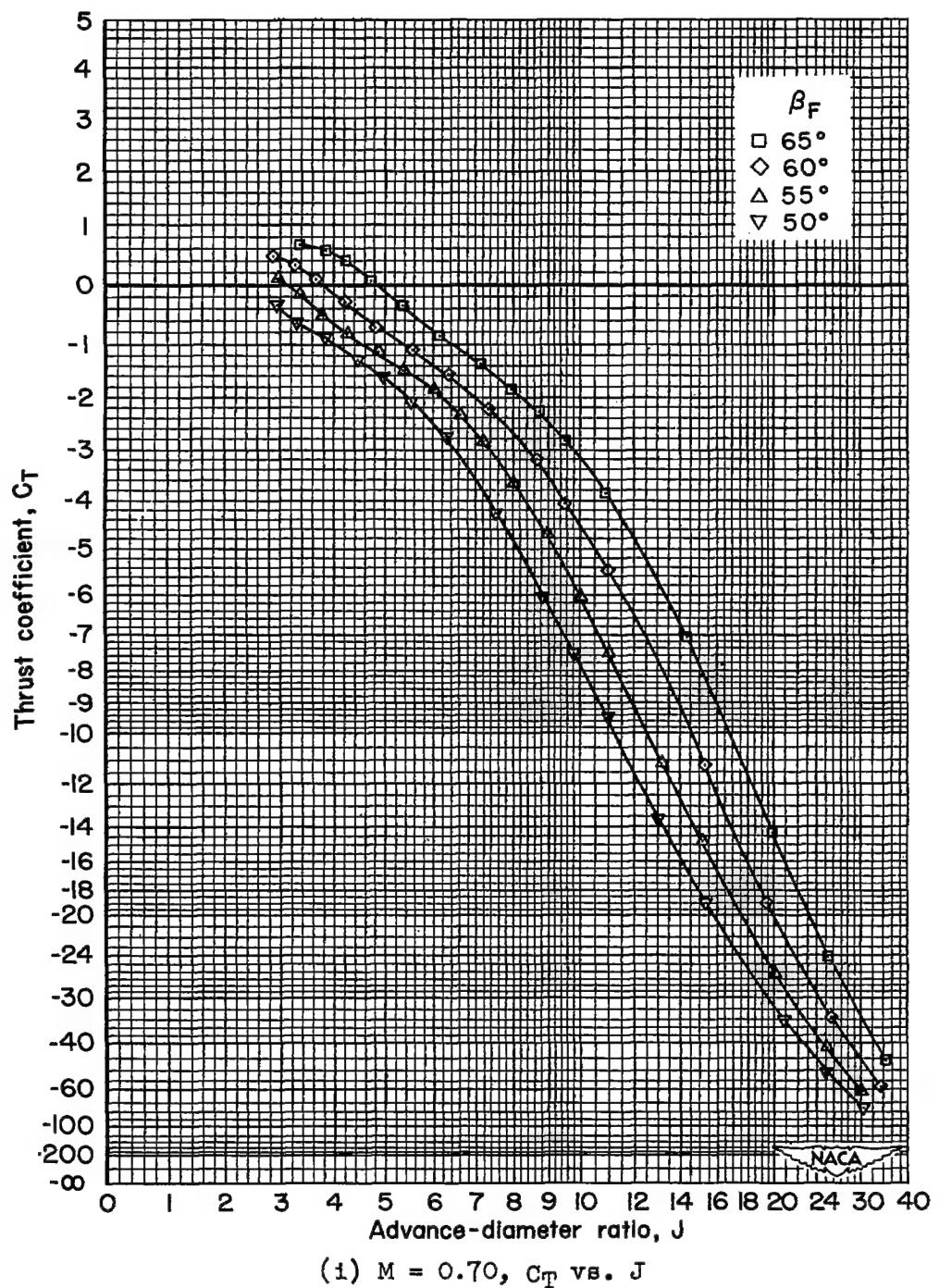


Figure 25.- Continued.

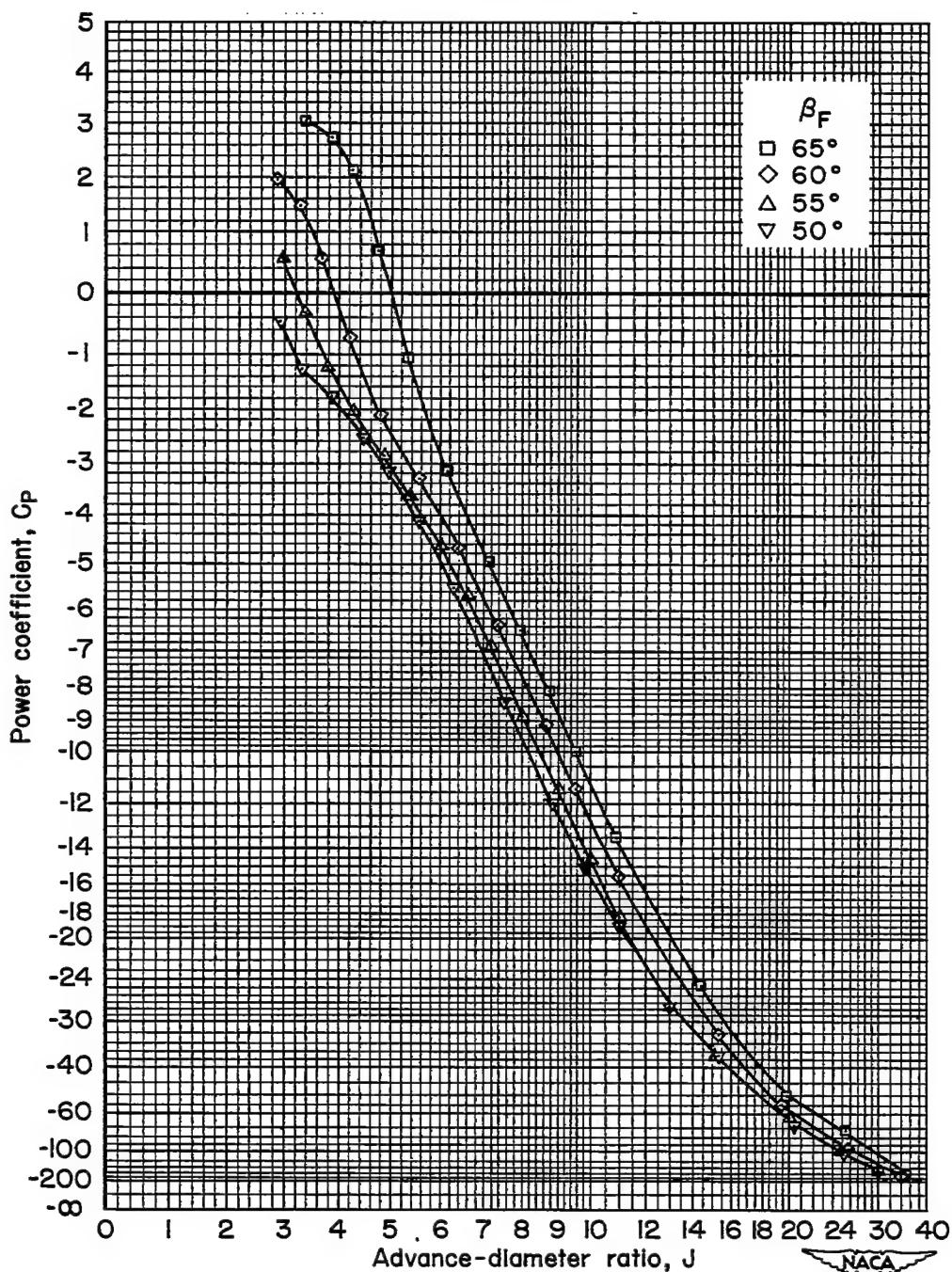
(j) $M = 0.70$, C_P vs. J

Figure 25.-- Continued.

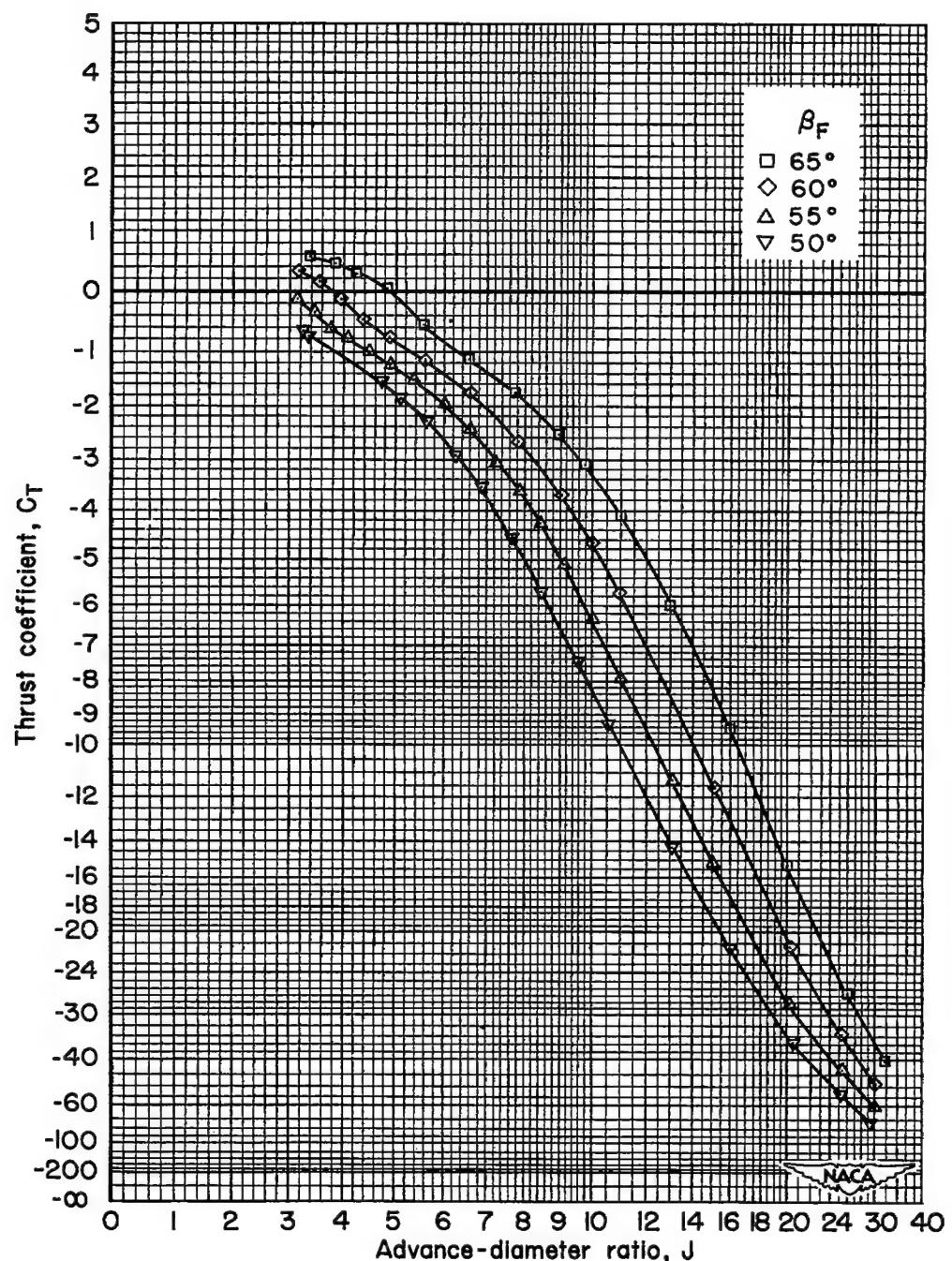
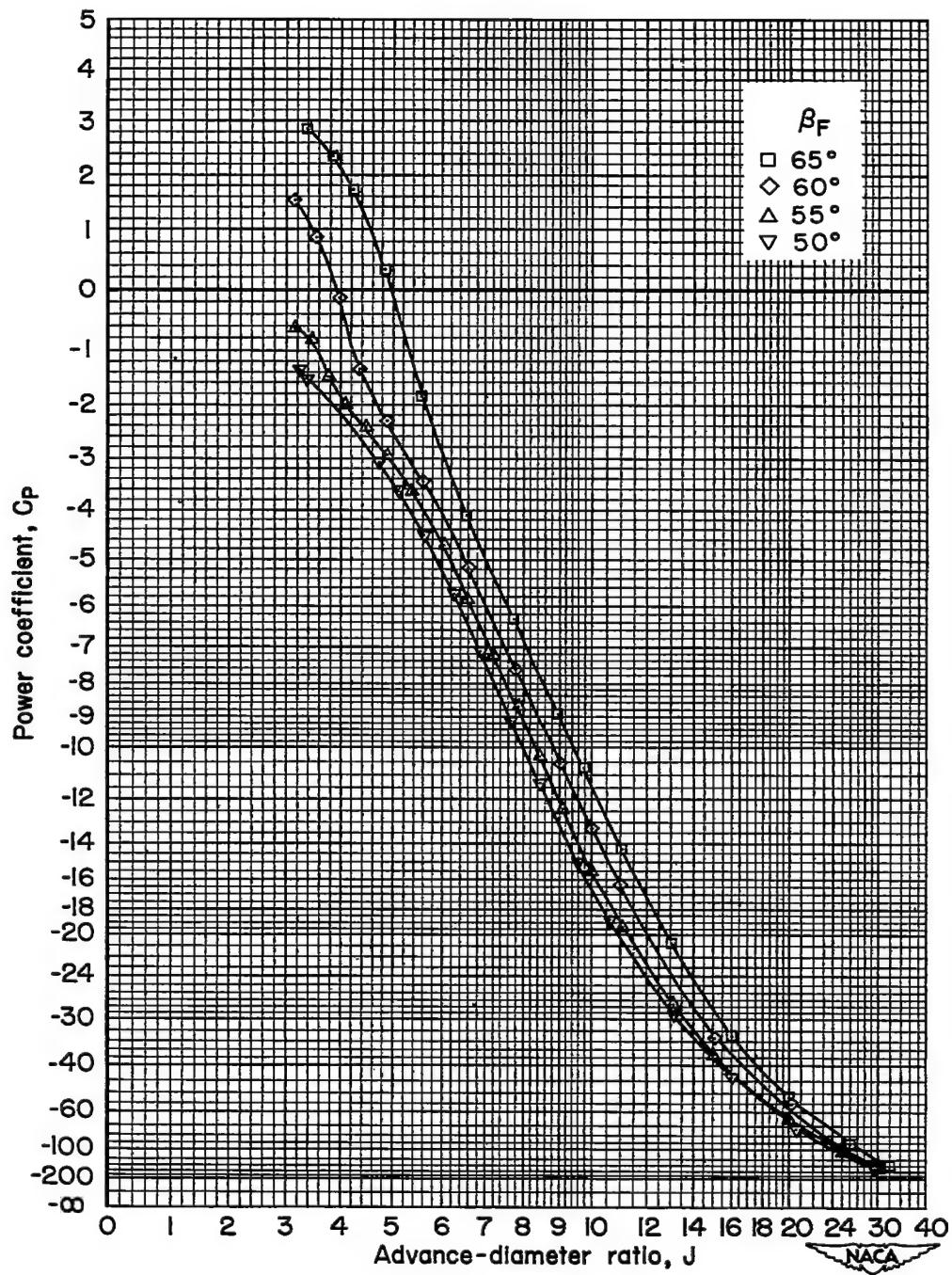
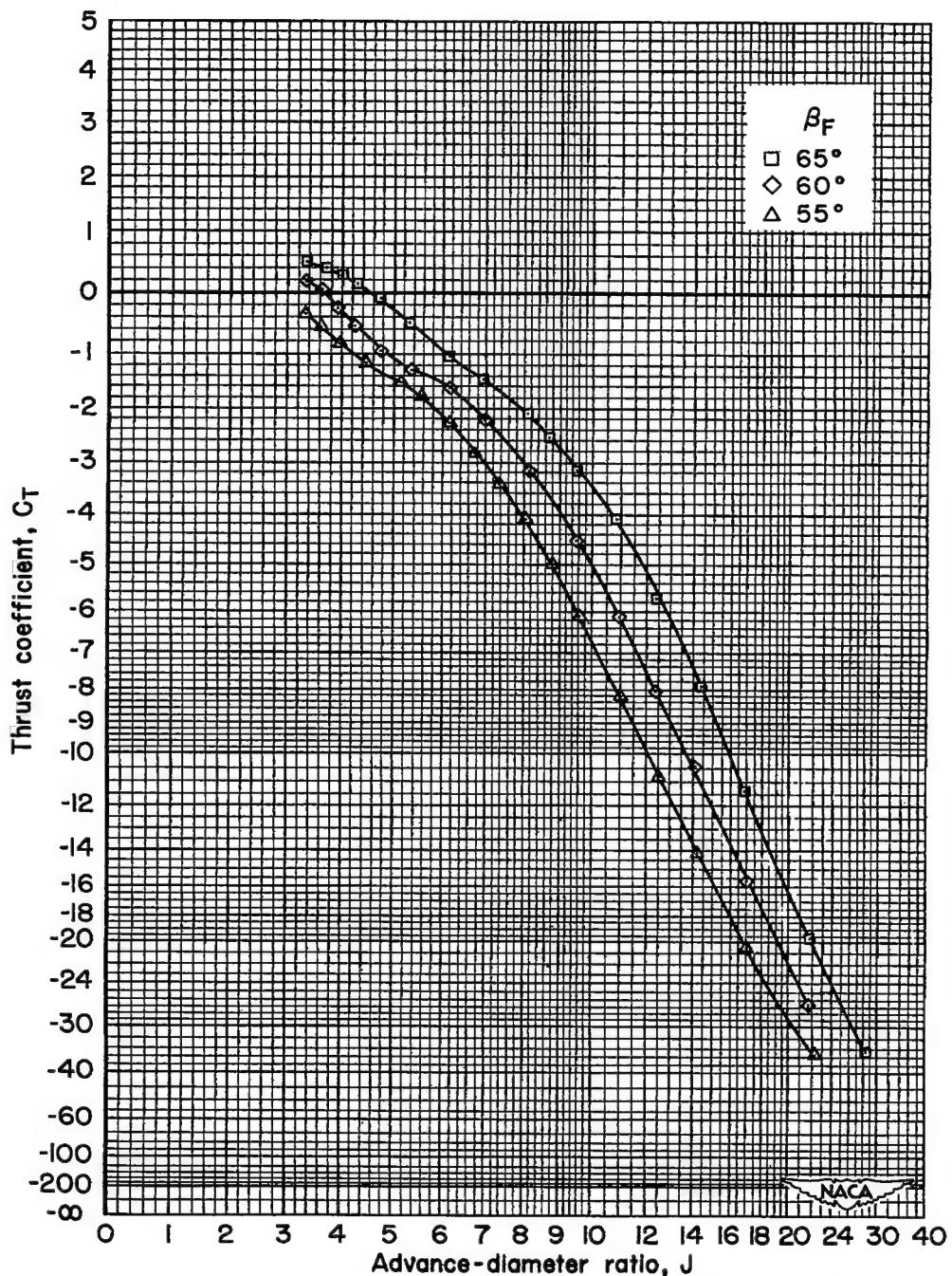
(k) $M = 0.75$, C_T vs. J

Figure 25.- Continued.



(1) $M = 0.75$, C_p vs. J

Figure 25.- Continued.



(m) $M = 0.80$, C_T vs. J

Figure 25.- Continued.

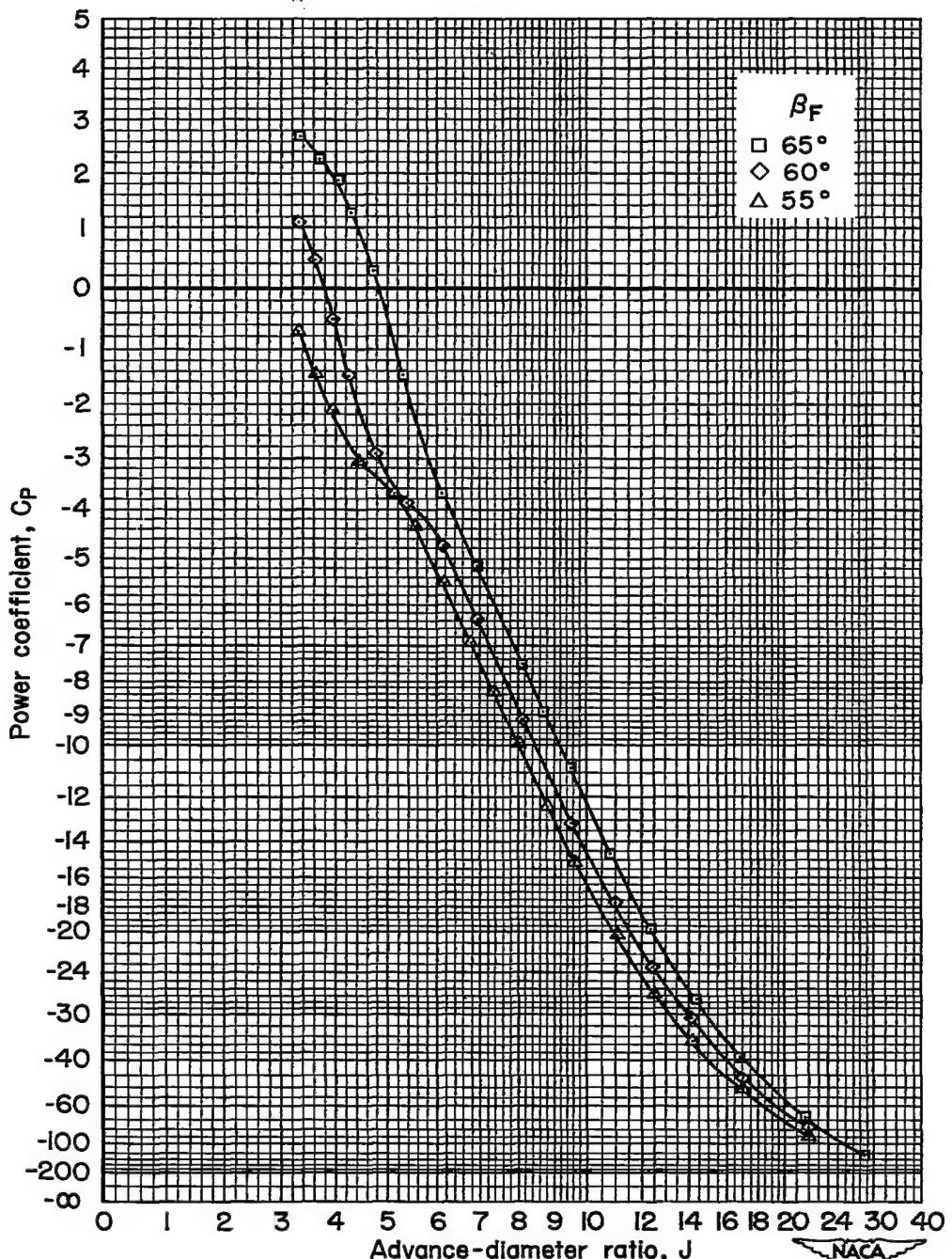
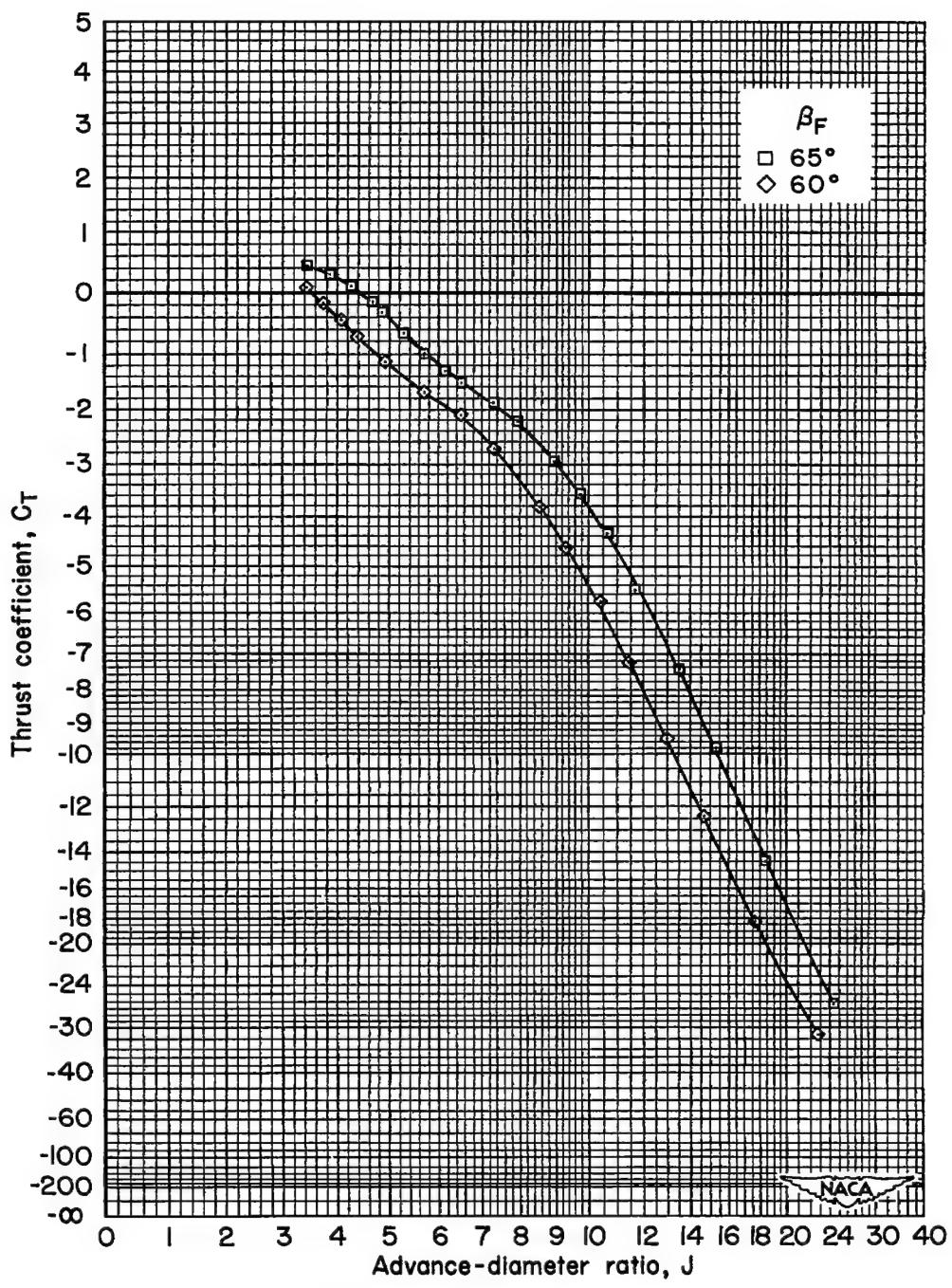
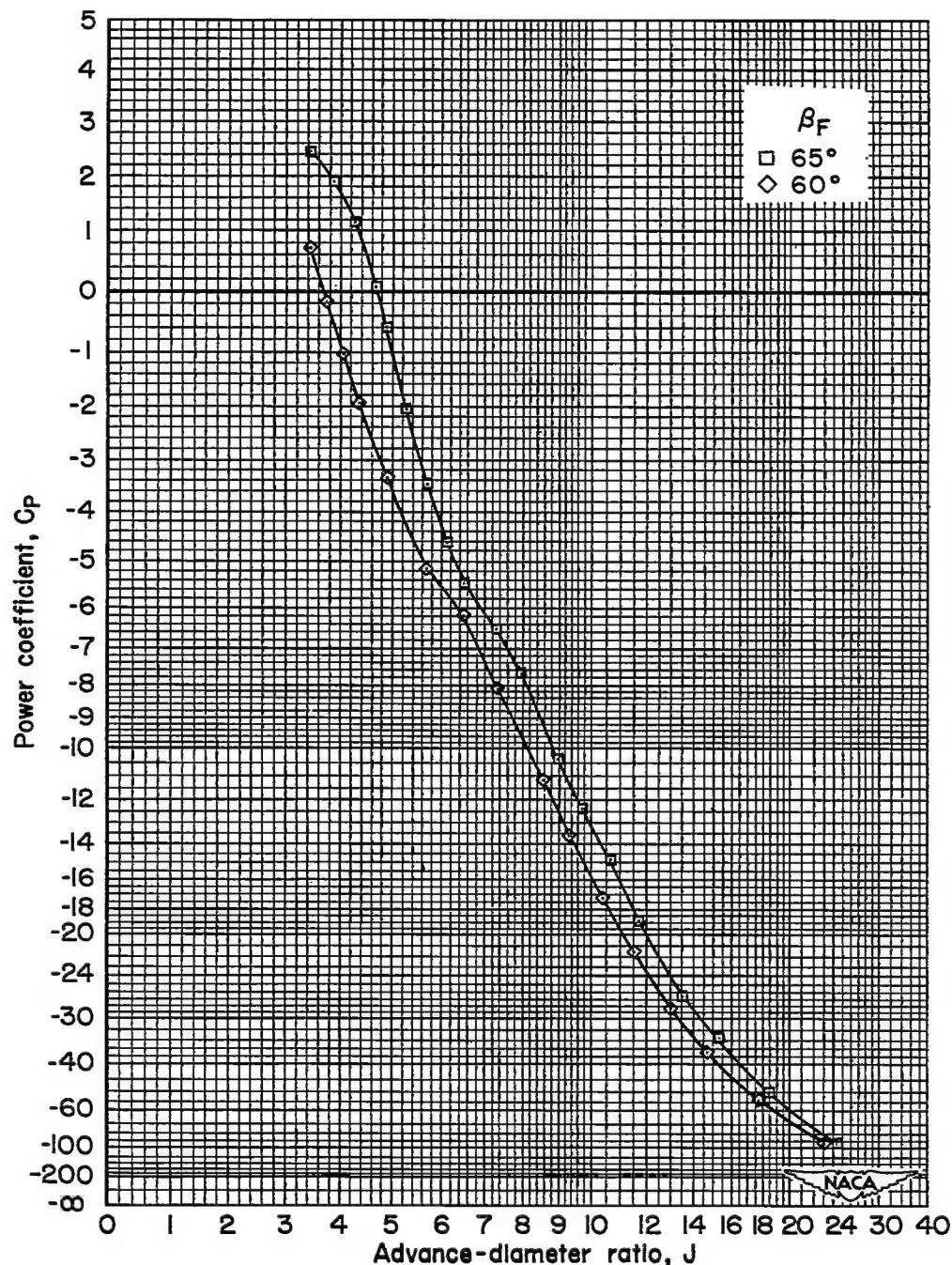


Figure 25.- Continued.



(o) $M = 0.84$, C_T vs. J

Figure 25.- Continued.



(p) $M = 0.84$, C_p vs. J

Figure 25.- Concluded.

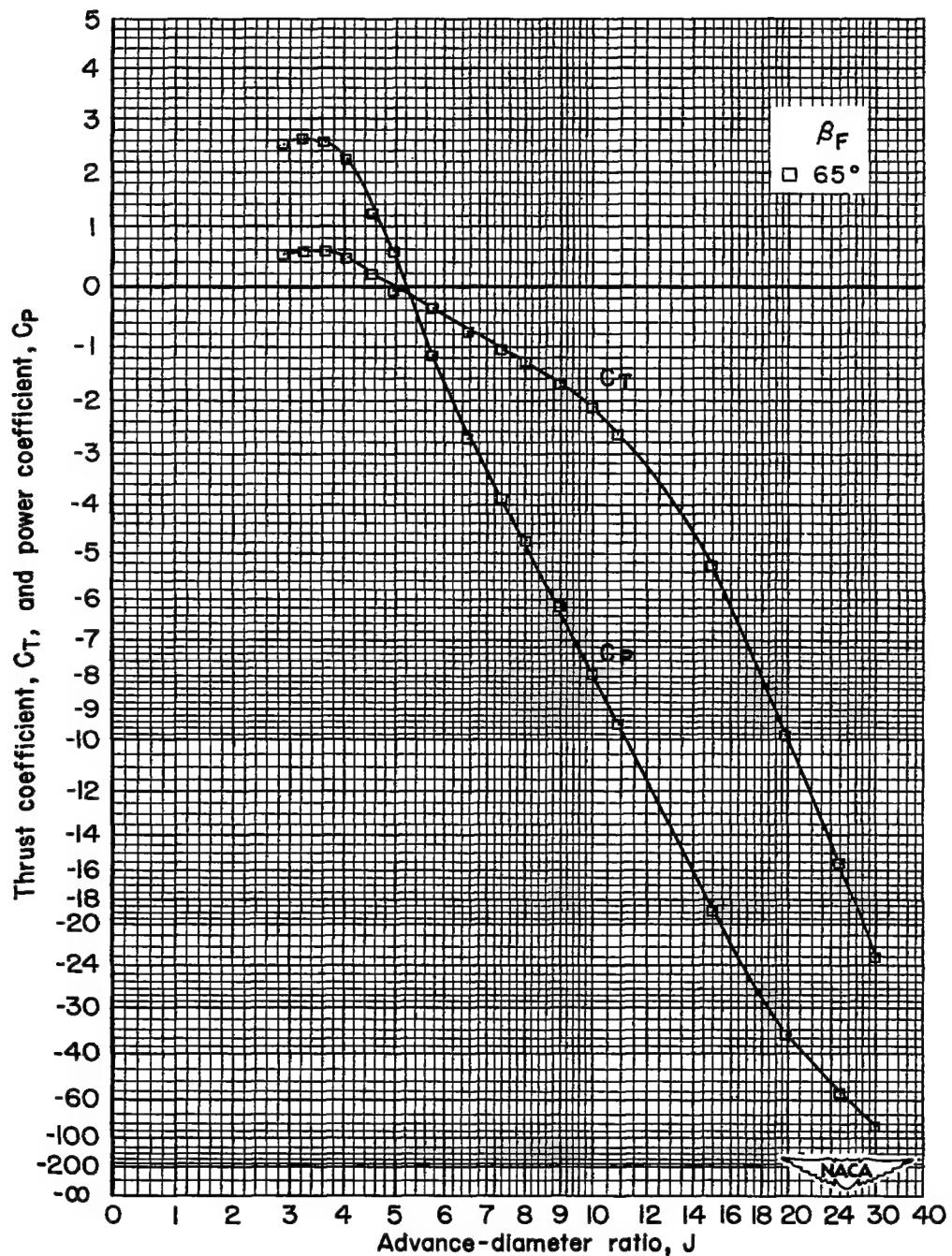
(a) $M = 0.60$

Figure 26.- Negative-thrust characteristics; NACA 4-(5)(05)-037 six-blade, dual-rotation propeller, $\Delta\beta = 0.8^\circ$, spinner A.

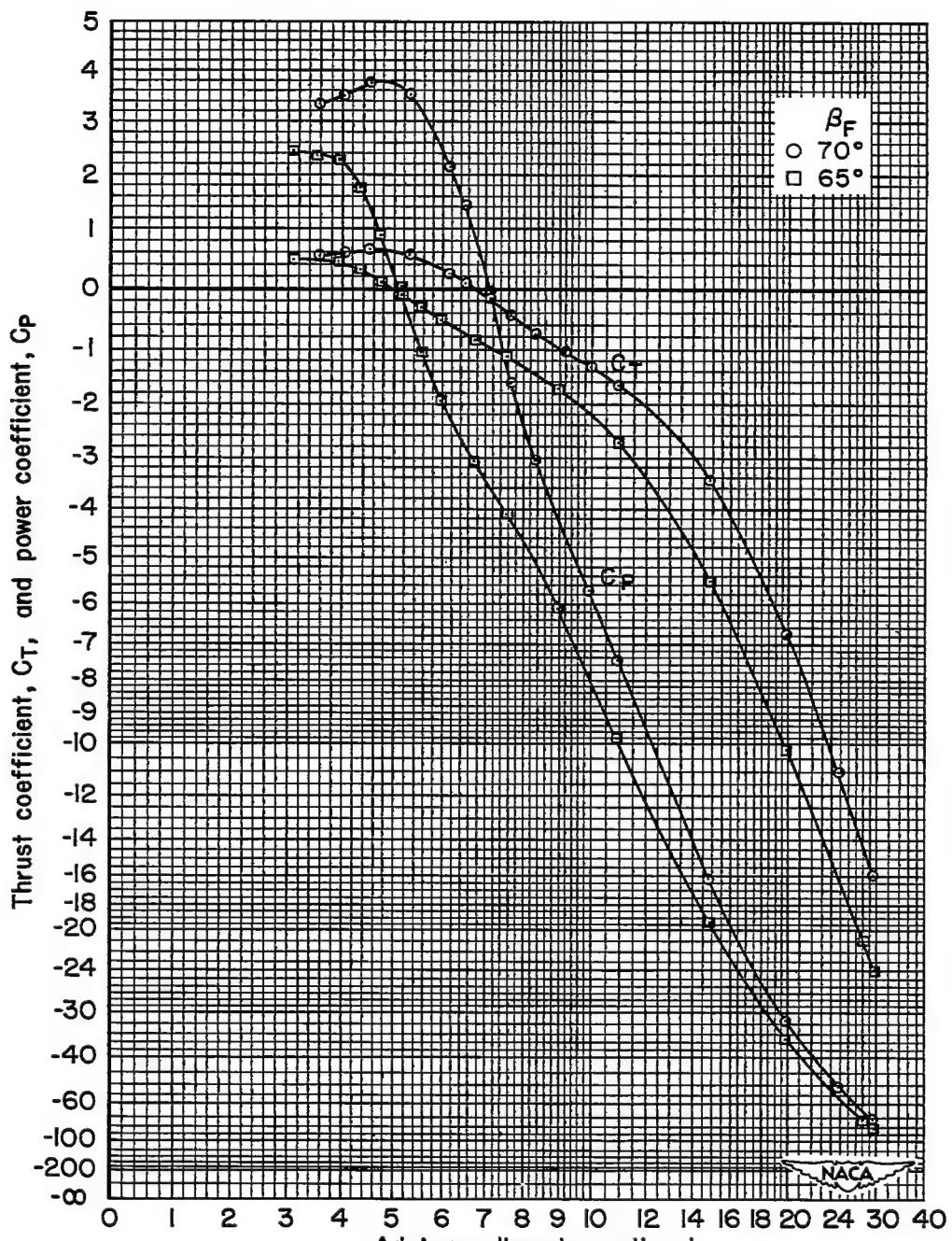
(b) $M = 0.70$

Figure 26.- Continued.

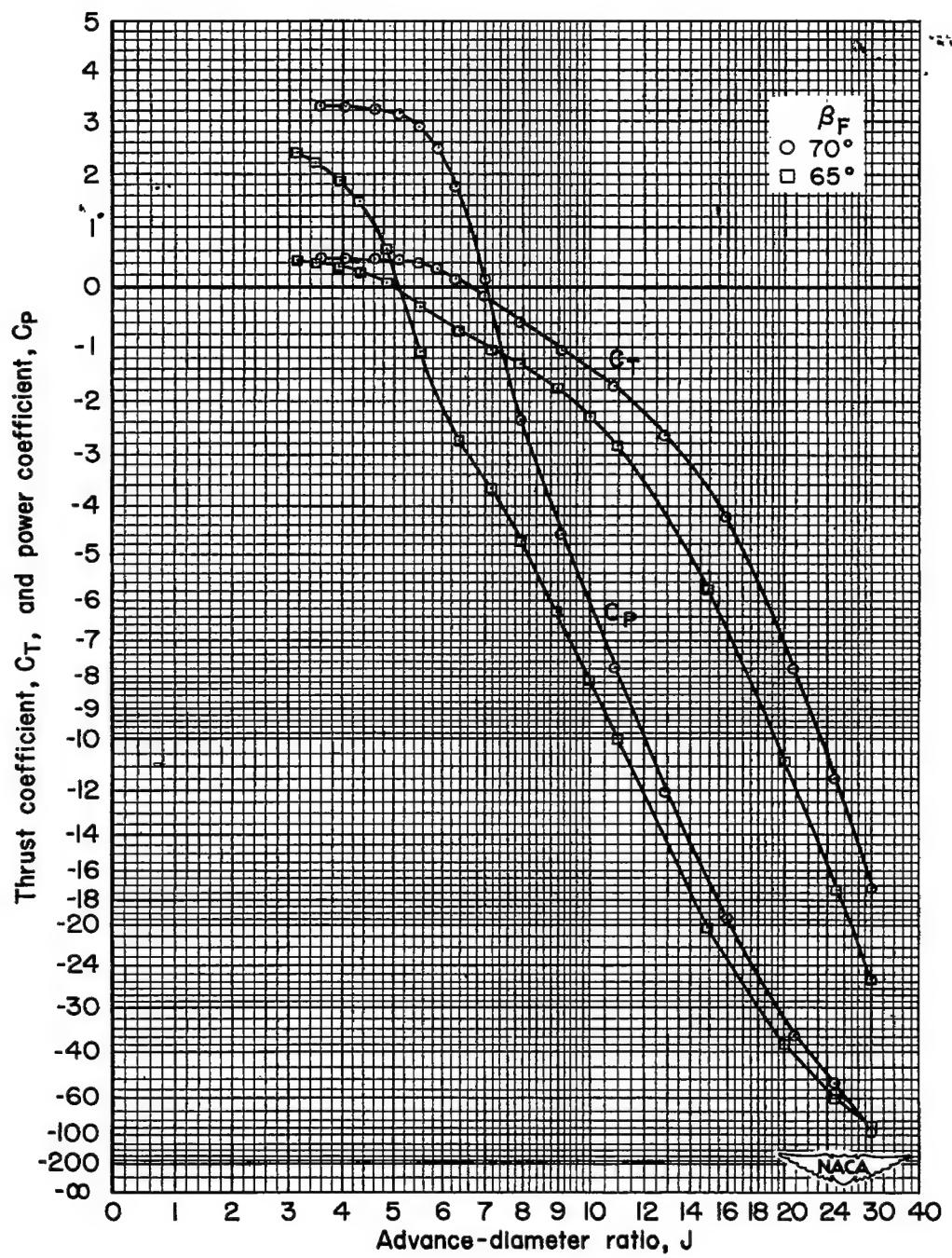
(c) $M = 0.75$

Figure 26.- Continued.

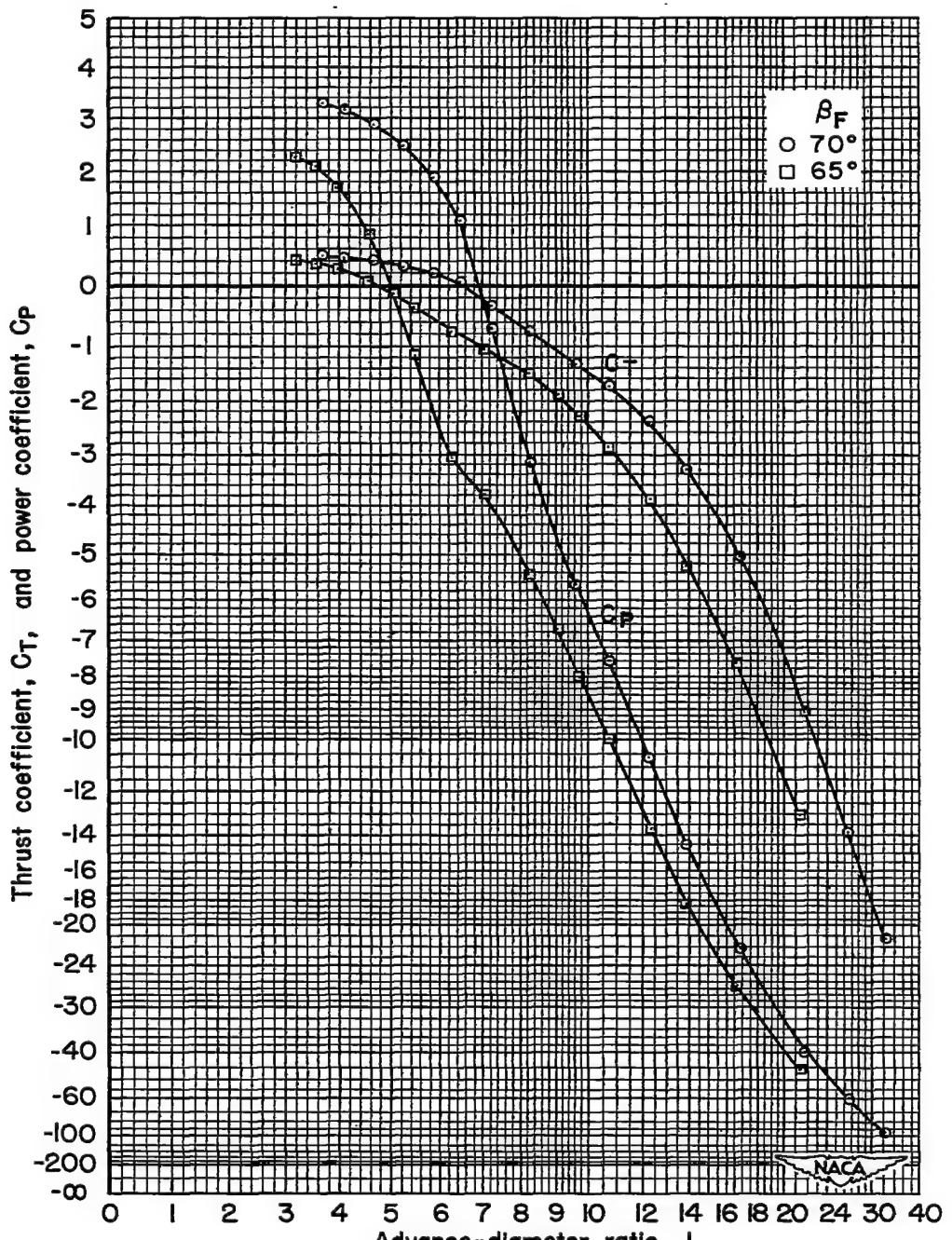
(d) $M = 0.80$

Figure 26.- Continued.

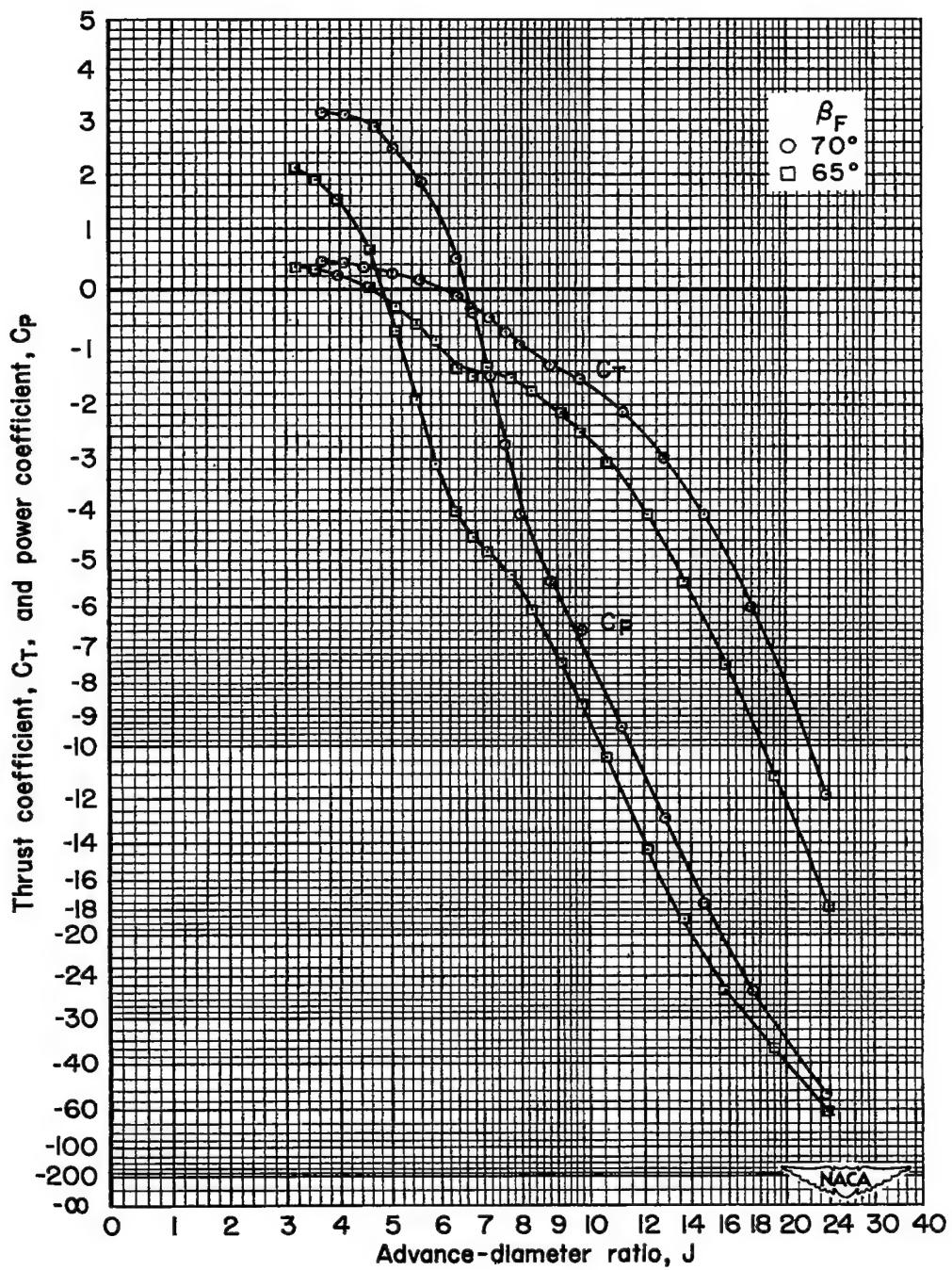
(e) $M = 0.84$

Figure 26.- Continued.

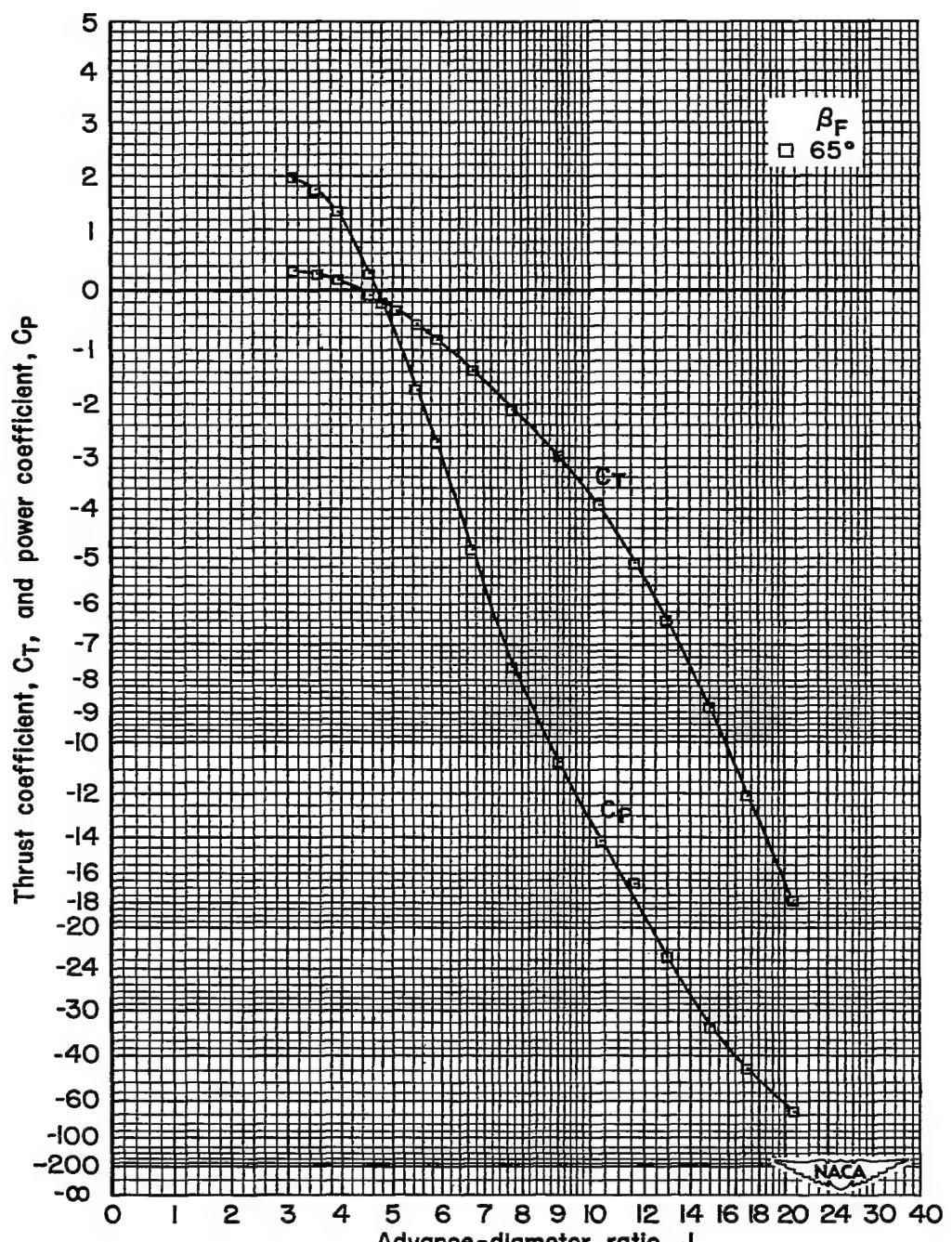
(f) $M = 0.90$

Figure 26.- Concluded.

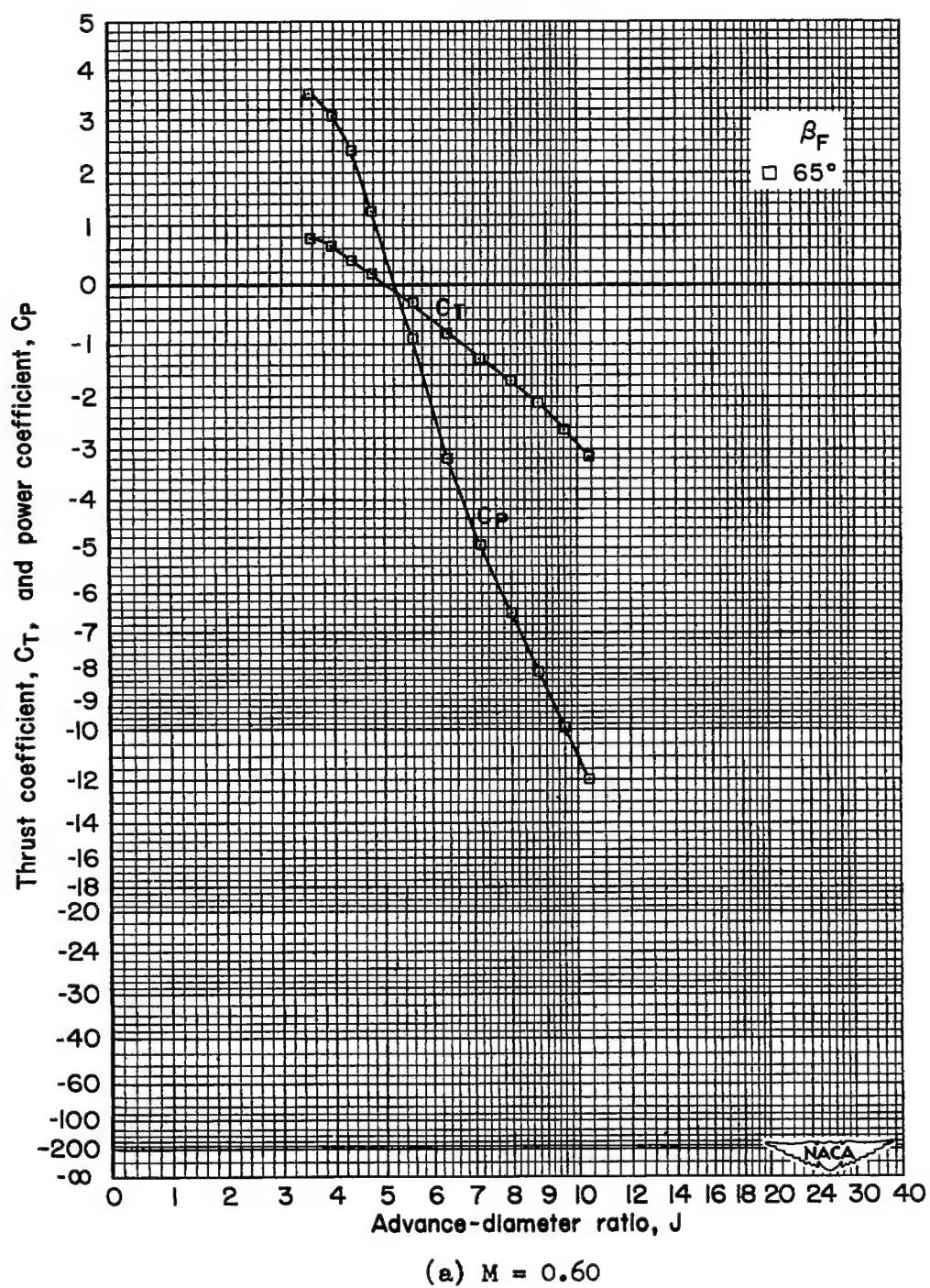


Figure 27.- Negative-thrust characteristics; NACA 4-(5)(05)-037 eight-blade, dual-rotation propeller, $\Delta\beta = 0.8^\circ$, spinner A.

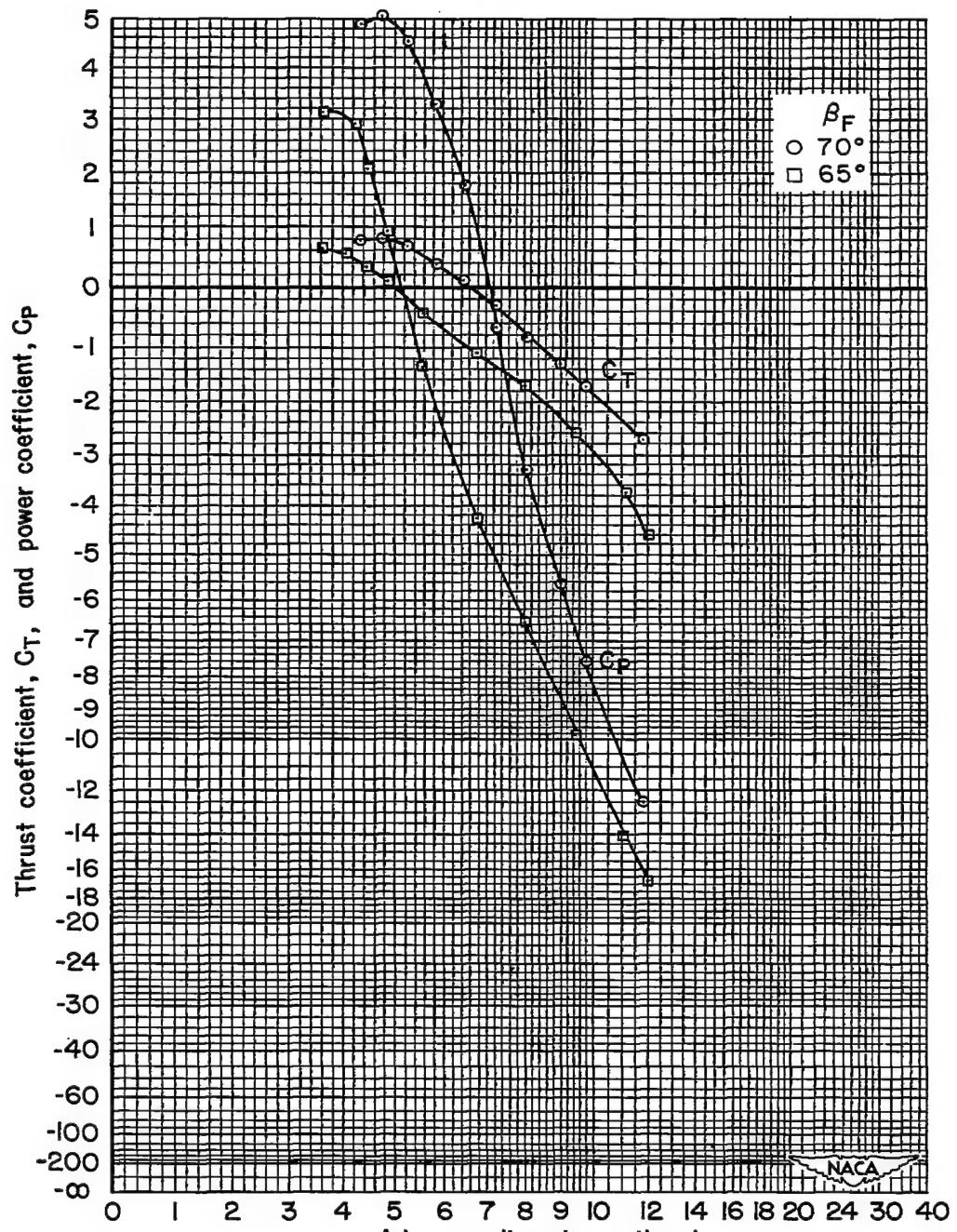
(b) $M = 0.70$

Figure 27.- Continued.

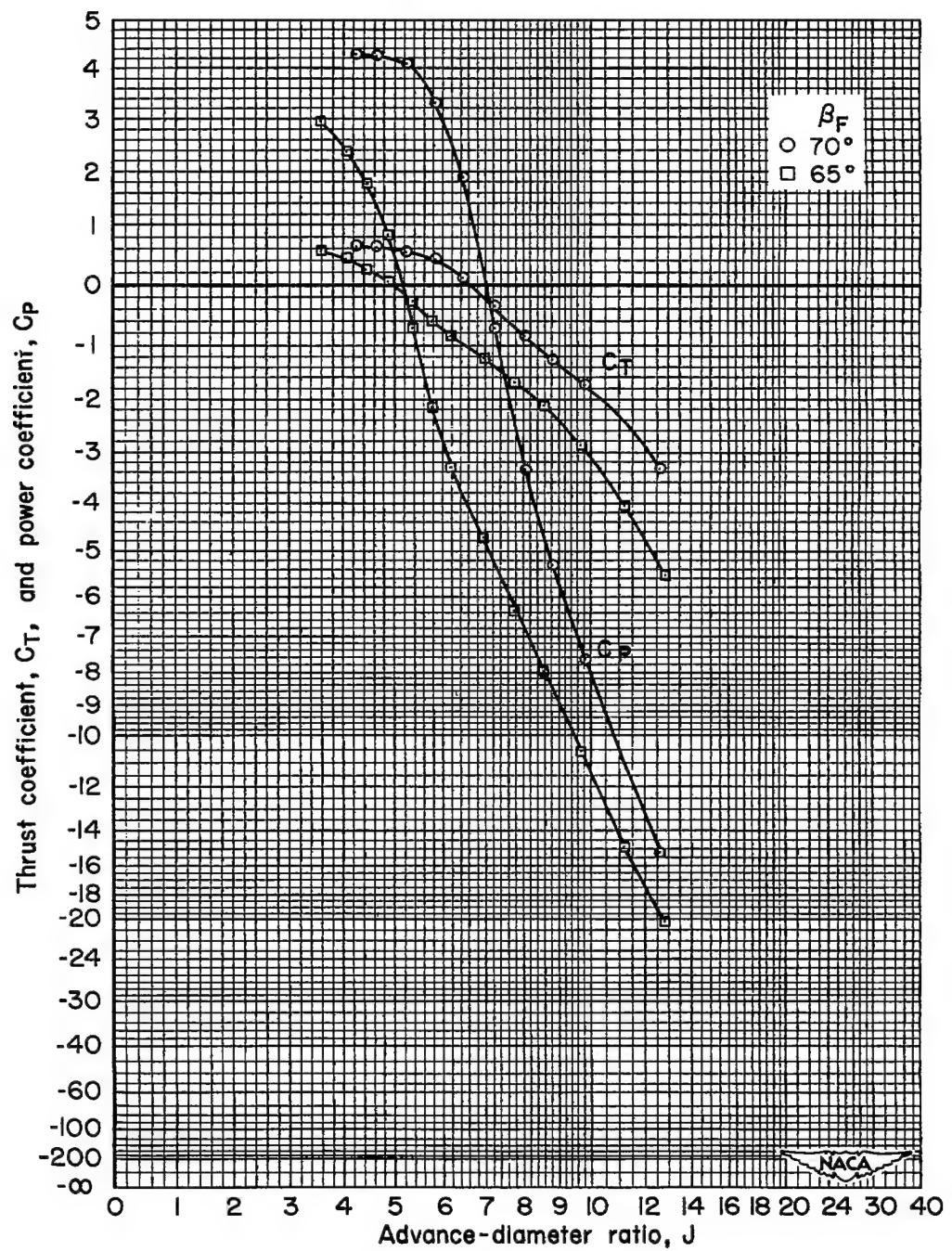
(c) $M = 0.75$

Figure 27.- Continued.

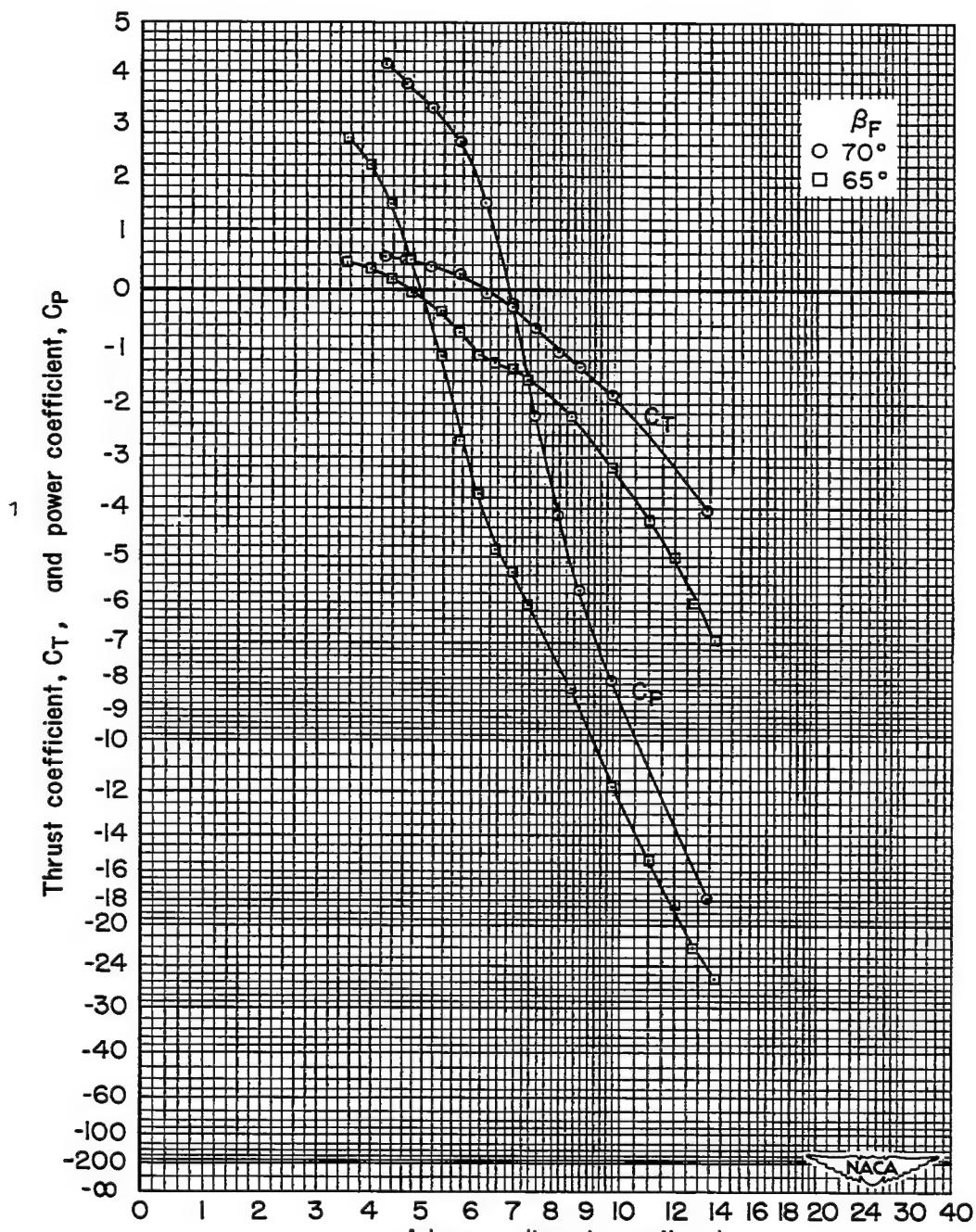
(d) $M = 0.80$

Figure 27.- Continued.

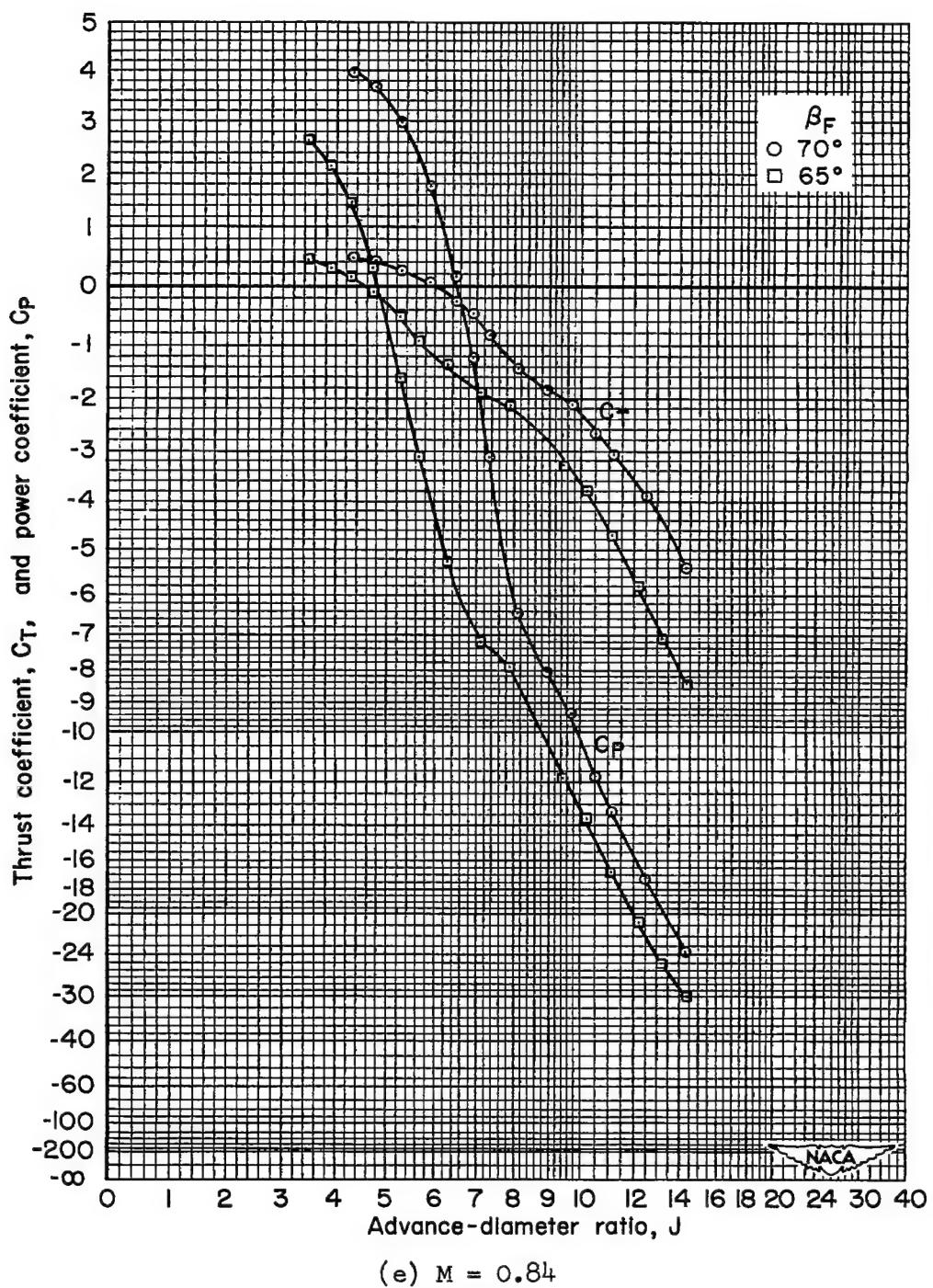


Figure 27.- Continued.

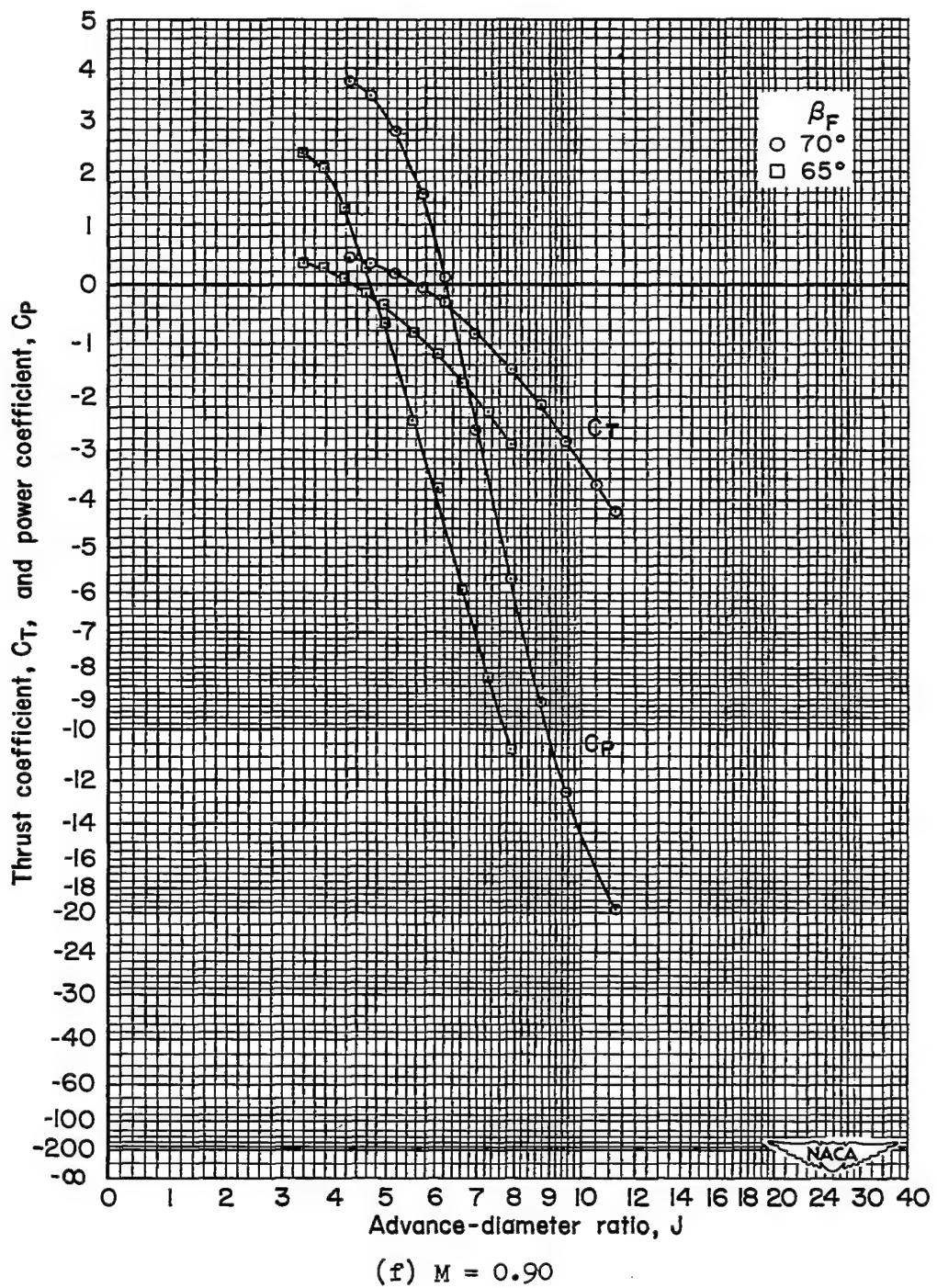


Figure 27.- Concluded.

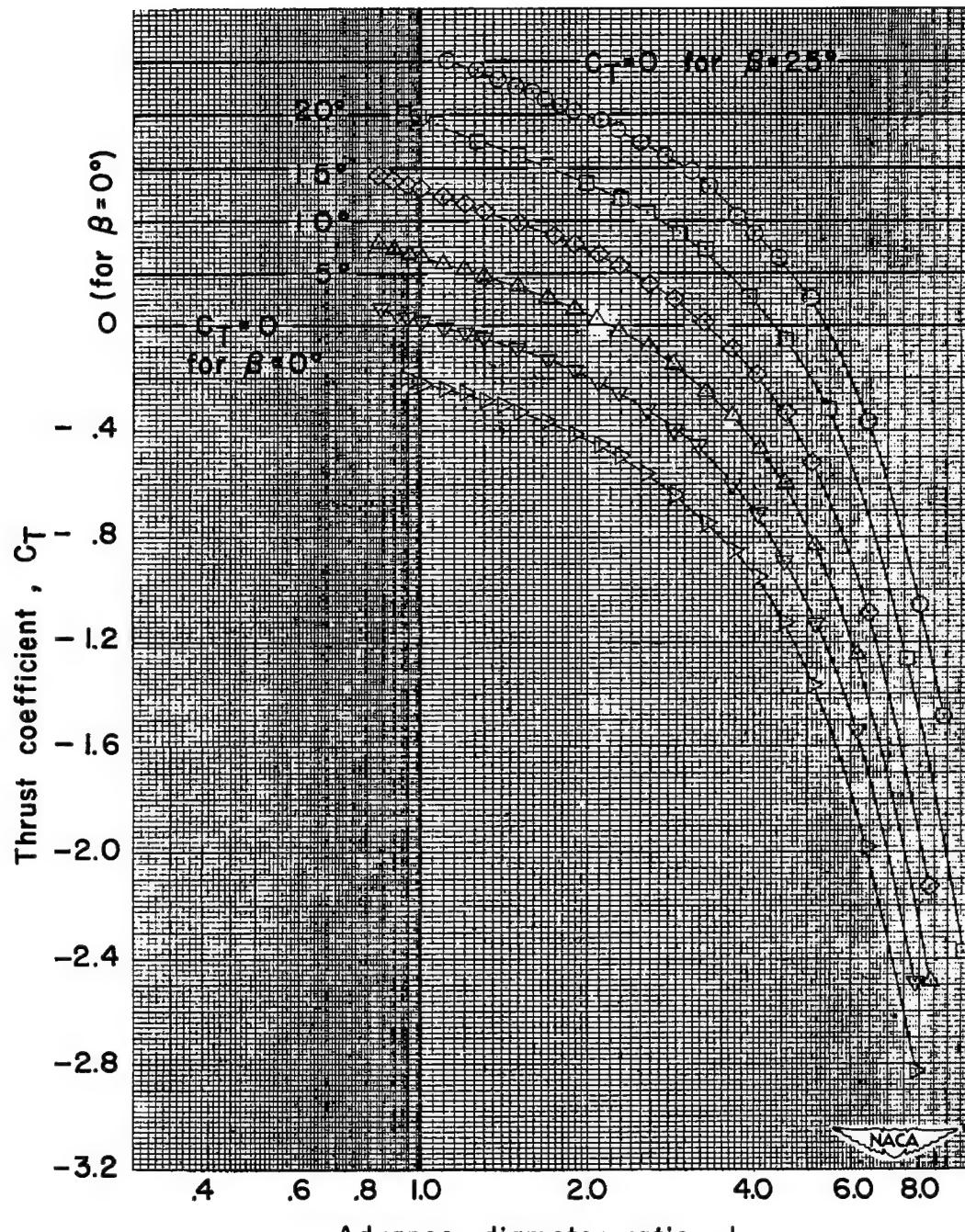
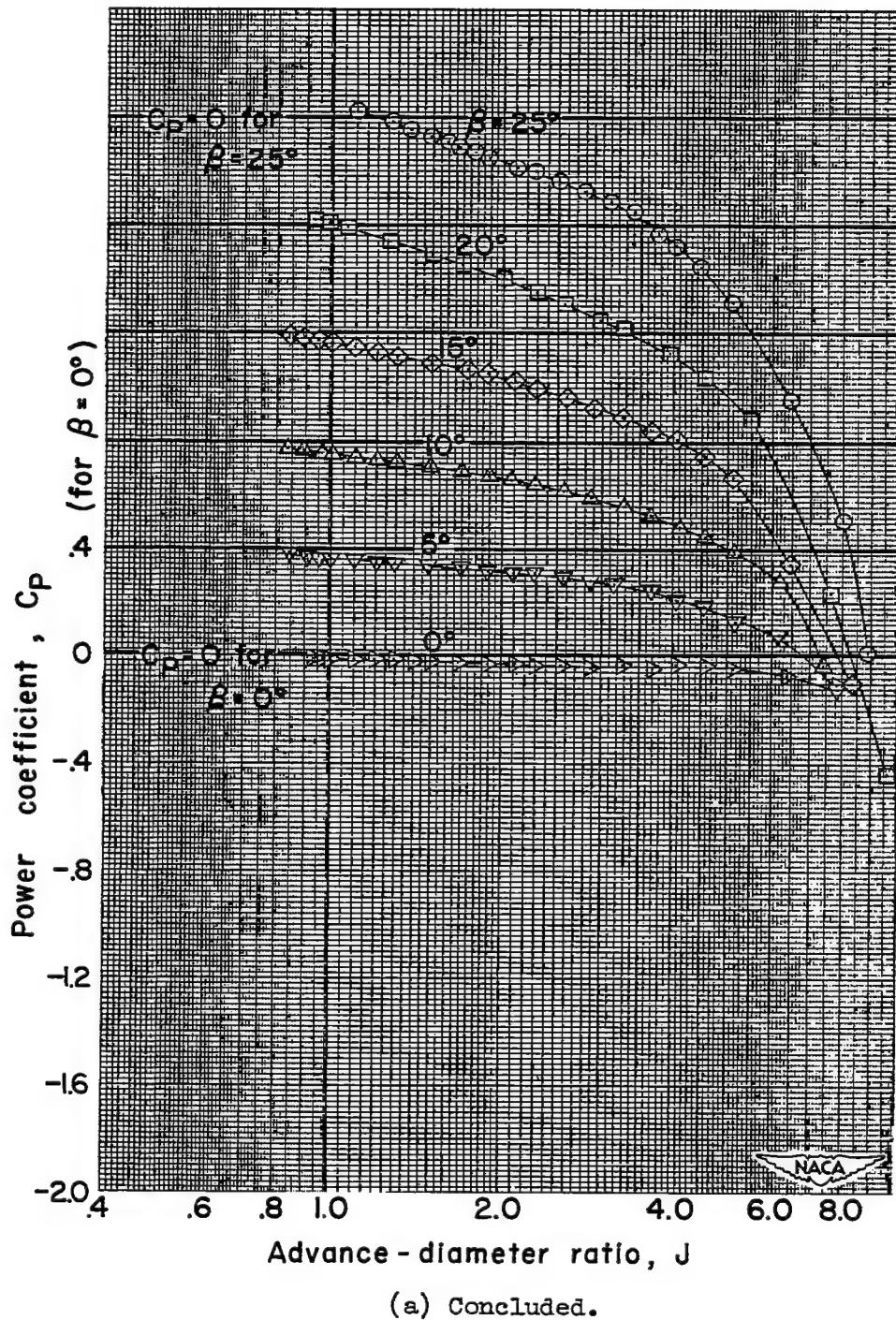
(a) $M = 0.15$

Figure 28.- Negative-thrust characteristics; NACA 4-(5)(05)-041 two-blade, single-rotation propeller, spinner C.



(a) Concluded.

Figure 28.- Continued.

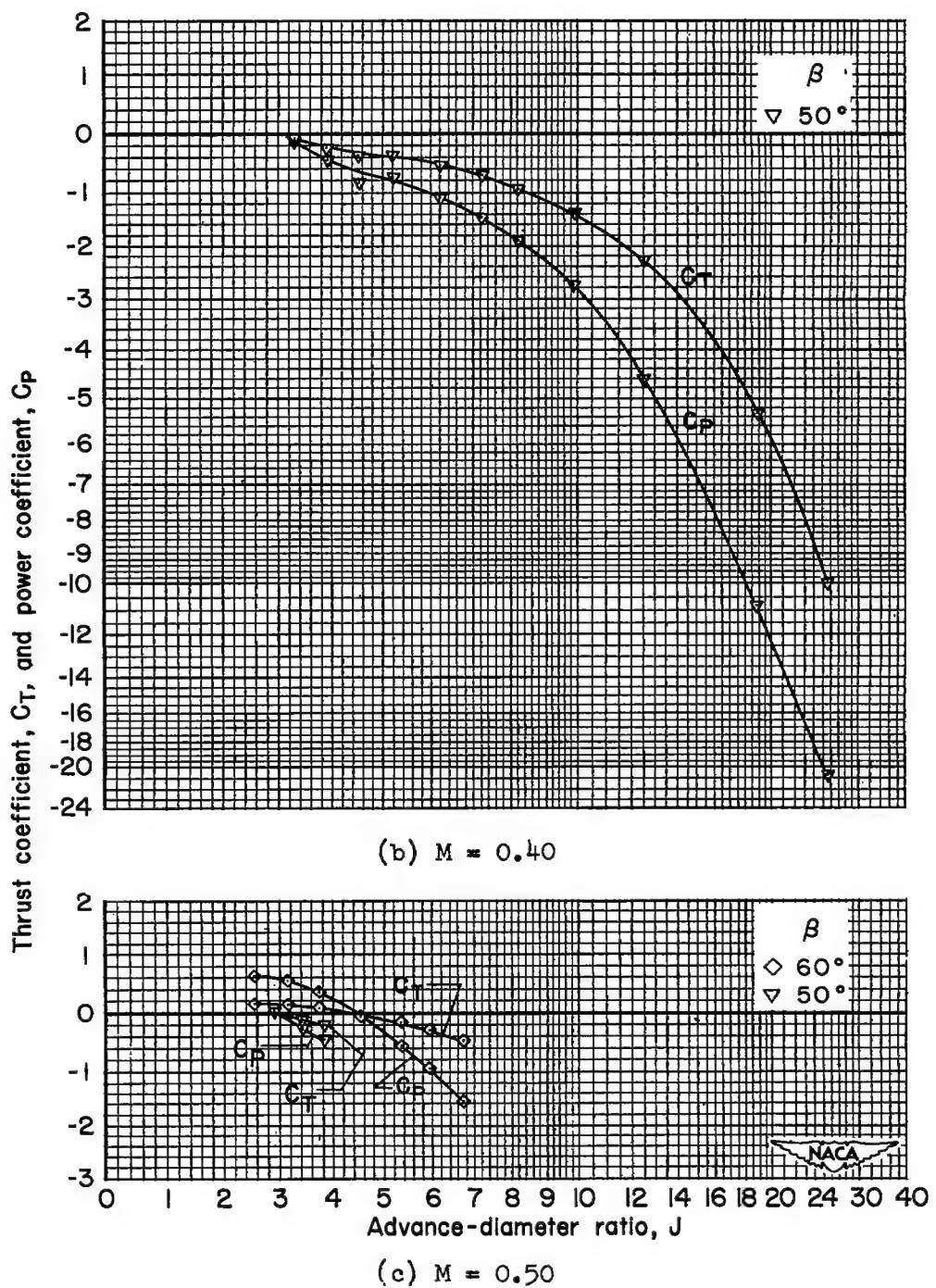


Figure 28.- Continued.

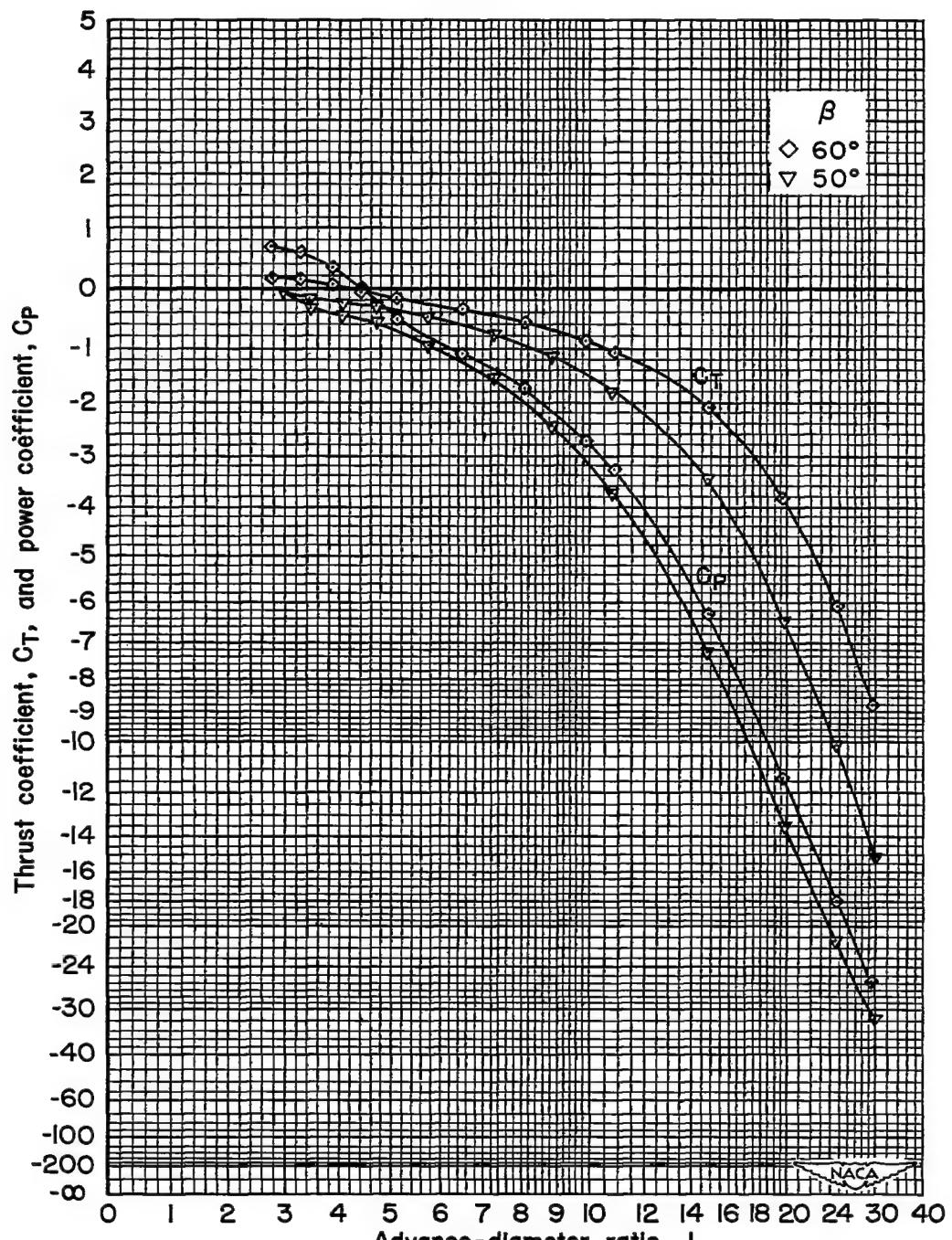
(d) $M = 0.60$

Figure 28.- Continued.

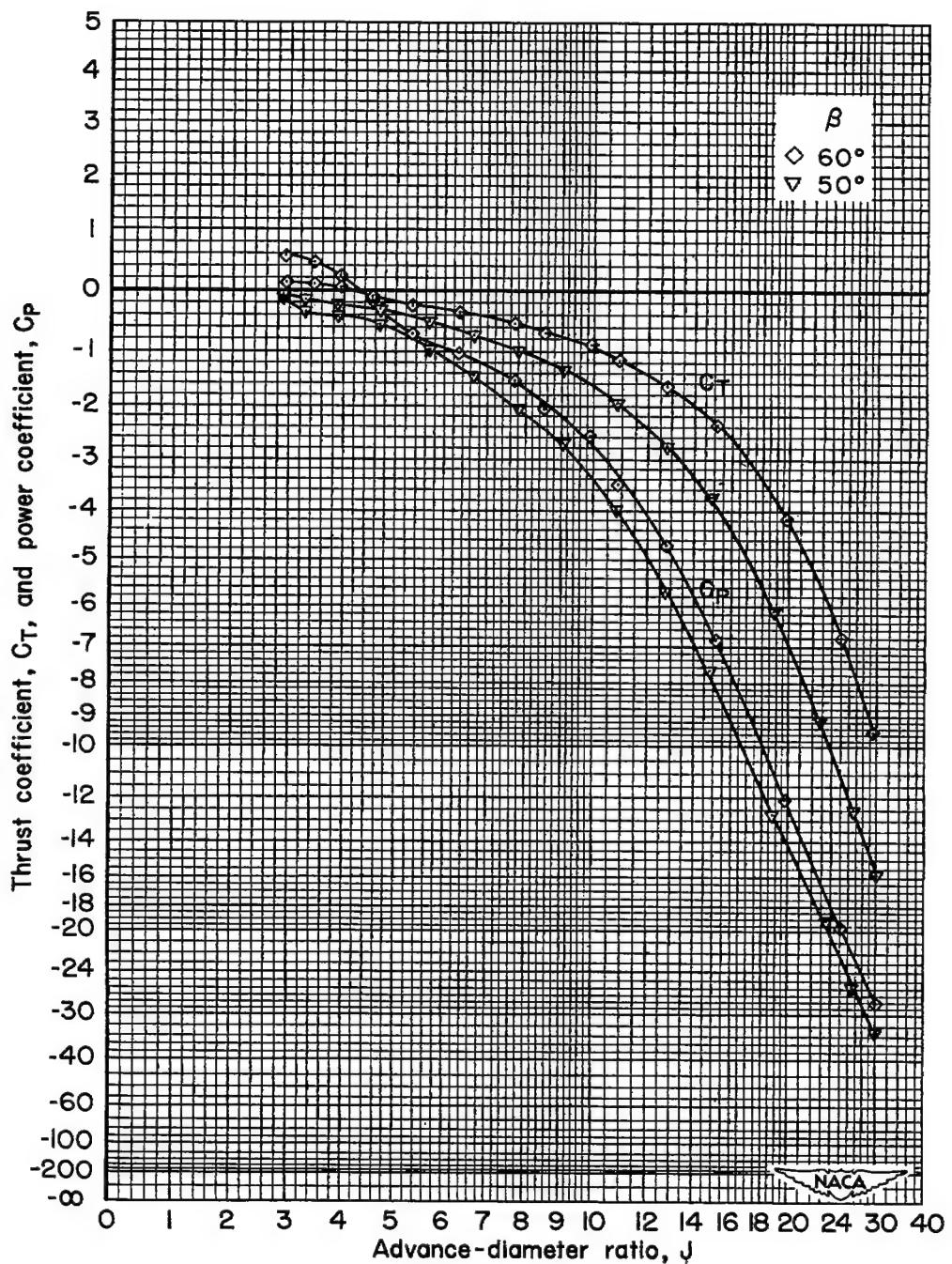
(e) $M = 0.70$

Figure 28.- Continued.

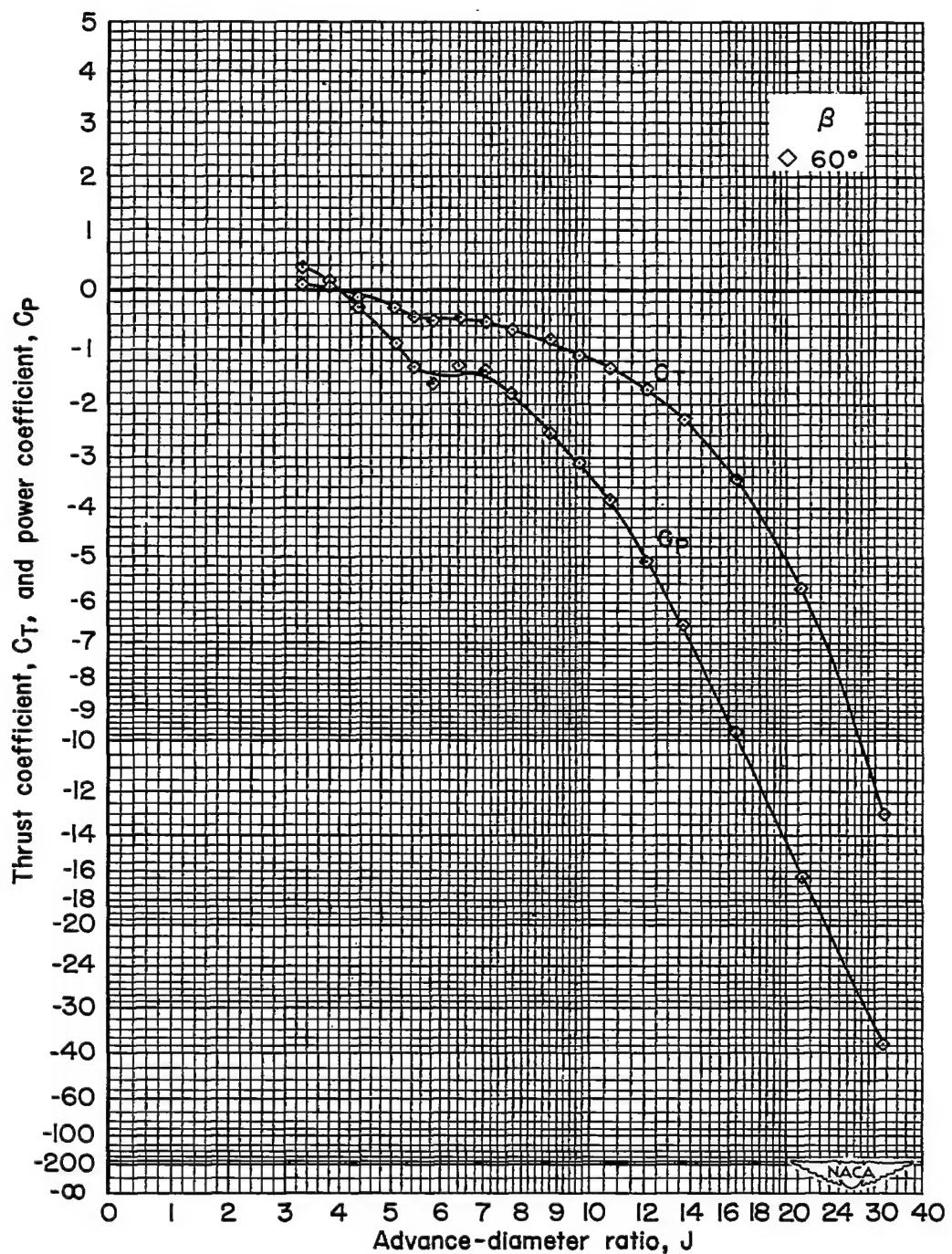
(f) $M = 0.80$

Figure 28.-- Concluded.

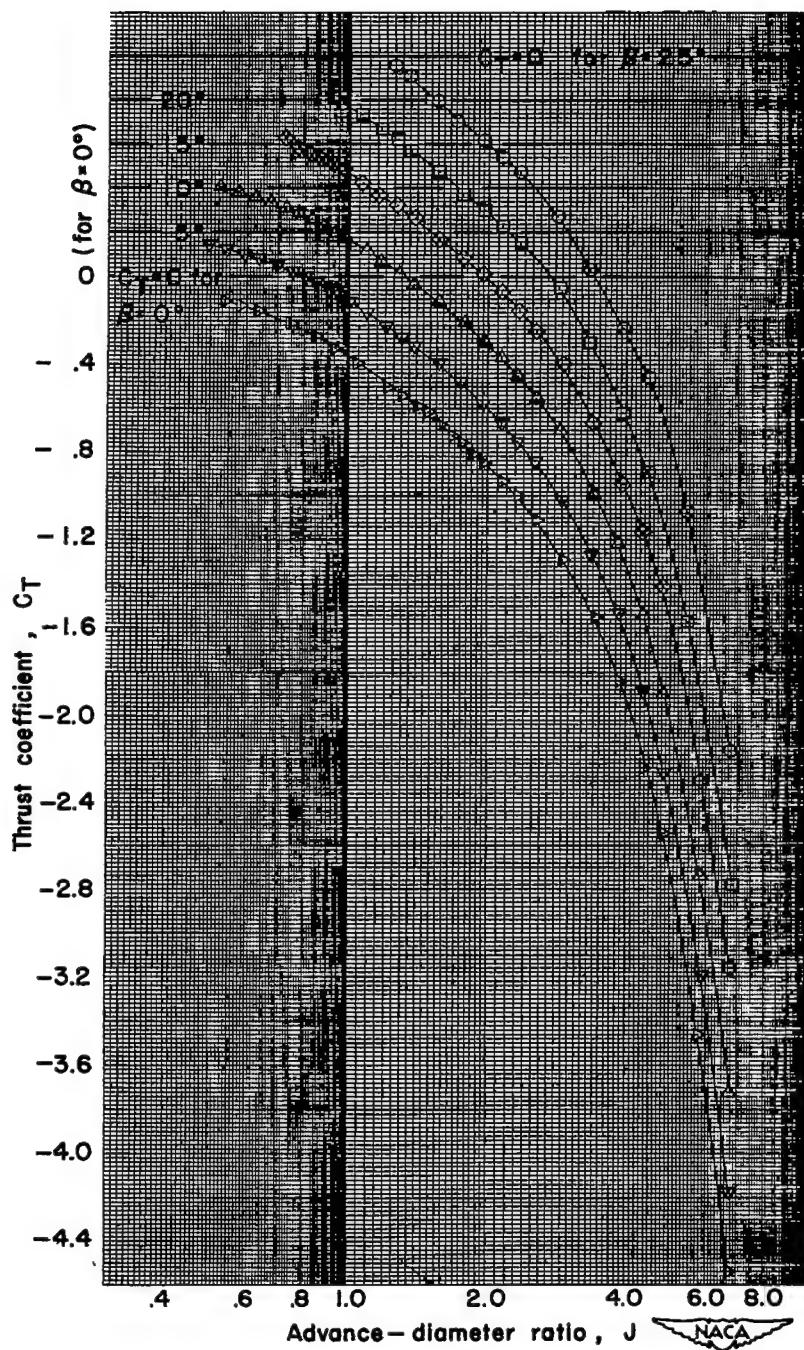
(a) $M = 0.15$, C_T vs. J

Figure 29.- Negative-thrust characteristics; NACA 4-(5)(05)-041 four-blade, single-rotation propeller, spinner C.

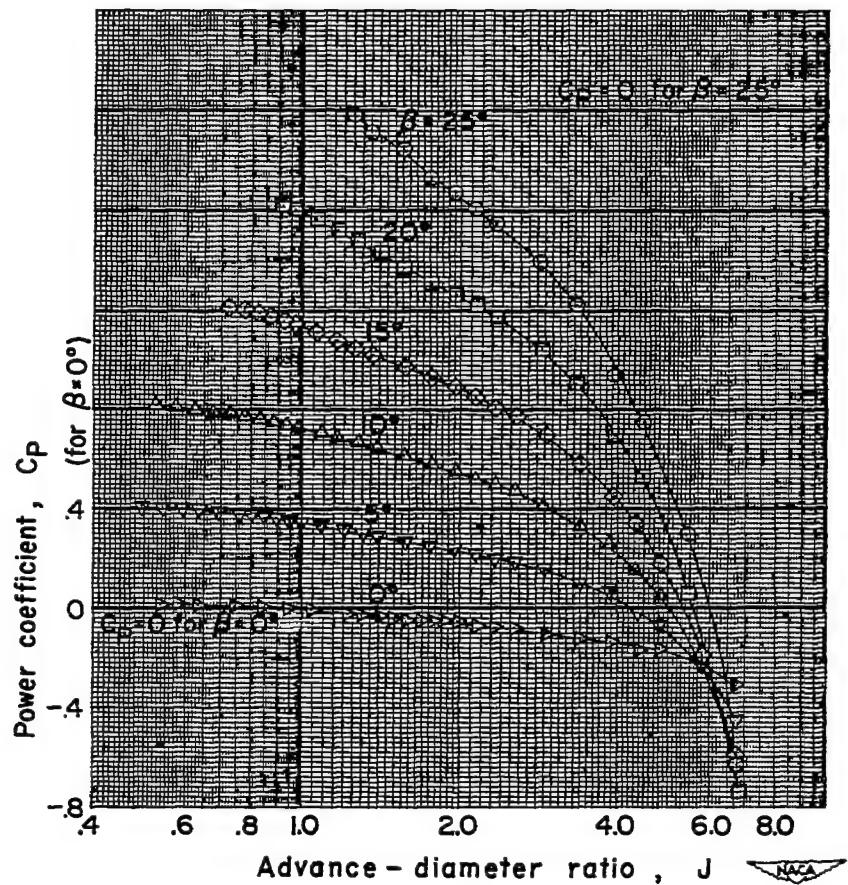
(b) $M = 0.15$, C_P vs. J

Figure 29-- Concluded.

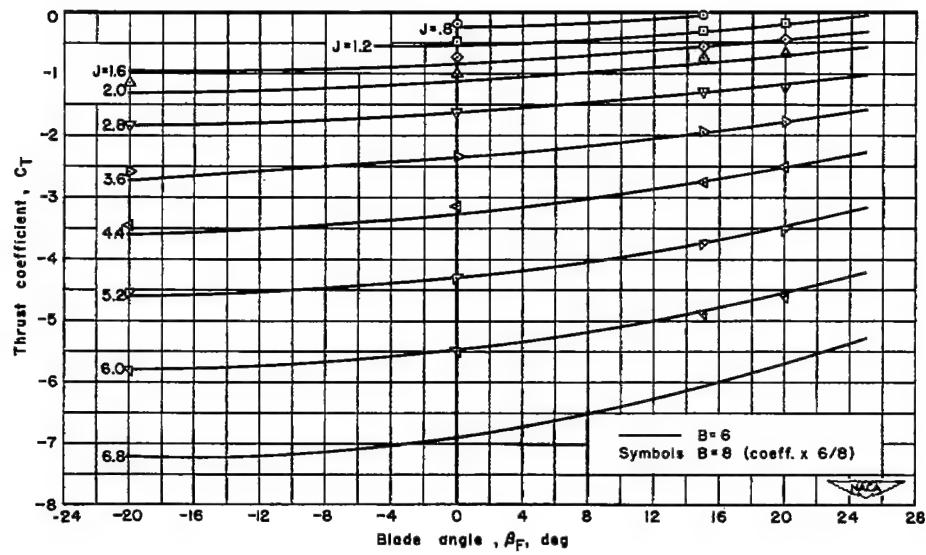
(a) $M = 0.15$, C_T vs. J

Figure 30.- The effect of blade angle on the negative-thrust characteristics; NACA 4-(5)(05)-037 six-blade, dual-rotation propeller,
 $\Delta\beta$ = optimum, spinner A.

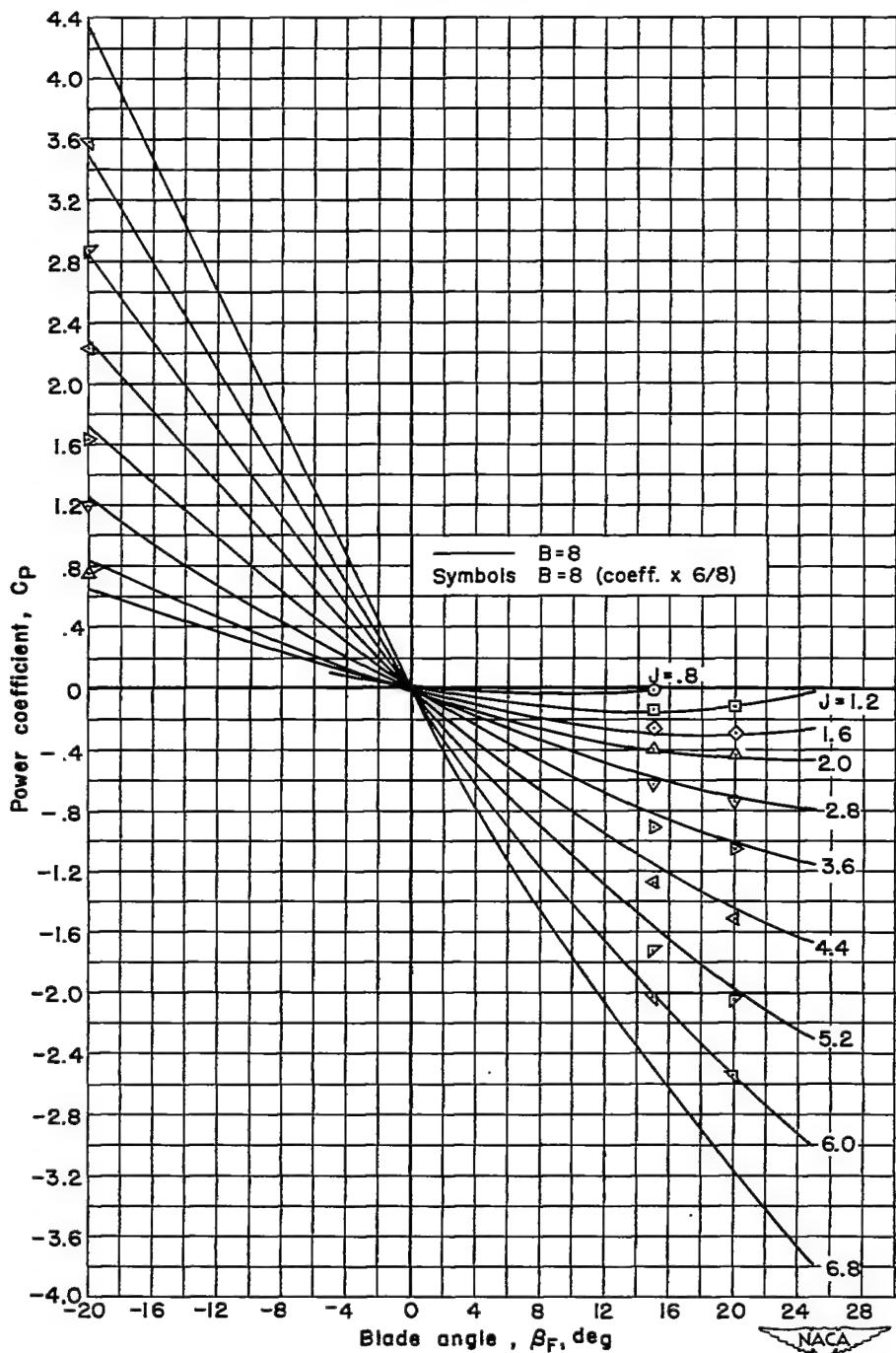
(b) $M = 0.15$, C_P vs. J

Figure 30.- Continued.

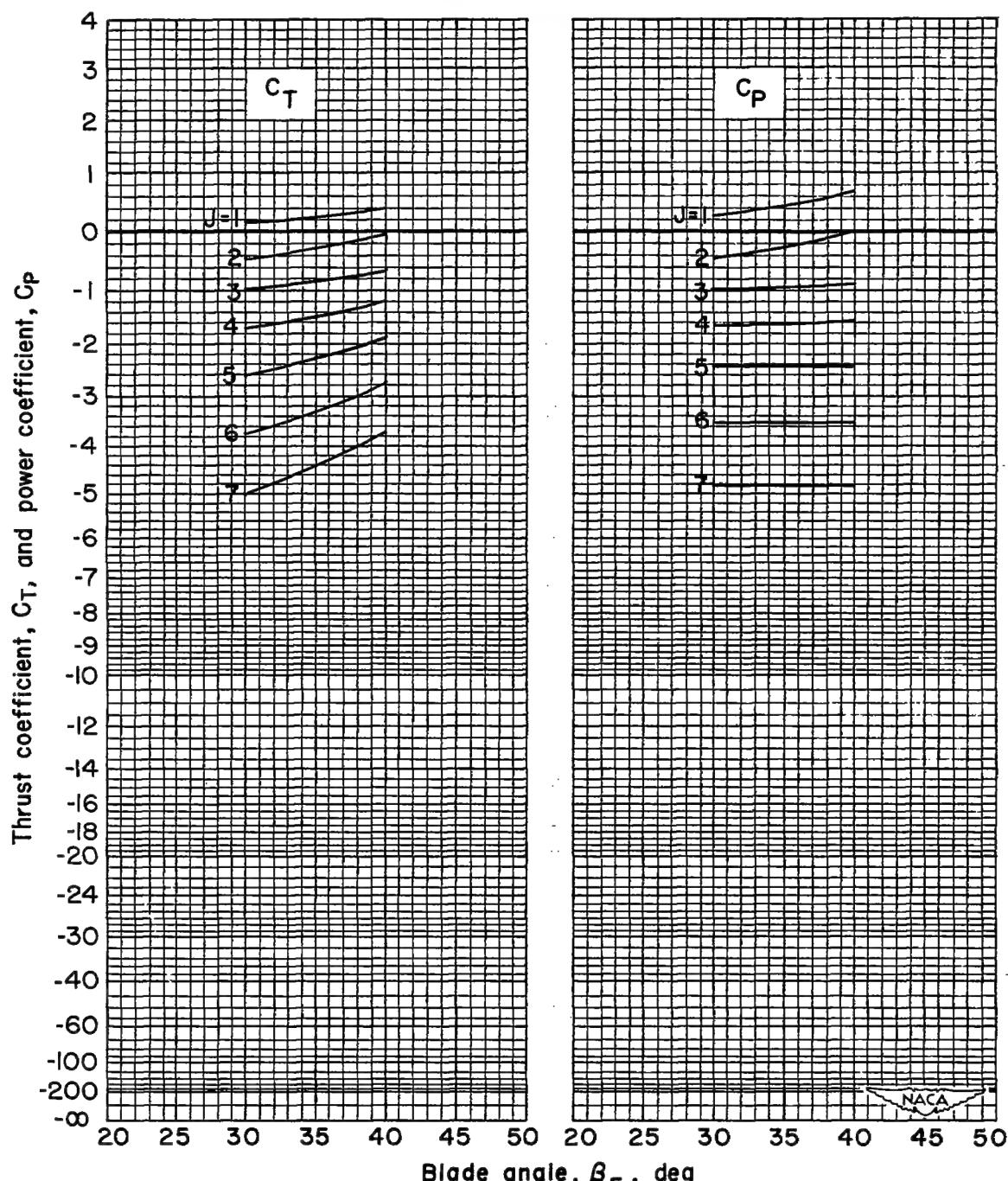
(c) $M = 0.20$

Figure 30.- Continued.

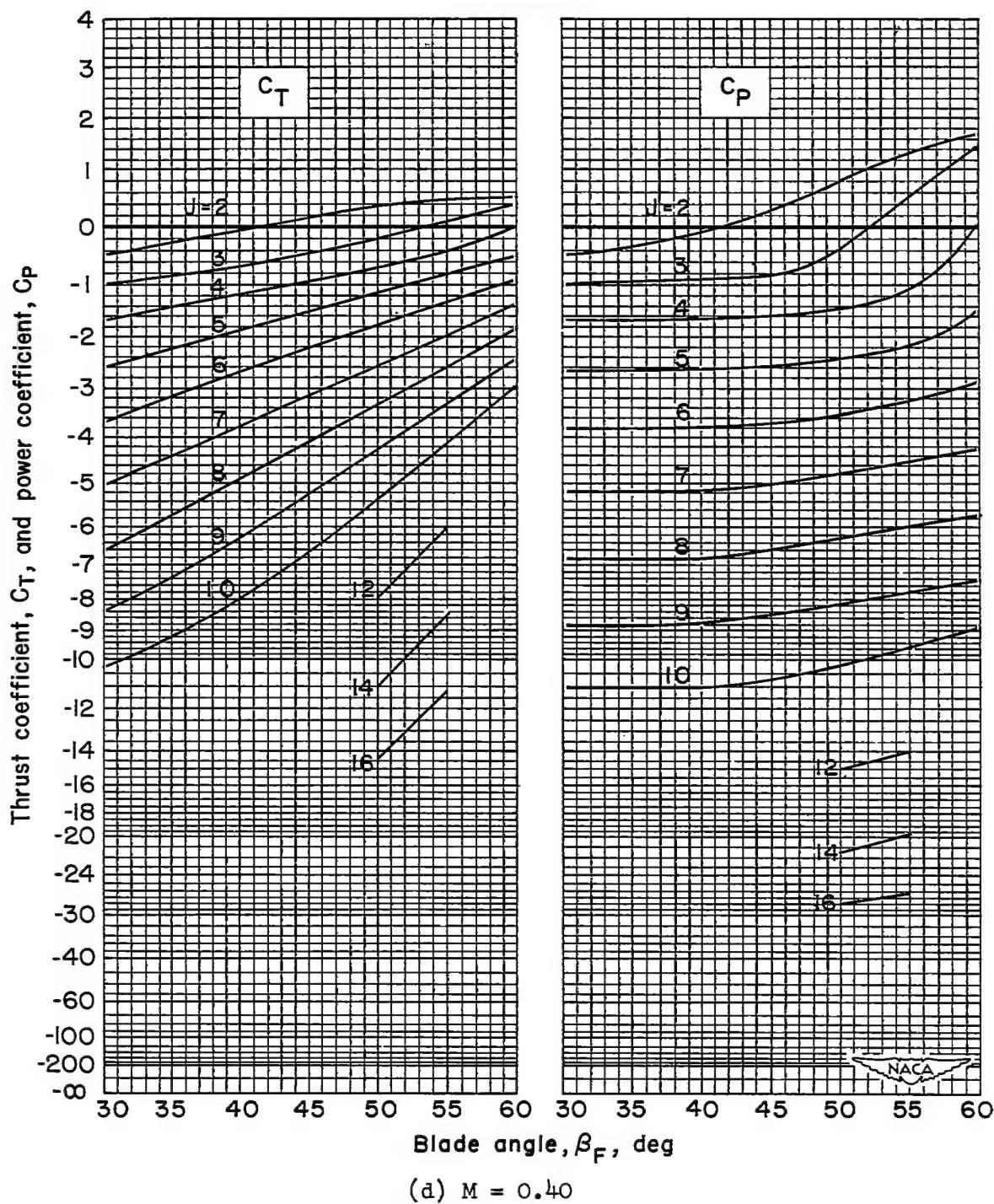
(d) $M = 0.40$

Figure 30.- Continued.

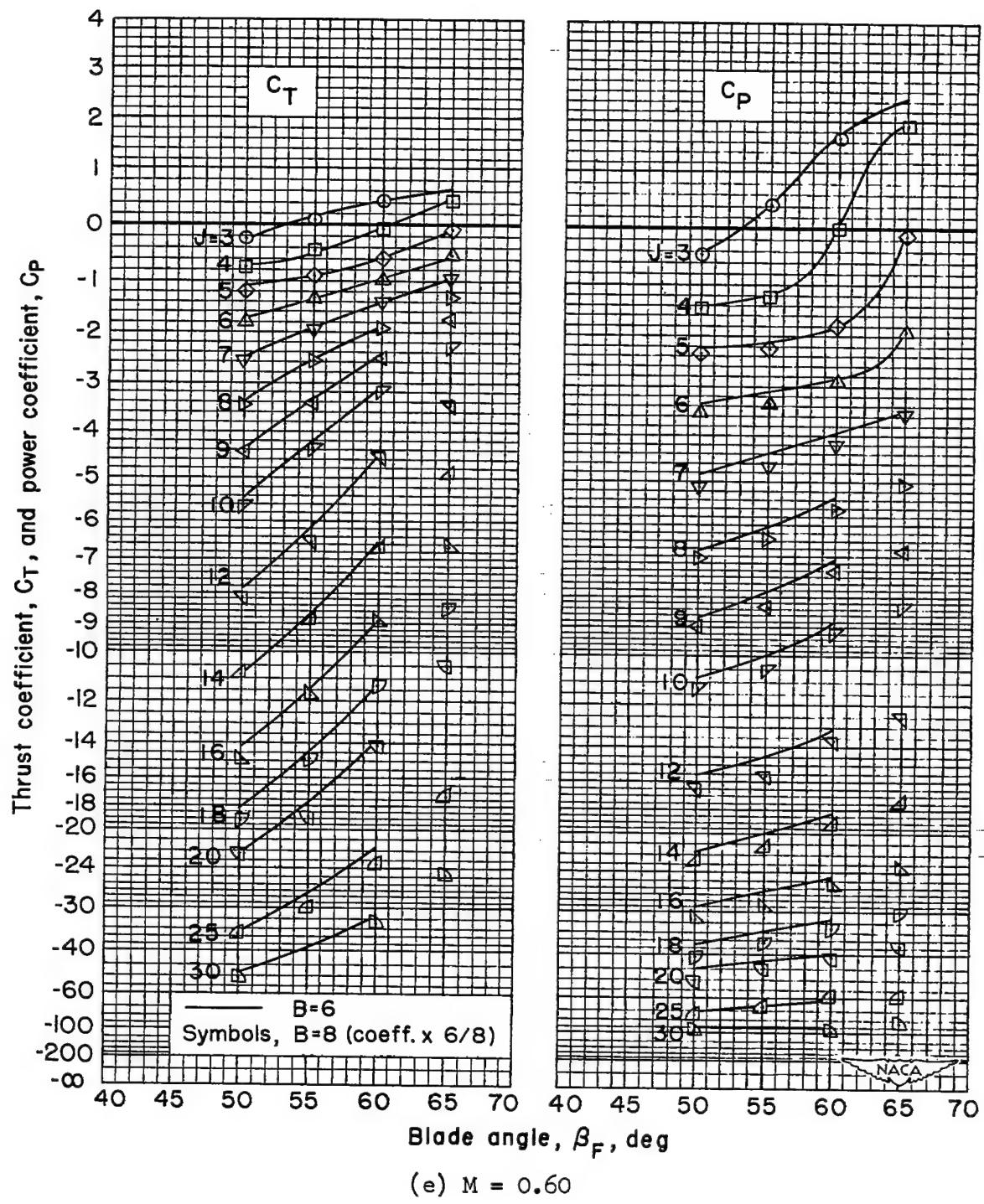


Figure 30.- Continued.

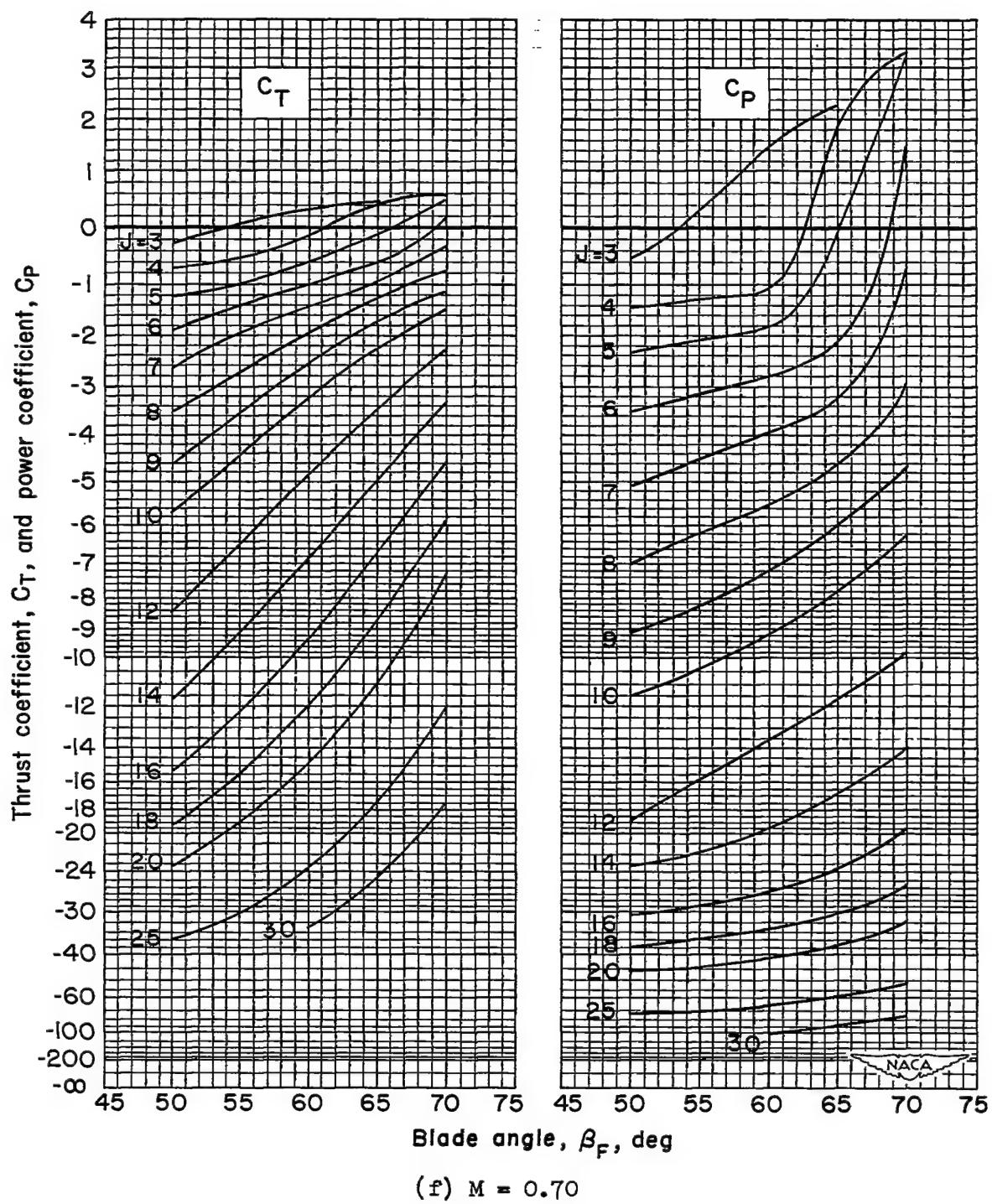


Figure 30.- Continued.

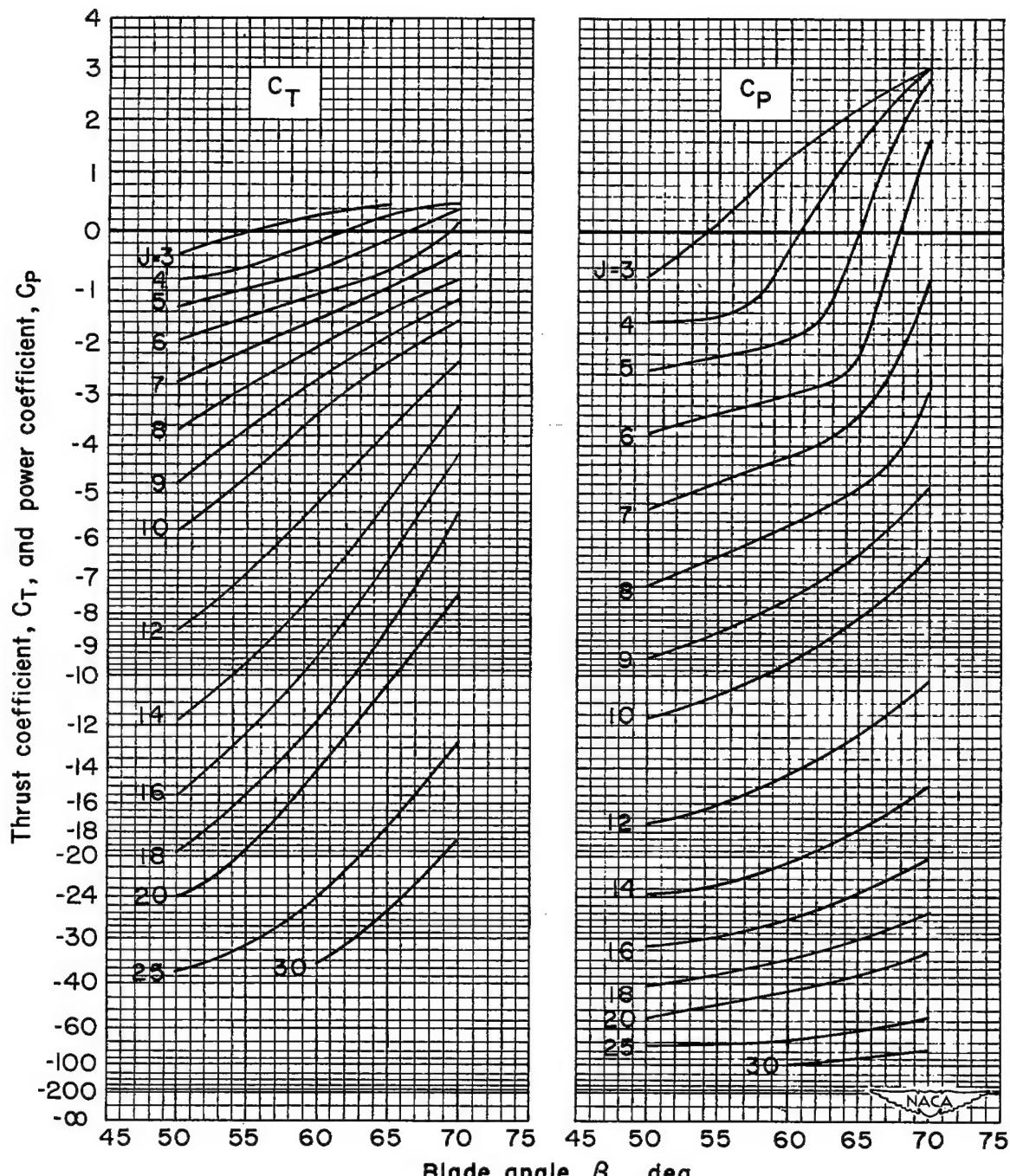
(g) $M = 0.75$

Figure 30.- Continued.

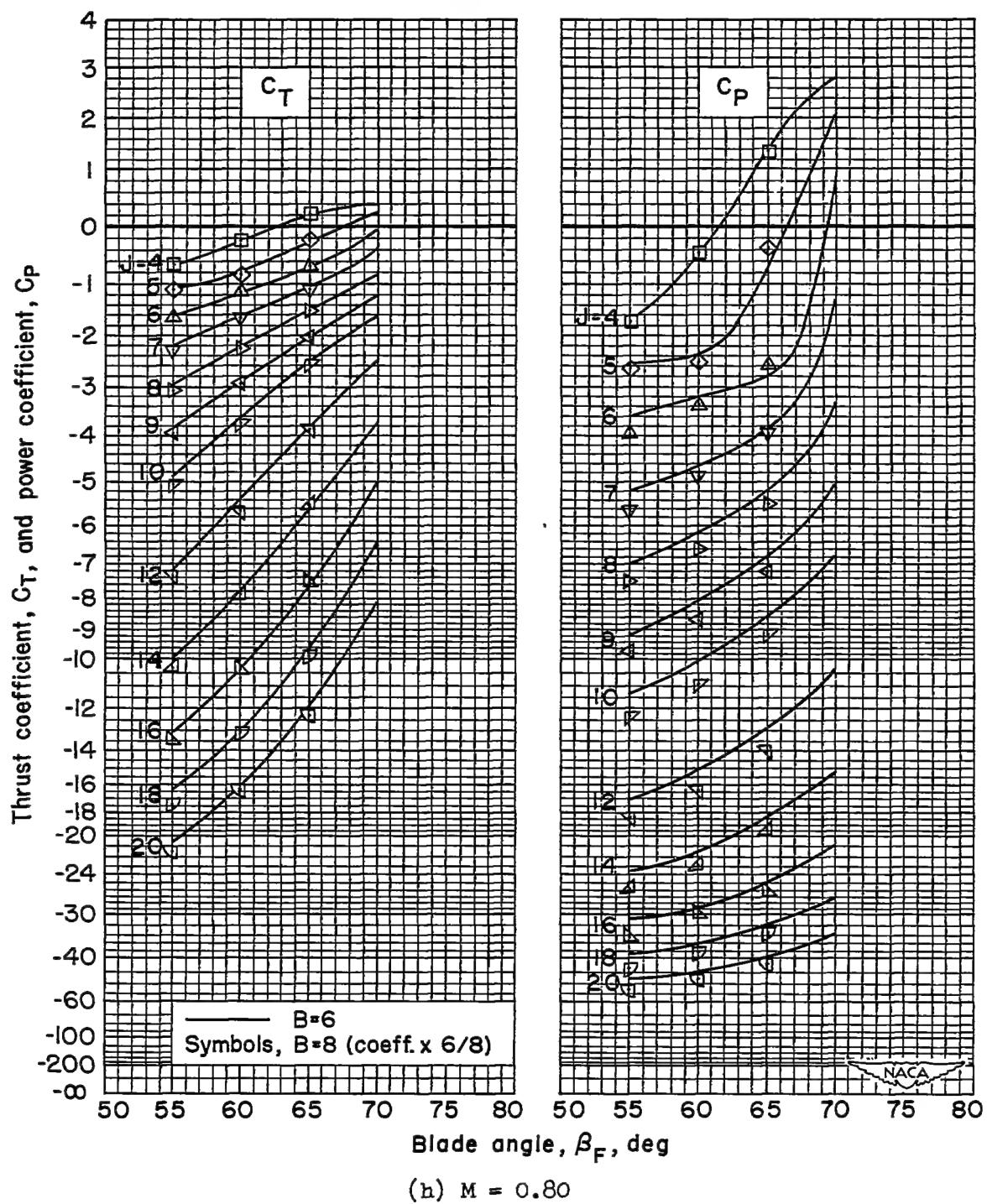
(h) $M = 0.80$

Figure 30.- Continued.

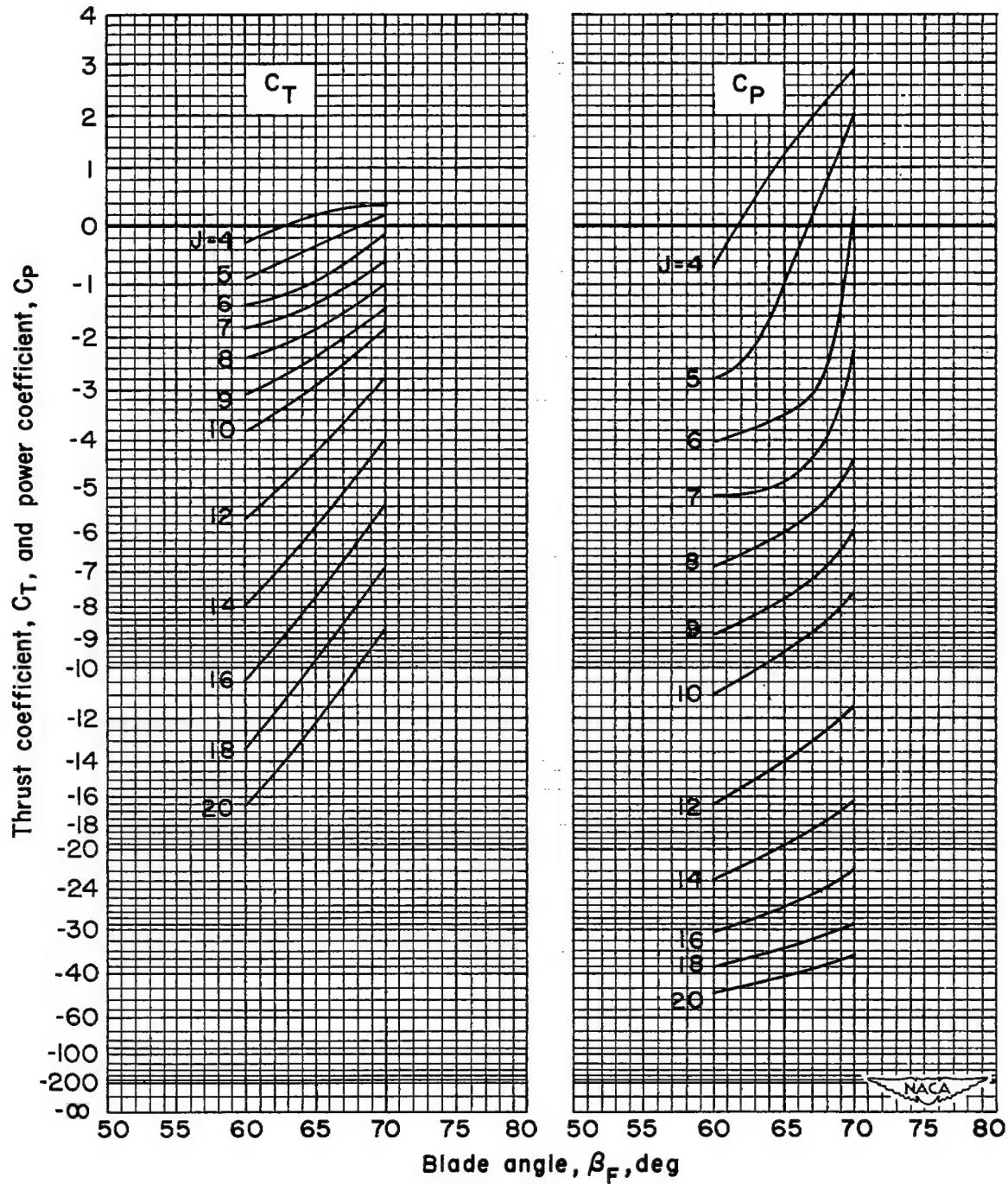
(i) $M = 0.84$

Figure 30.- Concluded.

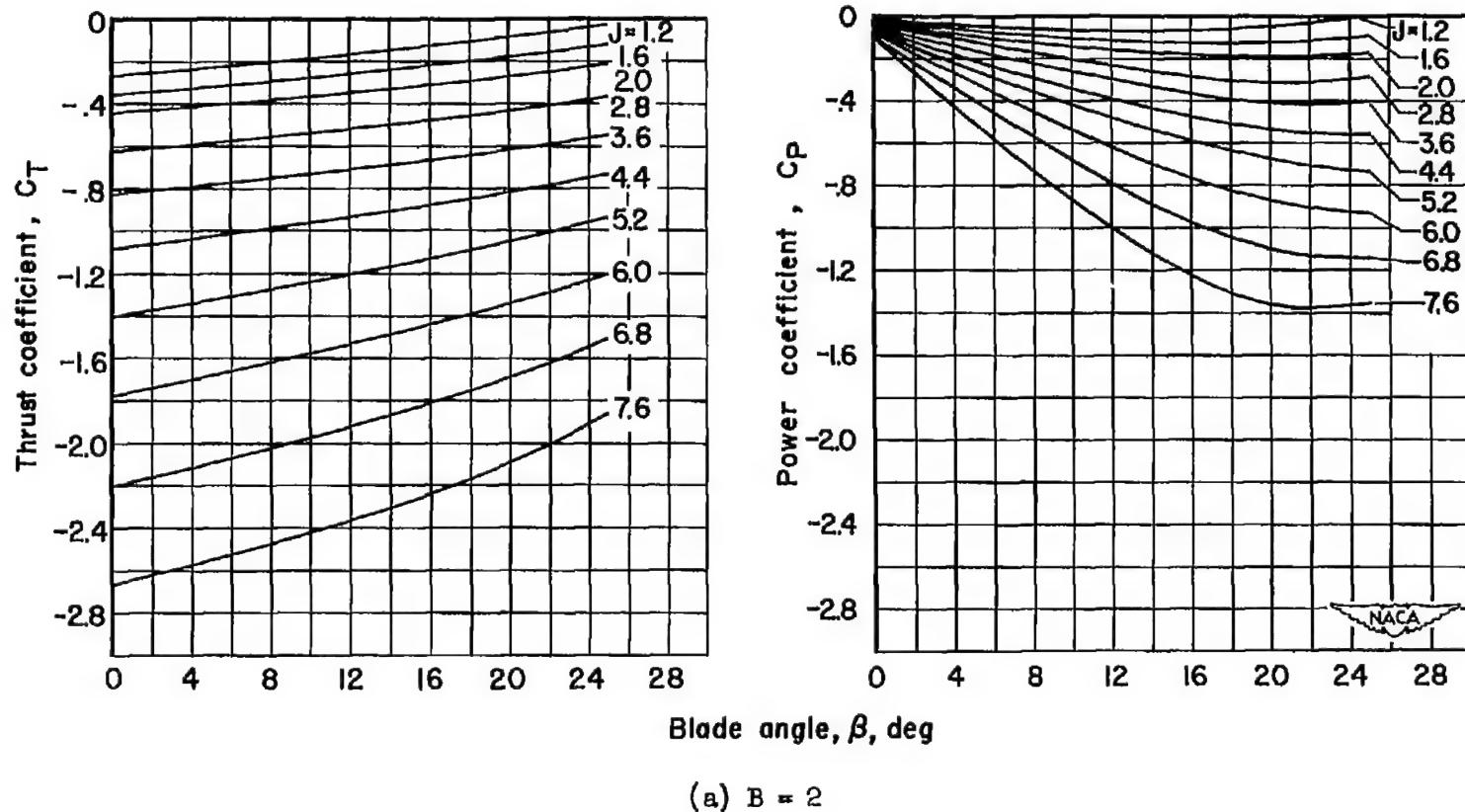


Figure 31.- The effect of blade angle on the negative-thrust characteristics; NACA 4-(5)(05)-041 two- and four-blade, single-rotation propellers, spinner C, $M = 0.15$.

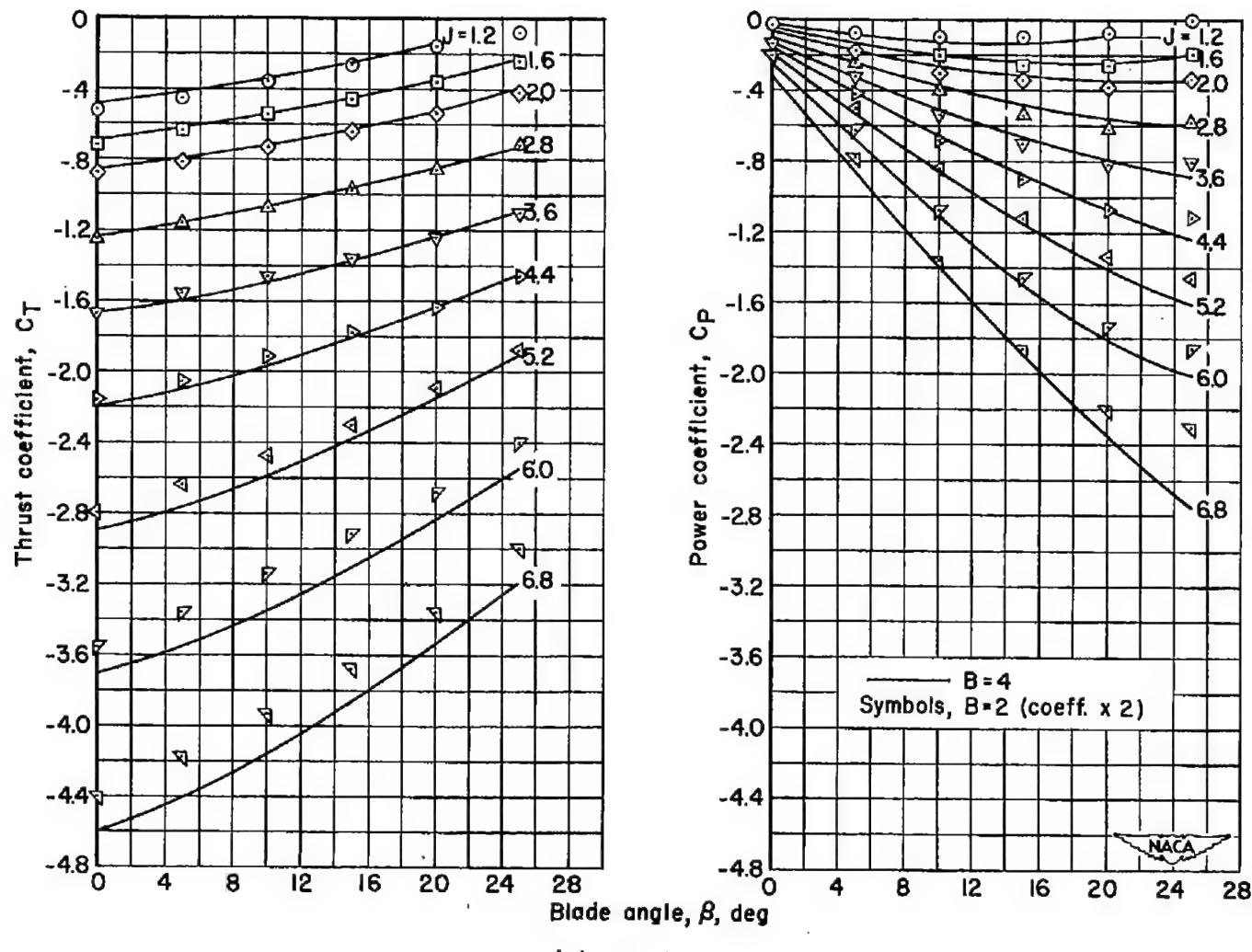
(b) $B = 4$

Figure 31.- Concluded.

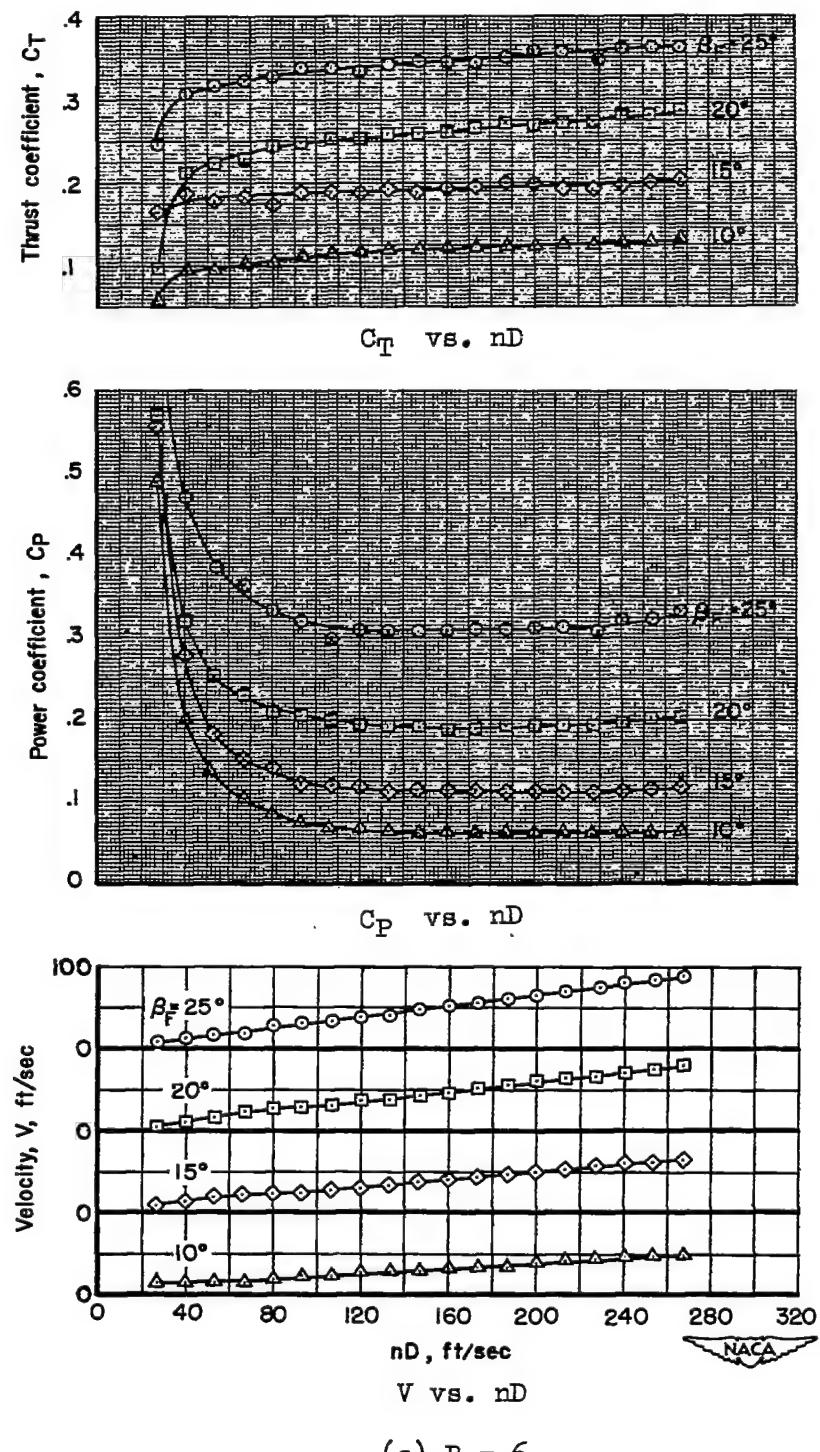
(a) $B = 6$

Figure 32.- Near static-thrust characteristics; NACA 4-(5)(05)-037 six- and eight-blade, dual-rotation propellers, $\Delta\beta$ = optimum, spinner A.

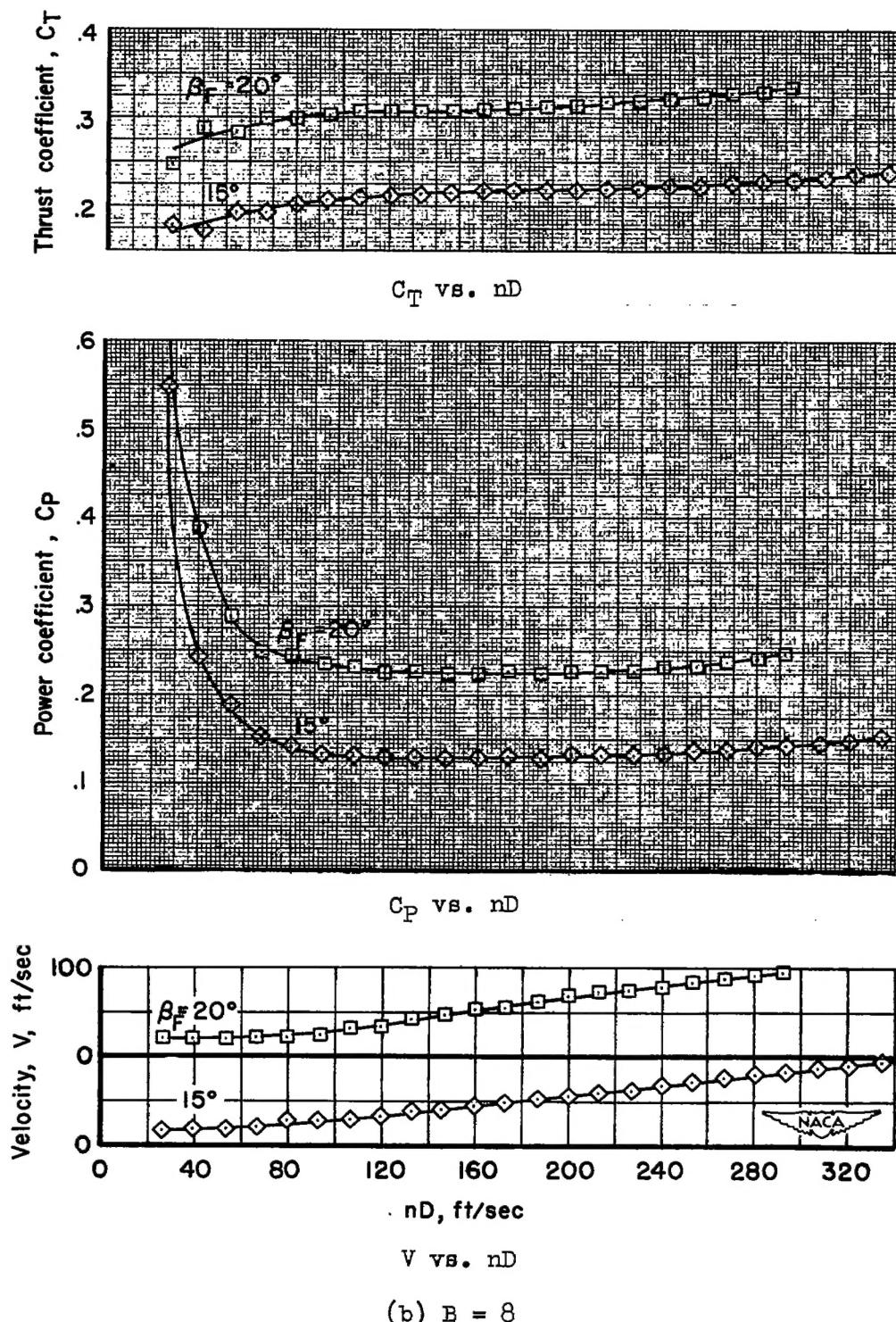


Figure 32.- Concluded.

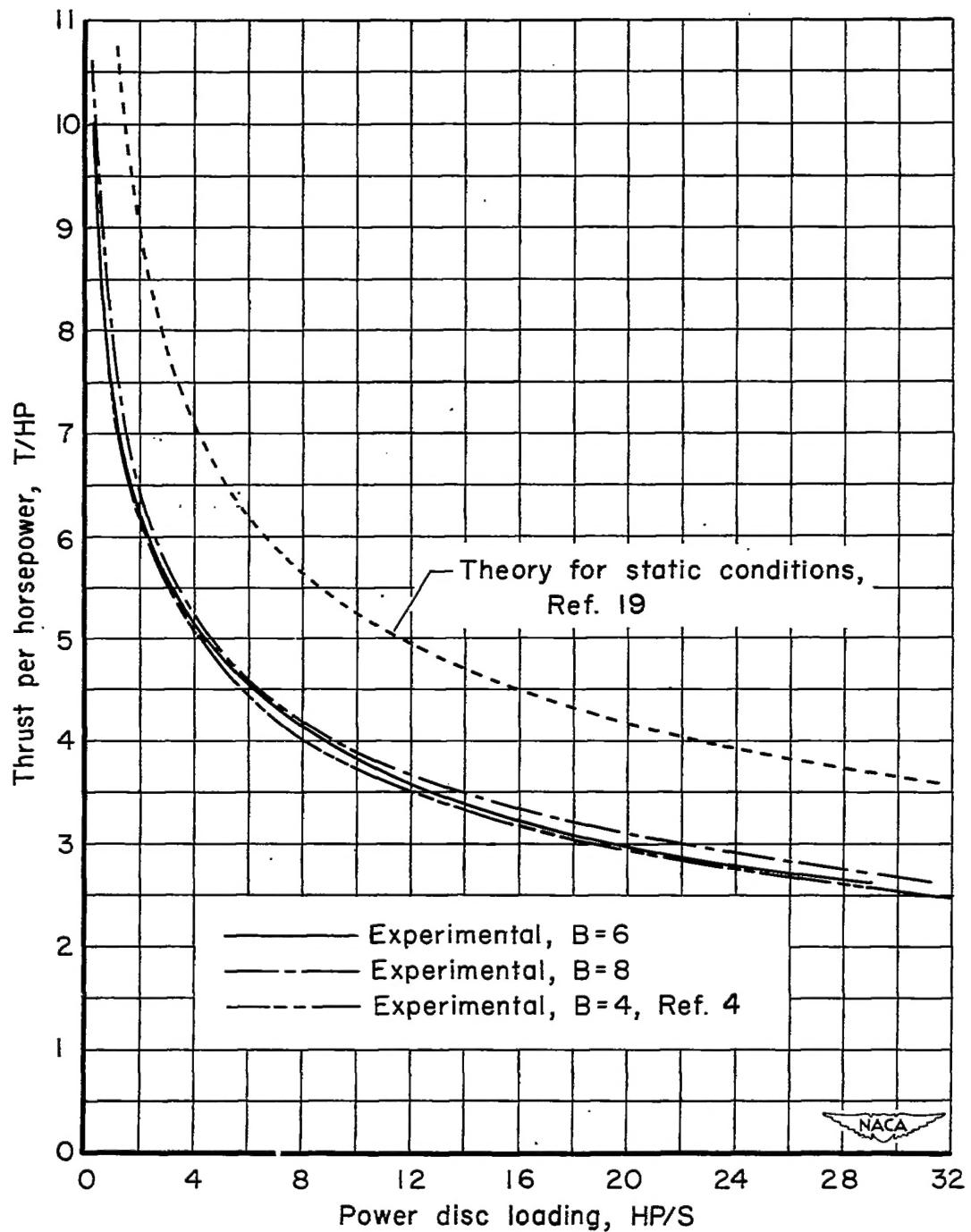


Figure 33.- Variation of the thrust per horsepower with power disc loading for operation of the NACA 4-(5)(05)-037 six- and eight-blade, dual-rotation propellers ($\Delta\beta$ = optimum, spinner A) at near static conditions, as compared with theory and with the results of a previous investigation.

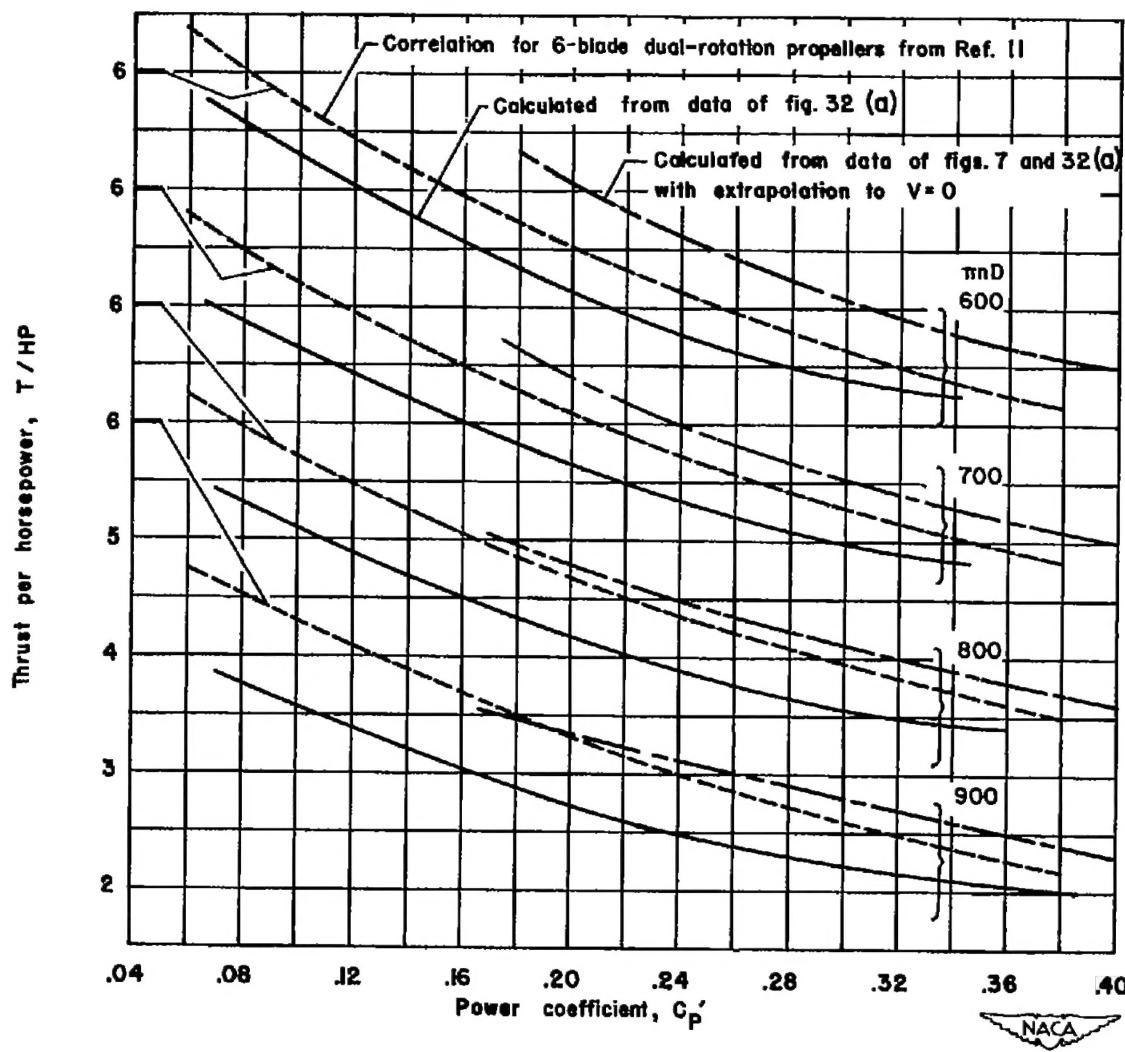


Figure 34.- Variation of thrust per horsepower with power coefficient obtained at near static conditions as compared with the results of previous investigations at static conditions.



3 1176 01434 7752